Towards controlled microneedle-mediated intradermal immunization

Schipper, P.

Towards Controlled Microneedle-Mediated Intradermal Immunization

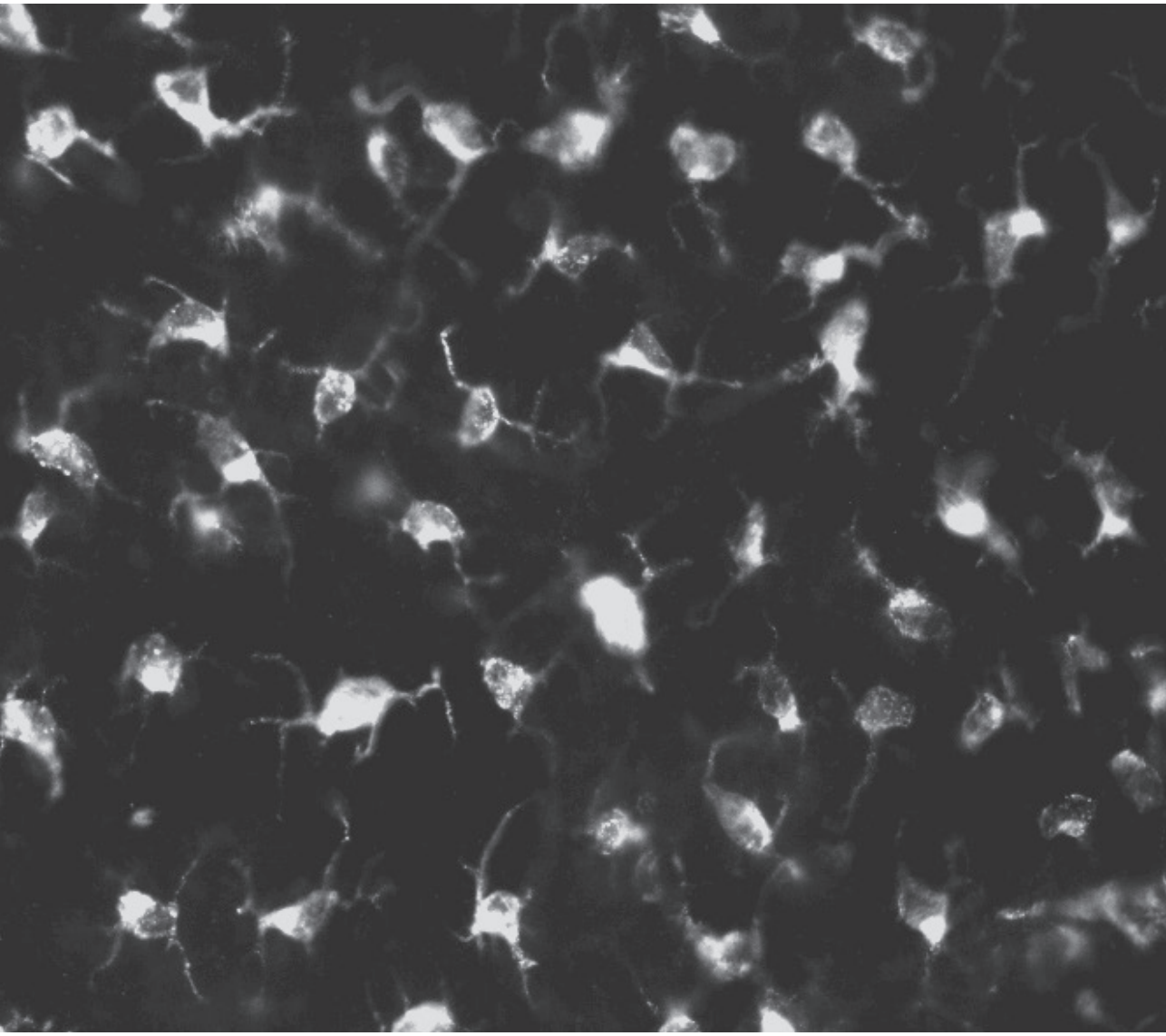

Pim Schipper

Towards Controlled Microneedle-Mediated Intradermal Immunization

Pim Schipper

The research described in this thesis was performed at the Division of BioTherapeutics of the Leiden Academic Centre for Drug Research (LACDR), Leiden University, Leiden, the Netherlands.

ISBN 978-94-6323-678-2

About the cover: the fluorescence microscopy cover image provides a view perpendicular to the skin surface and depicts Langerhans cells, which are immune cells residing in the most superficial skin layer (i.e., the epidermis) and are important for intradermal immunization.

Cover design by Pim Schipper, Chris Hansler and Gerrit Riezebos.
Layout design by Ilse Modder, www.ilsemodder.nl
Printed by Gildeprint Enschede, www.gildeprint.nl.

Towards Controlled Microneedle-Mediated Intradermal Immunization

PROEFSCHRIFT

ter verkrijging van
de graad van Doctor aan de Universiteit Leiden,
op gezag van Rector Magnificus Prof. Mr. C.J.J.M. Stolker,
volgens besluit van het College voor Promoties
te verdedigen op donderdag 20 juni 2019
klokke 13.45 uur

door

Pim Schipper
Geboren op 22 december 1985
te Alkmaar

Promotoren	Prof. Dr. Joke A. Bouwstra
	Prof. Dr. Wim Jiskoot
	Prof. Dr. Ir. Cees W.J. Oomens
Promotiecommissie	Prof. Dr. H. Irth, Universiteit Leiden (Voorzitter)
	Prof. Dr. A.P. IJzerman, Universiteit Leiden (Secretaris)
	Prof. Dr. C. Foged, Universiteit van Kopenhagen
	Prof. Dr. A.L.W. Huckriede, Rijksuniversiteit Groningen
	Prof. Dr. A. Kros, Universiteit Leiden
	Prof. Dr. F.A. Ossendorp, Universiteit Leiden

TABLE OF CONTENTS

Chapter 1 **9**
General introduction
Aim and outline of this thesis

Chapter 2 **27**
Determination of depth-dependent intradermal immunogenicity of adjuvanted inactivated polio vaccine delivered by microinjections via hollow microneedles

Chapter 3 **53**
Antigen uptake by skin dendritic cells as function of antigen dose and intradermal injection depth

Chapter 4 **83**
Repeated fractional intradermal dosing of an inactivated polio vaccine by a single hollow microneedle leads to superior immune responses

Chapter 5 **105**
Diphtheria toxoid and N-trimethyl chitosan layer-by-layer coated pH-sensitive microneedles induce potent immune responses upon dermal vaccination in mice

Chapter 6 **141**
Chemical modifications of gold surfaces with basic groups and a fluorescent nanoparticle adhesion assay to determine their surface pK_a

Chapter 7 **163**
Summary 164
Prospects 169
Conclusion 174

Appendices **181**
Nederlandse samenvatting 182
Curriculum Vitae 193
List of publications 194
List of abbreviations 195

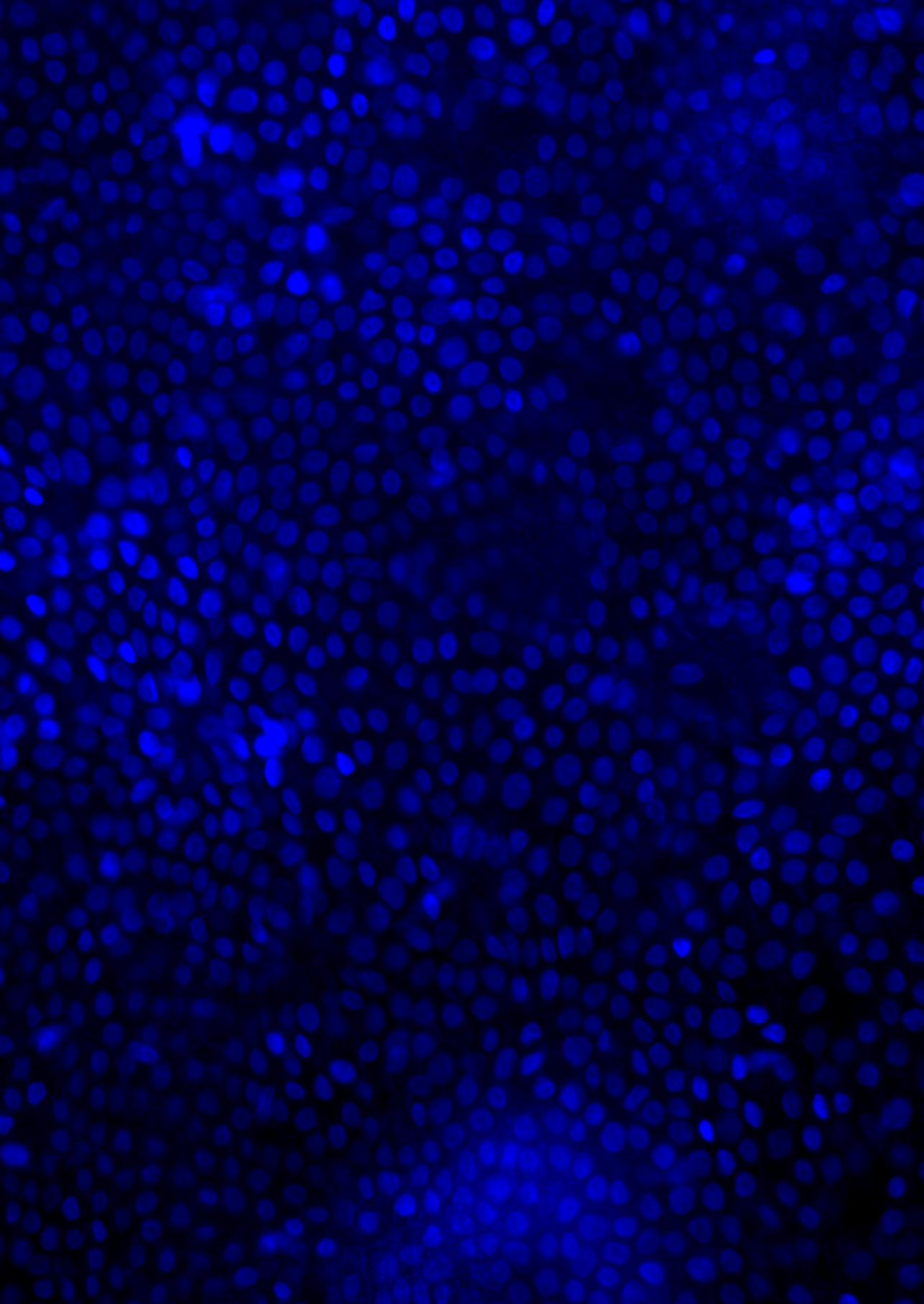

1

General introduction, aim and outline of this thesis

GENERAL INTRODUCTION

Vaccination

The advent of disease prevention by vaccination, introduced by pioneers such as Edward Jenner (1749-1823) and Louis Pasteur (1822-1895), started a revolution in medicine that is unparalleled to date. Vaccination strongly reduces disease burden, disability and death resulting from a variety of infectious diseases [1]. In fact, common (pediatric) diseases of the 20th century were reduced by 90% to 99% by modern vaccination programs in the United States [2, 3]. The success of vaccination even led to the eradication of smallpox, while an endgame strategic plan for polio eradication was drafted by the World Health Organization [4, 5]. Moreover, by preventing diseases, vaccination programs reduce healthcare costs drastically [6, 7].

Vaccination not only protects the vaccinated individuals, but in case of sufficiently high vaccination coverage also prevents the spread of disease, thereby indirectly protecting non-vaccinated individuals and those who do not respond to vaccination [8]. A successful vaccine must be highly effective, safe and have high vaccination coverage within the population [1, 8]. However, hesitance or refusal to vaccination is growing [9-11]. Religious views [12] and fear for side-effects [1] are cited as causes for growing refusal to vaccination. Furthermore, pain, fear and distress during vaccination leads to refusal, especially within the pediatric population [13].

Vaccine administration routes

Vaccination is usually performed *via* intramuscular and subcutaneous administration routes. These routes have the downsides of requiring trained personnel and painful injections by using hypodermic needles. Hypodermic needles also carry a risk for re-use and needle-stick injuries. Therefore, alternative administration routes have been investigated, including the intradermal and mucosal routes [14-19]. These alternative administration routes are easily accessible, potentially remove the requirement for trained personnel for administration and may enable painless administration of the vaccine. Vaccination *via* the skin is of high interest, owing to the presence of high numbers of immune cells in the skin [14, 20-24], which may enable increased immune responses at equal or lower doses. For example, intradermal rabies vaccination has been reported to result in a 60-80% dose reduction compared to intramuscular vaccination [25-27]. Dose sparing has also been reported for intradermal vaccination as compared to intramuscular vaccination against hepatitis B [28, 29], influenza [30-35] and polio [36, 37].

Intradermal vaccination: skin anatomy

An important role of the skin is to protect the body from pathogens in the environment [14, 24, 38]. Protection against invading pathogens is provided by two factors: 1) physical obstruction to invading pathogens and 2) a highly complex defense mechanism provided by the immune cells present in the skin.

The physical obstruction to invading pathogens by the skin is provided by the stratum corneum, which is the outermost layer of the epidermis (in human skin ca. 15-20 µm thickness) [39]. Underneath the stratum corneum is the viable epidermis. The viable epidermis is densely populated with keratinocytes and supplemented with melanocytes, Merkel cells and Langerhans Cells (LCs). The epidermis in human skin has a thickness of ca. 50-100 µm [14, 24, 38, 40]. The dermis is located below the epidermis, consists of a dense fibroelastic connective tissue and has a thickness of ca. 1-2 mm in human skin. Nerves, blood and lymphatic vessels, fibroblasts and a variety of immune cells are present throughout the dermis. The inner most layer of the skin is the subcutis, which consists of subcutaneous fat cells.

Intradermal vaccination: skin immunobiology

When an antigen from a pathogen or vaccine enters the skin, it can be taken up by (professional) antigen presenting cells (APCs), such as dendritic cells (DCs). After antigen uptake, DCs will process the antigen and subsequently migrate from the skin towards draining lymph nodes [24, 41, 42]. This process is facilitated by unspecific innate immune responses, which mainly function to induce inflammation and recruitment of immune cells. An example of this principle is the release of cytokines from the keratinocytes (the major cell type in the epidermis). Alternatively, the antigen itself migrates to a draining lymph node, after which the antigen is taken up by DCs residing in the lymph node [43-45]. Within draining lymph nodes, DCs present the antigen to B and T cells, initiating the adaptive immune response [24, 41, 42]. The adaptive immune response is capable of adapting and tailoring an immune response very specifically to the antigens of the invading pathogen or vaccine administered. The adaptive immune responses depend on antigen-specific B and T cells. Naïve B cells are inactive, until they encounter their specific antigen and are further activated by T helper cells. Upon activation, B cells proliferate into plasma cells, which produce high numbers of antibodies against the antigen. Antibodies provide a number of helpful functions to the immune system, which help neutralize and eliminate the invading pathogen. T cells may be divided into T helper ($CD4^+$) T cells and cytotoxic ($CD8^+$) T cells. Upon encountering their specific antigen, T helper cells are activated and help other immune cells, such as B cells, and help maximize the bactericidal activity of phagocytes (such as macrophages). Cytotoxic T

cells recognize and attack infected cells, effectively eliminating the pathogen.

Keratinocytes and LCs are present in the epidermis. As the human epidermis is only 50-100 µm in thickness, these immune cells are very close to the surface of the skin. Logically, they provide the first line of defense against invading pathogens. Keratinocytes function as sentries, providing key innate immune functions [46-48]. LCs are a special subset of DCs and provide a unique role to skin homeostasis and immunobiology. LCs form a high-density network, with their dendrites almost completely covering the skin surface [24, 41]. LCs are more specialized in cellular immunity than other skin DCs [49-54]. LCs react to viruses [49, 52-54], but weakly to bacteria [51, 55, 56]. This selective reactivity of LCs is most likely due to reduced expression of TLR2 [50, 51, 56] TLR4 [51, 56] and TLR5 [50, 51, 56], which are involved in recognition of bacterial ligands. Without the presence of antigens, LCs are known to be stationary in the skin for a long period of time [38].

Within the dermis, fibroblasts, subpopulations of dermal dendritic cells (DDCs), mast cells, macrophages, gamma-delta T cells and memory T cells (both $CD4^+$ and $CD8^+$) are present [57]. Fibroblasts play a role in the skin's innate immunity [38]. DDCs are also professional APCs and in human skin are comprised of two subsets, namely the $CD1a^+$ DDCs and the $CD14^+$ DDCs [24, 41, 50]. $CD14^+$ DDCs are more efficient in initiating humoral immunity than LCs or $CD1a^+$ DDCs. Naïve $CD4^+$ T cells are polarized by $CD14^+$ DDCs to develop into (follicular) helper T cells, which in turn induce naïve B cells to produce antibodies and to proliferate into plasma cells [49, 50, 58]. In comparison to LCs and $CD14^+$ DDCs, $CD1a^+$ DDCs are intermediately efficient in inducing humoral and cellular immune responses [49, 50, 59, 60]. Macrophages survey the dermis and have a critical role in innate immunity through phagocytosis and scavenging [61], and are involved in tissue repair [62]. Macrophages also bridge the innate and adaptive immunity by recruiting immune cells [61]. As the dermis is highly vascularized with blood- and lymph vessels, various immune cells may be recruited upon inflammation [63, 64].

After encounter and combating a pathogen, DCs perform antigen-imprinting on T cells specific for that pathogen [65], which marks them as memory T cells to be harbored in the skin. Upon re-encounter of the pathogen, memory T cells boost the immune responses to more effectively eliminate the pathogen. Thus, the skin is not only involved in local pathogen defense, but also on a systemic level, as the skin is home to twice the total number of circulating T cells in the blood. About 95% of T cells found in the skin is of the memory phenotype, while the other 5% is of the "revertant" memory phenotype [66, 67]. The epidermis houses mostly $CD8^+$ T cells in close proximity to the LCs [68].

Intradermal vaccination: methods of administration

The major hurdle to administer vaccines into the skin is to overcome the physical obstruction of the skin, provided by the stratum corneum [14]. Several techniques are developed to bypass the physical obstruction provided by the stratum corneum. The use of a conventional needle and syringe to inject vaccines into the skin, developed by Mendel and Mantoux in the early 1900s [69], is still being used today. However, such injections are hard to perform and require well-trained physicians. Therefore, alternative administration techniques are explored for safe and effective administration of vaccines into the skin.

Techniques explored to administer vaccines into the skin are nano-carriers (such as nanoparticles and liposomes) or micro-carriers, which are directly applied to the intact skin and may enter the hair follicles or are injected into the skin. Other administration techniques include the needle-free disruption of the stratum corneum by tape-stripping [70-74], abrasion [75-82], low-frequency ultrasound [83], electroporation [84-87] and thermo-ablation [88]. Jet injections of dry powder [89-96] or liquid formulations [97-99] have been investigated as well. Especially for polio vaccination, liquid jet injections were popular until the 1985 hepatitis outbreak [100], but have gained renewed interest [101-106]. However, of the novel administration techniques, microneedle-mediated administration of vaccines is regarded as highly promising and is widely explored [14, 107-109].

Microneedles

Microneedles are needles at a micrometer scale, usually with a length between 50-1000 µm [108]. Different types of microneedles exist, which can be classified into hollow microneedles and solid microneedles.

Hollow microneedles are hollow-bore needles at micrometer scale and can be used in the "poke and flow" approach to administer vaccine into the skin [108]:

1. In the "poke and flow" approach, either a single hollow microneedle or an array of hollow microneedles is used. The microneedle (array) is pierced into the skin, after which a liquid formulation flows through the bore of the microneedle(s), effectively injecting the liquid formulation into the skin.

As the name suggests, solid microneedles are solid needles at micrometer scale. Solid microneedles are usually utilized in arrays, which can be used in three distinctive approaches to administer vaccine into the skin:

2. In the "poke and patch" approach, an array of solid microneedles is pierced into the

skin, thereby creating microchannels. After removal of the (array of) microneedles, a patch containing a vaccine is applied onto the disrupted skin, allowing the vaccine to diffuse along the microchannels into the skin.

3. In the "poke and release" approach, vaccine is encapsulated in an array of dissolving microneedles. After piercing the (array of) microneedles into the skin, the microneedles start to dissolve, thereby releasing the vaccine. The "poke and release" approach can also be applied by using (array of) porous microneedles, allowing to release the encapsulated vaccine into the skin by a diffusion process.
4. In the "coat and poke" approach, the vaccine is coated onto the surface(s) of (an array of) solid microneedles. Upon piercing the skin, the vaccine is released from the coated microneedle surface(s).

In this thesis, studies have been described further exploring the "poke and flow" and "coat and poke" approaches, as detailed in the following section.

AIM AND OUTLINE OF THIS THESIS

The main goals of this research were to:

1. Investigate the dependency of immune responses on the depth at which the antigen is administered in skin by a single hollow microneedle by using the "poke and flow" approach.
2. Determine whether immune responses resulting from intradermal injections of repeated fractional doses differ from immune responses resulting from a single intradermal bolus injection. In these studies, the "poke and flow" approach has been explored by using a single hollow microneedle.
3. Evaluate the possibilities to create pH-sensitive surfaces on gold surfaces.
4. To examine whether a layer-by-layer vaccine-coating approach on pH-sensitive modified silicon surfaces of microneedles can be used for intradermal immunization purposes. In these studies, the "coat and poke" approach has been explored by using a high-density solid microneedle array.

In *chapter 2*, the performance of a single hollow microneedle together with an applicator system to perform depth-controlled minimally-invasive intradermal microinjections is described. The single hollow microneedle injection system allowed for precisely controlling the injection depth, injection rate and injection volume. By using this single hollow microneedle injection system, monovalent inactivated polio vaccine serotype

1 (IPV1) was injected intradermally at different depths in rats *in vivo*. The relationship between the intradermal injection depth and IPV1-specific immune responses was investigated. In addition, the potential of the adjuvants CpG oligodeoxynucleotide 1826 (CpG) and cholera toxin (CT) to enhance intradermal IPV1-specific immune responses was investigated. The results were compared against classic subcutaneous IPV1 injection using a conventional needle and syringe.

In *chapter 3*, a human skin DC crawl-out model was utilized to investigate responses of human skin DCs in relation to the depth at which vaccine was injected intradermally by using the single hollow microneedle injection system or a conventional needle and syringe. In this chapter, it was investigated whether the fraction and maturation of LCs and DDCs and the internalization of model antigen ovalbumin (OVA) by LCs and DDCs differs in response to the OVA dose or the depth at which OVA was administered intradermally.

Besides intradermal administration depth, the influence of repeated fractional intradermal dosing of IPV1 on IPV1-specific immune responses was investigated in *chapter 4*. The IPV1 dose was fractionated and administered over multiple days. The repeated fractional dosing schedules were compared to the classic (single) bolus dosing schedule and to CpG adjuvanted IPV1 bolus dosing. IPV1 was intradermally administered by using the single hollow microneedle injection system or subcutaneously administered by using a conventional needle and syringe.

A benefit of using solid microneedle arrays in the "coat and poke" approach, is that the vaccine is in a solid state and therefore is expected to be more stable at room temperature as compared to liquid vaccine formulations. To make use of the "coat and poke" approach, pH-sensitive microneedle surfaces provide a method to adhere antigen to the microneedle surface and to release antigen upon piercing the skin. The amount of antigen that can be coated in a single layer onto pH-sensitive surfaces of microneedle arrays is limited. In an effort to increase the amount of antigen that can be coated onto pH-sensitive silicon surfaces of microneedle arrays, two approaches were examined.

In *chapter 5*, the development of a layer-by-layer coating approach on pH-sensitive silicon microneedles is described. This layer-by-layer coating approach effectively enlarges the surface area available for coating, thereby increasing the amount of antigen that can be coated onto the microneedle array. In the layer-by-layer coating approach, a negatively charged antigen (diphtheria toxoid (DT)) was coated alternatingly with a positively charged polymer (N,N,N-trimethyl chitosan (TMC)) onto pH-sensitive silicon

surfaces of microneedle arrays. The coating and release properties of these layer-by-layer DT-TMC coated microneedle arrays were characterized. Furthermore, the potential of these DT-TMC coated microneedle arrays to induce immunization against diphtheria toxin was investigated, by using an *in vivo* mouse model. In these studies, immunization *via* the skin by using DT-TMC coated microneedle arrays was compared against intradermal or subcutaneous immunization with DT alone or in combination with TMC. Intradermal immunization was performed by using the single hollow microneedle injection system and subcutaneous immunization was performed by using a conventional needle and syringe.

Sponge-like surfaces can be created by sputtering gold-ions onto silicon surfaces, to enlarge the surface area available for coating. In *chapter 6*, chemical gold surface modifiers were used to create self-assembled pH-sensitive monolayers on gold surfaces. This pH-sensitivity depends on the surface pK_a. Therefore, the surface pK_a of these pH-sensitive modified gold surfaces was determined using a fluorescent nanoparticle adhesion assay as well.

Lastly, the results and conclusions of this thesis are summarized in *chapter 7*. Additionally, this chapter contains the prospects of intradermal immunization making use of microneedle-mediated administration of vaccines.

REFERENCES

1. W.A. Orenstein, R. Ahmed, Simply put: Vaccination saves lives, Proc Natl Acad Sci U S A, 114 (2017) 4031-4033.
2. Centers for Disease Control and Prevention (2016) Notifiable Diseases and Mortality Tables, MMWR Morb Mortal Wkly Rep, 65 ND-924-ND-941.
3. S.W. Roush, T.V. Murphy, G. Vaccine-Preventable Disease Table Working, Historical comparisons of morbidity and mortality for vaccine-preventable diseases in the United States, JAMA, 298 (2007) 2155-2163.
4. Fenner F, Henderson DA, Arita I, Jezek AZ, L. ID, Smallpox and its Eradication, World Health Organization, Geneva, 1988.
5. W. World Health Organization, Polio eradication and endgame strategic plan 2013 - 2018, World Health Organization (WHO), Geneva, Switserland, 2013.
6. F. Zhou, A. Shefer, J. Wenger, M. Messonnier, L.Y. Wang, A. Lopez, M. Moore, T.V. Murphy, M. Cortese, L. Rodewald, Economic evaluation of the routine childhood immunization program in the United States, 2009, Pediatrics, 133 (2014) 577-585.
7. S. Ozawa, S. Clark, A. Portnoy, S. Grewal, L. Brenzel, D.G. Walker, Return On Investment From Childhood Immunization In Low- And Middle-Income Countries, 2011-20, Health Aff (Millwood), 35 (2016) 199-207.
8. F. PEM, M. K, Community immunity, Elsevier, Philadelphia, 2013.
9. P.M. Frew, A.K. Fisher, M.M. Basket, Y. Chung, J. Schamel, J.L. Weiner, J. Mullen, S.B. Omer, W.A. Orenstein, Changes in childhood immunization decisions in the United States: Results from 2012 & 2014 National Parental Surveys, Vaccine, 34 (2016) 5689-5696.
10. C. Hough-Telford, D.W. Kimberlin, I. Aban, W.P. Hitchcock, J. Almquist, R. Kratz, K.G. O'Connor, Vaccine Delays, Refusals, and Patient Dismissals: A Survey of Pediatricians, Pediatrics, 138 (2016).
11. H.J. Larson, A. de Figueiredo, Z. Xiahong, W.S. Schulz, P. Verger, I.G. Johnston, A.R. Cook, N.S. Jones, The State of Vaccine Confidence 2016: Global Insights Through a 67-Country Survey, EBioMedicine, 12 (2016) 295-301.
12. C. NS, G. PA, F. AP, R. SB, W. GS, Centers for Disease Control and Prevention (CDC) Measles—United States, January 4–April 2, 2015, MMWR Morb Mortal Wkly Rep, 64 (2015) 373–376.
13. R.M. Jacobson, A. Swan, A. Adegbenro, S.L. Ludington, P.C. Wollan, G.A. Poland, G. Vaccine Research, Making vaccines more acceptable--methods to prevent and minimize pain and other common adverse events associated with vaccines, Vaccine, 19 (2001) 2418-2427.
14. S.M. Bal, Z. Ding, E. van Riet, W. Jiskoot, J.A. Bouwstra, Advances in transcutaneous vaccine delivery: do all ways lead to Rome?, J Control Release, 148 (2010) 266-282.
15. M.R. Neutra, P.A. Kozlowski, Mucosal vaccines: the promise and the challenge, Nat Rev Immunol, 6 (2006) 148-158.
16. T.R. Hird, N.C. Grassly, Systematic review of mucosal immunity induced by oral and inactivated poliovirus vaccines against virus shedding following oral poliovirus challenge, PLoS Pathog, 8 (2012) e1002599.
17. B. Slutter, N. Hagenaars, W. Jiskoot, Rational design of nasal vaccines, J Drug Target, 16 (2008) 1-17.

18. M.P. Girard, S.K. Osmanov, M.P. Kieny, A review of vaccine research and development: the human immunodeficiency virus (HIV), Vaccine, 24 (2006) 4062-4081.
19. P.A. Kozlowski, S. Cu-Uvin, M.R. Neutra, T.P. Flanigan, Comparison of the oral, rectal, and vaginal immunization routes for induction of antibodies in rectal and genital tract secretions of women, Infect Immun, 65 (1997) 1387-1394.
20. S. Kaushik, A.H. Hord, D.D. Denson, D.V. McAllister, S. Smitra, M.G. Allen, M.R. Prausnitz, Lack of pain associated with microfabricated microneedles, Anesth Analg, 92 (2001) 502-504.
21. B. Bonnotte, M. Gough, V. Phan, A. Ahmed, H. Chong, F. Martin, R.G. Vile, Intradermal injection, as opposed to subcutaneous injection, enhances immunogenicity and suppresses tumorigenicity of tumor cells, Cancer Res, 63 (2003) 2145-2149.
22. R.B. Belshe, F.K. Newman, J. Cannon, C. Duane, J. Treanor, C. Van Hoecke, B.J. Howe, G. Dubin, Serum antibody responses after intradermal vaccination against influenza, N Engl J Med, 351 (2004) 2286-2294.
23. J.F. Nicolas, B. Guy, Intradermal, epidermal and transcutaneous vaccination: from immunology to clinical practice, Expert Rev Vaccines, 7 (2008) 1201-1214.
24. C. Levin, H. Perrin, B. Combadiere, Tailored immunity by skin antigen-presenting cells, Hum Vaccin Immunother, 11 (2015) 27-36.
25. M.J. Warrell, K.G. Nicholson, D.A. Warrell, P. Suntharasamai, P. Chanthavanich, C. Viravan, A. Sinhaseni, M.K. Chiewbambroongkiat, X. Pouradier-Duteil, C. Xueref, et al., Economical multiple-site intradermal immunisation with human diploid-cell-strain vaccine is effective for post-exposure rabies prophylaxis, Lancet, 1 (1985) 1059-1062.
26. B.P. Quiambao, E.M. Dimaano, C. Ambas, R. Davis, A. Banzhoff, C. Malerczyk, Reducing the cost of post-exposure rabies prophylaxis: efficacy of 0.1 ml PCEC rabies vaccine administered intradermally using the Thai Red Cross post-exposure regimen in patients severely exposed to laboratory-confirmed rabid animals, Vaccine, 23 (2005) 1709-1714.
27. A. Ambrozaitis, A. Laiskonis, L. Balciuniene, A. Banzhoff, C. Malerczyk, Rabies post-exposure prophylaxis vaccination with purified chick embryo cell vaccine (PCECV) and purified Vero cell rabies vaccine (PVRV) in a four-site intradermal schedule (4-0-2-0-1-1): an immunogenic, cost-effective and practical regimen, Vaccine, 24 (2006) 4116-4121.
28. T. Propst, A. Propst, K. Lhotta, W. Vogel, P. Konig, Reinforced intradermal hepatitis B vaccination in hemodialysis patients is superior in antibody response to intramuscular or subcutaneous vaccination, Am J Kidney Dis, 32 (1998) 1041-1045.
29. H. Micozkadioglu, A. Zumrutdal, D. Torun, S. Sezer, F.N. Ozdemir, M. Haberal, Low dose intradermal vaccination is superior to high dose intramuscular vaccination for hepatitis B in unresponsive hemodialysis patients, Ren Fail, 29 (2007) 285-288.
30. Y.C. Kim, F.S. Quan, D.G. Yoo, R.W. Compans, S.M. Kang, M.R. Prausnitz, Improved influenza vaccination in the skin using vaccine coated microneedles, Vaccine, 27 (2009) 6932-6938.
31. D. Holland, R. Booy, F. De Looze, P. Eizenberg, J. McDonald, J. Karrasch, M. McKeirnan, H. Salem, G. Mills, J. Reid, F. Weber, M. Saville,

Intradermal influenza vaccine administered using a new microinjection system produces superior immunogenicity in elderly adults: a randomized controlled trial, J Infect Dis, 198 (2008) 650-658.

32. F.S. Quan, Y.C. Kim, A. Vunnava, D.G. Yoo, J.M. Song, M.R. Prausnitz, R.W. Compans, S.M. Kang, Intradermal vaccination with influenza virus-like particles by using microneedles induces protection superior to that with intramuscular immunization, J Virol, 84 (2010) 7760-7769.
33. D.G. Koutsonanos, E.V. Vassilieva, A. Stavropoulou, V.G. Zarnitsyn, E.S. Esser, M.T. Taherbhai, M.R. Prausnitz, R.W. Compans, I. Skountzou, Delivery of subunit influenza vaccine to skin with microneedles improves immunogenicity and long-lived protection, Sci Rep, 2 (2012) 357.
34. E.V. Vassilieva, H. Kalluri, D. McAllister, M.T. Taherbhai, E.S. Esser, W.P. Pewin, J.A. Pulit-Penaloza, M.R. Prausnitz, R.W. Compans, I. Skountzou, Improved immunogenicity of individual influenza vaccine components delivered with a novel dissolving microneedle patch stable at room temperature, Drug Deliv Transl Res, 5 (2015) 360-371.
35. R. Arakane, R. Annaka, A. Takahama, K. Ishida, M. Yoshiike, T. Nakayama, F. Takeshita, Superior immunogenicity profile of the new intradermal influenza vaccine compared to the standard subcutaneous vaccine in subjects 65 years and older: A randomized controlled phase III study, Vaccine, 33 (2015) 6650-6658.
36. J. Cadorna-Carlos, E. Vidor, M.C. Bonnet, Randomized controlled study of fractional doses of inactivated poliovirus vaccine administered intradermally with a needle in the Philippines, Int J Infect Dis, 16 (2012) e110-116.
37. S.B. Troy, D. Kouiavskaia, J. Siik, E. Kochba, H. Beydoun, O. Mirochnitchenko, Y. Levin, N. Khardori, K. Chumakov, Y. Maldonado, Comparison of the Immunogenicity of Various Booster Doses of Inactivated Polio Vaccine Delivered Intradermally Versus Intramuscularly to HIV-Infected Adults, J Infect Dis, 211 (2015) 1969-1976.
38. B. Combadiere, C. Liard, Transcutaneous and intradermal vaccination, Hum Vaccin, 7 (2011) 811-827.
39. J. van Smeden, M. Janssens, G.S. Gooris, J.A. Bouwstra, The important role of stratum corneum lipids for the cutaneous barrier function, Biochim Biophys Acta, 1841 (2014) 295-313.
40. H.J. Hirschberg, E. van Riet, D. Oosterhoff, J.A. Bouwstra, G.F. Kersten, Animal models for cutaneous vaccine delivery, Eur J Pharm Sci, 71 (2015) 112-122.
41. M.B. Teunissen, M. Haniffa, M.P. Collin, Insight into the immunobiology of human skin and functional specialization of skin dendritic cell subsets to innovate intradermal vaccination design, Curr Top Microbiol Immunol, 351 (2012) 25-76.
42. T. Worbs, S.I. Hammerschmidt, R. Forster, Dendritic cell migration in health and disease, Nat Rev Immunol, 17 (2017) 30-48.
43. R.S. Allan, C.M. Smith, G.T. Belz, A.L. van Lint, L.M. Wakim, W.R. Heath, F.R. Carbone, Epidermal viral immunity induced by CD8alpha+ dendritic cells but not by Langerhans cells, Science, 301 (2003) 1925-1928.
44. A. Kissenpfennig, B. Malissen, Langerhans cells--revisiting the paradigm using genetically engineered mice, Trends Immunol, 27 (2006) 132-139.

45. X. Zhao, E. Deak, K. Soderberg, M. Linehan, D. Spezzano, J. Zhu, D.M. Knipe, A. Iwasaki, Vaginal submucosal dendritic cells, but not Langerhans cells, induce protective Th1 responses to herpes simplex virus-2, J Exp Med, 197 (2003) 153-162.
46. M.C. Lebre, A.M. van der Aar, L. van Baarsen, T.M. van Capel, J.H. Schuitemaker, M.L. Kapsenberg, E.C. de Jong, Human keratinocytes express functional Toll-like receptor 3, 4, 5, and 9, J Invest Dermatol, 127 (2007) 331-341.
47. P. Di Meglio, G.K. Perera, F.O. Nestle, The multitasking organ: recent insights into skin immune function, Immunity, 35 (2011) 857-869.
48. W.R. Heath, F.R. Carbone, The skin-resident and migratory immune system in steady state and memory: innate lymphocytes, dendritic cells and T cells, Nat Immunol, 14 (2013) 978-985.
49. E. Klechevsky, R. Morita, M. Liu, Y. Cao, S. Coquery, L. Thompson-Snipes, F. Briere, D. Chaussabel, G. Zurawski, A.K. Palucka, Y. Reiter, J. Banchereau, H. Ueno, Functional specializations of human epidermal Langerhans cells and CD14+ dermal dendritic cells, Immunity, 29 (2008) 497-510.
50. C.M. Fehres, S.C. Bruijns, B.N. Sotthewes, H. Kalay, L. Schaffer, S.R. Head, T.D. de Gruijl, J.J. Garcia-Vallejo, Y. van Kooyk, Phenotypic and Functional Properties of Human Steady State CD14+ and CD1a+ Antigen Presenting Cells and Epidermal Langerhans Cells, PLoS One, 10 (2015) e0143519.
51. A.M. van der Aar, R.M. Sylva-Steenland, J.D. Bos, M.L. Kapsenberg, E.C. de Jong, M.B. Teunissen, Loss of TLR2, TLR4, and TLR5 on Langerhans cells abolishes bacterial recognition, J Immunol, 178 (2007) 1986-1990.
52. E. Klechevsky, M. Liu, R. Morita, R. Banchereau, L. Thompson-Snipes, A.K. Palucka, H. Ueno, J. Banchereau, Understanding human myeloid dendritic cell subsets for the rational design of novel vaccines, Hum Immunol, 70 (2009) 281-288.
53. G. Ratzinger, J. Baggers, M.A. de Cos, J. Yuan, T. Dao, J.L. Reagan, C. Munz, G. Heller, J.W. Young, Mature human Langerhans cells derived from CD34+ hematopoietic progenitors stimulate greater cytolytic T lymphocyte activity in the absence of bioactive IL-12p70, by either single peptide presentation or cross-priming, than do dermal-interstitial or monocyte-derived dendritic cells, J Immunol, 173 (2004) 2780-2791.
54. A.M. van der Aar, R. de Groot, M. Sanchez-Hernandez, E.W. Taanman, R.A. van Lier, M.B. Teunissen, E.C. de Jong, M.L. Kapsenberg, Cutting edge: virus selectively primes human langerhans cells for CD70 expression promoting CD8+ T cell responses, J Immunol, 187 (2011) 3488-3492.
55. J. Takeuchi, E. Watari, E. Shinya, Y. Norose, M. Matsumoto, T. Seya, M. Sugita, S. Kawana, H. Takahashi, Down-regulation of Toll-like receptor expression in monocyte-derived Langerhans cell-like cells: implications of low-responsiveness to bacterial components in the epidermal Langerhans cells, Biochem Biophys Res Commun, 306 (2003) 674-679.
56. V. Flacher, M. Bouschbacher, E. Verronese, C. Massacrier, V. Sisirak, O. Berthier-Vergnes, B. de Saint-Vis, C. Caux, C. Dezutter-Dambuyant, S. Lebecque, J. Valladeau, Human Langerhans cells express a specific TLR profile and differentially respond to viruses and Gram-positive bacteria, J Immunol, 177 (2006) 7959-7967.
57. Y. Nakanishi, B. Lu, C. Gerard, A. Iwasaki, CD8(+) T

lymphocyte mobilization to virus-infected tissue requires CD4(+) T-cell help, Nature, 462 (2009) 510-513.

58. C. Caux, C. Massacrier, B. Vanbervliet, B. Dubois, I. Durand, M. Cella, A. Lanzavecchia, J. Banchereau, CD34+ hematopoietic progenitors from human cord blood differentiate along two independent dendritic cell pathways in response to granulocyte-macrophage colony-stimulating factor plus tumor necrosis factor alpha: II. Functional analysis, Blood, 90 (1997) 1458-1470.
59. A.E. Morelli, J.P. Rubin, G. Erdos, O.A. Tkacheva, A.R. Mathers, A.F. Zahorchak, A.W. Thomson, L.D. Falo, Jr., A.T. Larregina, $CD4^+$ T cell responses elicited by different subsets of human skin migratory dendritic cells, J Immunol, 175 (2005) 7905-7915.
60. L.C. Zaba, J. Fuentes-Duculan, R.M. Steinman, J.G. Krueger, M.A. Lowes, Normal human dermis contains distinct populations of CD11c+BDCA-1+ dendritic cells and CD163+FXIIIA+ macrophages, J Clin Invest, 117 (2007) 2517-2525.
61. F.O. Martinez, A. Sica, A. Mantovani, M. Locati, Macrophage activation and polarization, Front Biosci, 13 (2008) 453-461.
62. C.D. Mills, M1 and M2 Macrophages: Oracles of Health and Disease, Crit Rev Immunol, 32 (2012) 463-488.
63. T.S. Kupper, R.C. Fuhlbrigge, Immune surveillance in the skin: mechanisms and clinical consequences, Nat Rev Immunol, 4 (2004) 211-222.
64. F.O. Nestle, P. Di Meglio, J.Z. Qin, B.J. Nickoloff, Skin immune sentinels in health and disease, Nat Rev Immunol, 9 (2009) 679-691.
65. H. Sigmundsdottir, E.C. Butcher, Environmental cues, dendritic cells and the programming of tissue-selective lymphocyte trafficking, Nat Immunol, 9 (2008) 981-987.
66. R.A. Clark, Skin-resident T cells: the ups and downs of on site immunity, J Invest Dermatol, 130 (2010) 362-370.
67. R.A. Clark, B. Chong, N. Mirchandani, N.K. Brinster, K. Yamanaka, R.K. Dowgiert, T.S. Kupper, The vast majority of CLA+ T cells are resident in normal skin, J Immunol, 176 (2006) 4431-4439.
68. C.A. Foster, H. Yokozeki, K. Rappersberger, F. Koning, B. Volc-Platzer, A. Rieger, J.E. Coligan, K. Wolff, G. Stingl, Human epidermal T cells predominantly belong to the lineage expressing alpha/beta T cell receptor, J Exp Med, 171 (1990) 997-1013.
69. B.G. Weniger, M.J. Papania, Alternative vaccine delivery methods, Elsevier, Amsterdam, the Netherlands, 2008.
70. B. Combadiere, A. Vogt, B. Mahe, D. Costagliola, S. Hadam, O. Bonduelle, W. Sterry, S. Staszewski, H. Schaefer, S. van der Werf, C. Katlama, B. Autran, U. Blume-Peytavi, Preferential amplification of CD8 effector-T cells after transcutaneous application of an inactivated influenza vaccine: a randomized phase I trial, PLoS One, 5 (2010) e10818.
71. A. Vogt, B. Mahe, D. Costagliola, O. Bonduelle, S. Hadam, G. Schaefer, H. Schaefer, C. Katlama, W. Sterry, B. Autran, U. Blume-Peytavi, B. Combadiere, Transcutaneous anti-influenza vaccination promotes both CD4 and CD8 T cell immune responses in humans, J Immunol, 180 (2008) 1482-1489.
72. H. Yagi, H. Hashizume, T. Horibe, Y. Yoshinari, M. Hata, A. Ohshima, T. Ito, M. Takigawa, A. Shibaki,

H. Shimizu, N. Seo, Induction of therapeutically relevant cytotoxic T lymphocytes in humans by percutaneous peptide immunization, Cancer Res, 66 (2006) 10136-10144.

73. B. Mahe, A. Vogt, C. Liard, D. Duffy, V. Abadie, O. Bonduelle, A. Boissonnas, W. Sterry, B. Verrier, U. Blume-Peytavi, B. Combadiere, Nanoparticle-based targeting of vaccine compounds to skin antigen-presenting cells by hair follicles and their transport in mice, J Invest Dermatol, 129 (2009) 1156-1164.
74. T. Scharton-Kersten, J. Yu, R. Vassell, D. O'Hagan, C.R. Alving, G.M. Glenn, Transcutaneous immunization with bacterial ADP-ribosylating exotoxins, subunits, and unrelated adjuvants, Infect Immun, 68 (2000) 5306-5313.
75. G.M. Glenn, C.P. Villar, D.C. Flyer, A.L. Bourgeois, R. McKenzie, R.M. Lavker, S.A. Frech, Safety and immunogenicity of an enterotoxigenic Escherichia coli vaccine patch containing heat-labile toxin: use of skin pretreatment to disrupt the stratum corneum, Infect Immun, 75 (2007) 2163-2170.
76. R. McKenzie, A.L. Bourgeois, S.A. Frech, D.C. Flyer, A. Bloom, K. Kazempour, G.M. Glenn, Transcutaneous immunization with the heat-labile toxin (LT) of enterotoxigenic Escherichia coli (ETEC): protective efficacy in a double-blind, placebo-controlled challenge study, Vaccine, 25 (2007) 3684-3691.
77. G.M. Glenn, D.N. Taylor, X. Li, S. Frankel, A. Montemarano, C.R. Alving, Transcutaneous immunization: a human vaccine delivery strategy using a patch, Nat Med, 6 (2000) 1403-1406.
78. S.A. Frech, H.L. Dupont, A.L. Bourgeois, R. McKenzie, J. Belkind-Gerson, J.F. Figueroa, P.C. Okhuysen, N.H. Guerrero, F.G. Martinez-Sandoval, J.H. Melendez-Romero, Z.D. Jiang, E.J. Asturias, J. Halpern, O.R. Torres, A.S. Hoffman, C.P. Villar, R.N. Kassem, D.C. Flyer, B.H. Andersen, K. Kazempour, S.A. Breisch, G.M. Glenn, Use of a patch containing heat-labile toxin from Escherichia coli against travellers' diarrhoea: a phase II, randomised, double-blind, placebo-controlled field trial, Lancet, 371 (2008) 2019-2025.
79. J. Inoue, Y. Aramaki, Toll-like receptor-9 expression induced by tape-stripping triggers on effective immune response with CpG-oligodeoxynucleotides, Vaccine, 25 (2007) 1007-1013.
80. G.M. Glenn, D.C. Flyer, L.R. Ellingsworth, S.A. Frech, D.M. Frerichs, R.C. Seid, J. Yu, Transcutaneous immunization with heat-labile enterotoxin: development of a needle-free vaccine patch, Expert Rev Vaccines, 6 (2007) 809-819.
81. S.A. Frech, R.T. Kenney, C.A. Spyr, H. Lazar, J.F. Viret, C. Herzog, R. Gluck, G.M. Glenn, Improved immune responses to influenza vaccination in the elderly using an immunostimulant patch, Vaccine, 23 (2005) 946-950.
82. G.R. Matyas, A.M. Friedlander, G.M. Glenn, S. Little, J. Yu, C.R. Alving, Needle-free skin patch vaccination method for anthrax, Infect Immun, 72 (2004) 1181-1183.
83. A. Tezel, S. Paliwal, Z. Shen, S. Mitragotri, Low-frequency ultrasound as a transcutaneous immunization adjuvant, Vaccine, 23 (2005) 3800-3807.
84. A.D. Cristillo, D. Weiss, L. Hudacik, S. Restrepo, L. Galmin, J. Suschak, R. Draghia-Akli, P. Markham,

R. Pal, Persistent antibody and T cell responses induced by HIV-1 DNA vaccine delivered by electroporation, Biochem Biophys Res Commun, 366 (2008) 29-35.

85. L.A. Hirao, L. Wu, A.S. Khan, A. Satishchandran, R. Draghia-Akli, D.B. Weiner, Intradermal/subcutaneous immunization by electroporation improves plasmid vaccine delivery and potency in pigs and rhesus macaques, Vaccine, 26 (2008) 440-448.
86. Y.L. Zhao, S.N. Murthy, M.H. Manjili, L.J. Guan, A. Sen, S.W. Hui, Induction of cytotoxic T-lymphocytes by electroporation-enhanced needle-free skin immunization, Vaccine, 24 (2006) 1282-1290.
87. G. Vandermeulen, L. Daugimont, H. Richiardi, M.L. Vanderhaeghen, N. Lecouturier, B. Ucakar, V. Preat, Effect of tape stripping and adjuvants on immune response after intradermal DNA electroporation, Pharm Res, 26 (2009) 1745-1751.
88. S. Garg, M. Hoelscher, J.A. Belser, C. Wang, L. Jayashankar, Z. Guo, R.H. Durland, J.M. Katz, S. Sambhara, Needle-free skin patch delivery of a vaccine for a potentially pandemic influenza virus provides protection against lethal challenge in mice, Clin Vaccine Immunol, 14 (2007) 926-928.
89. L.K. Roberts, L.J. Barr, D.H. Fuller, C.W. McMahon, P.T. Leese, S. Jones, Clinical safety and efficacy of a powdered Hepatitis B nucleic acid vaccine delivered to the epidermis by a commercial prototype device, Vaccine, 23 (2005) 4867-4878.
90. R.J. Drape, M.D. Macklin, L.J. Barr, S. Jones, J.R. Haynes, H.J. Dean, Epidermal DNA vaccine for influenza is immunogenic in humans, Vaccine, 24 (2006) 4475-4481.
91. Z. Dincer, S. Jones, R. Haworth, Preclinical safety assessment of a DNA vaccine using particle-mediated epidermal delivery in domestic pig, minipig and mouse, Exp Toxicol Pathol, 57 (2006) 351-357.
92. R.D. Cassaday, P.M. Sondel, D.M. King, M.D. Macklin, J. Gan, T.F. Warner, C.L. Zuleger, A.J. Bridges, H.G. Schalch, K.M. Kim, J.A. Hank, D.M. Mahvi, M.R. Albertini, A phase I study of immunization using particle-mediated epidermal delivery of genes for gp100 and GM-CSF into uninvolved skin of melanoma patients, Clin Cancer Res, 13 (2007) 540-549.
93. R.P. Braun, L. Dong, S. Jerome, R. Herber, L.K. Roberts, L.G. Payne, Multi-antigenic DNA immunization using herpes simplex virus type 2 genomic fragments, Hum Vaccin, 4 (2008) 36-43.
94. S. Jones, K. Evans, H. McElwaine-Johnn, M. Sharpe, J. Oxford, R. Lambkin-Williams, T. Mant, A. Nolan, M. Zambon, J. Ellis, J. Beadle, P.T. Loudon, DNA vaccination protects against an influenza challenge in a double-blind randomised placebo-controlled phase 1b clinical trial, Vaccine, 27 (2009) 2506-2512.
95. R. Wang, J. Epstein, F.M. Baraceros, E.J. Gorak, Y. Charoenvit, D.J. Carucci, R.C. Hedstrom, N. Rahardjo, T. Gay, P. Hobart, R. Stout, T.R. Jones, T.L. Richie, S.E. Parker, D.L. Doolan, J. Norman, S.L. Hoffman, Induction of CD4(+) T cell-dependent CD8(+) type 1 responses in humans by a malaria DNA vaccine, Proc Natl Acad Sci U S A, 98 (2001) 10817-10822.
96. J.E. Epstein, E.J. Gorak, Y. Charoenvit, R. Wang, N. Freydberg, O. Osinowo, T.L. Richie, E.L. Stoltz, F. Trespalacios, J. Nerges, J. Ng, V. Fallarme-Majam, E. Abot, L. Goh, S. Parker, S. Kumar, R.C. Hedstrom, J. Norman, R. Stout, S.L.

Hoffman, Safety, tolerability, and lack of antibody responses after administration of a PfCSP DNA malaria vaccine via needle or needle-free jet injection, and comparison of intramuscular and combination intramuscular/intradermal routes, Hum Gene Ther, 13 (2002) 1551-1560.

97. S. Aboud, C. Nilsson, K. Karlen, M. Marovich, B. Wahren, E. Sandstrom, H. Gaines, G. Biberfeld, K. Godoy-Ramirez, Strong HIV-specific $CD4^+$ and $CD8^+$ T-lymphocyte proliferative responses in healthy individuals immunized with an HIV-1 DNA vaccine and boosted with recombinant modified vaccinia virus ankara expressing HIV-1 genes, Clin Vaccine Immunol, 17 (2010) 1124-1131.
98. K. Raviprakash, D. Ewing, M. Simmons, K.R. Porter, T.R. Jones, C.G. Hayes, R. Stout, G.S. Murphy, Needle-free Biojector injection of a dengue virus type 1 DNA vaccine with human immunostimulatory sequences and the GM-CSF gene increases immunogenicity and protection from virus challenge in Aotus monkeys, Virology, 315 (2003) 345-352.
99. A.H. Choi, K. Smiley, M. Basu, M.M. McNeal, M. Shao, J.A. Bean, J.D. Clements, R.R. Stout, R.L. Ward, Protection of mice against rotavirus challenge following intradermal DNA immunization by Biojector needle-free injection, Vaccine, 25 (2007) 3215-3218.
100. J. Canter, K. Mackey, L.S. Good, R.R. Roberto, J. Chin, W.W. Bond, M.J. Alter, J.M. Horan, An outbreak of hepatitis B associated with jet injections in a weight reduction clinic, Arch Intern Med, 150 (1990) 1923-1927.
101. A.J. Mohammed, S. AlAwaidy, S. Bawikar, P.J. Kurup, E. Elamir, M.M. Shaban, S.M. Sharif, H.G. van der Avoort, M.A. Pallansch, P. Malankar, A. Burton, M. Sreevatsava, R.W. Sutter, Fractional doses of inactivated poliovirus vaccine in Oman, N Engl J Med, 362 (2010) 2351-2359.
102. D. Soonawala, P. Verdijk, A.J. Wijmenga-Monsuur, C.J. Boog, P. Koedam, L.G. Visser, N.Y. Rots, Intradermal fractional booster dose of inactivated poliomyelitis vaccine with a jet injector in healthy adults, Vaccine, 31 (2013) 3688-3694.
103. S. Resik, A. Tejeda, P.M. Lago, M. Diaz, A. Carmenates, L. Sarmiento, N. Alemani, B. Galindo, A. Burton, M. Friede, M. Landaverde, R.W. Sutter, Randomized controlled clinical trial of fractional doses of inactivated poliovirus vaccine administered intradermally by needle-free device in Cuba, J Infect Dis, 201 (2010) 1344-1352.
104. S. Resik, A. Tejeda, R.W. Sutter, M. Diaz, L. Sarmiento, N. Alemani, G. Garcia, M. Fonseca, L.H. Hung, A.L. Kahn, A. Burton, J.M. Landaverde, R.B. Aylward, Priming after a fractional dose of inactivated poliovirus vaccine, N Engl J Med, 368 (2013) 416-424.
105. S. Resik, A. Tejeda, O. Mach, M. Fonseca, M. Diaz, N. Alemany, G. Garcia, L.H. Hung, Y. Martinez, R. Sutter, Immune responses after fractional doses of inactivated poliovirus vaccine using newly developed intradermal jet injectors: a randomized controlled trial in Cuba, Vaccine, 33 (2015) 307-313.
106. C.F. Estivariz, H. Jafari, R.W. Sutter, T.J. John, V. Jain, A. Agarwal, H. Verma, M.A. Pallansch, A.P. Singh, S. Guirguis, J. Awale, A. Burton, S. Bahl, A. Chatterjee, R.B. Aylward, Immunogenicity of supplemental doses of poliovirus vaccine for children aged 6-9 months in Moradabad, India:

a community-based, randomised controlled trial, Lancet Infect Dis, 12 (2012) 128-135.

107. M.R. Prausnitz, Microneedles for transdermal drug delivery, Adv Drug Deliv Rev, 56 (2004) 581-587.

108. K. van der Maaden, W. Jiskoot, J. Bouwstra, Microneedle technologies for (trans)dermal drug and vaccine delivery, J Control Release, 161 (2012) 645-655.

109. Y.C. Kim, J.H. Park, M.R. Prausnitz, Microneedles for drug and vaccine delivery, Adv Drug Deliv Rev, 64 (2012) 1547-1568.

2

Determination of depth-dependent intradermal immunogenicity of adjuvanted inactivated polio vaccine delivered by microinjections via hollow microneedles

Pharm. Res., 33 (2016) 2269-2279

Pim Schipper[1], Koen van der Maaden[1], Stefan Romeijn[1], Cees Oomens[2], Gideon Kersten[1,3], Wim Jiskoot[1], Joke Bouwstra[1]

[1] Division of Drug Delivery Technology, Cluster BioTherapeutics, Leiden Academic Centre for Drug Research, Leiden University, Leiden, the Netherlands

[2] Soft Tissue Biomechanics and Engineering, Department of Biomedical Engineering, Eindhoven University of Technology, Eindhoven, the Netherlands

[3] Intravacc (Institute for Translational Vaccinology), Bilthoven, the NetherlandS

ABSTRACT

PURPOSE

The aim of this study was to investigate the depth-dependent intradermal immunogenicity of inactivated polio vaccine (IPV) delivered by depth-controlled microinjections *via* hollow microneedles (HMN) and to investigate antibody response enhancing effects of IPV immunization adjuvanted with CpG oligodeoxynucleotide 1826 (CpG) or cholera toxin (CT).

METHODS

A novel applicator for HMN was designed to permit depth- and volume-controlled microinjections. The applicator was used to immunize rats intradermally with monovalent IPV serotype 1 (IPV1) at injection depths ranging from 50-550 µm, or at 400 µm for CpG and CT adjuvanted immunization, which were compared to intramuscular immunization.

RESULTS

The applicator allowed accurate microinjections into rat skin at predetermined injection depths (50-900 µm), -volumes (1-100 µL) and -rates (up to 60 µL/min) with minimal volume loss (±1-2%). HMN-mediated intradermal immunization resulted in similar IgG and virus-neutralizing antibody titers as conventional intramuscular immunization. No differences in IgG titers were observed as function of injection depth, however IgG titers were significantly increased in the CpG and CT adjuvanted groups (7-fold).

CONCLUSION

Intradermal immunogenicity of IPV1 was not affected by injection depth. CpG and CT were potent adjuvants for both intradermal and intramuscular immunization, allowing effective vaccination upon a minimally-invasive single intradermal microinjection by HMN.

INTRODUCTION

Poliomyelitis can be prevented through vaccination by either oral polio vaccine (OPV) or inactivated polio vaccine (IPV). Although OPV is an inexpensive and easy to administer vaccine, it may cause outbreaks of vaccine-derived polioviruses [1]. Therefore, the World Health Organization aims to eliminate the use of OPV and substitute it by IPV in its goal towards worldwide polio eradication [2]. However, IPV vaccination is more costly because of higher production costs and a higher dose requirement in comparison to OPV. Therefore, several strategies for dose sparing to reduce the cost of IPV vaccination have been proposed, including intradermal immunization and IPV adjuvantation [3].

Although intradermal IPV immunization at reduced doses in human resulted in seroconversion, [4] intradermal injection by the Mantoux technique is difficult to perform. Therefore, there is an urgent need for novel intradermal injection methods. Intradermal IPV immunization *via* jet injectors resulted in seroconversion at reduced doses [5, 6]. Another novel strategy for intradermal injection is microneedles, which are micron-sized needles [7]. Microneedles were investigated on their ability to induce protective immune responses upon intradermal IPV delivery on rats and rhesus macaques [8-12]. Hollow microneedle (HMN) mediated intradermal IPV immunization at reduced doses was also investigated in humans, which resulted in similar seroconversion rates in comparison to a full intramuscular dose [13].

Although intradermal immunization is a promising immunization strategy, it is unknown whether the immunogenicity of intradermally administered IPV is affected as a function of injection depth. This is of interest, as several classes of dendritic cells (DCs) reside in either the epidermis or the dermis. Langerhans cells (LCs) reside in the epidermis (topmost skin layer) and dermal dendritic cells (DDCs) reside in the dermis (lower layer) [14]. Both LCs and DDCs have distinct immune functions and may therefore have a different role in immunization [14]. Therefore, targeting different skin depths may affect the efficiency of intradermal IPV immunization. Hence, the objective of the present study is to investigate intradermal IPV immunization efficiency as function of skin injection depth by using a HMN system. To this end, precise and reproducible injection of IPV into the skin at a predefined depth is a requirement. This requirement can be fulfilled by using our previously developed in-house applicator [8]. However, this applicator only allowed a maximum flow rate of 2 µL/min without leakage in the microinjection system. Therefore, the system was thoroughly redesigned to allow increased pressures, resulting in increased ranges of injection rates, -volumes and -depths without leakages.

Besides establishing the potential effect of intradermal injection depth on the immune response, the use of adjuvants can improve IPV immunization efficiency and therefore may result in IPV dose sparing and thus cost reduction [3, 15]. Although colloidal aluminum hydroxide or aluminum phosphate salts have been used with IPV for intramuscular immunization [16-20], they are not for intradermal use as they cause severe side effects. Therefore, in this study we examined the immune potentiating effects of CpG oligodeoxynucleotide 1826 (CpG) and cholera toxin (CT) as potentially suitable adjuvants for intradermal IPV immunization.

In this study we demonstrate a HMN applicator that allows for injection depth, -rate and -volume controllable minimally-invasive intradermal microinjections. This applicator allowed to investigate the dependence of intradermal immunogenicity to the injection depth of IPV1. To our knowledge this is the first systematic study where the influence of injection depth on antigen-specific immune responses is investigated. Additionally, the potential of adjuvants CpG and CT to enhance intradermal IPV immunization for dose sparing was investigated.

MATERIALS

Polyimide coated fused silica capillary (375 µm outer diameter, 100 and 20 µm inner diameter) was obtained from Polymicro, Phoenix, USA. Silicone oil AK 350 was purchased from Boom Chemicals, Meppel, the Netherlands. CapTite™ connections were obtained from Labsmith, USA. Parafilm M® was purchased from Bemis, Monceau-sur-Sambre, Belgium. Tissue-Tek O.C.T. compound was ordered at Sakura Finetek, Alphen aan den Rijn, the Netherlands. Phosphate buffered saline, pH 7.4 (PBS pH 7.4: 163.9 mM Na^+, 140.3 mM Cl^-, 8.7 mM HPO_4^{2-} and 1.8 mM $H_2PO_4^-$, pH 7.4) was purchased from B. Braun Melsungen, Melsungen, Germany. IsoFlo® (isoflurane 100% w/w) was obtained from Abbott Laboratories, Maidenhead, UK. CpG was purchased from Invivogen, Toulouse, France. Hydrofluoric acid (49% w/w), concentrated sulfuric acid (95-98%), fluorescein, trypan blue, CT (holotoxin) and 3,3'5,5'-tetramethylbenzidine (TMB) were obtained from Sigma-Aldrich, Zwijndrecht, the Netherlands. Polystyrene 96 well microtiter plates and 2.5 mL Vacuette® Z serum separator clot activator premium tubes were ordered at Greiner Bio-One, Alphen aan den Rijn, the Netherlands. Tween 80 and 30% w/w hydrogen peroxide were obtained from Merck, Amsterdam, the Netherlands. PBS pH 7.2 (160.6 mM Na^+, 155.2 mM Cl^-, 2.7 mM HPO_4^{2-}, 1.5 mM $H_2PO_4^-$ and 1.5 mM K^+, pH 7.2) was purchased from Gibco (Life Technologies), Bleiswijk, the Netherlands. Protifar was obtained from Nutricia, Zoetermeer, the Netherlands. Bovine anti-poliovirus type 1 serum, monovalent IPV vaccine serotype 1 (IPV1), 1.1 M sodium acetate and 2M sulfuric acid were kindly provided by Intravacc, Bilthoven, the Netherlands. Horseradish peroxidase-conjugated goat-anti-rat IgG was obtained from Southern Biotech, Birmingham, AL, USA. Female Wistar Han IGS rats (Crl:WI(Han), strain code 273) of 175-225 g were ordered from Charles River Laboratories, Saint-Germain-sur-l'Arbresle, France.

METHODS

Fabrication of HMN

HMN were produced by an in-house process as described previously [8]. In short, the inner lumen of 20 µm inner diameter polyimide coated fused silica capillaries were filled overnight with silicone oil AK 350 by use of a vacuum oven at 100 °C. These silicone oil-filled capillaries were subsequently wet etched into HMN by immersing the ends in a container with hydrofluoric acid (49% w/w) for 4 h. To expose the microneedle tips, the polyimide coating at the etched ends of the capillaries was removed by immersing them in concentrated sulfuric acid (95-98%) at 250 °C for 5 min.

HMN applicator

The HMN applicator that was previously developed in-house [8] was thoroughly redesigned to enable better depth-controlled intradermal microinjections. This HMN applicator is depicted in Fig. 1A and 1B. Optimization was dedicated to improve accuracy, precision and reproducibility of microinjections, to allow for increased injection rates to decrease the injection time, to allow for higher injection volumes and to achieve skin depth-controlled injections. To achieve these improvements, high-pressure resistance in the fluidics system was required. Therefore, flexible materials were replaced by non-flexible rigid materials and all previous connectors in the fluidics system were replaced by high-pressure resistant CapTite™ connectors. For the fluidics system, an 100 µL Hamilton gas-tight Luer-Lock syringe (model 1710 TLL, Hamilton Robotics, Bonaduz, Switzerland) with a barrel inner diameter of 1.46 mm was used in conjunction with a syringe pump (NE-300, Prosense, Oosterhout, the Netherlands) and 100 µm inner diameter polyimide coated fused silica capillaries.

HMN applicator performance validation with *ex vivo* rat skin

Microinjections into *ex vivo* rat skin were performed to determine the range of injection rates, -volumes and –depths that can be used for leakage-free microinjections. *Ex vivo* shaved rat skin was isolated from sacrificed female Wistar Han rats. The skin was stretched on Styrofoam covered with parafilm. Subsequently, microinjections of a solution of 10 µg/mL fluorescein in PBS pH 7.4 were performed at various injection rates, -volumes and -depths. To determine the accuracy and repeatability of the microinjections, volume loss that occurred at i) connections of the fluidics system, ii) on the skin surface at the injection site or iii) due to retained volume on the microneedle after its withdrawal from the injection site was measured by pipetting the lost volume with a 0.2-2 µL pipette. A pipetted volume below 0.2 µL was measured as a volume loss of 0.2 µL. The percentage volume loss was calculated as the percentage of volume loss (as measured by pipetting) from the digitally-displayed dispensed volume (as indicated by the syringe pump).

In the first series of experiments, the injection rate performance was investigated by varying injection rates from 1 – 60 µL/min, while both the injection volume and -depth were kept constant at 10 µL and at 500 µm, respectively. The maximum injection rate of the syringe pump for the 1.46 mm inner diameter 100 µL Hamilton syringe was 62 µL/min. In the second series of experiments, the injection volume was investigated by varying injection volumes from 1 – 100 µL, while both the injection rate and -depth were kept constant at 20 µL/min and at 500 µm, respectively. Finally, injection depths ranging from 50 to 900 µm were investigated by performing 10 µL microinjections at an injection rate of 20 µL/min.

Visualization of depth-controlled microinjections in *ex vivo* rat skin

In order to visualize microinjections at different preselected depths in *ex vivo* rat skin, trypan blue solution (0.4% w/v in PBS pH 7.4) was used. *Ex vivo* rat skin was isolated and prepared as described above. Next, trypan blue solution was injected at 250, 400 and 550 µm depths with an injection volume of 10 µL and at an injection rate of 20 µL/min. The microinjections in *ex vivo* rat skin were photographed on outer and inner skin sides by utilizing a stereo microscope at 2.5x magnification (Zeiss Stemi 2000-c, paired with a Zeiss AxioCam ICc5 camera).

Furthermore, *ex vivo* rat skin injected with 0.5 µL trypan blue solution at the same injection depths and at an injection rate of 1 µL/min was embedded in Tissue-Tek O.C.T. compound and subsequently snap-frozen in liquid nitrogen, from which 10 µm thick cryosections were made on a Leica CM3050s cryostat. Subsequently, unstained and hematoxylin and eosin (H&E) stained images were made to visualize the injection depth of the microinjections. Images were made with a Zeiss 10x plan-Apochromat objective mounted onto a Zeiss Axio Imager D2 microscope coupled with a MRc5 camera.

Investigation of depth-dependent intradermal immunogenicity

Two immunization studies were performed under the guidelines and regulations enforced by the animal ethic committee of the Netherlands, and were approved by the "Dierexperimentencommissie Universiteit Leiden (UDEC)" under number 12084. Female Wistar Han rats with a weight of 175-225 g on arrival were accommodated under standardized conditions in the animal facilities of the Leiden Academic Centre for Drug Research, Leiden University. The animals were housed in groups of five and were assigned to different immunization groups (10 rats per immunization group). Prior to blood withdrawal or immunization, the rats were anaesthetized with isoflurane. Anaesthetized animals that were assigned to the intradermal injection groups were shaved minimally (an area of 4 cm^2 on the left flank) prior to the intradermal injection.

To investigate the depth-dependent intradermal immunogenicity of IPV1, the rats were immunized intradermally *via* HMN mediated microinjections of 10 µL containing 5 DU of IPV1 at an injection rate of 20 µL/min and at injection depths of 250, 400, 550 µm for animal study 1, and 50, 150, 250 µm for animal study 2. As a control in both animal studies, 5 DU of IPV1 in 200 µL PBS pH 7.4 was administered intramuscularly divided over each hind leg (100 µL per hind leg). Furthermore, both animal studies contained a mock treated group *via* the intramuscular route (100 µL PBS pH 7.4 per hind leg). In the first animal study the immunogenicity enhancing effects of adjuvants were investigated: two groups were immunized intradermally *via* HMN mediated microinjections of 10 µL

(injection rate 20 µL/min and injection depth 400 µm) and two groups were immunized intramuscularly (100 µL per hind leg) with 5 DU IPV1 adjuvanted with either CpG or CT. These previously described immunization procedures were performed at day 1 (prime immunization) and were repeated at day 21 (booster immunization). Collection of blood samples were performed at day 1, day 21 (prime) and day 42 (boost). Blood samples were collected in 2.5 mL Vacuette® tubes and stored on ice before centrifugation at 2000g for 10 min to isolate serum.

Serum IgG titers

To measure serum IgG titers, a capture ELISA was performed. Bovine anti-poliovirus type 1 serum in PBS pH 7.2 was used to coat polystyrene 96 well microtiter plates overnight at 4 °C. Subsequently, washing was performed with 0.05% Tween 80 in tap water. Afterwards, assay buffer consisting of PBS pH 7.2, 0.5% (w/v) Protifar and 0.05% (v/v) Tween 80 was used to add 4.5 DU IPV1/well (100 µL/well). Plates were incubated at 37 °C for 2 h before a wash step was performed. Afterwards, threefold serial dilutions of serum samples in assay buffer were added at 100 µL/well and subsequently incubated at 37 °C for 2 h. Plates were washed before horseradish peroxidase-conjugated goat-anti-rat IgG was added to the wells (4000-fold dilution, 100 µL/well) and subsequently incubated at 37 °C for 1 h. Subsequently, plates were thoroughly washed before adding TMB substrate solution (100 µL/well) which consisted of 1.1 M sodium acetate, 100 mg/mL TMB and 0.006% (v/v) hydrogen peroxide. 2 M sulfuric acid was used after 10 min to stop the reaction (100 µL/well). Finally, sample absorbance was measured at 450 nm by a Biotek ELx808 plate reader (Winooski, VT, USA).

The Biotek Gen5 2.0 data analysis software was used to determine endpoint titers by 4-parameter analysis. The endpoint titer was defined as the reciprocal of the serum dilution producing a 450 nm absorbance equal to that of the mean 450 nm absorbance with addition of three times the standard deviation of eight samples of IPV1-specific-antibody negative serum samples.

Virus-neutralizing antibodies

Determination of the antibody titers able to neutralize wildtype poliovirus serotype 1 was outsourced to Bilthoven Biologicals and performed as previously described [21, 22]. In short, average virus-neutralizing (VN) antibody titers were measured after pooling of the serum samples of all rats per immunization group. Subsequently, two-fold serial dilutions of the pooled sera were made (2^{11}–2^{22}) after inactivation of sera at 56 °C for 30 min prior to testing. 100$TCID_{50}$ of the Mahoney wild-type strain (poliovirus type 1) was added to the resulting serum dilutions and these virus/serum mixtures were incubated

for 3 h at 36 °C and 5% CO_2 before incubation at 4 °C overnight. Subsequently, to each sample $1x10^4$ Vero cells were added and the resulting mixtures were incubated for 7 days at 36 °C and 5% CO_2. Finally, samples were fixed with formalin, stained with crystal violet and were analyzed macroscopically. VN titers were displayed as the last serum dilution which did not exhibit cytopathogenic effects.

Statistical analysis

Statistics were performed using GraphPad Prism (v.6.00, GraphPad Software, LaJolla, CA, USA). Kruskall-Wallis tests with Dunn's post-hoc tests were performed as IgG titers were non-normally distributed and considered significant at $p < 0.05$.

RESULTS

HMN applicator optimization and performance

To allow for increased injection rates and thereby short injection times, connections in the fluidics system of the HMN applicator were optimized by applying high-pressure resistant CapTite™ connectors and high-pressure resistant polyimide fused silica capillaries, as shown in Fig. 1A and 1B. Furthermore, the dead volume in the fluidics system was kept to a minimum to maximize injection volume accuracy and minimize the loss of vaccine formulation. The hydrofluoric acid etching procedure of polyimide coated fused silica capillaries resulted in sharp HMN (Fig. 1C).

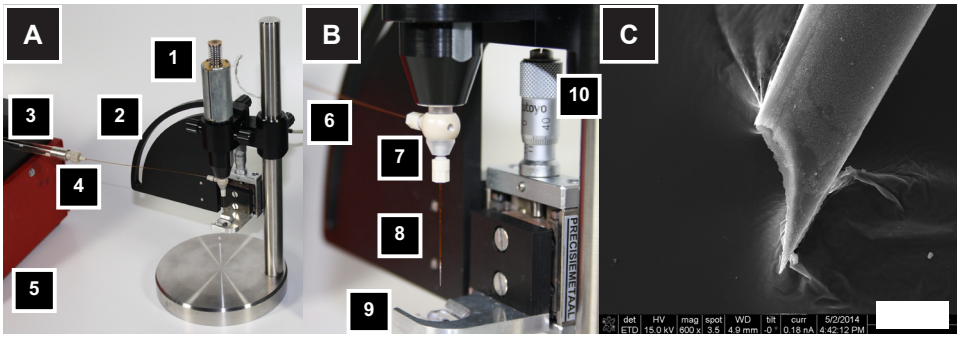

Fig. 1 Images of the HMN applicator (**A** and **B**) and a scanning electron microscopy image of a HMN (**C**, bar represents 50 µm). The microneedle insertion speed (1 to 3 m/s) is controlled by an electromagnet (1). Angled injections are possible *via* a guided rail (2). The injection depth of the microneedle into the skin is accurately controlled by a micrometer actuator (10) and a guide plate (9). Fluid flow starts with a 100 µL Hamilton gas-tight Luer-Lock syringe (3) which is driven by a controllable syringe pump (5) that is connected to a 100 µm inner diameter capillary (6) *via* a Luer-Lock-CapTite adapter (4). This capillary feeds the fluid flow *via* a specially designed connection piece (7) into a HMN (8) that enables the intradermal injections. Because the syringe pump is programmable, injection rates and -volumes can be accurately controlled.

The performance of the fluidics system was examined by varying the injection rate during intradermal microinjections into *ex vivo* rat skin, mimicking back pressure during actual microinjections on live animals. As shown in Fig. 2A, the volume loss was ±1-2% for all investigated injection rates at an injection volume and -depth of 10 µL and 500 µm, respectively. Volume loss was only observed at the skin surface of the microinjection sites or on the HMN after retracting the microneedle from the skin. No additional volume loss was observed. Owing to the achieved increase in injection rate, a significant

reduction in injection time was achieved.

As shown in Fig. 2B, volumes up to 100 µL could be injected into *ex vivo* rat skin with volume loss that was ±1-2%, independent of injection volume, at an injection depth and -rate of 500 µm and 20 µL/min, respectively. This volume loss was observed on the skin surface at the microinjection sites.

Finally, variation in injection depth was studied by injecting 10 µL in *ex vivo* rat skin at different injection depths. As shown in Fig. 2C, microinjections were performed between 50 to 900 µm injection depths. At all investigated injection depths, all microinjections resulted in ±1-2% volume loss. Moreover, there was no increase in volume loss at any particular injection depth.

Visualization of depth-controlled microinjections in *ex vivo* rat skin

To obtain evidence that skin layers at different preselected depths were targeted, microinjections of a trypan blue solution were performed on *ex vivo* rat skin, which was then photographed at both sides (Fig. 3A). Whereas the trypan blue spot of the shallower microinjection at a skin injection depth of 250 µm was more clearly visible at the outer side of the skin, the trypan blue spot of the deeper injection at 550 µm was hardly visible. Contrarily, the trypan blue spot of the deeper microinjection at a skin injection depth of 550 µm was more clearly visible at the inner side of the skin than the trypan blue spot of the shallower injection (250 µm). Moreover, as shown in Fig. 3B, visualization of the skin injection depth in cross-sectioned skin indicated that the microinjections were indeed performed at different pre-defined skin injection depths.

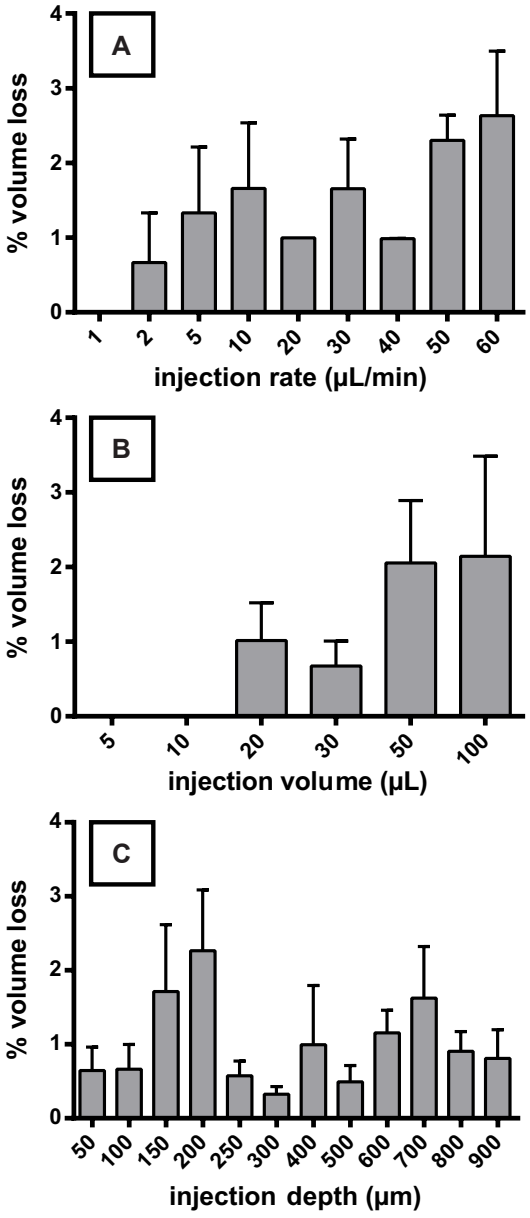

Fig. 2 Accuracy of the HMN applicator, expressed as percent volume loss, as function of (**A**) injection rate (1-60 µL/min (pump-syringe combination maximum)) at constant injection depth (500 µm) and volume (10 µL); (**B**) injection volume (5-100 µL) at constant injection depth (500 µm) and rate (20 µL/min); and (**C**) injection depth (50-900 µm) at constant injection volume (10 µL) and rate (20 µL/min). Bars represent mean ± SEM (n = 6).

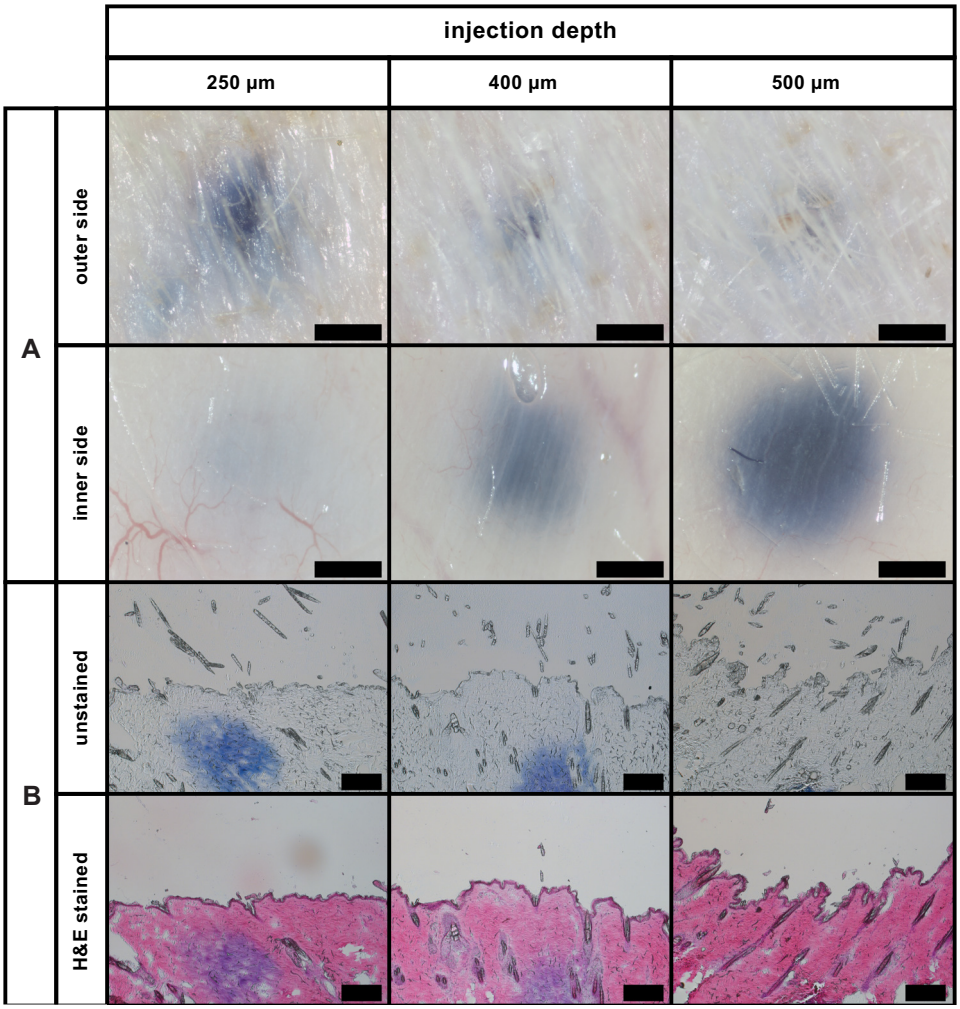

Fig. 3 Visualization of depth-controlled microinjections of trypan blue solution by HMN into rat skin at 10 µL and 20 µL/min (**A**), visualized by light microscopy at 4x magnification; bars represent 500 µm. Visualization of cross-sections of cryofixed rat skin after depth-controlled microinjections of trypan blue solution into rat skin at 0.5 µL at 10 µL/min were performed (**B**), visualized either before or after H&E staining by bright-field microscopy at 10x magnification; bars represent 200 µm.

Injection depth-dependent intradermal immunogenicity

To assess whether injection of IPV1 at different injection depths in the skin affects IPV1-specific antibody responses, two immunization studies in rats were conducted. Intradermal immunization was performed using the HMN applicator in a depth-controlled manner and this was compared to intramuscular immunization with a conventional 26G

hypodermic needle. IPV1-specific IgG titers obtained after intradermal immunization with non-adjuvanted IPV1 at injection depths ranging between 50 and 550 µm are shown in Fig. 4. Three weeks after prime immunization (Fig. 4A) and boost immunization (Fig. 4B), no significant differences in IPV1-specific IgG titers were observed at different injection depths. Moreover, IPV1-specific IgG titers obtained after intradermal immunization were similar to those obtained after intramuscular IPV1 immunization. No IPV1-specific antibody responses were observed in the mock treated group.

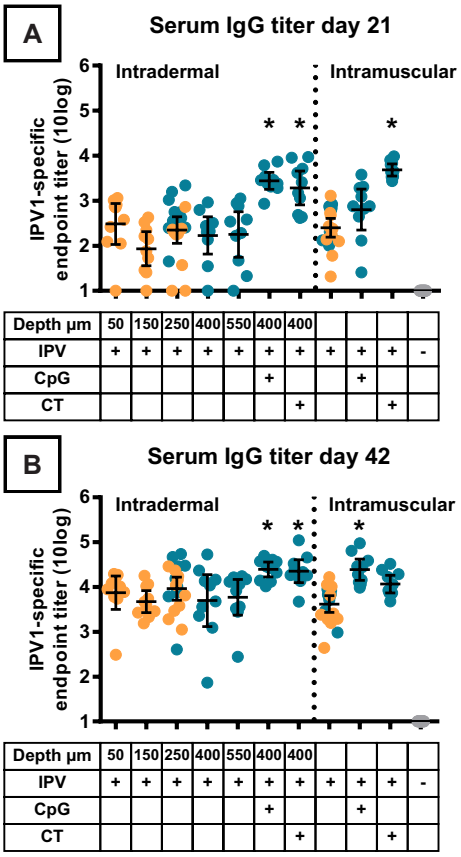

Fig. 4 IPV1-specific IgG antibody responses measured in serum obtained in study 1 or 2, after prime immunization (**A**, day 21) or boost immunization (**B**, day 42) with PBS pH 7.4, 5 DU IPV1 or 5 DU IPV1 adjuvanted with either CpG or CT. Formulations were injected intradermally *via* HMN at the indicated injection depths or intramuscularly *via* conventional 26G needles. Aqua or orange rounds represent animals from study 1 or 2, respectively. Bars represent mean ± 95% confidence interval (n = 10) and stars represent a significant increase ($p < 0.05$).

Immunogenicity enhancing effects of adjuvants CpG and CT

To assess the potential increase in antibody responses and the applicability for use as intradermal adjuvants, CpG and CT were used as adjuvants in intradermal and intramuscular IPV immunization (Fig. 4A and 4B). Intradermal IPV1 immunization adjuvanted with CpG led to statistically significant increased IgG titers in comparison to non-adjuvanted 400 and 550 µm injection depths and intramuscular IPV1 group after prime immunization. Contrarily, intramuscular IPV1 immunization adjuvanted with CpG did not result in any significant increase in IgG titer after prime immunization. After boost immunization however, IPV1 immunization adjuvanted with CpG *via* both the intradermal and intramuscular route resulted in significantly increased IgG titers in comparison to the non-adjuvanted intramuscular IPV1 group.

Intradermal IPV1 immunization adjuvanted with CT led to statistically significant increased IgG titers after prime immunization (non-adjuvanted 400 µm injection depth) and booster immunization (non-adjuvanted intramuscular control group). Intramuscular IPV1 immunization adjuvanted with CT resulted in statistically significant increased IgG titers in comparison to all non-adjuvanted groups (250, 400 and 550 µm injection depths and intramuscular IPV1 group) after prime immunization. However, after boost immunization there were no significant differences for intramuscular IPV1 immunization adjuvanted with CT.

Furthermore, there were no statistically significant differences in IgG titers between CpG or CT adjuvanted groups, neither for the intradermal or the intramuscular immunization routes and neither after prime or boost immunization. However, some differences were observed between CpG and CT, when they were compared against non-adjuvanted groups. After prime intradermal immunization, CpG and CT adjuvanted IPV1 immunization resulted in 6.9 and 7.3 fold increased IgG titers on average, respectively, in comparison to the non-adjuvanted intradermal IPV1 groups. After prime intramuscular immunization, CpG and CT adjuvanted IPV1 immunization resulted in 2.7 and 12.1 fold increased IgG titers, respectively, in comparison to the non-adjuvanted intramuscular IPV1 group. Thus in prime immunization, CpG enhanced IgG titers more in intradermal immunization in comparison to intramuscular immunization, whereas CT enhanced IgG titers in both immunization routes. After the booster intradermal immunization, CpG and CT adjuvanted IPV1 immunization resulted in 1.9 and 2.2 fold increased IgG titers on average, respectively, in comparison to the non-adjuvanted intradermal IPV1 groups. After the booster intramuscular immunization, CpG and CT adjuvanted IPV1 immunization resulted in 5.5 and 2.4 fold increased IgG titers, respectively, in comparison to the non-adjuvanted intramuscular IPV1 group. Thus, the IgG titer enhancing effect was more

pronounced in prime immunization than in booster immunization. Intramuscular IPV1 immunization adjuvanted with CpG resulted in the strongest increase in IgG titers in booster immunization.

Besides increasing IgG titers, intradermal IPV1 immunization adjuvanted with CpG and both intradermal and intramuscular IPV1 immunization adjuvanted with CT, resulted in less low-responders in comparison to the non-adjuvanted groups after prime immunization. Moreover, these adjuvanted groups resulted in IPV1-specific IgG titers after a single immunization that were comparable to the ones obtained after two non-adjuvanted immunizations.

Virus-neutralizing antibodies

In addition to the determination of the IPV1-specific IgG antibody responses by ELISA, protectivity of these antibodies against wildtype poliovirus was measured in a wildtype poliovirus-neutralizing antibody assay. VN antibody titers were observed in all IPV1 immunization groups (Table 1). No VN antibody titer was observed in the mock treated group. Although the VN titers were measured on pooled serum samples, some slight differences in mean VN titer per immunization group were observed. For example, for the 400 µm injection depth, a VN titer of 13 was observed, which was higher than those of the other injection depths and the intramuscular IPV1 immunization. Moreover, this VN titer was similar to the VN titers of intradermal and intramuscular IPV1 immunization adjuvanted with CpG, however lower than the VN titer of intradermal IPV1 immunization adjuvanted with CT, which had the highest VN titer. VN titers of non-adjuvanted intradermal and intramuscular IPV1 immunization were similar. Intramuscular IPV1 immunization adjuvanted with CT resulted in a similar VN titer as non-adjuvanted intradermal and intramuscular immunization and was lower in comparison to intradermal IPV1 immunization adjuvanted with CT. Thus, CpG enhanced VN antibody titers in both intradermal and intramuscular IPV1 immunization, whereas CT only in intradermal IPV1 immunization.

Table 1 Virus neutralizing (VN) antibody titers measured in serum obtained in study 1 and 2 after prime and boost immunization (day 42) with PBS pH 7.4, 5 DU IPV1 or 5 DU IPV1 adjuvanted with either CpG or CT. Formulations were injected intradermally *via* HMN at indicated injection depths or intramuscularly *via* conventional 26G needles. Presented data represents VN titers which were measured on pooled serum samples of all rats per immunization group.

VN antibody titers (log_2)											
	Intradermal							**Intramuscular**			
Depth (µm)	50	150	250	400	550	400	400				
IPV1	+	+	+	+	+	+	+	+	+	+	-
CpG						+			+		
CT							+			+	
VN titer study 1			11	13	11	13	14	12	13	11	0
VN titer study 2	11	12	12					11			0

Both during and immediately after intradermal immunization with HMN, a small bleb was observed on the skin. This bleb disappeared within 5 min after injection. No erythema was observed during and after intradermal injections with HMN, with one exception. Mild erythema was observed after intradermal injection of IPV1 with CT. This effect was only observed after the prime immunization and started 60 min post injection and lasted up to 7 days. Other adverse effects were not observed.

DISCUSSION

The relationship between injection depth and intradermal immunization has not been studied before, because this requires accurate, precise and reproducible depth-controlled intradermal injections with small injection volumes. For these reasons, an HMN applicator was thoroughly redesigned and improved in this study. This improved HMN applicator allowed for accurately controllable injection rates, -volumes and -depths, which allowed to investigate the depth-dependent intradermal immunogenicity of IPV1, in an effort for IPV1 dose sparing.

Skin resistance during injection might significantly inhibit injection rate and accuracy [23]. However, the redesigned applicator allowed for a 30-fold increased injection rate (60 µL/min) compared to previously achieved rates (2 µL/min) [8]. Increased injection rates were needed to increase injection accuracy and shorten injection duration. Achieved injection rates were higher than those reported in literature for rat skin with a single HMN (0.17 µL/min/HMN, 1 µL/min/HMN after needle retraction, [24]) or with HMN arrays (0.001 µL/min/HMN, [25]) and for human skin with a single HMN (0.25-1.6 µL/min/HMN), which required hyaluronidase and needle retraction to increase rates to 18.83 µL/min/HMN [23]. In contrast, by using the improved applicator, no additional methods were required to achieve even higher injection rates. Therefore, the utilization of non-flexible materials allowed increased pressure during injection, which allowed to easily overcome skin resistance and to achieve increased injection rates.

In addition, injection volumes achieved with this improved applicator were increased 11-fold in comparison to those previously achieved in rat skin (9 µL/HMN) [8]. These volumes were also much higher as those reported for single HMN in human skin (20 µL/HMN) [23] or HMN arrays in mice skin (0.22 µL/HMN) [26]. Additionally, achieved volumes were comparable to HMN arrays in porcine skin (83.33 µL/HMN) [27]. Furthermore, a single hollow needle design reduces the risk of volume loss (dose loss) compared to HMN arrays, as in arrays all needles need to be penetrated and unclogged to ensure an accurate injection and prevent leakage [28, 29].

The improved applicator allowed for an increased injection depth range (50-900 µm) compared to the previously reported range (100-400 µm) [8]. This injection depth range was larger than the previously reported depth range in hairless rat skin (150-770µm, [24]) and smaller than the previously reported depth range in human skin (180-1080 µm, [23]). However, these studies do not report the influence of injection depth on antigen-specific immune responses.

In contrast to our hypothesis, there was no injection depth-dependent intradermal immunogenicity observed for IPV1. However, the limited thickness (20-30 μm) of rat epidermis prevented injection into the epidermis where LCs reside [30]. The attempt to inject IPV1 as close to the epidermis as possible did not result in a significant change in IPV1-specific IgG titers. It is not known whether the distribution of the injected volume in the skin influences the targeting of intradermal injection depths. Furthermore, it is unclear whether local changes in innate immunity can be expected, as antigen-bearing DCs will migrate to lymph nodes, where lymph node-residing DCs may influence any immunological effect [14, 30]. This behavior, chemotaxis and chemoattraction of other DCs and the complex interplay between different DC classes, may explain the absence of differences in immune response as function of the injection depth. Contrarily to rat skin though, in human skin the epidermis has a thickness of 50-100 μm [30]. As the redesigned applicator is able to inject at a depth of 50 μm, injection directly into the human epidermis is possible. This allows to study LC function in intradermal immunity in the future. In conclusion, our applicator could provide a method to investigate depth-dependent intradermal vaccine immunogenicity in human.

Furthermore, results presented in this study are important in microneedle patch design for intradermal IPV immunization as the independence of IPV1 immunization on skin depth suggests that microneedle length will not affect the immune response and thus precise dosing at a certain skin depth is not required. This may put a smaller burden on the design specifications of microneedle applicators.

Besides, an effort was made to find a dose sparing strategy for IPV immunization. However, intradermal and intramuscular immunization without use of adjuvants led to similar results, likewise as reported for other microneedle strategies: HMN in rats [8, 11] or humans [13], coated microneedles in rats, [9] dissolving microneedles in rats [10] or rhesus macaques [12]. Furthermore, clinical trials in humans have been performed to investigate IPV dose sparing, by comparison of a 80% reduced IPV dose (20% of full dose) administered intradermally against a full IPV dose administered intramuscularly. For polio prime immunization in newborn infants, intradermal 20% IPV dose resulted in similar [4, 5] or inferior [31-33] seroconversion rates compared to a full intramuscular dose. Similarly, for polio booster immunization, intradermal 20% IPV dose resulted in either similar [6, 13] or inferior [34, 35] seroconversion rates in comparison to full intramuscular dose. However, intradermal immunization generally resulted in significantly lowered antibody titers [5, 6, 31-35]. These findings were seemingly not dependent on the intradermal immunization method used, because jet injectors [5, 6, 31, 32, 34, 35], the Mantoux technique [4, 35] or HMN arrays [13, 33] evenly resulted in either similar or inferior results to full intramuscular dose.

In this study, it is shown that the depth at which the antigen was administered by these different intradermal immunization techniques cannot explain this phenomenon either. However, the 80% dose-reduction goal may be unrealistic, as a 60% dose-reduction was achieved by HMN mediated intradermal immunization without use of adjuvants [11, 13].

Adjuvants may be used as another strategy for IPV dose sparing [3]. For example, aluminum hydroxide [16, 17] and aluminum phosphate [18, 19] have been successfully used as an adjuvant for intramuscular IPV immunization. Because aluminum salts cannot be administered intradermally due to local adverse effects, adjuvants CpG and CT were assessed for intradermal IPV1 immunization. Both CpG and CT have shown to be safe as adjuvant in intradermal immunization in humans [36, 37]. In the present study, immune-enhancing effects on IPV1-specific IgG responses by the adjuvants CpG and CT were significant, which indicates that CpG and CT might be potential adjuvant candidates for intradermal IPV1 immunization and may lead to dose sparing. Indeed, CpG was reported by others to be an effective immune enhancing adjuvant for IPV immunization [38]. Although this latter study utilized mice and a different CpG motif (ODN2006), both studies report on the potential for CpG as adjuvant in IPV immunization. Furthermore, we have reported a 6.9- and 7.3-fold increase in IPV1-specific IgG serum titers for intradermally IPV co-administered with CpG and CT, respectively. This increase was larger as reported for intradermal IPV immunization in mice in combination with CpG-ODN2006 (4-fold) or double mutant heat-labile enterotoxin from E. coli LT (R192G/L211A) (2.5-fold) [38, 39]. Contrarily, a 10-fold increase was achieved by CAF01 liposomal IPV formulation for intradermal IPV immunization in mice [40].

CONCLUSION

In this study, an unique dose sparing strategy for IPV1 was investigated by intradermal microinjections of small volumes of IPV1 formulation at different pre-determined depths in rat skin *in vivo*. To enable this, a HMN applicator controllable in injection rate, -volume and –depth was developed that allowed for intradermal microinjections. Results indicated however, that intradermal immunogenicity was not dependent on the injection depth. Nonetheless, IPV1 immunization by minimally-invasive intradermal microinjections resulted in similar IPV1-specific antibody responses in comparison to IPV1 immunization by more invasive and painful intramuscular injections. Moreover, intradermal IPV1 immunization antibody responses were significantly increased (7-fold) by adjuvants CpG and CT, such that a single minimally-invasive intradermal immunization by HMN resulted in comparable antibody responses to two intramuscular immunizations.

ACKNOWLEDGEMENTS

The authors thank Heleen Kraan for contributions to analysis of IPV-specific IgG and VN responses, Raphael Zwier for contributions to the applicator design and Anne Römgens for contributions to discussions related to this study.

REFERENCES

1. O.M. Kew, R.W. Sutter, E.M. de Gourville, W.R. Dowdle, M.A. Pallansch, Vaccine-derived polioviruses and the endgame strategy for global polio eradication, Annu Rev Microbiol, 59 (2005) 587-635.
2. W. World Health Organization, Polio eradication and endgame strategic plan 2013 - 2018, World Health Organization (WHO), Geneva, Switserland, 2013.
3. H. Okayasu, R.W. Sutter, H.S. Jafari, M. Takane, R.B. Aylward, Affordable inactivated poliovirus vaccine: strategies and progress, J Infect Dis, 210 Suppl 1 (2014) S459-464.
4. J. Cadorna-Carlos, E. Vidor, M.C. Bonnet, Randomized controlled study of fractional doses of inactivated poliovirus vaccine administered intradermally with a needle in the Philippines, Int J Infect Dis, 16 (2012) e110-116.
5. A.J. Mohammed, S. AlAwaidy, S. Bawikar, P.J. Kurup, E. Elamir, M.M. Shaban, S.M. Sharif, H.G. van der Avoort, M.A. Pallansch, P. Malankar, A. Burton, M. Sreevatsava, R.W. Sutter, Fractional doses of inactivated poliovirus vaccine in Oman, N Engl J Med, 362 (2010) 2351-2359.
6. D. Soonawala, P. Verdijk, A.J. Wijmenga-Monsuur, C.J. Boog, P. Koedam, L.G. Visser, N.Y. Rots, Intradermal fractional booster dose of inactivated poliomyelitis vaccine with a jet injector in healthy adults, Vaccine, 31 (2013) 3688-3694.
7. K. van der Maaden, W. Jiskoot, J. Bouwstra, Microneedle technologies for (trans)dermal drug and vaccine delivery, J Control Release, 161 (2012) 645-655.
8. K. van der Maaden, S.J. Trietsch, H. Kraan, E.M. Varypataki, S. Romeijn, R. Zwier, H.J. van der Linden, G. Kersten, T. Hankemeier, W. Jiskoot, J. Bouwstra, Novel hollow microneedle technology for depth-controlled microinjection-mediated dermal vaccination: a study with polio vaccine in rats, Pharm Res, 31 (2014) 1846-1854.
9. K. van der Maaden, E. Sekerdag, P. Schipper, G. Kersten, W. Jiskoot, J.A. Bouwstra, Layer-by-layer assembly of inactivated poliovirus and N-trimethyl chitosan on pH-sensitive microneedles for dermal vaccination, Langmuir, (2015).
10. H. Kraan, I. Ploemen, G. van de Wijdeven, I. Que, C. Lowik, G. Kersten, J.P. Amorij, Alternative delivery of a thermostable inactivated polio vaccine, Vaccine, 33 (2015) 2030-2037.
11. D. Kouiavskaia, O. Mirochnitchenko, E. Dragunsky, E. Kochba, Y. Levin, S. Troy, K. Chumakov, Intradermal inactivated poliovirus vaccine: a preclinical dose-finding study, J Infect Dis, 211 (2015) 1447-1450.
12. C. Edens, N.C. Dybdahl-Sissoko, W.C. Weldon, M.S. Oberste, M.R. Prausnitz, Inactivated polio vaccination using a microneedle patch is immunogenic in the rhesus macaque, Vaccine, (2015).
13. S.B. Troy, D. Kouiavskaia, J. Siik, E. Kochba, H. Beydoun, O. Mirochnitchenko, Y. Levin, N. Khardori, K. Chumakov, Y. Maldonado, Comparison of the Immunogenicity of Various Booster Doses of Inactivated Polio Vaccine Delivered Intradermally Versus Intramuscularly to HIV-Infected Adults, J Infect Dis, 211 (2015) 1969-1976.
14. B. Combadiere, C. Liard, Transcutaneous and intradermal vaccination, Hum Vaccin, 7 (2011) 811-827.

15. J. Hawken, S.B. Troy, Adjuvants and inactivated polio vaccine: a systematic review, Vaccine, 30 (2012) 6971-6979.
16. W. Auerswald, O. Juergenssen, [On the problem of antibody formation against poliomyelitis in small children. Studies on the effect of an adjuvant vaccine with antigen components against poliomyelitis, diphtheria, pertussis and tetanus], Wien Med Wochenschr, 110 (1960) 646-648.
17. R.C. Li, F.X. Li, Y.P. Li, Q.M. Hou, C.G. Li, Y.N. Li, F.S. Chen, X.Z. Hu, W.B. Su, S.M. Zhang, H.H. Fang, Q. Ye, T.D. Zeng, T.X. Liu, X.B. Li, Y.N. Huang, M.L. Deng, Y.P. Zhang, E. Ortiz, Immunogenicity and safety of a pentavalent acellular pertussis combined vaccine including diphtheria, tetanus, inactivated poliovirus and conjugated Haemophilus Influenzae type b polysaccharide for primary vaccination at 2, 3, 4 or 3, 4, 5 months of age in infants in China, Vaccine, 29 (2011) 1913-1920.
18. S.H. Yeh, J.I. Ward, S. Partridge, S.M. Marcy, H. Lee, J. Jing, E.S. Curry, B.J. Howe, Safety and immunogenicity of a pentavalent diphtheria, tetanus, pertussis, hepatitis B and polio combination vaccine in infants, Pediatr Infect Dis J, 20 (2001) 973-980.
19. F.A. Guerra, M.M. Blatter, D.P. Greenberg, M. Pichichero, F.R. Noriega, G. Pentacel Study, Safety and immunogenicity of a pentavalent vaccine compared with separate administration of licensed equivalent vaccines in US infants and toddlers and persistence of antibodies before a preschool booster dose: a randomized, clinical trial, Pediatrics, 123 (2009) 301-312.
20. R.K. Gupta, Aluminum compounds as vaccine adjuvants, Adv Drug Deliv Rev, 32 (1998) 155-172.
21. P. Albrecht, G. van Steenis, A.L. van Wezel, J. Salk, Standardization of poliovirus neutralizing antibody tests, Rev Infect Dis, 6 Suppl 2 (1984) S540-544.
22. J. Westdijk, P. Koedam, M. Barro, B.P. Steil, N. Collin, T.S. Vedvick, W.A. Bakker, P. van der Ley, G. Kersten, Antigen sparing with adjuvanted inactivated polio vaccine based on Sabin strains, Vaccine, 31 (2013) 1298-1304.
23. W. Martanto, J.S. Moore, O. Kashlan, R. Kamath, P.M. Wang, J.M. O'Neal, M.R. Prausnitz, Microinfusion using hollow microneedles, Pharm Res, 23 (2006) 104-113.
24. P.M. Wang, M. Cornwell, J. Hill, M.R. Prausnitz, Precise microinjection into skin using hollow microneedles, J Invest Dermatol, 126 (2006) 1080-1087.
25. N. Roxhed, B. Samel, L. Nordquist, P. Griss, G. Stemme, Painless drug delivery through microneedle-based transdermal patches featuring active infusion, IEEE Trans Biomed Eng, 55 (2008) 1063-1071.
26. U.O. Hafeli, A. Mokhtari, D. Liepmann, B. Stoeber, In vivo evaluation of a microneedle-based miniature syringe for intradermal drug delivery, Biomed Microdevices, 11 (2009) 943-950.
27. S.A. Burton, C.Y. Ng, R. Simmers, C. Moeckly, D. Brandwein, T. Gilbert, N. Johnson, K. Brown, T. Alston, G. Prochnow, K. Siebenaler, K. Hansen, Rapid intradermal delivery of liquid formulations using a hollow microstructured array, Pharm Res, 28 (2011) 31-40.
28. Y.C. Kim, J.H. Park, M.R. Prausnitz, Microneedles for drug and vaccine delivery, Adv Drug Deliv

Rev, 64 (2012) 1547-1568.

29. N. Roxhed, P. Griss, G. Stemme, Membrane-sealed hollow microneedles and related administration schemes for transdermal drug delivery, Biomed Microdevices, 10 (2008) 271-279.
30. H.J. Hirschberg, E. van Riet, D. Oosterhoff, J.A. Bouwstra, G.F. Kersten, Animal models for cutaneous vaccine delivery, Eur J Pharm Sci, 71 (2015) 112-122.
31. S. Resik, A. Tejeda, P.M. Lago, M. Diaz, A. Carmenates, L. Sarmiento, N. Alemani, B. Galindo, A. Burton, M. Friede, M. Landaverde, R.W. Sutter, Randomized controlled clinical trial of fractional doses of inactivated poliovirus vaccine administered intradermally by needle-free device in Cuba, J Infect Dis, 201 (2010) 1344-1352.
32. S. Resik, A. Tejeda, R.W. Sutter, M. Diaz, L. Sarmiento, N. Alemani, G. Garcia, M. Fonseca, L.H. Hung, A.L. Kahn, A. Burton, J.M. Landaverde, R.B. Aylward, Priming after a fractional dose of inactivated poliovirus vaccine, N Engl J Med, 368 (2013) 416-424.
33. A. Anand, K. Zaman, C.F. Estivariz, M. Yunus, H.E. Gary, W.C. Weldon, T.I. Bari, M. Steven Oberste, S.G. Wassilak, S.P. Luby, J.D. Heffelfinger, M.A. Pallansch, Early priming with inactivated poliovirus vaccine (IPV) and intradermal fractional dose IPV administered by a microneedle device: A randomized controlled trial, Vaccine, 33 (2015) 6816-6822.
34. C.F. Estivariz, H. Jafari, R.W. Sutter, T.J. John, V. Jain, A. Agarwal, H. Verma, M.A. Pallansch, A.P. Singh, S. Guirguis, J. Awale, A. Burton, S. Bahl, A. Chatterjee, R.B. Aylward, Immunogenicity of supplemental doses of poliovirus vaccine for children aged 6-9 months in Moradabad, India: a community-based, randomised controlled trial, Lancet Infect Dis, 12 (2012) 128-135.
35. S. Resik, A. Tejeda, O. Mach, M. Fonseca, M. Diaz, N. Alemany, G. Garcia, L.H. Hung, Y. Martinez, R. Sutter, Immune responses after fractional doses of inactivated poliovirus vaccine using newly developed intradermal jet injectors: a randomized controlled trial in Cuba, Vaccine, 33 (2015) 307-313.
36. J. Scheiermann, D.M. Klinman, Clinical evaluation of CpG oligonucleotides as adjuvants for vaccines targeting infectious diseases and cancer, Vaccine, 32 (2014) 6377-6389.
37. E.H. Eypper, P.V. Johnson, E.I. Purro, E.L. Hohmann, Transcutaneous immunization of healthy volunteers with an attenuated Listeria monocytogenes vaccine strain and cholera toxin adjuvant, Vaccine, 31 (2013) 3257-3261.
38. C. Yang, H. Shi, J. Zhou, Y. Liang, H. Xu, CpG oligodeoxynucleotides are a potent adjuvant for an inactivated polio vaccine produced from Sabin strains of poliovirus, Vaccine, 27 (2009) 6558-6563.
39. E.B. Norton, D.L. Bauer, W.C. Weldon, M.S. Oberste, L.B. Lawson, J.D. Clements, The novel adjuvant dmLT promotes dose sparing, mucosal immunity and longevity of antibody responses to the inactivated polio vaccine in a murine model, Vaccine, 33 (2015) 1909-1915.
40. J. Dietrich, L.V. Andreasen, P. Andersen, E.M. Agger, Inducing dose sparing with inactivated polio virus formulated in adjuvant CAF01, PLoS One, 9 (2014) e100879.

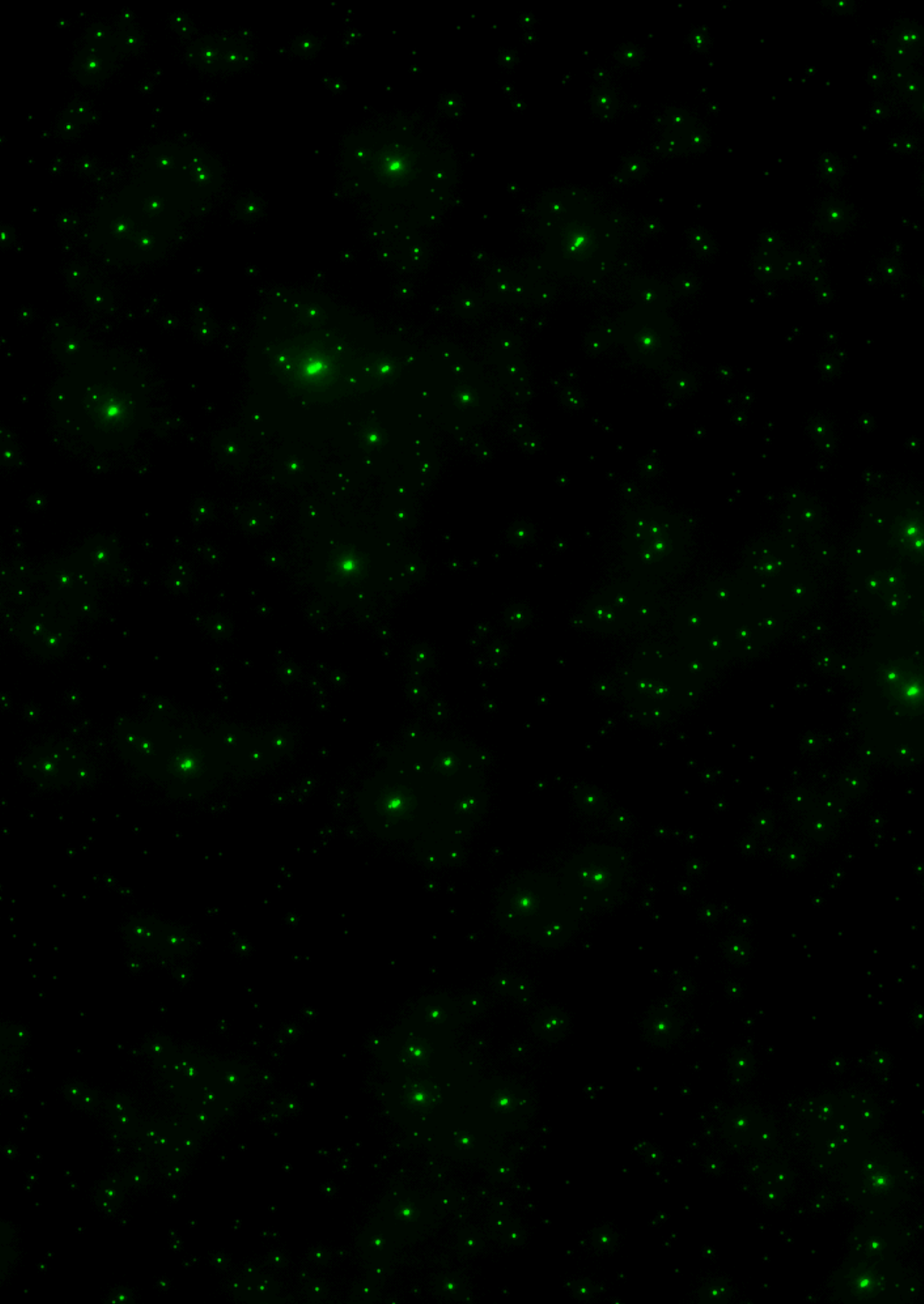

3

Antigen uptake by skin dendritic cells as function of antigen dose and intradermal injection depth

Prepared for submission

Pim Schipper[1], Koen van der Maaden[1], Toni M.M. van Capel[2], Anne M. Römgens[3], Cees W. Oomens[3], Esther C. de Jong[2], Joke Bouwstra[1]

[1] Division of BioTherapeutics, Leiden Academic Centre for Drug Research, Leiden University, Leiden, the Netherlands

[2] Department of Experimental Immunology; Academic Medical Center; Amsterdam, the Netherlands

[3] Soft Tissue Biomechanics and Engineering, Department of Biomedical Engineering, Eindhoven University of Technology, Eindhoven, the Netherlands

ABSTRACT

The skin is an attractive administration route for vaccines, as the skin is rich in dendritic cells (DCs) and is easily accessible. Multiple subsets of DCs with distinct roles reside at different depths in the skin. The aim of this study was to determine whether migration of, maturation of and antigen uptake by the different DC subsets in skin differ as a result of administration of antigen at various doses (1-50 μg) or injection depths (50-1000 μm) in *ex vivo* human skin. Ovalbumin (OVA) was selected as model antigen. Migrated skin cells were collected by using a skin explant model and the migration, maturation and OVA uptake were determined per DC subset by using flow cytometric analysis. An increase in OVA dose decreased the percentage of $CD1a^+$ and $CD14^+$ dermal DCs (DDCs) within the migrated $HLA\text{-}DR^+$ DC population. Moreover, with increasing OVA doses, only $CD1a^+$ DDCs demonstrated increased maturation, determined as increased expression of costimulatory molecule CD86. Furthermore, with increasing dose the amount of OVA taken up and percentage of OVA-containing cells increased for Langerhans cells (12-99%) and $CD1a^+$ DDCs (91-99%). $CD14^+$ DDCs were most efficient in antigen uptake, as demonstrated by a seemingly saturated amount of OVA uptake and very high percentage of OVA-containing cells (±99%), even at the lowest dose tested. Intradermal administration of OVA at various depths in skin did not result in differences in migration, maturation and OVA uptake, most likely due to a high diffusion coefficient of OVA in human skin. However, intradermal microinjection by using a single hollow microneedle using a 50x reduced injection volume resulted in similar antigen uptake as compared to using a conventional hypodermic needle-and-syringe. Thus using hollow microneedles, the injection volume for intradermal injections may be strongly reduced, avoiding discomfort associated with intradermal injections.

INTRODUCTION

The skin is an attractive immunization route, owing to the presence of high numbers of dendritic cells (DCs) within the skin, allowing for the induction of a potent immune response [1-4]. Previous studies have shown that an equally effective immune response was induced by intradermal rabies immunization using a 60-80% dose reduction, as compared to intramuscular immunization [5-7]. Furthermore, dose sparing has been reported for intradermal immunization (compared to conventional intramuscular immunization) for hepatitis B [8, 9], influenza [10-15] and polio [16, 17], making intradermal immunization an attractive alternative to conventional intramuscular immunization.

DCs are key immune cells for (intradermal) immunization [18-20]. However, to administer a sufficient amount of antigen to DCs located in the skin, the physical barrier of the skin (i.e., the stratum corneum) must be bypassed [1]. Several techniques are available to administer a sufficient amount of antigen into the skin. One of the more attractive approaches are the use of hollow and solid microneedles, which are able to disrupt the stratum corneum effectively and potentially without pain sensation [21, 22]. Upon administration of the antigen into the skin, DCs will take up and process the antigen and migrate from the skin towards draining lymph nodes [23-25]. Alternatively, the antigen itself migrates to draining lymph nodes after which it is taken up by lymph node residing DCs. Within the draining lymph nodes, DCs present the antigen to B- and T-cells, initiating the adaptive immune response [23-25].

Three phenotypically and functionally distinct subsets of DCs are known to reside in human skin [24, 26-34]. LCs reside in the epidermis, forming a tight knit network with their dendrites just below the surface of the skin [23, 24, 33]. Human LCs are recognized by their expression of Langerin and CD1a, but lack of expression of CD14 on the cell surface. LCs are more efficient in inducing cytotoxic T-lymphocyte (CTL) responses [29, 32, 35-38] than other skin DCs. LCs are known to respond to viruses [29, 36-38], but not to bacteria [35, 39, 40], probably due to reduced expression of TLR 2, 4 and 5 [35]. Dermal DCs (DDCs) reside in the dermis and are comprised of $CD1a^+$ DDCs and $CD14^+$ DDCs [23, 24, 32-34]. $CD14^+$ DDCs lack expression of Langerin and CD1a, but do express CD14 on the cell surface. $CD14^+$ DDCs are reported to be more efficient in initiating humoral immunity than LCs or $CD1a^+$ DDCs. $CD14^+$ DDCs polarize naïve $CD4^+$ T cells to develop into follicular helper T cells, which in turn induce naïve B cells to produce antibodies and to proliferate into plasma cells [29, 32, 41]. $CD1a^+$ DDCs lack expression of Langerin and CD14, but do express CD1a on the cell surface. $CD1a^+$ DDCs are intermediately efficient in inducing humoral and cellular immune responses, in comparison to LCs and $CD14^+$ DDCs [28, 29, 32, 42].

Due to differences in immunological function and location in skin, it is important to examine to which extent LCs, CD1a$^+$ and CD14$^+$ DDCs are involved in antigen uptake. Therefore, the aim of this study was to determine the effects of administration of antigen at various doses and injection depths in skin on antigen uptake by human LCs, CD1a$^+$ and CD14$^+$ DDCs.

Ovalbumin (OVA) was selected as model protein antigen and a human skin explant model was used, to examine the antigen uptake, migration and maturation by/of LCs, CD1a$^+$ and CD14$^+$ DDCs [43-45]. To be able to perform intradermal depth-controlled microinjections, a single hollow microneedle and an applicator system was used [46-49]. In addition, a combination of fluorescence recovery after photobleaching (FRAP) experiments with finite element analysis was used to determine the diffusion coefficient of OVA in various depths in skin.

In this study, we demonstrated that the amount and efficiency of OVA uptake differs between LCs, CD1a$^+$ and CD14$^+$ DDCs, but that the intradermal injection depth did not result in different uptake. We also demonstrated that OVA uptake was similar at equal dose for intradermal administration by using a conventional hypodermic needle-and-syringe (standard volume of 10 µL) and by using a single hollow microneedle using a 50x reduced injection volume.

MATERIALS

OVA conjugated with Alexa Fluor® 488 (OVA) or FITC (OVA-FITC), Hoechst 33342, Iscove's Modified Dulbecco's Medium (IMDM), Hank's balanced salt solution and anti-human CD11c-PE-Cy7 antibodies (catalogue number 25-0116-42) were purchased from Thermo Fisher Scientific (Bleiswijk, the Netherlands). Cholecalciferol (vitamin D3) and ethanol 96% (v/v) were obtained from Sigma Aldrich (Zwijndrecht, the Netherlands). Sterile phosphate buffered saline (PBS) (163.9 mM Na^+, 140.3 mM Cl^-, 8.7 mM HPO_4^{2-} and 1.8 mM $H_2PO_4^-$, pH 7.4) was ordered at B. Braun Melsungen (Oss, the Netherlands). Skin biopsy punches were purchased from Kai Europe (Solingen, Germany). BD Micro-Fine™+ 30G 0.3 mL needle-syringes and anti-human CD1a-APC, CD86-PE and HLA-DR-PerCP antibodies (catalogue numbers 559775, 555665 and 347364, respectively) were obtained from Becton Dickinson (Breda, the Netherlands). Anti-human CD14-APC-Cy7 antibodies (catalogue number 301820) were ordered at Biolegend (Koblenz, Germany). HyClone™ Fetal calf serum (FCS) was purchased from GE Healthcare Life Sciences (Eindhoven, the Netherlands). GM-CSF was obtained from Schering-Plough (Uden, the Netherlands). Costar® 48-well plates were ordered at Corning Life Sciences (Amsterdam, the Netherlands). Styrofoam were purchased from a local hardware store.

METHODS

Preparation of human skin for intradermal injections

Abdominal *ex vivo* human skin was obtained from local hospitals after cosmetic surgery and after obtaining informed consent from the donors, which was handled according to the ethical principles of the Declaration of Helsinki. The skin was stored at 4 °C until use within 24 h after surgery. To clean the skin, the epidermal side of the skin was sequentially rinsed with sterile PBS, 70% (v/v) ethanol and sterile PBS again. The skin was slightly pre-stretched by pinning the skin on a flat piece of Styrofoam, in an effort to simulate the stretch conditions of skin in normal conditions.

Dose-dependent antigen uptake

For each experiment, sterile formulations of OVA and vitamin D3 were prepared. To determine the effect of the administered OVA dose on antigen uptake, migration and maturation by/of LCs, $CD1a^+$ and $CD14^+$ DDCs, 1, 5, 25, or 50 µg OVA in 10 µL PBS was injected intradermally using a conventional hypodermic needle-and-syringe (30G needle-syringes). As controls, $1.25{\cdot}10^{-9}$ mole Vitamin D3 in 10 µL PBS (positive control)

or 10 µL PBS alone (negative control) were injected intradermally using a conventional hypodermic needle-and-syringe (30G needle-syringes). Additionally, plain biopsies of untreated skin were included (negative control).

System for single hollow microneedle-mediated depth-controlled intradermal microinjections

To allow for intradermal microinjections at an accurate depth, intradermal microinjections were performed using a digitally-controlled single hollow microneedle injection system (DC-shMN-iSystem). This system comprises of a single hollow microneedle, which is fixed in an applicator, as explained in detail elsewhere [47, 49]. Accurate intradermal microinjections of very low volumes were feasible by controlling the microneedle applicator and syringe pump (NE-300, Prosense, Oosterhout, the Netherlands) *via* a microneedle applicator controller unit (uPRAX Microsolutions, Delft, The Netherlands) [46, 50]. Single hollow microneedles were fabricated using hydrofluoric acid etching as previously described [49]. Prior to use, the fluidics part of the DC-shMN-iSystem was sterilized by flushing it with 70% ethanol.

Depth-controlled intradermal microinjections

To maximize the accuracy of the depth at which an antigen is administered intradermally, very low volumes have to be injected, due to possible perfusion. Therefore, the microinjection volume was reduced to 0.2 µL (as compared to the 10 µL intradermal injections using a conventional hypodermic needle-and-syringe), and contained 0.1 µg OVA. Intradermal microinjections were performed at a pre-selected depth of 50, 500 or 1000 µm using the DC-shMN-iSystem. As control, 0.1 µg OVA in 10 µL PBS was injected intradermally using a conventional hypodermic needle-and-syringe (30G needle-syringes).

Culturing of human skin explants

A skin biopsy was harvested immediately after intradermal injection and was cultured to observe the immunological behavior of migrating cells, as reported earlier [44, 45]. A full thickness skin biopsy of 6 mm in diameter was taken from the *ex vivo* skin at the injection site, whilst simultaneously removing the subcutaneous fat. For each treatment, 12 biopsies were harvested. Each biopsy was floated with the epidermal side up for 1 hour in 0.5 mL IMDM containing 1% FCS in a 48-well plate. Subsequently, the biopsies were transferred to 1 mL of IMDM containing 10% FCS and 100 ng/mL GM-CSF in a new 48-well plate and were cultured with the epidermal side up at 37 °C and 5% CO_2 for 3 days. After removal of the biopsies, migrated cells (crawled out the biopsies) were harvested and pooled for flow cytometric analysis.

Analysis by flow cytometry

The percentage of specific subsets of total migrated HLA-DR$^+$ DCs, maturation and uptake of OVA by migrated LCs, CD1a$^+$ and CD14$^+$ DDCs were analyzed by using flow cytometry. Migrated DCs were isolated and stained with fluorescently labeled antibodies. During flow cytometric analysis, migrated DCs were distinguished by their forward and sideward scatter properties, in combination with high expression levels of HLA-DR and CD11c, after which LCs (defined as CD1a^{high}), CD1a$^+$ and CD14$^+$ DDCs were discriminated from this population, see Supplementary Materials. Absolute cell counts and percentages of specific subsets of total migrated HLA-DR$^+$ DCs and relative changes in comparison to PBS treatment (%cells treatment group / %cells PBS group * 100) of LCs, CD1a$^+$ and CD14$^+$ DDCs were calculated. Subsequently, OVA uptake by LCs, CD1a$^+$ and CD14$^+$ DDCs was quantified by measuring the median fluorescence intensity (MFI) of (fluorescently labeled) OVA within each LC, CD1a$^+$ or CD14$^+$ DDC. Moreover, the percentage of cells within the LC, CD1a$^+$ and CD14$^+$ DDC subpopulations which had taken up OVA was determined. Additionally, maturation of LCs, CD1a$^+$ or CD14$^+$ DDCs was analyzed by measuring the MFI of the markers HLA-DR and CD86. Multicolor flow cytometry was performed on a FACS Canto II (Becton Dickinson) and FlowJo v10.3 (Tree Star, Ashland, OR, USA) was used for data analysis.

Determination of the diffusion coefficient of OVA in skin

A method combining FRAP experiments with finite element analysis was used to determine the diffusion coefficient of OVA at various depths in the skin, as described in detail elsewhere [51]. In short, human skin samples were prepared by cutting slices perpendicular to the skin surface using a cutting device to create a flat cutting plane. Subsequently, the skin samples were immerged in 1 mg/mL OVA-FITC in Hank's balanced salt solution with 20 µg/mL Hoechst 33342 and stored at 4 °C for at least 20 h. After equilibrating the skin samples to room temperature (15-25 °C) for at least 30 min, the skin samples were prepared for FRAP experiments, so that dehydration during the experiments was prevented. During FRAP experiments, the fluorescent molecules in a spot in the skin were bleached with a high laser power. Due to diffusion of bleached and unbleached molecules, the fluorescence level of the bleached spot recovers. This recovery is recorded with a confocal microscope with low laser power. The locations tested in FRAP experiments were at 50% of the epidermal thickness, 50% of the papillary dermal thickness and at the upper 10% of the reticular dermis, corresponding to average depths in skin of approximately 90, 300 and 1000 µm, respectively. The resulting images of the FRAP experiments were processed using MATLAB (2013a, The MathWorks Inc., Natick, MA, USA). Using Abaqus/Standard (v6-11.2, Dassault Systèmes Simulia Corp., Providence, RI, USA), a two-dimensional finite element model was designed simulating

the FRAP experiments, to solve the diffusion equation for OVA. Finally, the results of the finite element simulation were fitted to results of the processed data from the microscopy images of the FRAP experiments, whereby the diffusion coefficient of OVA at various depths in skin was estimated.

Statistical analysis

Graphs were plotted as mean ± SEM by using GraphPad Prism (v.7.00, GraphPad Software, LaJolla, CA, USA). The data was considered to be non-parametric paired data with multiple test groups. Therefore, statistical analysis was performed using linear mixed models (covariance type: compound symmetry) on rank transformed data with donor as covariate, followed by the post-hoc least significant difference (LSD) test for pairwise comparisons. Effects of the combination of the injected formulations and type of injection (single hollow microneedle, conventional hypodermic needle-and-syringe or no injection) were measured by assessing markers related to five different outcome groups: cell counts, percentage of specific subsets of total migrated HLA-DR$^+$ DCs, relative changes in comparison to PBS treatment, DC maturation marker expression and OVA uptake. The linear mixed model was adjusted for 5 outcome groups and was considered to be statistically significant at $p < 0.01$. The LSD was considered to be statistically significant at $p < 0.05$. Statistical analyses were performed using IBM SPSS Statistics (version 23, International Business Machines Corporation, Armonk, NY, USA).

RESULTS

Dose-dependent antigen uptake

Antigen uptake by skin DCs may be influenced by the amount of antigen that is administered into the skin. Therefore, various amounts of model antigen OVA were administered intradermally using a conventional hypodermic needle-and-syringe.

Migration of skin DC subsets

Increasing OVA doses (1-50 µg) resulted in a trend of enhanced migration of LCs out of the skin, as determined in absolute cell counts (Fig. 1A), percentage of total migrated HLA-DR$^+$ DCs (Fig. 1B) and relative changes in comparison to PBS treatment (Fig. 1C). When focusing on CD1a$^+$ DDCs, the migration was independent of the OVA dose when determined in absolute cell counts (Fig. 1A). Contrarily, increasing OVA doses resulted in decreased CD1a$^+$ DDC migration, taking into account the percentage of total migrated HLA-DR$^+$ DCs (Fig. 1B) and relative changes in comparison to PBS treatment (Fig. 1C). Furthermore, a dose-dependent decrease in CD14$^+$ DDC migration was also found, expressed as absolute cell counts (Fig. 1A), percentage of total migrated HLA-DR$^+$ DCs (Fig. 1B) and relative changes in comparison to PBS treatment (Fig. 1C). Summarizing, intradermal administration of increasing OVA doses resulted in a trend in enhanced migration of LCs, whilst it resulted in statistically significant decreased migration of CD1a$^+$ and CD14$^+$ DDCs.

Vitamin D3 was selected as a positive control, as it is known to influence the migration of skin DCs [45]. Intradermal administration of vitamin D3 resulted in decreased migration of CD1a$^+$ DDCs, but increased migration of CD14$^+$ DDCs, expressed as absolute cell counts (Fig. 1A), percentage of total migrated HLA-DR$^+$ DCs (Fig. 1B) and in relative changes in comparison to PBS treatment (Fig. 1C).

PBS treatment and biopsy alone were selected as negative controls. By comparing PBS treatment with biopsy alone, it was possible to determine whether the migration of skin DCs is affected by intradermal injection. After intradermal injection of PBS, in comparison to biopsy alone, only an enhanced migration of CD1a$^+$ DDCs was observed, expressed as increase in percentage of total migrated HLA-DR$^+$ DCs (Fig. 1B) and in relative changes in comparison to PBS treatment (Fig. 1C).

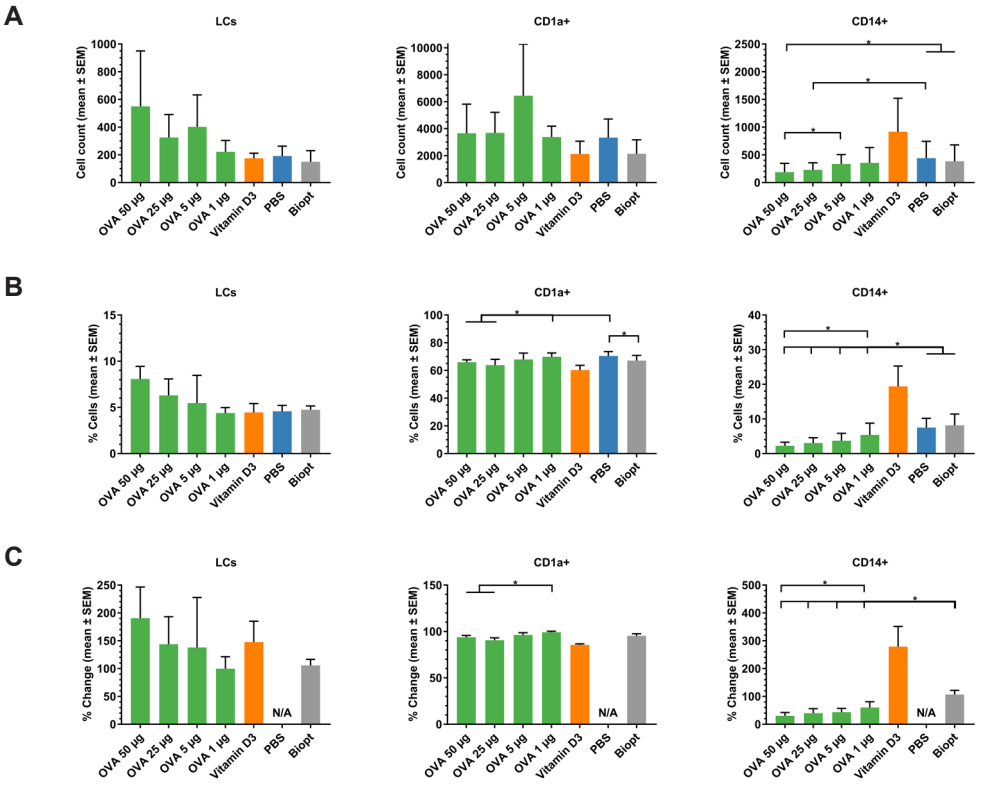

Fig. 1 Migration of LCs, CD1a⁺ and CD14⁺ DDCs is independent of administered OVA dose.

For LCs, CD1a⁺ and CD14⁺ DDCs, the absolute cell count (**A**), the percentage of total migrated HLA-DR⁺ DCs (**B**) and the relative changes in comparison to PBS treatment (**C**) was analyzed as function of OVA dose, vitamin D3 or PBS after intradermal administration by using a conventional hypodermic needle-and-syringe or as function of biopsy alone. The data represents mean ± SEM (n = 3). Statistical significant differences ($p < 0.05$) are indicated with an asterisk (*).The statistical significant differences for the vitamin D3 group are omitted and are as follows: Fig. 1A CD14⁺ DDCs (vitamin D3 against all other treatments, except PBS), Fig. 1B CD1a⁺ DDCs and Fig. 1B CD14⁺ DDCs (vitamin D3 against all other treatments), Fig. 1C CD1a⁺ DDCs (vitamin D3 against 5 and 1 µg OVA and biopt) and Fig. 1C CD14⁺ DDCs (vitamin D3 against all other groups).

Maturation

DCs must activate and maturate after antigen uptake, in order to be able to induce adaptive immune responses, important to immunization. Maturation is characterized by an increase in expression of HLA-DR and co-stimulatory molecule CD86 on the cell surface. Therefore, it is important to determine the effect of increasing OVA doses on

the expression of HLA-DR and CD86 on LCs, CD1a$^+$ and CD14$^+$ DDCs. Representative histograms of flow cytometric analysis after administration of 50 µg OVA or PBS is shown in Fig. 2A and 2B for HLA-DR and CD86, respectively.

The expression of HLA-DR (Fig. 2C) by LCs, CD1a$^+$ and CD14$^+$ DDCs was independent of administered OVA dose. However, CD86 expression by CD1a$^+$ DDCs, but not by LCs or CD14$^+$ DDCs, was significantly increased in a dose-dependent manner after intradermal administration of OVA (Fig. 2D). Vitamin D3 treatment resulted in a significant increase in CD86 expression by CD1a$^+$ DDCs in comparison to negative controls. No differences between PBS injection and biopsy alone were observed for HLA-DR or CD86 expression.

OVA uptake

The effect of the OVA dose on OVA uptake by LCs, CD1a$^+$ and CD14$^+$ DDCs was determined by intradermal administration of increasing (fluorescently labeled) OVA doses. Representative histograms of OVA fluorescence after intradermal administration of 50 µg OVA or PBS are shown in Fig. 3A.

A dose-dependent OVA uptake by LCs and CD1a$^+$ DDCs was observed, illustrated by an increasing MFI for OVA with increasing OVA doses (presented in Fig. 3B). Contrarily, the OVA uptake by CD14$^+$ DDCs was independent of OVA dose, indicating that CD14$^+$ DDCs are very efficient in uptake of OVA. In fact, when examining the 50 µg OVA dose, OVA uptake was highest in CD14$^+$ DDCs, followed by that of CD1a$^+$ DDCs (3.5-fold lower) and LCs (15.7-fold lower). As expected, no OVA fluorescence was detected after intradermal administration of control formulations.

Next, the percentage of cells within the LC, CD1a$^+$ and CD14$^+$ DDC subpopulations that took up OVA was determined, as detailed in Fig. 3A. Nearly each CD14$^+$ DDC had taken up OVA, even at the lowest OVA dose (99%), as presented in Fig. 3C. Similarly, the percentage of CD1a$^+$ DDCs which had taken up OVA was high (91-99%). However, an OVA dose-dependent increase in OVA uptake was observed, as administration of 50 or 25 µg OVA doses resulted in a statistically significant higher percentage of CD1a$^+$ DDCs which had taken up OVA (99% and 97%, respectively), as compared to intradermal administration of 5 and 1 µg OVA (95 and 91%, respectively). Furthermore, the percentage of LCs which had taken up OVA strongly depended on the OVA dose, as an equal percentage of LCs and CD1a+ or CD14$^+$ DDCs that had taken up OVA was only reached using the highest OVA doses. Moreover, nearly each LC had taken up OVA after intradermal administration of 50 and 25 µg OVA (99%), whereas only approximately 60% or 12% of LCs had taken up OVA after intradermal administration of 5 and 1 µg OVA, respectively.

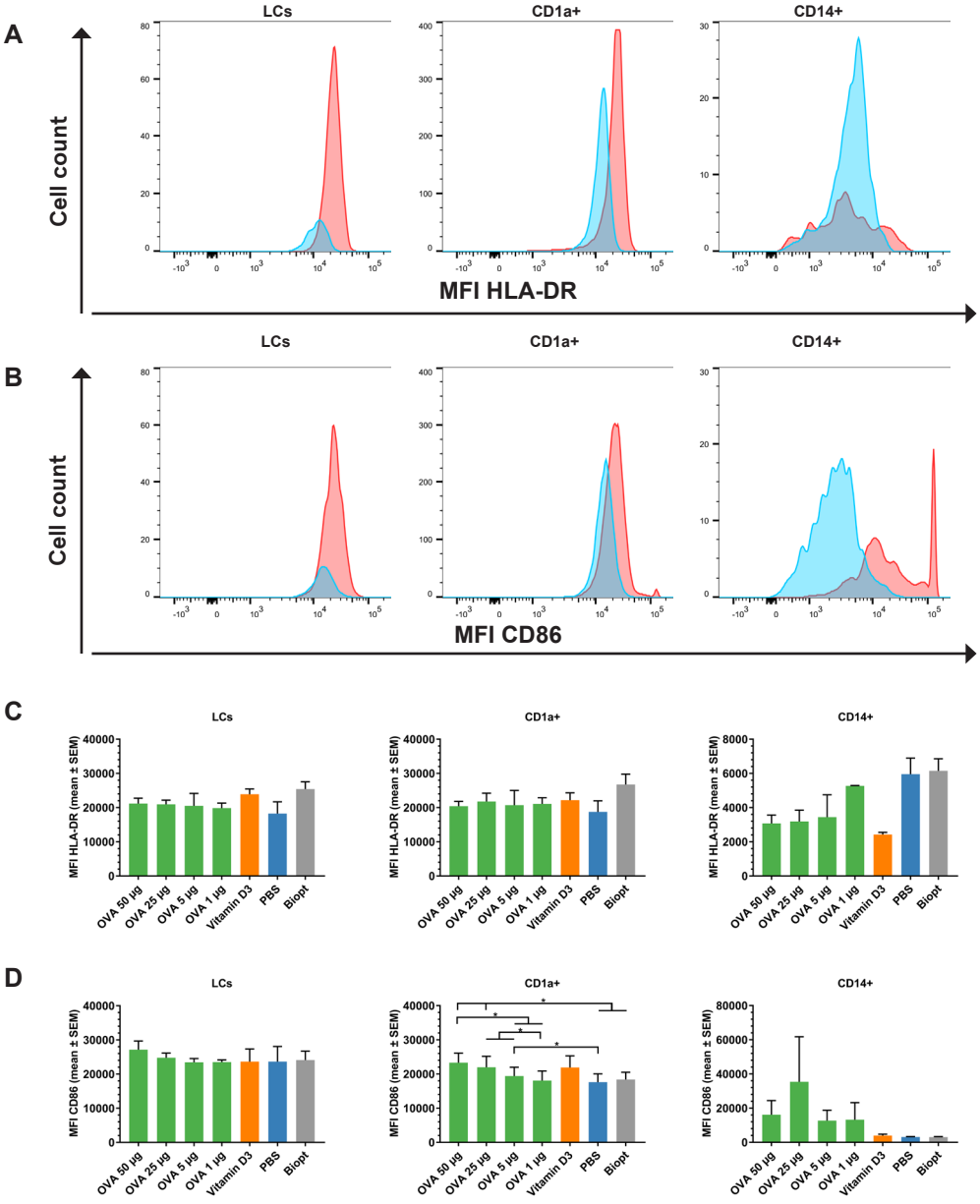

Fig. 2 Maturation of LCs, CD1a⁺ and CD14⁺ DDCs is affected by the administered OVA dose.

The maturation of LCs, CD1a⁺ and CD14⁺ DDCs was analyzed by measuring the MFI of HLA-DR and co-stimulatory molecule CD86. Representative histograms are shown for LCs, CD1a⁺ and CD14⁺ DDCs, for 50 µg of OVA (red) and PBS (blue), for HLA-DR (**A**) and CD86 (**B**). The MFI was analyzed as function of OVA dose, vitamin D3 or PBS after intradermal administration by using a conventional hypodermic needle-and-syringe or biopsy alone. The MFI is represented for HLA-DR in (**C**) and for

CD86 in (**D**). The data represents mean ± SEM (n = 3). Statistical significant differences ($p < 0.05$) are indicated with an asterisk (*). The statistical significant differences for vitamin D3 treatment are omitted and are as follows: Fig. 2D CD1a$^+$ DDCs (vitamin D3 against 1 µg OVA, PBS and biopt).

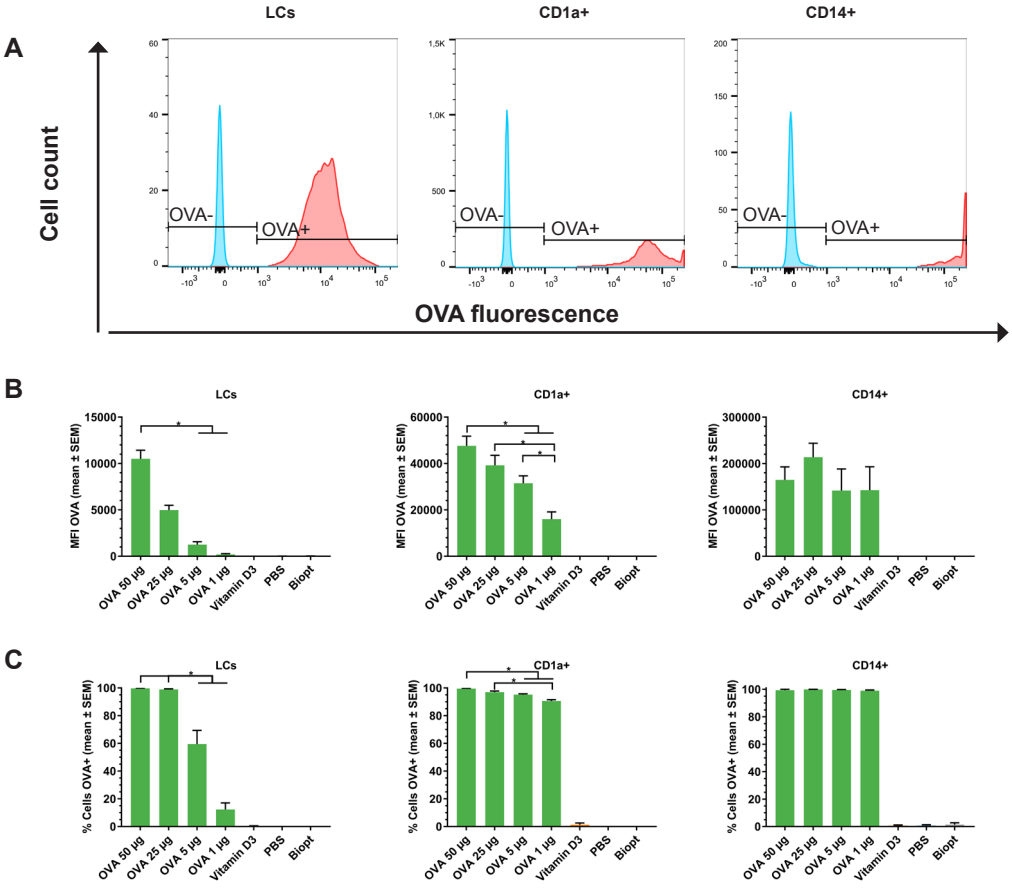

Fig. 3 OVA uptake differs between LCs, CD1a$^+$ and CD14$^+$ DDCs and is affected by the administered OVA dose.

OVA uptake by LCs, CD1a$^+$ and CD14$^+$ DDCs was investigated by flow cytometry as function of the OVA dose, vitamin D3 or PBS after intradermal administration by using a conventional hypodermic needle-and-syringe or biopsy alone. OVA fluorescence was measured within migrated LCs, CD1a$^+$ and CD14$^+$ DDCs. This is demonstrated in representative histograms (**A**), where OVA fluorescence from migrated LCs, CD1a$^+$ and CD14$^+$ DDCs after administration of 50 µg of (fluorescently labeled) OVA (red) or PBS (blue) is depicted. The amount of OVA uptake by LCs, CD1a$^+$ and CD14$^+$ DDCs was quantified by measuring the MFI of (fluorescently labeled) OVA, represented in (**B**). The discrimination between LCs, CD1a$^+$ and CD14$^+$ DDCs which had taken up OVA or not was based on

a threshold for OVA fluorescence (**A**). Following this discrimination, the percentage of cells within each LC, CD1a$^+$ or CD14$^+$ DDC subpopulation which had taken up OVA is represented in (**C**). The data represents mean ± SEM (n = 3). Statistical significant differences ($p < 0.05$) are indicated with an asterisk (*).

Single hollow microneedle-mediated depth-controlled intradermal microinjections of OVA

Because LCs, CD1a$^+$ and CD14$^+$ DDCs reside at different depths in the skin, we hypothesized that OVA uptake may be influenced by administration of OVA at different depths in skin. Therefore, 0.1 µg OVA was administered intradermally in 0.2 µL at shallow (50 µm), medium (500 µm) and deep (1000 µm) depths in skin, by using single hollow microneedle-mediated depth-controlled microinjections. Subsequent percentages of specific subsets of total migrated HLA-DR$^+$ DCs, maturation and OVA uptake of migrated LCs, CD1a$^+$ and CD14$^+$ DDCs were analyzed and compared to intradermal administration of 0.1 µg OVA in 10 µL by using a conventional hypodermic needle-and-syringe.

Migration of skin DC subsets

No differences were found in absolute cell counts (Fig. 4A), percentage of specific subsets of total migrated HLA-DR$^+$ DCs (Fig. 4B) or in relative changes in comparison to PBS treatment (Fig. 4C) of LCs, CD1a$^+$ and CD14$^+$ DDCs upon administration of OVA at different depths into the skin (50, 500 and 1000 µm). Similarly, no differences were found between intradermal administration of OVA by using a single hollow microneedle at different depths or a conventional hypodermic needle-and-syringe. However, intradermal administration of OVA by using a single hollow microneedle (at 500 or 1000 µm depths) resulted in an increased percentage of CD14$^+$ DDCs of total migrated HLA-DR$^+$ DCs in comparison to biopsy alone (Fig. 4B). Likewise, intradermal administration of OVA by using a single hollow microneedle (at 500 or 1000 µm depths) or by using a conventional hypodermic needle-and-syringe resulted in an increase of CD14$^+$ DDCs in relative changes in comparison to PBS treatment (Fig. 4C).

The percentage of CD14$^+$ DDCs of total migrated HLA-DR$^+$ DCs and relative changes in comparison to PBS treatment increased upon intradermal administration of vitamin D3. Neither PBS or biopsy treatment resulted in any effect.

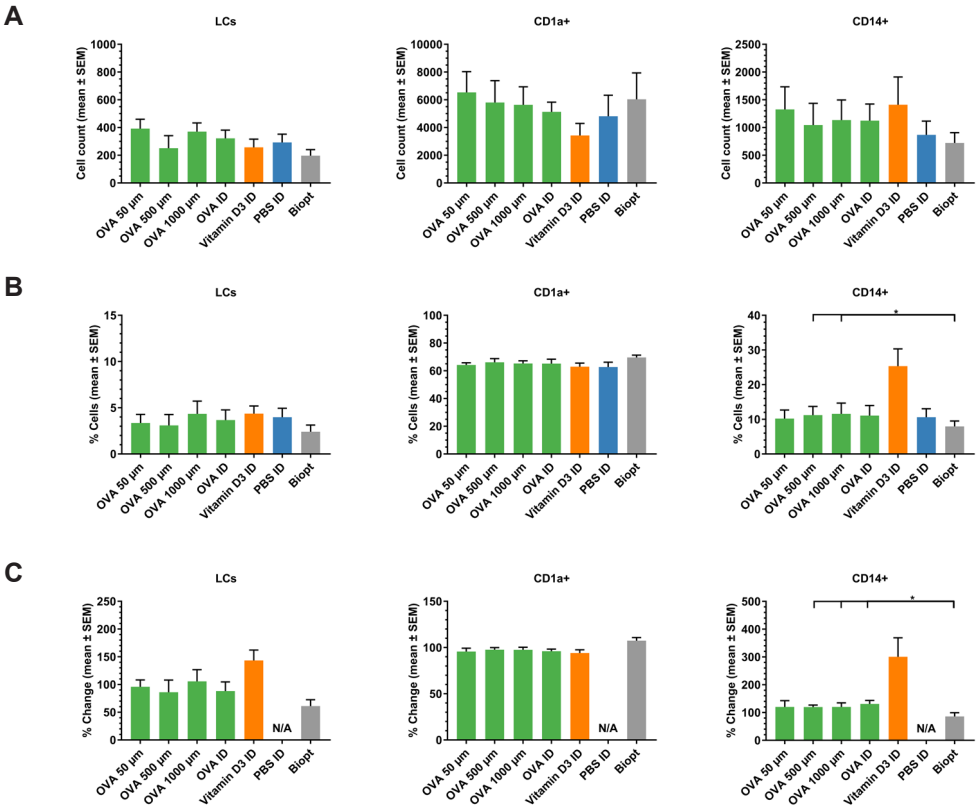

Fig. 4 Migration of LCs, CD1a⁺ and CD14⁺ DDCs is independent of the injection depth in skin and by injection method.

For LCs, CD1a⁺ and CD14⁺ DDCs, the absolute cell count (**A**), the percentage of total migrated HLA-DR⁺ DCs (**B**) and the relative changes in comparison to PBS treatment (**C**) was investigated as function of the injection depth in skin by using a single hollow microneedle and as function of intradermal administration by using a conventional hypodermic needle-and-syringe (ID) of OVA, vitamin D3 or PBS or as function of biopsy alone. The data represents mean ± SEM (n = 5). Statistical significant differences ($p < 0.05$) are indicated with an asterisk (*). The statistical significant differences for the vitamin D3 group are omitted and are as follows: Fig. 4B CD14⁺ DDCs and Fig. 4C CD14⁺ DDCs (vitamin D3 against all other groups).

Maturation

As demonstrated in Fig. 5, the expression of HLA-DR and co-stimulatory molecule CD86 was independent of intradermal administration of OVA at different depths or upon comparing intradermal administration of OVA either by using a single hollow microneedle or by using a conventional hypodermic needle-and-syringe. Nor was the expression of HLA-DR or CD86 affected by treatment with OVA, vitamin D3, PBS or biopsy alone.

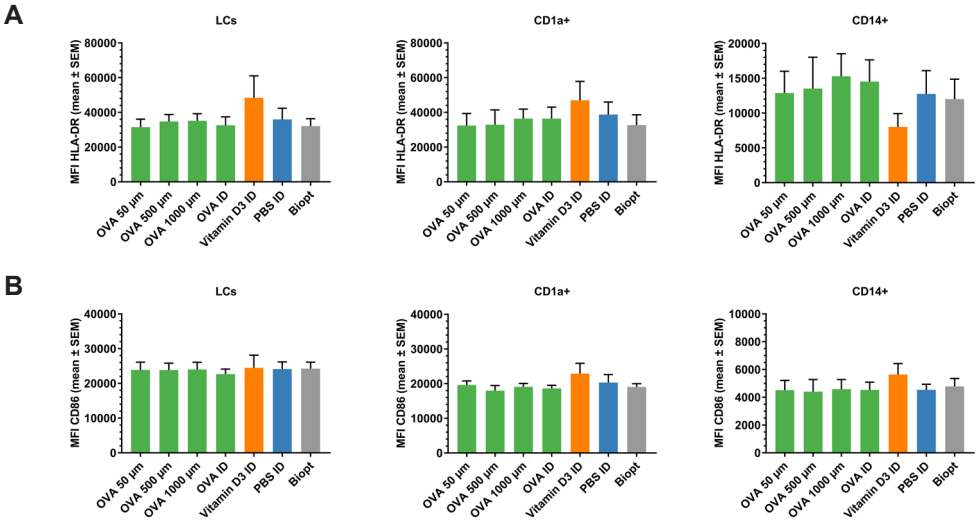

Fig. 5 Maturation of LCs, CD1a⁺ and CD14⁺ DDCs is independent of the depth in skin at which OVA is administered and intradermal administration method.

The maturation of LCs, CD1a⁺ and CD14⁺ DDCs was analyzed by measuring the MFI of HLA-DR (**A**) and co-stimulatory molecule CD86 (**B**). Maturation was investigated as function of the depth in skin at which OVA was administered by using a single hollow microneedle or as function of intradermal administration by using a conventional hypodermic needle-and-syringe (ID) of OVA, vitamin D3 or PBS or as function of biopsy alone. The data represents mean ± SEM (n = 5).

OVA uptake

Upon analyzing the effect of depth-controlled intradermal administration of OVA on antigen uptake by skin DCs (Fig. 6A and -B), no differences were found, with one exception. Intradermal administration of OVA at 50 µm depth resulted in a decreased percentage of LCs that had taken up OVA compared to intradermal administration of OVA at 500 and 1000 µm depths by using a single hollow microneedle and by using a

conventional hypodermic needle-and-syringe. However, the amount of OVA which had been taken up on average by an individual LC was independent of injection depth, as indicated by the MFI in Fig. 6A. Furthermore, the amount of OVA uptake by CD14$^+$ DDCs was highest, followed by that of CD1a$^+$ DDCs and LCs (Fig. 6A). As expected, controls did not result in the detection of OVA uptake by LCs, CD1a$^+$ or CD14$^+$DDCs.

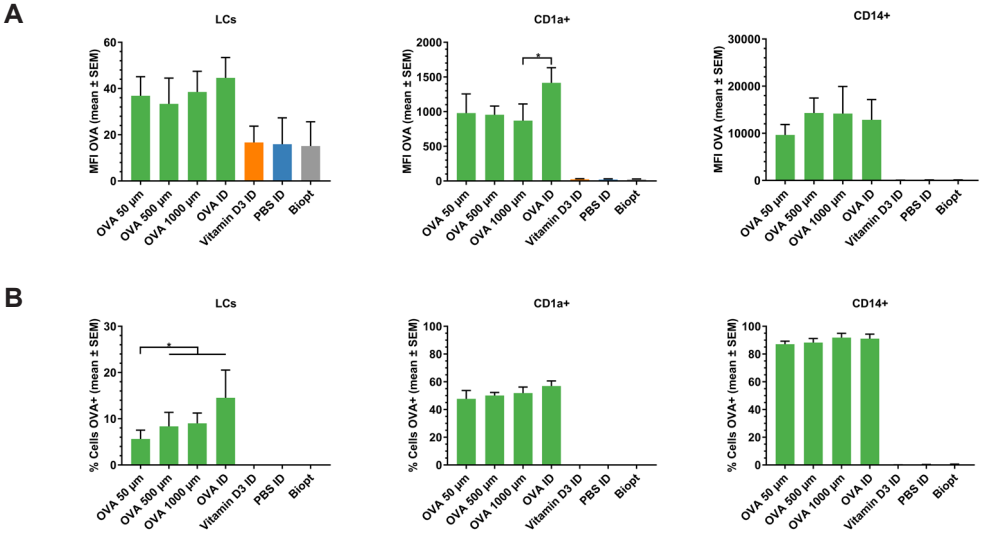

Fig. 6 OVA uptake differs between LCs, CD1a$^+$ and CD14$^+$ DDCs and is independent of the depth in skin at which OVA is administered and intradermal administration method.

OVA uptake by LCs, CD1a$^+$ and CD14$^+$ DDCs was investigated by flow cytometry as function of the depth in skin at which OVA was administered by using a single hollow microneedle, as function of intradermal administration by using a conventional hypodermic needle-and-syringe (ID) of OVA, vitamin D3 or PBS or as function of biopsy alone. The amount of OVA uptake by LCs, CD1a$^+$ and CD14$^+$ DDCs was quantified by measuring the MFI of OVA, represented in (**A**). The percentage of cells which had taken up OVA is represented in (**B**). The data represents mean ± SEM (n = 5). Statistical significant differences ($p < 0.05$) are indicated with an asterisk (*).

Determination of the diffusion coefficient of OVA in skin

No differences in OVA uptake by skin DCs were observed upon OVA administration at different depths into the skin. For this reason, it was decided to measure the diffusion coefficient of OVA at different depths in skin, which was done using FRAP.

From the fluorescence recovery monitored with confocal microscopy combined with finite element analysis, the OVA diffusion coefficient was determined on 3 locations in the skin within 10 samples. Based on the criteria for the quality of experiments and quality of the fit, 17 of the 30 measurements were selected for further analysis. As demonstrated in Fig. 7, the mean diffusion coefficient of OVA was 17 $\mu m^2/s$ at a depth of about 90 µm in the epidermis and was approximately two-fold higher in the dermis, namely 35 $\mu m^2/s$ at a depth of about 300 µm and 27 $\mu m^2/s$ at a depth of about 1000 µm.

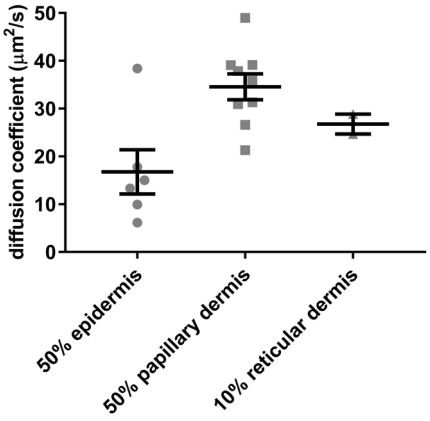

Fig. 7 The diffusion coefficient of OVA in the epidermis and dermis.

The diffusion coefficient of OVA at 50% of the depth of the epidermis, at 50% of the depth of the papillary dermis and at 10% of the depth of the reticular dermis was determined by a combination of FRAP experiments and finite elements analysis. The data represents mean ± SEM (*n* = 6, 9, 2 for 50% epidermis, 50% papillary dermis and 10% reticular dermis, respectively).

DISCUSSION

In this study, OVA was administered into *ex vivo* human skin at various doses and depths in skin to examine the resulting migration of, maturation of and OVA uptake by LCs, $CD1a^+$ and $CD14^+$ DDCs. Upon intradermal administration of increasing OVA doses, an (non-significant) increased percentage of LCs was detected amongst the migrated DCs, while significantly decreased percentages of $CD1a^+$ and $CD14^+$ DDCs were observed. Moreover, an increase in the expression of costimulatory molecule CD86 was found on $CD1a^+$ DDCs, whereas no differential expression was detected on LCs and $CD14^+$ DDCs. Intradermal administration of increasing OVA doses correlated with increased OVA uptake by LCs and $CD1a^+$ DDCs, whereas $CD14^+$ DDCs were seemingly saturated even at the lowest dose investigated, demonstrating a very high level of OVA uptake. In addition, nearly each individual $CD14^+$ DDC took up OVA at the examined doses, closely followed by $CD1a^+$ DDCs, whereas LCs only reached similar levels as $CD1a^+$ and $CD14^+$ DDC at the highest OVA doses tested. Taken together, $CD1a^+$ and $CD14^+$ DDCs were more efficient in OVA uptake compared to LCs. Furthermore, no difference in OVA uptake was observed between intradermal administration of OVA, either by using a conventional hypodermic needle-and-syringe or by using a single hollow microneedle for depth-controlled microinjections at a 50x reduced injection volume. These results indicate however, that the volume of vaccine formulations for intradermal administration can be significantly reduced, lowering discomfort associated with intradermal injections [17], while maintaining high antigen uptake by skin DCs.

Using single cell suspensions consisting of DCs extracted from human skin, it was demonstrated that $CD14^+$ DDCs were superior in OVA uptake compared to $CD1a^+$ DDCs, which were superior compared to LCs [32]. Our findings are similar to those, but resulting from *in situ* intradermal administration of OVA. Although the $CD14^+$ DDCs subpopulation was not distinctively determined, similar results were presented in another study in which OVA uptake was examined upon *in situ* intradermal administration of OVA by using a conventional needle-and-syringe [52]. In addition, by using cryo-sectioned and stained samples of skin analyzed by using confocal microscopy, it was shown that DDCs had superior OVA uptake compared to LCs [52]. Uptake of antigen by LCs in the epidermis upon intradermal administration was demonstrated in other studies, both in human [53] and mice skin [54-59], but were limited in distinguishing between LCs and the two subsets of DDCs or did not quantify antigen uptake.

DDCs are also superior in uptake of bacteria in comparison to LCs, as DDCs more efficiently internalized Gram-negative [35, 60, 61] and Gram-positive bacteria [35, 61] than

LCs. In this case, the reduced expression of TLR 2, 4 and 5 [35], important to bacterial recognition, may play an important role. In fact, it has been proposed that LCs provide an immune regulating role in the epidermis, maintaining tolerance to commensal skin bacteria [61-63].

A comparison of the diffusion coefficient of macromolecules at various depths in human skin has previously only been performed for fluorescein dextran of 40 and 500 kDa [51]. Although dextran (at 40 kDa MW) and OVA (at 42.7 kDa MW [64]) share a similar molecular weight, a direct comparison of dextran and OVA cannot be made as the molecular structure is dissimilar: dextran is a complex branched glucan and OVA is a protein. For this reason, we decided to determine the diffusion coefficient of OVA in the epidermis as well as in the dermis. In comparison, the diffusion coefficient of OVA is somewhat higher than that of 40 kDa dextran [51]. The diffusion coefficient of both OVA and 40 kDa dextran was two-fold higher in the dermis compared to the epidermis [51]. Owing to this relatively high diffusion coefficient, within the 3-day culturing period used in the human skin explant model, the administered OVA might diffuse in all compartments of the skin and subsequently be taken up by the LCs or DDCs independent of the injection depth. Therefore, the relatively high diffusion rate might be partly responsible for the absence of differences as function of the injection depth. Interestingly, a study tracking motility of the DCs in skin demonstrated that DDCs actually take up antigen from the highest skin regions [59], which may further clarify why a high OVA loading was observed in DDCs as compared to LCs.

Historically, performance of vaccines is evaluated on the ability to induce antibody responses. In some studies, elevated antibody responses at reduced doses have been reported for intradermal immunization in comparison to intramuscular and subcutaneous routes [17], while other studies report no difference in response [65]. It is suggested that intradermal immunization route may provide a dose-sparing strategy, as the skin is rich in a variety of DCs [66]. Our study showed that $CD14^+$ DDCs easily internalized large amounts of OVA, even at low dose. This suggests efficient processing and presentation and subsequent initiation of adaptive immune responses [29, 32, 41].

Recently, however, attention has shifted to the role of cellular responses in vaccination, especially in the scope of therapeutic vaccines (e.g., against cancer) and intercellular pathogens. LCs are more efficient than $CD1a^+$ or $CD14^+$ DDCs in initiating CTL responses [29, 32, 35-38]. For cellular responses, a higher abundance of antigen seems to lead towards a stronger CTL response [67]. Our results and those by others [32] indicate that LC uptake of OVA at low dose is inefficient and a high dose must be utilized to achieve high antigen

loading in LCs. If this can be translated to other antigens, vaccination strategies aiming for high CTL responses may require a high dose to load LCs. However, increasing antigen doses may affect specificity, affinity and stability of a peptide binding to MHCI molecules, the internal processing by DCs for presentation on MHCI molecules and gene and protein expression levels, which may influence CTL responses [68, 69]. Therefore, it remains to be elucidated whether there is a correlation between high antigen loading in LCs and high CTL responses. Moreover, glycosylation of antigens may enhance their uptake and therefore alter the efficiency of T cell priming [70-73].

CONCLUSION

In this study, the role of antigen uptake by individual DC subsets in skin was further investigated. We demonstrated that the uptake of antigen is most efficient by $CD14^+$ DDCs followed by $CD1a^+$ DDCs. Furthermore, LCs require high antigen doses to internalize large quantities of protein antigen (OVA). There was no influence of the injection depth in skin on antigen uptake by skin DCs. Importantly, intradermal microinjection by a single hollow microneedle using a 50x reduced injection volume results in similar antigen uptake as compared to intradermal administration with a conventional hypodermic needle-and-syringe, which opens possibilities for improved vaccination strategies using hollow microneedles.

REFERENCES

1. J.F. Nicolas, B. Guy, Intradermal, epidermal and transcutaneous vaccination: from immunology to clinical practice, Expert Rev Vaccines, 7 (2008) 1201-1214.
2. B. Bonnotte, M. Gough, V. Phan, A. Ahmed, H. Chong, F. Martin, R.G. Vile, Intradermal injection, as opposed to subcutaneous injection, enhances immunogenicity and suppresses tumorigenicity of tumor cells, Cancer Res, 63 (2003) 2145-2149.
3. R.B. Belshe, F.K. Newman, J. Cannon, C. Duane, J. Treanor, C. Van Hoecke, B.J. Howe, G. Dubin, Serum antibody responses after intradermal vaccination against influenza, N Engl J Med, 351 (2004) 2286-2294.
4. S. Kaushik, A.H. Hord, D.D. Denson, D.V. McAllister, S. Smitra, M.G. Allen, M.R. Prausnitz, Lack of pain associated with microfabricated microneedles, Anesth Analg, 92 (2001) 502-504.
5. M.J. Warrell, K.G. Nicholson, D.A. Warrell, P. Suntharasamai, P. Chanthavanich, C. Viravan, A. Sinhaseni, M.K. Chiewbambroongkiat, X. Pouradier-Duteil, C. Xueref, et al., Economical multiple-site intradermal immunisation with human diploid-cell-strain vaccine is effective for post-exposure rabies prophylaxis, Lancet, 1 (1985) 1059-1062.
6. B.P. Quiambao, E.M. Dimaano, C. Ambas, R. Davis, A. Banzhoff, C. Malerczyk, Reducing the cost of post-exposure rabies prophylaxis: efficacy of 0.1 ml PCEC rabies vaccine administered intradermally using the Thai Red Cross post-exposure regimen in patients severely exposed to laboratory-confirmed rabid animals, Vaccine, 23 (2005) 1709-1714.
7. A. Ambrozaitis, A. Laiskonis, L. Balciuniene, A. Banzhoff, C. Malerczyk, Rabies post-exposure prophylaxis vaccination with purified chick embryo cell vaccine (PCECV) and purified Vero cell rabies vaccine (PVRV) in a four-site intradermal schedule (4-0-2-0-1-1): an immunogenic, cost-effective and practical regimen, Vaccine, 24 (2006) 4116-4121.
8. T. Propst, A. Propst, K. Lhotta, W. Vogel, P. Konig, Reinforced intradermal hepatitis B vaccination in hemodialysis patients is superior in antibody response to intramuscular or subcutaneous vaccination, Am J Kidney Dis, 32 (1998) 1041-1045.
9. H. Micozkadioglu, A. Zumrutdal, D. Torun, S. Sezer, F.N. Ozdemir, M. Haberal, Low dose intradermal vaccination is superior to high dose intramuscular vaccination for hepatitis B in unresponsive hemodialysis patients, Ren Fail, 29 (2007) 285-288.
10. R. Arakane, R. Annaka, A. Takahama, K. Ishida, M. Yoshiike, T. Nakayama, F. Takeshita, Superior immunogenicity profile of the new intradermal influenza vaccine compared to the standard subcutaneous vaccine in subjects 65 years and older: A randomized controlled phase III study, Vaccine, 33 (2015) 6650-6658.
11. D. Holland, R. Booy, F. De Looze, P. Eizenberg, J. McDonald, J. Karrasch, M. McKeirnan, H. Salem, G. Mills, J. Reid, F. Weber, M. Saville, Intradermal influenza vaccine administered using a new microinjection system produces superior immunogenicity in elderly adults: a randomized controlled trial, J Infect Dis, 198 (2008) 650-658.
12. Y.C. Kim, F.S. Quan, D.G. Yoo, R.W. Compans,

S.M. Kang, M.R. Prausnitz, Improved influenza vaccination in the skin using vaccine coated microneedles, Vaccine, 27 (2009) 6932-6938.

13. D.G. Koutsonanos, E.V. Vassilieva, A. Stavropoulou, V.G. Zarnitsyn, E.S. Esser, M.T. Taherbhai, M.R. Prausnitz, R.W. Compans, I. Skountzou, Delivery of subunit influenza vaccine to skin with microneedles improves immunogenicity and long-lived protection, Sci Rep, 2 (2012) 357.
14. F.S. Quan, Y.C. Kim, A. Vunnava, D.G. Yoo, J.M. Song, M.R. Prausnitz, R.W. Compans, S.M. Kang, Intradermal vaccination with influenza virus-like particles by using microneedles induces protection superior to that with intramuscular immunization, J Virol, 84 (2010) 7760-7769.
15. E.V. Vassilieva, H. Kalluri, D. McAllister, M.T. Taherbhai, E.S. Esser, W.P. Pewin, J.A. Pulit-Penaloza, M.R. Prausnitz, R.W. Compans, I. Skountzou, Improved immunogenicity of individual influenza vaccine components delivered with a novel dissolving microneedle patch stable at room temperature, Drug Deliv Transl Res, 5 (2015) 360-371.
16. J. Cadorna-Carlos, E. Vidor, M.C. Bonnet, Randomized controlled study of fractional doses of inactivated poliovirus vaccine administered intradermally with a needle in the Philippines, Int J Infect Dis, 16 (2012) e110-116.
17. S.B. Troy, D. Kouiavskaia, J. Siik, E. Kochba, H. Beydoun, O. Mirochnitchenko, Y. Levin, N. Khardori, K. Chumakov, Y. Maldonado, Comparison of the Immunogenicity of Various Booster Doses of Inactivated Polio Vaccine Delivered Intradermally Versus Intramuscularly to HIV-Infected Adults, J Infect Dis, 211 (2015) 1969-1976.
18. J. Banchereau, R.M. Steinman, Dendritic cells and the control of immunity, Nature, 392 (1998) 245-252.
19. M.L. Kapsenberg, Dendritic-cell control of pathogen-driven T-cell polarization, Nat Rev Immunol, 3 (2003) 984-993.
20. I. Mellman, R.M. Steinman, Dendritic cells: specialized and regulated antigen processing machines, Cell, 106 (2001) 255-258.
21. S.M. Bal, Z. Ding, E. van Riet, W. Jiskoot, J.A. Bouwstra, Advances in transcutaneous vaccine delivery: do all ways lead to Rome?, J Control Release, 148 (2010) 266-282.
22. K. van der Maaden, W. Jiskoot, J. Bouwstra, Microneedle technologies for (trans)dermal drug and vaccine delivery, J Control Release, 161 (2012) 645-655.
23. C. Levin, H. Perrin, B. Combadiere, Tailored immunity by skin antigen-presenting cells, Hum Vaccin Immunother, 11 (2015) 27-36.
24. M.B. Teunissen, M. Haniffa, M.P. Collin, Insight into the immunobiology of human skin and functional specialization of skin dendritic cell subsets to innovate intradermal vaccination design, Curr Top Microbiol Immunol, 351 (2012) 25-76.
25. T. Worbs, S.I. Hammerschmidt, R. Forster, Dendritic cell migration in health and disease, Nat Rev Immunol, 17 (2017) 30-48.
26. F.O. Nestle, X.G. Zheng, C.B. Thompson, L.A. Turka, B.J. Nickoloff, Characterization of dermal dendritic cells obtained from normal human skin reveals phenotypic and functionally distinctive subsets, J Immunol, 151 (1993) 6535-6545.

27. J. Valladeau, S. Saeland, Cutaneous dendritic cells, Semin Immunol, 17 (2005) 273-283.
28. A.E. Morelli, J.P. Rubin, G. Erdos, O.A. Tkacheva, A.R. Mathers, A.F. Zahorchak, A.W. Thomson, L.D. Falo, Jr., A.T. Larregina, CD4+ T cell responses elicited by different subsets of human skin migratory dendritic cells, J Immunol, 175 (2005) 7905-7915.
29. E. Klechevsky, R. Morita, M. Liu, Y. Cao, S. Coquery, L. Thompson-Snipes, F. Briere, D. Chaussabel, G. Zurawski, A.K. Palucka, Y. Reiter, J. Banchereau, H. Ueno, Functional specializations of human epidermal Langerhans cells and CD14+ dermal dendritic cells, Immunity, 29 (2008) 497-510.
30. N. Romani, M. Thurnher, J. Idoyaga, R.M. Steinman, V. Flacher, Targeting of antigens to skin dendritic cells: possibilities to enhance vaccine efficacy, Immunol Cell Biol, 88 (2010) 424-430.
31. E. Segura, J. Valladeau-Guilemond, M.H. Donnadieu, X. Sastre-Garau, V. Soumelis, S. Amigorena, Characterization of resident and migratory dendritic cells in human lymph nodes, J Exp Med, 209 (2012) 653-660.
32. C.M. Fehres, S.C. Bruijns, B.N. Sotthewes, H. Kalay, L. Schaffer, S.R. Head, T.D. de Gruijl, J.J. Garcia-Vallejo, Y. van Kooyk, Phenotypic and Functional Properties of Human Steady State CD14+ and CD1a+ Antigen Presenting Cells and Epidermal Langerhans Cells, PLoS One, 10 (2015) e0143519.
33. G. Rowden, M.G. Lewis, A.K. Sullivan, Ia antigen expression on human epidermal Langerhans cells, Nature, 268 (1977) 247-248.
34. F.O. Nestle, L. Filgueira, B.J. Nickoloff, G. Burg, Human dermal dendritic cells process and present soluble protein antigens, J Invest Dermatol, 110 (1998) 762-766.
35. A.M. van der Aar, R.M. Sylva-Steenland, J.D. Bos, M.L. Kapsenberg, E.C. de Jong, M.B. Teunissen, Loss of TLR2, TLR4, and TLR5 on Langerhans cells abolishes bacterial recognition, J Immunol, 178 (2007) 1986-1990.
36. E. Klechevsky, M. Liu, R. Morita, R. Banchereau, L. Thompson-Snipes, A.K. Palucka, H. Ueno, J. Banchereau, Understanding human myeloid dendritic cell subsets for the rational design of novel vaccines, Hum Immunol, 70 (2009) 281-288.
37. A.M. van der Aar, R. de Groot, M. Sanchez-Hernandez, E.W. Taanman, R.A. van Lier, M.B. Teunissen, E.C. de Jong, M.L. Kapsenberg, Cutting edge: virus selectively primes human langerhans cells for CD70 expression promoting CD8+ T cell responses, J Immunol, 187 (2011) 3488-3492.
38. G. Ratzinger, J. Baggers, M.A. de Cos, J. Yuan, T. Dao, J.L. Reagan, C. Munz, G. Heller, J.W. Young, Mature human Langerhans cells derived from CD34+ hematopoietic progenitors stimulate greater cytolytic T lymphocyte activity in the absence of bioactive IL-12p70, by either single peptide presentation or cross-priming, than do dermal-interstitial or monocyte-derived dendritic cells, J Immunol, 173 (2004) 2780-2791.
39. J. Takeuchi, E. Watari, E. Shinya, Y. Norose, M. Matsumoto, T. Seya, M. Sugita, S. Kawana, H. Takahashi, Down-regulation of Toll-like receptor expression in monocyte-derived Langerhans cell-like cells: implications of low-

responsiveness to bacterial components in the epidermal Langerhans cells, Biochem Biophys Res Commun, 306 (2003) 674-679.

40. V. Flacher, M. Bouschbacher, E. Verronese, C. Massacrier, V. Sisirak, O. Berthier-Vergnes, B. de Saint-Vis, C. Caux, C. Dezutter-Dambuyant, S. Lebecque, J. Valladeau, Human Langerhans cells express a specific TLR profile and differentially respond to viruses and Gram-positive bacteria, J Immunol, 177 (2006) 7959-7967.
41. C. Caux, C. Massacrier, B. Vanbervliet, B. Dubois, I. Durand, M. Cella, A. Lanzavecchia, J. Banchereau, CD34+ hematopoietic progenitors from human cord blood differentiate along two independent dendritic cell pathways in response to granulocyte-macrophage colony-stimulating factor plus tumor necrosis factor alpha: II. Functional analysis, Blood, 90 (1997) 1458-1470.
42. L.C. Zaba, J. Fuentes-Duculan, R.M. Steinman, J.G. Krueger, M.A. Lowes, Normal human dermis contains distinct populations of CD11c+BDCA-1+ dendritic cells and CD163+FXIIIA+ macrophages, J Clin Invest, 117 (2007) 2517-2525.
43. T.D. de Gruijl, S.A. Luykx-de Bakker, B.W. Tillman, A.J. van den Eertwegh, J. Buter, S.M. Lougheed, G.J. van der Bij, A.M. Safer, H.J. Haisma, D.T. Curiel, R.J. Scheper, H.M. Pinedo, W.R. Gerritsen, Prolonged maturation and enhanced transduction of dendritic cells migrated from human skin explants after in situ delivery of CD40-targeted adenoviral vectors, J Immunol, 169 (2002) 5322-5331.
44. L.P. Schneider, A.J. Schoonderwoerd, M. Moutaftsi, R.F. Howard, S.G. Reed, E.C. de Jong, M.B. Teunissen, Intradermally administered TLR4 agonist GLA-SE enhances the capacity of human skin DCs to activate T cells and promotes emigration of Langerhans cells, Vaccine, 30 (2012) 4216-4224.
45. G. Bakdash, L.P. Schneider, T.M. van Capel, M.L. Kapsenberg, M.B. Teunissen, E.C. de Jong, Intradermal application of vitamin D3 increases migration of $CD14^+$ dermal dendritic cells and promotes the development of Foxp3+ regulatory T cells, Hum Vaccin Immunother, 9 (2013) 250-258.
46. P. Schipper, K. van der Maaden, V. Groeneveld, M. Ruigrok, S. Romeijn, S. Uleman, C. Oomens, G. Kersten, W. Jiskoot, J. Bouwstra, Diphtheria toxoid and N-trimethyl chitosan layer-by-layer coated pH-sensitive microneedles induce potent immune responses upon dermal vaccination in mice, J Control Release, (2017).
47. P. Schipper, K. van der Maaden, S. Romeijn, C. Oomens, G. Kersten, W. Jiskoot, J. Bouwstra, Determination of Depth-Dependent Intradermal Immunogenicity of Adjuvanted Inactivated Polio Vaccine Delivered by Microinjections via Hollow Microneedles, Pharm Res, 33 (2016) 2269-2279.
48. P. Schipper, K. van der Maaden, S. Romeijn, C. Oomens, G. Kersten, W. Jiskoot, J. Bouwstra, Repeated fractional intradermal dosing of an inactivated polio vaccine by a single hollow microneedle leads to superior immune responses, J Control Release, 242 (2016) 141-147.
49. K. van der Maaden, S.J. Trietsch, H. Kraan, E.M. Varypataki, S. Romeijn, R. Zwier, H.J. van der Linden, G. Kersten, T. Hankemeier, W. Jiskoot, J. Bouwstra, Novel hollow microneedle technology

for depth-controlled microinjection-mediated dermal vaccination: a study with polio vaccine in rats, Pharm Res, 31 (2014) 1846-1854.

50. K. van der Maaden, J. Heuts, M. Camps, M. Pontier, A. Terwisscha van Scheltinga, W. Jiskoot, F. Ossendorp, J. Bouwstra, Hollow microneedle-mediated micro-injections of a liposomal HPV E743-63 synthetic long peptide vaccine for efficient induction of cytotoxic and T-helper responses, J Control Release, 269 (2018) 347-354.
51. A.M. Römgens, D.L. Bader, J.A. Bouwstra, F.P. Baaijens, C.W. Oomens, Diffusion profile of macromolecules within and between human skin layers for (trans)dermal drug delivery, J Mech Behav Biomed Mater, 50 (2015) 215-222.
52. E. Bond, W.C. Adams, A. Smed-Sorensen, K.J. Sandgren, L. Perbeck, A. Hofmann, J. Andersson, K. Lore, Techniques for time-efficient isolation of human skin dendritic cell subsets and assessment of their antigen uptake capacity, J Immunol Methods, 348 (2009) 42-56.
53. M. Pearton, S.M. Kang, J.M. Song, A.V. Anstey, M. Ivory, R.W. Compans, J.C. Birchall, Changes in human Langerhans cells following intradermal injection of influenza virus-like particle vaccines, PLoS One, 5 (2010) e12410.
54. B. Mahe, A. Vogt, C. Liard, D. Duffy, V. Abadie, O. Bonduelle, A. Boissonnas, W. Sterry, B. Verrier, U. Blume-Peytavi, B. Combadiere, Nanoparticle-based targeting of vaccine compounds to skin antigen-presenting cells by hair follicles and their transport in mice, J Invest Dermatol, 129 (2009) 1156-1164.
55. X. Su, B.S. Kim, S.R. Kim, P.T. Hammond, D.J. Irvine, Layer-by-layer-assembled multilayer films for transcutaneous drug and vaccine delivery, ACS Nano, 3 (2009) 3719-3729.
56. V. Flacher, C.H. Tripp, P. Stoitzner, B. Haid, S. Ebner, B. Del Frari, F. Koch, C.G. Park, R.M. Steinman, J. Idoyaga, N. Romani, Epidermal Langerhans cells rapidly capture and present antigens from C-type lectin-targeting antibodies deposited in the dermis, J Invest Dermatol, 130 (2010) 755-762.
57. F. Sparber, C.H. Tripp, M. Hermann, N. Romani, P. Stoitzner, Langerhans cells and dermal dendritic cells capture protein antigens in the skin: possible targets for vaccination through the skin, Immunobiology, 215 (2010) 770-779.
58. C. Liard, S. Munier, A. Joulin-Giet, O. Bonduelle, S. Hadam, D. Duffy, A. Vogt, B. Verrier, B. Combadiere, Intradermal immunization triggers epidermal Langerhans cell mobilization required for CD8 T-cell immune responses, J Invest Dermatol, 132 (2012) 615-625.
59. T. Rattanapak, J.C. Birchall, K. Young, A. Kubo, S. Fujimori, M. Ishii, S. Hook, Dynamic visualization of dendritic cell-antigen interactions in the skin following transcutaneous immunization, PLoS One, 9 (2014) e89503.
60. L. Filgueira, F.O. Nestle, M. Rittig, H.I. Joller, P. Groscurth, Human dendritic cells phagocytose and process Borrelia burgdorferi, J Immunol, 157 (1996) 2998-3005.
61. A.M. van der Aar, D.I. Picavet, F.J. Muller, L. de Boer, T.M. van Capel, S.A. Zaat, J.D. Bos, H. Janssen, T.C. George, M.L. Kapsenberg, S.M. van Ham, M.B. Teunissen, E.C. de Jong, Langerhans cells favor skin flora tolerance through limited presentation of bacterial antigens and induction

of regulatory T cells, J Invest Dermatol, 133 (2013) 1240-1249.

62. D.J. Campbell, S.F. Ziegler, FOXP3 modifies the phenotypic and functional properties of regulatory T cells, Nat Rev Immunol, 7 (2007) 305-310.
63. D.A. Vignali, L.W. Collison, C.J. Workman, How regulatory T cells work, Nat Rev Immunol, 8 (2008) 523-532.
64. A.D. Nisbet, R.H. Saundry, A.J. Moir, L.A. Fothergill, J.E. Fothergill, The complete amino-acid sequence of hen ovalbumin, Eur J Biochem, 115 (1981) 335-345.
65. N.G. Rouphael, M. Paine, R. Mosley, S. Henry, D.V. McAllister, H. Kalluri, W. Pewin, P.M. Frew, T. Yu, N.J. Thornburg, S. Kabbani, L. Lai, E.V. Vassilieva, I. Skountzou, R.W. Compans, M.J. Mulligan, M.R. Prausnitz, T.-M.S. Group, The safety, immunogenicity, and acceptability of inactivated influenza vaccine delivered by microneedle patch (TIV-MNP 2015): a randomised, partly blinded, placebo-controlled, phase 1 trial, Lancet, 390 (2017) 649-658.
66. H. Okayasu, R.W. Sutter, H.S. Jafari, M. Takane, R.B. Aylward, Affordable inactivated poliovirus vaccine: strategies and progress, J Infect Dis, 210 Suppl 1 (2014) S459-464.
67. E.J. Wherry, K.A. Puorro, A. Porgador, L.C. Eisenlohr, The induction of virus-specific CTL as a function of increasing epitope expression: responses rise steadily until excessively high levels of epitope are attained, J Immunol, 163 (1999) 3735-3745.
68. D.C. Tscharke, N.P. Croft, P.C. Doherty, N.L. La Gruta, Sizing up the key determinants of the CD8(+) T cell response, Nat Rev Immunol, 15 (2015) 705-716.
69. F. Luciani, M.T. Sanders, S. Oveissi, K.C. Pang, W. Chen, Increasing viral dose causes a reversal in CD8$^+$ T cell immunodominance during primary influenza infection due to differences in antigen presentation, T cell avidity, and precursor numbers, J Immunol, 190 (2013) 36-47.
70. D. Sancho, O.P. Joffre, A.M. Keller, N.C. Rogers, D. Martinez, P. Hernanz-Falcon, I. Rosewell, C. Reis e Sousa, Identification of a dendritic cell receptor that couples sensing of necrosis to immunity, Nature, 458 (2009) 899-903.
71. J. Idoyaga, A. Lubkin, C. Fiorese, M.H. Lahoud, I. Caminschi, Y. Huang, A. Rodriguez, B.E. Clausen, C.G. Park, C. Trumpfheller, R.M. Steinman, Comparable T helper 1 (Th1) and CD8 T-cell immunity by targeting HIV gag p24 to CD8 dendritic cells within antibodies to Langerin, DEC205, and Clec9A, Proc Natl Acad Sci U S A, 108 (2011) 2384-2389.
72. L. Bonifaz, D. Bonnyay, K. Mahnke, M. Rivera, M.C. Nussenzweig, R.M. Steinman, Efficient targeting of protein antigen to the dendritic cell receptor DEC-205 in the steady state leads to antigen presentation on major histocompatibility complex class I products and peripheral CD8$^+$ T cell tolerance, J Exp Med, 196 (2002) 1627-1638.
73. K. Mahnke, M. Guo, S. Lee, H. Sepulveda, S.L. Swain, M. Nussenzweig, R.M. Steinman, The dendritic cell receptor for endocytosis, DEC-205, can recycle and enhance antigen presentation via major histocompatibility complex class II-positive lysosomal compartments, J Cell Biol, 151 (2000) 673-684.

SUPPLEMENTARY MATERIALS

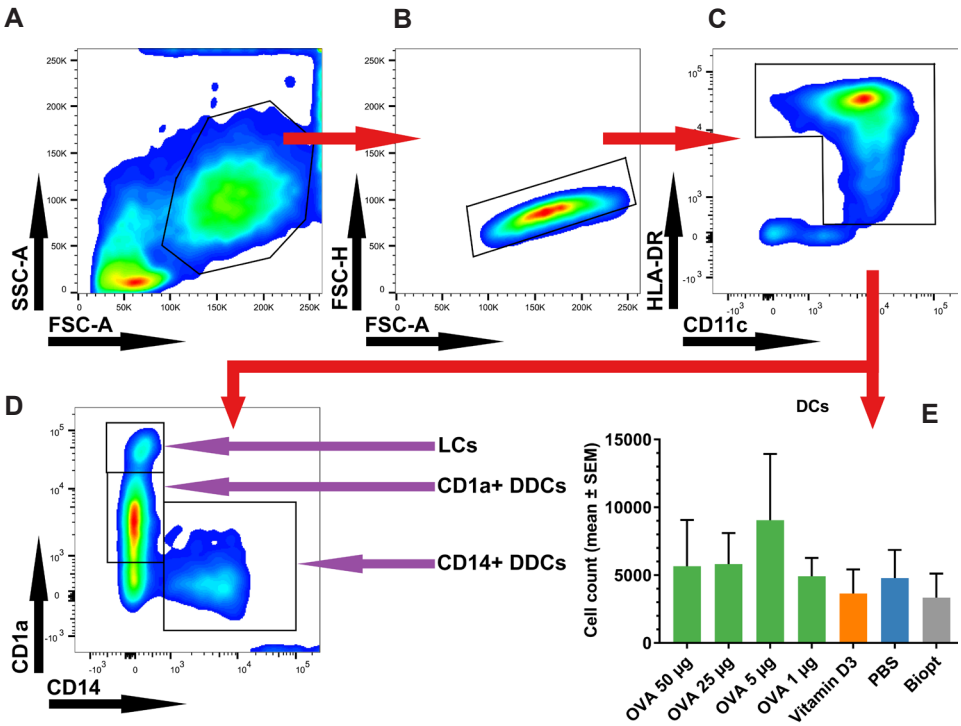

Supplementary Fig. 1 The absolute cell counts of migrated skin DCs was independent of administered OVA dose.

Leukocytes were selected on their forward-scatter and sideward-scatter characteristics (**A**), doublet-cells were excluded by selection on forward-scatter area and -height characteristics (**B**) and finally skin DCs were selected on the expression of CD11c and HLA-DR (**C**). The skin DCs were discriminated in three skin DC subsets, based on the expression of CD14 and CD1a (**D**). LCs were discriminated as $CD1a^{high}/CD14^{-}$, while DDCs were distinguished as $CD1a^{+}$ DDCs (discriminated as $CD1a^{mid}/CD14^{-}$) and $CD14^{+}$ DDCs (discriminated as $CD1a^{-}$/ $CD14^{+}$). The absolute cell counts of migrated skin DCs selected from (**C**) are expressed in (**E**) and are independent of the OVA dose. The dot plots are representative for the flow cytometry experiments. The data in (**E**) represents mean ± SEM (n = 3).

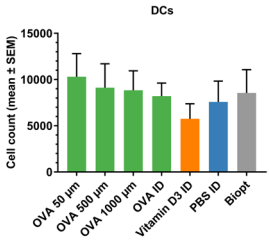

Supplementary Fig. 2 Migration of skin DCs is independent of the depth in skin at which OVA is administered and intradermal administration method.

The absolute cell counts of migrated skin DCs was investigated as function of the depth in skin at which OVA was administered by using a single hollow microneedle, as function of intradermal administration by using a conventional hypodermic needle-and-syringe (ID) of OVA, vitamin D3 or PBS or as function of biopsy alone. The data represents mean ± SEM (*n* = 5).

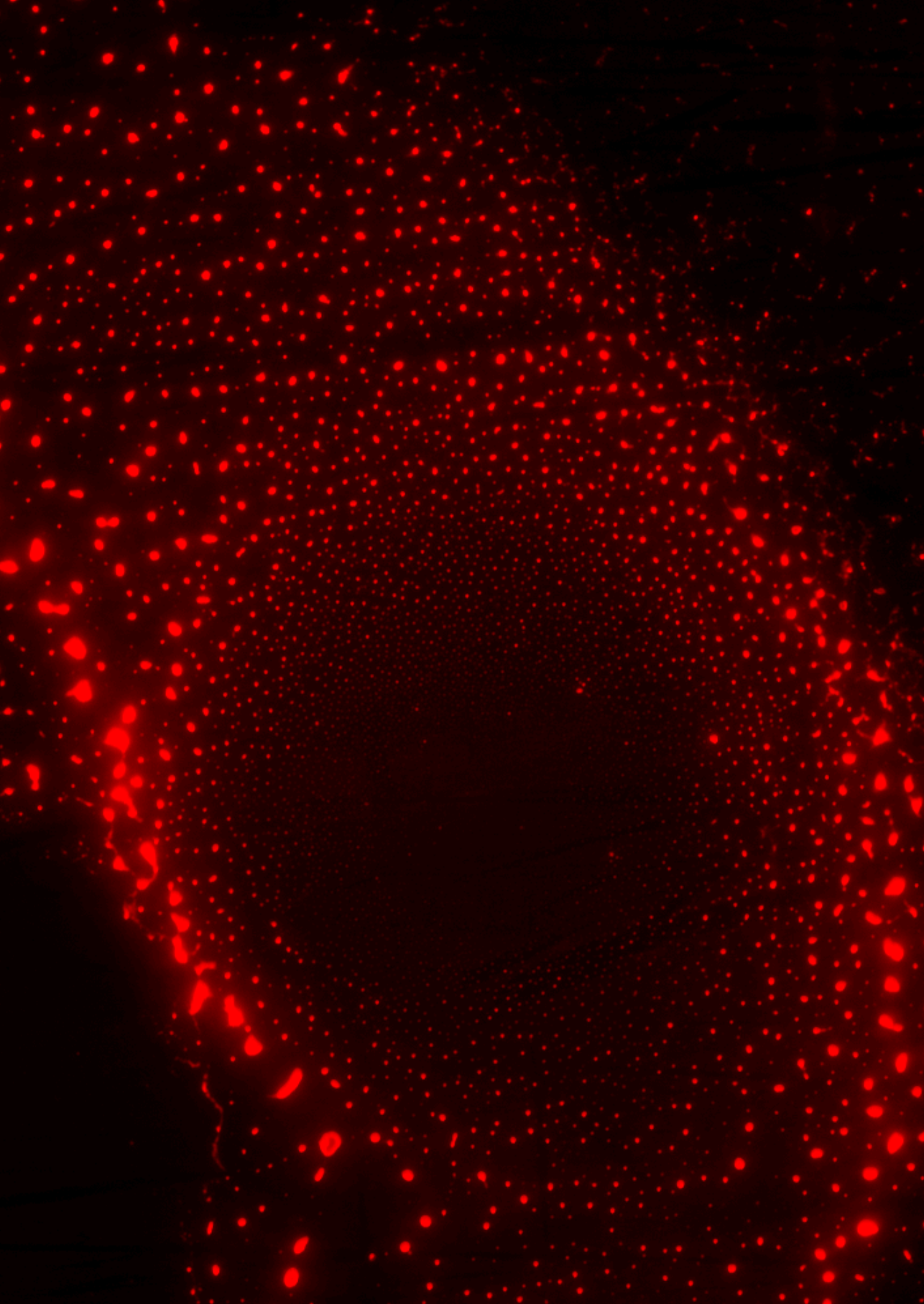

4

Repeated fractional intradermal dosing of an inactivated polio vaccine by a single hollow microneedle leads to superior immune responses

J. Control. Release, 242 (2016) 141-147

Pim Schipper[1], Koen van der Maaden[1], Stefan Romeijn[1], Cees Oomens[2], Gideon Kersten[1,3], Wim Jiskoot[1], Joke Bouwstra[1]

[1] Division of Drug Delivery Technology, Cluster BioTherapeutics, Leiden Academic Centre for Drug Research, Leiden University, Leiden, the Netherlands

[2] Soft Tissue Biomechanics and Engineering, Department of Biomedical Engineering, Eindhoven University of Technology, Eindhoven, the Netherlands

[3] Intravacc (Institute for Translational Vaccinology), Bilthoven, the Netherlands

ABSTRACT

The purpose of this study was to investigate the effect of various repeated fractional intradermal dosing schedules of inactivated polio vaccine serotype 1 (IPV1) on IPV1-specific IgG responses in rats. By utilizing an applicator that allowed for precisely controlled intradermal microinjections by using a single hollow microneedle, rats were immunized intradermally with 5 D-antigen units (DU) of IPV1 at 150 µm skin depth. This dose was administered as a bolus, or in a repeated fractional dosing schedule: 4 doses of 1.25 DU (1/4th of total dose) were administered on four consecutive days or every other day; 8 doses of 0.625 DU (1/8th of total dose) were administered on eight consecutive days; or 4 exponentially increasing doses (0.04, 0.16, 0.8 and 4 DU), either with or without an exponentially increasing CpG oligodeoxynucleotide 1826 (CpG) dose, were administered on four consecutive days. All of these fractional dosing schedules resulted in up to ca. 10-fold higher IPV1-specific IgG responses than intradermal and intramuscular bolus dosing. IPV1 combined with adjuvant CpG in exponential dosing did not significantly increase the IPV1-specific IgG responses further, which demonstrated that maximal responses were achieved by fractional dosing. In conclusion, repeated fractional intradermal IPV1 dosing leads to superior IPV1-specific IgG responses without the use of adjuvants. These results indicate that a controlled release delivery system for intradermal IPV1 delivery can potentiate IPV1-specific IgG responses.

GRAPHICAL ABSTRACT

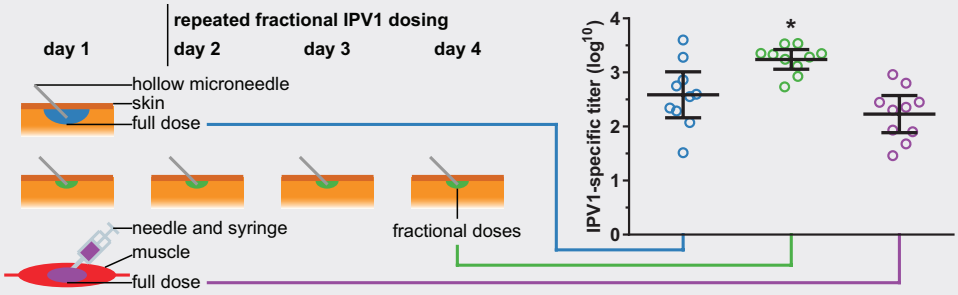

INTRODUCTION

The World Health Organization has initiated a plan to eradicate poliomyelitis completely. Extensive vaccination programs play a major role in this plan [1]. Currently, inactivated polio vaccine (IPV) and oral polio vaccine (OPV) are both used to prevent poliomyelitis. IPV is expensive, because of high production costs and the requirement of a relatively large dose for protection [2]. However, because OPV is based on attenuated live polio virus strains, it carries the risk that it may revert to wildtype poliovirus and cause outbreaks of vaccine-derived polioviruses. Sometimes this results in vaccine-associated paralytic poliomyelitis in vaccinated individuals or their contacts [3, 4]. For that reason, the strategy of the World Health Organization is to replace OPV by IPV [1]. Simultaneously, several strategies to reduce costs for IPV immunization are investigated, including dose sparing strategies, such as adjuvanting IPV [2]. Studies have been conducted focusing on the IPV-specific immune response-enhancing effects of adjuvants, such as aluminum salts, calcium phosphate, oil emulsions, chitosan, vitamin D, CpG oligodeoxynucleotides, stearyl tyrosine, liposomes and others [5-13]. Although adjuvants may increase (antigen-specific) immune responses and may result in antigen dose sparing, they can also cause side-effects, may be expensive and may introduce vaccine formulation stability problems [14]. Therefore, avoidance of adjuvants in vaccine formulations can increase vaccine safety and stability and reduce costs.

As an alternative strategy for dose sparing, other delivery routes than the intramuscular route have gained much interest in recent years [2]. The intradermal delivery route has been regarded as very attractive, as it has been reported that intradermal immunization may result in increased immune responses, owing to the unique immunological properties of the densely packed skin dendritic cells [15]. Indeed, IPV dose sparing has been reported for intradermal IPV immunization of infants by intradermal injections with conventional needles [16]. However, intradermal injections with conventional needles are difficult to perform and painful. Therefore, there is a need for alternative intradermal immunization methods. Microneedle-mediated vaccine delivery is a relatively new strategy to intradermally deliver vaccines in a minimally invasive and potentially pain-free manner [17]. For this reason, microneedle-mediated intradermal IPV immunization was examined in rats, rhesus macaques and humans [6, 13, 18-23]. Previously, we developed hollow microneedles and an applicator for hollow microneedles, [18] that allows precisely controlled intradermal microinjections [13], taking full advantage of the unique immunological properties of the skin. Furthermore, prolonged delivery of a peptide antigen has led to increased immune responses [24]. However, it is unknown whether prolonged delivery of a vaccine antigen that is used in vaccine programs will lead to

increased immune responses as well and whether precise dosing in time is affecting antigen-specific IgG responses.

In the present study, the IPV dose was divided over multiple days using various multi-day dosing schedules and injected into the skin by hollow microneedle-mediated microinjections. In this way, the IPV dose was delivered into the skin in repeated fractional doses. We present that superior IPV-specific immune responses by immunization with repeated fractional doses are induced, without the use of adjuvants and taking advantage of the potentially pain-free IPV delivery into skin by hollow microneedles. This demonstrates that a controlled release delivery system which delivers IPV1 intradermally over multiple days may substantially increase IPV1-specific IgG responses.

MATERIALS

Concentrated sulfuric acid 95-98% and hydrofluoric acid 49% w/w were purchased from Sigma-Aldrich, Zwijndrecht, the Netherlands. Silicone oil AK350 was ordered at Boom, Meppel, the Netherlands and 20 µm inner diameter polyimide coated fused silica capillary at Polymicro, Phoenix, USA. Female Wistar Han IGS rats (Crl:WI(Han), strain code 273, 175-225 g) were obtained from Charles River, Saint-Germain-sur-l'Arbresle, France. Isoflurane 100% w/w was purchased from Abbott, Maidenhead, UK. Phosphate buffered saline (PBS: 163.9 mM Na^+, 140.3 mM Cl^-, 8.7 mM HPO_4^{2-} and 1.8 mM $H_2PO_4^-$, pH 7.4) was ordered at B. Braun Melsungen, Melsungen, Germany and CpG oligodeoxynucleotide 1826 (CpG) at Invivogen, Toulouse, France. 2.5 mL Vacuette® Z-serum-separator clot-activator premium-tubes were obtained from Greiner Bio-One, Alphen a/d Rijn, the Netherlands. Monovalent IPV type-1 (IPV1) was kindly provided by Intravacc, Bilthoven, the Netherlands.

METHODS

Applicator and fabrication of hollow microneedles

Hollow microneedles were produced in-house as previously described [13, 18]. In short, the inner lumen of 20 µm inner diameter polyimide-coated fused-silica capillaries was filled with silicone oil overnight *in vacuo* at 100 °C. These capillaries were wet-etched into hollow microneedles, by immersing one side (± 10 mm) of the capillaries in 49% hydrofluoric acid for 4 h. Next, the polyimide coating was removed by immersing the etched capillaries in concentrated sulfuric acid at 250 °C for 5 min, which resulted in hollow microneedles. An in-house designed hollow microneedle applicator [18], allowing for controllable injection rate, volume and depth [13], was used for intradermal microinjections by these hollow microneedles.

Immunization studies

Animal studies were performed obeying the guidelines and regulations enforced by Dutch law and the animal ethic committee. These studies were approved by the "Dierexperimentencommissie Universiteit Leiden (UDEC)" under number 12084. Female Wistar Han rats (weight on arrival 175-225 g) were housed in groups of five in a controlled environment subjected to guidelines of the animal facilities of the Leiden Academic Centre for Drug Research, Leiden University. The animals were randomly assigned to immunization groups (10 animals per group). Animals were anesthetized

with isoflurane prior to shaving, blood withdrawal and immunization. Animals that were assigned to intradermal immunization groups were shaved (an area of 4 cm^2 on the left posterior flank) prior to the intradermal microinjection. For intradermal immunization, a single hollow microneedle was applied by using an applicator for hollow microneedles to perform microinjections into the skin at a pre-defined skin injection depth, rate and volume of 150 µm, 20 µL/min and 10 µL, respectively. Control groups received intramuscular injections of 100 µL per hind leg (200 µL in total).

Two immunization studies were performed to investigate effects of repeated fractional IPV1 dosing. The dosing schedule of the first study is presented in Table 1. In detail, all groups (except the PBS treated group) received a total IPV1 dose of 5 D-antigen units (5 DU, 1/8th human dose) per immunization course, injected either by intradermal microinjections or by intramuscular injections by a hypodermic 26G needle. The total IPV1 dose was either given at once (bolus), was divided into four 1/4th doses and delivered over four consecutive days (4 x 1/4th (4 d)) or was divided into four exponentially increasing doses and delivered over four consecutive days (Exp). The latter dosing schedule was also performed for IPV1 doses combined with adjuvant CpG (Exp-CpG). The total CpG dose was 10 µg and this dose was also divided into four exponentially increasing doses over four consecutive days, similar to the IPV1 dose. A bolus dose was delivered either by a single hollow microneedle-mediated intradermal microinjection (ID-bolus) or by a single conventional intramuscular injection by a hypodermic needle (IM-bolus). These dosing schedules were performed on day 0 as prime immunization course and these same dosing schedules were repeated, starting on day 21, for a booster immunization course. Blood samples of each individual animal were collected on 7-day intervals, which started on day 0 and ended on day 42. Blood samples were collected in 2.5 mL Vacuette® tubes and stored on ice before centrifugation at 2000g for 10 min to isolate serum, which was stored at -80 °C prior to analysis.

Table 1 Dosing schedule of the first immunization study.

The IPV1 dose delivered during each immunization course (prime and boost) was 5 DU. This dose was delivered as single injection (bolus) or was delivered over 4 days (4 d). The total IPV1 dose delivered in this study after two courses of immunizations (prime and boost) was 10 DU.

Delivery route	Group name	IPV1 dose (DU) on day				IPV1 dose (DU)	
		0 and 21	1 and 22	2 and 23	3 and 24	Per immunization	Total
Intradermal	ID-Bolus	5	-	-	-	**5**	**10**
	4x1/4th (4d)	1.25	1.25	1.25	1.25	**5**	**10**
	Exp	0.04	0.2	0.8	3.96	**5**	**10**
	Exp-CpG*	0.04	0.2	0.8	3.96	**5**	**10**
Intramuscular	IM-Bolus	5	-	-	-	**5**	**10**
	PBS	0	-	-	-	**0**	**0**

* The IPV1 dose was combined with an exponentially increasing CpG dose of 0.08, 0.32, 1.6 and 8 µg, respectively (total CpG dose 10 µg)

A second immunization study was performed to further examine the effect of repeated fractional IPV1 dosing. The dosing schedule of the second study is presented in Table 2. All groups (except the PBS treated group) received a total IPV1 dose of 5 DU in this study. During this study, the total IPV1 dose was either given in bolus, in four 1/4th doses over four consecutive days (4 x 1/4th (4 d)), in four 1/4th doses on every other day over 7 days (4 x 1/4th (7 d)), or in eight 1/8th doses over eight consecutive days (8 x 1/8th (8 d)). No boost immunization course was performed. Blood sampling, collection and storage was performed as described above.

Table 2 Dosing schedule of the second immunization study.

The total IPV1 dose delivered in this study after the single (prime) immunization course was 5 DU. This dose was delivered as single injection (bolus) or was delivered over 4 days (4 d), 7 days (7 d) or 8 days (8 d).

Delivery route	Group name	IPV1 dose (DU) on day								Total IPV1 dose (DU)
		0	1	2	3	4	5	6	7	
Intradermal	ID-Bolus	5	-	-	-	-	-	-	-	**5**
	4 x 1/4th (4 d)	1.25	1.25	1.25	1.25	-	-	-	-	**5**
	4 x 1/4th (7 d)	1.25	-	1.25	-	1.25	-	1.25	-	**5**
	8 x 1/8th (8 d)	0.625	0.625	0.625	0.625	0.625	0.625	0.625	0.625	**5**
Intramuscular	IM-Bolus	5	-	-	-	-	-	-	-	**5**
	PBS	0	-	-	-	-	-	-	-	**0**

IPV1-specific serum IgG titers and virus-neutralization (VN) titers

A capture ELISA was performed to measure IPV1-specific serum IgG titers of the collected serum samples, as previously described [12, 13]. Endpoint titers were determined, which were defined as the reciprocal of the serum dilution that resulted in an absorbance (at 450 nm) equal to the mean plus three times the standard deviation of the absorbance (at 450 nm) of IPV1-specific-antibody negative serum samples. The titer determination of antibodies that neutralize wildtype poliovirus serotype-1 was outsourced to Bilthoven Biologicals (Bilthoven, the Netherlands) and was performed as previously described [12, 25]. VN antibody titers were analyzed on two-fold serially diluted (2^{11}-2^{22}) pooled serum samples of each immunization group of the first immunization study.

Statistical analysis

Statistics were performed by using GraphPad Prism (v.6.00, GraphPad Software, LaJolla, CA, USA). Kruskall-Wallis tests with Dunn's post-hoc tests were performed, as IPV1-specific IgG titers were non-normally distributed. Differences were considered significant at $p < 0.05$.

RESULTS

First immunization study

In the first immunization study, a prime-boost immunization was performed as presented in Table 1. IPV1-specific immune responses resulting from repeated fractional doses delivered by hollow microneedle-mediated intradermal microinjections, were compared to the responses resulting from ID-bolus and IM-bolus dosing. CpG was selected as adjuvant, as in a previous study CpG acted as a potent adjuvant for intradermal IPV1 immunization [13].

As presented in Fig. 1A, at day 21, IPV1-specific IgG responses resulting from any repeated fractional intradermal dosing schedule were significantly increased, compared to conventional IM-bolus dosing. 4 x 1/4th (4 d), Exp and Exp-CpG dosing led to 8.1, 10.2 and 13.2-fold increased IPV1-specific IgG responses, respectively, compared to IM-bolus dosing. Compared to ID-bolus dosing, 4 x 1/4th (4 d), Exp and Exp-CpG dosing resulted in 3.5, 4.5 and 5.8-fold increased IPV1-specific IgG responses, respectively. The IPV1-specific IgG response resulting from Exp-CpG dosing was significantly increased compared to ID-bolus dosing. Although not significantly different, IPV1-specific IgG responses resulting from ID-bolus dosing were 2.3-fold increased versus those resulting from IM-bolus dosing. Additionally, a higher number of low responding individuals (log10 titer < 2) was observed after IM-bolus dosing than ID-bolus dosing. Interestingly, adjuvanted Exp-CpG dosing did not result in significantly increased IPV1-specific IgG responses, compared to unadjuvanted Exp dosing.

After the booster immunization course, the potent IPV1-specific IgG response-enhancing effects by repeated fractional dosing were maintained at day 42 (presented in Fig. 1B). 4 x 1/4th (4 d), Exp and Exp-CpG dosing resulted in 2.9, 4.3 and 7.8-fold increased IPV1-specific IgG responses, respectively, compared to conventional IM-bolus dosing. Compared to ID-bolus dosing, 4 x 1/4th (4 d), Exp and Exp-CpG dosing led to 3.6, 5.4 and 9.6-fold increased IPV1-specific IgG responses, respectively. The latter two dosing schedules resulted in significantly increased IPV1-specific IgG responses compared to IM-bolus and ID-bolus dosing. In contrast to day 21, at this time IM-bolus resulted in a non-significant 1.2-fold higher IPV1-specific IgG responses than those resulting from ID-bolus dosing.

Kinetics of IPV1-specific IgG responses were also determined at 7-day intervals, to examine whether an accelerated response occurs, resulting from repeated fractional intradermal dosing (presented in Fig. 1C and in supplementary Fig. 1 (S1)). At day 7, IPV1-

specific IgG responses in IPV1 immunized groups were significantly increased compared to IPV1-specific IgG responses of these same groups at day 0. From day 14 onwards, Exp and Exp-CpG dosing resulted in significantly increased IPV1-specific IgG responses compared to IM-bolus dosing and Exp-CpG also compared to ID-bolus dosing. At day 28, 7 days after the boost immunization course, IPV1-specific IgG responses had increased sharply, whereafter they leveled off. At day 28 and day 35, significantly higher IPV1-specific IgG responses were observed for any group treated with repeated fractional intradermal dosing (4 x 1/4th (4 d), Exp and Exp-CpG), compared to ID-bolus dosing. As expected, no IPV1-specific IgG responses were observed in the PBS treated group.

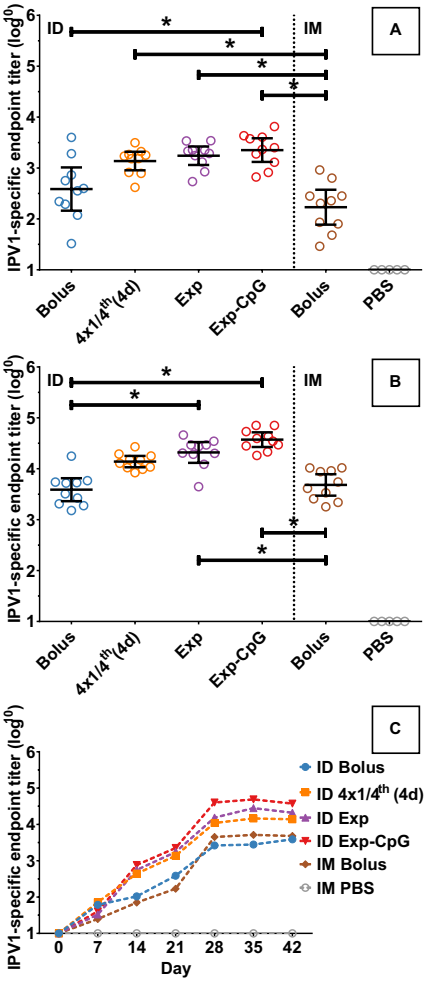

Fig. 1 IPV1-specific serum IgG antibody responses of study 1, at 21 days past the prime immunization course (**A**, day 21), 21 days past the boost immunization course (**B**, day 42) or from day 0 to 42 (**C**).

Dosing schedules are presented in Table 1. Formulations were delivered intradermally by hollow microneedle-mediated microinjections (ID) or intramuscularly by conventional 26G hypodermic needles (IM). In part A and B, bars represent the mean IPV1-specific IgG titer, the error bars the 95% confidence interval and an asterisk (*) designates a statistical significant difference ($p < 0.05$).

Besides measurements of IPV1-specific IgG antibody responses in serum as determined by ELISA, functionality of these serum antibodies was assessed in a VN assay. The serum antibodies resulting from any IPV1-treated group were able to neutralize virus, except the serum antibodies resulting from the PBS treated group (Table 3). VN titers resulting from Exp and Exp-CpG dosing was 2-fold and 4-fold increased, respectively, compared to the VN titer resulting from IM-bolus dosing. Compared to the VN titer resulting from ID-bolus dosing, VN titers resulting from Exp and Exp-CpG dosing were 4-fold and 8-fold increased, respectively.

Table 3 Virus-neutralization (VN) titers for study 1.

Study 1 VN antibody titers measured in serum obtained at day 42, after prime and booster immunization courses. The presented data was measured on a pool of serum samples of all individuals per immunization group. Dosing schedules are presented in Table 1. Formulations were delivered intradermally by hollow microneedle-mediated microinjections or intramuscularly by conventional 26G hypodermic needles.

Immunization route	Dosing schedule	VN titer (log_2)
Intradermal	ID-Bolus	11
	4 x 1/4th (4 d)	11
	Exp	13
	Exp-CpG	14
Intramuscular	IM-Bolus	12
	PBS	0

Second immunization study

In the second immunization study, the effect of different repeated fractional intradermal dosing schedules (see Table 2) was examined. In contrast to the first study, a single immunization course was performed. The IPV1-specific IgG responses resulting from 4 x 1/4th (4 d), 4 x 1/4th (7 d) and 8 x 1/8th (8 d) dosing schedules were compared to responses resulting from IM-bolus and ID-bolus dosing over an extended period of time. The non-responders (one in the 4 x 1/4th (7 d) dosing group and one in the IM-bolus dosing group) were excluded from analyses.

Similar to study 1, all repeated fractional intradermal dosing schedules examined in study 2 led to significantly increased IPV1-specific IgG responses after 21 days, compared to conventional IM-bolus dosing (Fig. 2A). Compared to IM-bolus dosing, 4 x 1/4th (4 d), 4 x 1/4th (7 d) and 8 x 1/8th (8 d) dosing resulted in 15.1, 9.5 and 17.9-fold significantly increased IPV1-specific IgG responses, respectively. Compared to ID-bolus dosing, 4 x 1/4th (4 d), 4 x 1/4th (7 d) and 8 x 1/8th (8 d) dosing resulted in 9.3 (significantly), 5.9 (not significantly) and 11.1-fold (significantly) increased IPV1-specific IgG responses, respectively.

At day 42, only 8 x 1/8th (8 d) dosing resulted in significantly increased IPV1-specific IgG responses, compared to both IM-bolus and ID-bolus dosing (Fig. 2B). Groups treated with 4 x 1/4th (4 d), 4 x 1/4th (7 d) and 8 x 1/8th (8 d) dosing led to 3.8, 3.8 and 9.4-fold increased IPV1-specific IgG responses, respectively, compared to IM-bolus dosing and led to 1.8, 1.8 and 4.5-fold increased responses, respectively, compared to ID-bolus dosing.

Similar to study 1, IPV1-specific IgG responses were examined at 7-day intervals. As presented in Fig. 2C, IPV1-specific IgG responses were already maximal at day 21 for the repeated fractional intradermal dosing groups. The differences in IPV1-specific IgG responses between the repeated fractional intradermal dosing groups and the bolus dosing groups was most evident at day 21 as well, as presented in Fig. 2A and C and in supplementary Fig. 2 (S2). IM-bolus and ID-bolus dosing reached maximal IPV1-specific IgG responses at day 28. From day 28 onwards, IPV1-specific IgG responses resulting from IM-bolus and ID-bolus dosing were comparable and those resulting from 4 x 1/4th (4 d) and 4 x 1/4th (7 d) dosing were comparable. Interestingly, 8 x 1/8th (8 d) dosing already led to a significantly increased IPV1-specific IgG response at day 14 and retained this significant difference, until the end of the study. No IPV1-specific IgG responses were observed in the PBS treated group. Alike the first study, although not significantly different, IPV1-specific IgG responses resulting from ID-bolus dosing were 1.6-fold and

2.1-fold increased at day 21 and at day 42 of the study, respectively, versus the IPV1-specific IgG responses resulting from IM-bolus dosing at those respective days.

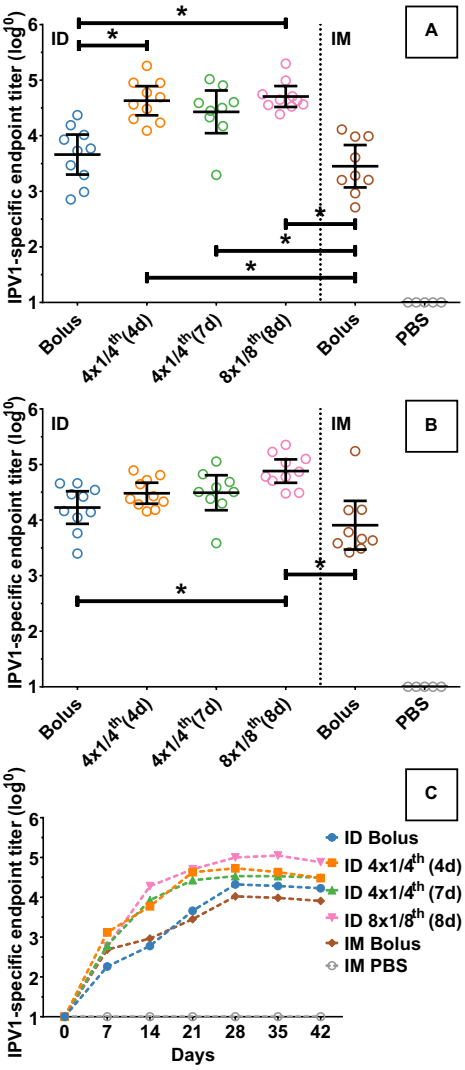

Fig. 2 IPV1-specific serum IgG antibody responses of study 2, at 21 days past the prime immunization course (**A**, day 21), 42 days past the prime immunization course (**B**, day 42) or from day 0 to 42 (**C**). Dosing schedules are presented in Table 2. Formulations were delivered intradermally by hollow microneedle-mediated microinjections (ID) or intramuscularly by conventional 26G hypodermic needles (IM). In part A and B, bars represent the mean IPV1-specific IgG titer, the error bars the 95% confidence interval and an asterisk (*) designates a statistical significant difference ($p < 0.05$).

DISCUSSION

In this study, we investigated whether repeated fractional intradermal dosing would enhance IPV1-specific IgG responses compared to the responses after conventional bolus dosing. To this end, four (4 x 1/4th (4 d), 4 x 1/4th (7 d), Exp or Exp-CpG) or eight (8 x 1/8th (8 d)) fractional IPV1 doses were delivered into skin over an extended time period, or a conventional bolus dose was administered. Repeated fractional intradermal IPV1 dosing led to a significant increase in IPV1-specific IgG responses compared to bolus dosing. Moreover, this effect was robust, as similar IPV1-specific IgG responses resulting from prime immunization by repeated fractional intradermal IPV1 dosing (4 x 1/4th (4 d)) were observed in two individual immunization studies. Therefore, repeated fractional intradermal dosing has a potential for dose sparing, but additional studies need to be performed to further substantiate this.

The use of adjuvants is an important strategy to achieve antigen dose sparing [2]. Although aluminum hydroxide and aluminum phosphate are normally used as adjuvants, they are not allowed for intradermal immunization, due to granuloma formation [26]. However, alternative adjuvants for intradermal IPV bolus dosing have been studied in mouse models: double mutant heat-labile enterotoxin from E. coli LT (R192G/L211A), CpG ODN 2006, CpG ODN 1826, cholera toxin and the CAF01 liposomal formulation resulted in a 2.5-, 4-, 6.9-, 7.3- and 10-fold increase in IPV-specific IgG responses after prime immunization, respectively, compared to unadjuvanted intradermal IPV bolus dosing [7, 10, 13, 27]. In our study, similarly potent increases in IPV1-specific IgG responses were observed upon intradermal delivery of fractional IPV1 doses, even without co-delivery of an adjuvant. In fact, IPV1-specific IgG responses of the Exp-CpG dosing group were similar to those of the (unadjuvanted) Exp dosing group. This demonstrates that by using alternative dosing strategies, antigen-specific immune responses can be increased and the use of an adjuvant can be avoided.

A fast induction of polio immunity is important for disease control during a polio outbreak. Therefore, the kinetics of IPV1-specific IgG responses were examined to determine whether different repeated fractional dosing schedules alter the kinetics of IPV1-specific IgG responses after prime immunization. In both studies, it was observed that repeated fractional dosing resulted in a faster increase in IPV1-specific IgG responses compared to bolus dosing. As presented in the second study, repeated fractional dosing reached maximal IPV1-specific IgG responses at day 21, whereas bolus dosing reached maximal IPV1-specific IgG responses 7 days later. Moreover, it is also important for disease control to boost immunity to stop pathogen replication in previously immunized

individuals. Therefore, booster responses are also important. In the first study, at 7 days after boost immunization, a similarly fast increase in IPV1-specific IgG responses was observed. Although responses were already maximal at that time, fractional dosing retained its significantly increased IPV1-specific IgG titers compared to ID-bolus and IM-bolus dosing. So, repeated fractional dosing resulted in both faster and higher IPV1-specific IgG responses.

For the delivery of IPV, this study was focused on the potential of minimally-invasive intradermal immunization by hollow microneedle-mediated microinjections. In this study, ID-bolus and IM-bolus dosing resulted in two individual immunization studies in slightly (but not-significantly) higher IPV1-specific IgG responses. In the literature, similar results on the comparison of ID-bolus and IM-bolus dosing have been reported in rats, mice and rhesus macaque animal models [6, 7, 13, 18-21]. In humans, the IPV seroconversion rates after intradermal and intramuscular immunization have been compared. Intradermal immunization of IPV naïve newborn infants resulted in either similar [16, 28] or inferior [23, 29, 30] seroconversion rates, compared to intramuscular immunization. Additionally, intradermal booster immunization of previously IPV vaccinated adults resulted in either similar [22, 31] or inferior [32, 33] seroconversion rates, compared to intramuscular immunization. However, intradermal immunization in these studies was performed with 1/5th of a full IPV dose and the resulting seroconversion was compared to the seroconversion which resulted from intramuscular immunization with a full IPV dose. To fully elucidate whether intradermal immunization results in dose-sparing in humans, a dose-response study should be performed comparing intradermal and intramuscular immunization.

Interestingly, there was no significant difference observed between the different repeated fractional dosing schedules. Therefore, fractional dose delivery over 4 or 8 days did not influence the observed effects on IPV1-specific IgG responses. Moreover, in the 4 x 1/4th (4 d) and 4 x 1/4th (7 d) dosing schedules, an equal dose and concentration was delivered at a differentiating time period, but this still resulted in similarly increased IPV1-specific IgG responses. Therefore, it seems that the observed increased IPV1-specific IgG responses are not sensitive to the time period in which the dose is delivered. This demonstrates that flexibility in the fractional dosing schedules is allowed. Therefore, our studies demonstrate that enhanced IgG responses are expected to be achieved, by making use of a controlled release delivery system that is administered by using a single injection and which releases IPV1 over a certain time period, but that the exact release profile does not affect the IPV1-specific IgG levels. The latter observation makes it more easy and attractive to design a controlled release delivery system. This will be subject of

future studies in our group.

The increased immune responses resulting from repeated fractional dosing might stem from prolonged exposure of the antigen to relevant immune cells. It was previously described that antigen depots are formed in germinal centers and that this depot is needed for B-cells to proliferate into plasma B-cells and memory B-cells [34, 35]. Moreover, it has been presented that the exposure time of T-cells to antigens determines the type of responses and level of responses by T-cells, including induction of T-cell memory [24, 36-39]. Therefore, it is likely that by repeated fractional dosing, an immune modulation is triggered by prolonged exposure of the antigen to relevant immune cells. Another potential influencing factor is that antigen delivery over a prolonged time period targets more dendritic cells, as opposed to bolus dosing, as migrated dendritic cells will be replaced by new skin dendritic cells within 16 h [40, 41]. Therefore, whether pulsatile or continuous dosing or alternatively dosing at multiple injection sites is better remains to be elucidated. Furthermore, repeated fractional dosing should be examined in a dose-response study, to precisely quantify dose-sparing effects.

CONCLUSION

In this study, the IPV1 dose was fractionated in 4, 8 or exponential increasing doses and was delivered intradermally over multiple days by minimally-invasive hollow microneedle-mediated microinjections. These repeated fractional intradermal dosing schedules resulted in superior immune responses, compared to ID-bolus and IM-bolus dosing, without the use of adjuvants. Moreover, there were no increased immune responses when fractionated IPV1 doses were adjuvanted with CpG. Furthermore, our data suggests that a controlled release delivery system for the intradermal delivery of IPV1 can lead to increased IPV1-specific IgG responses.

ACKNOWLEDGEMENTS

The authors thank Heleen Kraan for contributions to analysis of IPV1-specific IgG and VN responses; Raphaël Zwier for contributions to improvements of the hollow microneedle applicator; and Anne Römgens for stimulating discussions related to this study.

REFERENCES

1. W. World Health Organization, Polio eradication and endgame strategic plan 2013 - 2018, World Health Organization (WHO), Geneva, Switserland, 2013.
2. H. Okayasu, R.W. Sutter, H.S. Jafari, M. Takane, R.B. Aylward, Affordable inactivated poliovirus vaccine: strategies and progress, J Infect Dis, 210 Suppl 1 (2014) S459-464.
3. C.C. Burns, O.M. Diop, R.W. Sutter, O.M. Kew, Vaccine-derived polioviruses, J Infect Dis, 210 Suppl 1 (2014) S283-293.
4. L.R. Platt, C.F. Estivariz, R.W. Sutter, Vaccine-associated paralytic poliomyelitis: a review of the epidemiology and estimation of the global burden, J Infect Dis, 210 Suppl 1 (2014) S380-389.
5. J. Hawken, S.B. Troy, Adjuvants and inactivated polio vaccine: a systematic review, Vaccine, 30 (2012) 6971-6979.
6. H. Kraan, I. Ploemen, G. van de Wijdeven, I. Que, C. Lowik, G. Kersten, J.P. Amorij, Alternative delivery of a thermostable inactivated polio vaccine, Vaccine, 33 (2015) 2030-2037.
7. E.B. Norton, D.L. Bauer, W.C. Weldon, M.S. Oberste, L.B. Lawson, J.D. Clements, The novel adjuvant dmLT promotes dose sparing, mucosal immunity and longevity of antibody responses to the inactivated polio vaccine in a murine model, Vaccine, 33 (2015) 1909-1915.
8. J.A. White, J.S. Blum, N.A. Hosken, J.O. Marshak, L. Duncan, C. Zhu, E.B. Norton, J.D. Clements, D.M. Koelle, D. Chen, W.C. Weldon, M.S. Oberste, M. Lal, Serum and mucosal antibody responses to inactivated polio vaccine after sublingual immunization using a thermoresponsive gel delivery system, Hum Vaccin Immunother, 10 (2014) 3611-3621.
9. F. de Costa, A.C. Yendo, S.P. Cibulski, J.D. Fleck, P.M. Roehe, F.R. Spilki, G. Gosmann, A.G. Fett-Neto, Alternative inactivated poliovirus vaccines adjuvanted with Quillaja brasiliensis or Quil-a saponins are equally effective in inducing specific immune responses, PLoS One, 9 (2014) e105374.
10. J. Dietrich, L.V. Andreasen, P. Andersen, E.M. Agger, Inducing dose sparing with inactivated polio virus formulated in adjuvant CAF01, PLoS One, 9 (2014) e100879.
11. B.P. Steil, P. Jorquera, J. Westdijk, W.A. Bakker, R.E. Johnston, M. Barro, A mucosal adjuvant for the inactivated poliovirus vaccine, Vaccine, 32 (2014) 558-563.
12. J. Westdijk, P. Koedam, M. Barro, B.P. Steil, N. Collin, T.S. Vedvick, W.A. Bakker, P. van der Ley, G. Kersten, Antigen sparing with adjuvanted inactivated polio vaccine based on Sabin strains, Vaccine, 31 (2013) 1298-1304.
13. P. Schipper, K. van der Maaden, S. Romeijn, C. Oomens, G. Kersten, W. Jiskoot, J. Bouwstra, Determination of Depth-Dependent Intradermal Immunogenicity of Adjuvanted Inactivated Polio Vaccine Delivered by Microinjections via Hollow Microneedles, Pharm Res, 33 (2016) 2269-2279.
14. O.S. Kumru, S.B. Joshi, D.E. Smith, C.R. Middaugh, T. Prusik, D.B. Volkin, Vaccine instability in the cold chain: mechanisms, analysis and formulation strategies, Biologicals, 42 (2014) 237-259.
15. C. Levin, H. Perrin, B. Combadiere, Tailored immunity by skin antigen-presenting cells, Hum Vaccin Immunother, 11 (2015) 27-36.
16. J. Cadorna-Carlos, E. Vidor, M.C. Bonnet, Randomized controlled study of fractional

doses of inactivated poliovirus vaccine administered intradermally with a needle in the Philippines, Int J Infect Dis, 16 (2012) e110-116.

17. K. van der Maaden, W. Jiskoot, J. Bouwstra, Microneedle technologies for (trans)dermal drug and vaccine delivery, J Control Release, 161 (2012) 645-655.
18. K. van der Maaden, S.J. Trietsch, H. Kraan, E.M. Varypataki, S. Romeijn, R. Zwier, H.J. van der Linden, G. Kersten, T. Hankemeier, W. Jiskoot, J. Bouwstra, Novel hollow microneedle technology for depth-controlled microinjection-mediated dermal vaccination: a study with polio vaccine in rats, Pharm Res, 31 (2014) 1846-1854.
19. K. van der Maaden, E. Sekerdag, P. Schipper, G. Kersten, W. Jiskoot, J. Bouwstra, Layer-by-Layer Assembly of Inactivated Poliovirus and N-Trimethyl Chitosan on pH-Sensitive Microneedles for Dermal Vaccination, Langmuir, 31 (2015) 8654-8660.
20. D. Kouiavskaia, O. Mirochnitchenko, E. Dragunsky, E. Kochba, Y. Levin, S. Troy, K. Chumakov, Intradermal inactivated poliovirus vaccine: a preclinical dose-finding study, J Infect Dis, 211 (2015) 1447-1450.
21. C. Edens, N.C. Dybdahl-Sissoko, W.C. Weldon, M.S. Oberste, M.R. Prausnitz, Inactivated polio vaccination using a microneedle patch is immunogenic in the rhesus macaque, Vaccine, (2015).
22. S.B. Troy, D. Kouiavskaia, J. Siik, E. Kochba, H. Beydoun, O. Mirochnitchenko, Y. Levin, N. Khardori, K. Chumakov, Y. Maldonado, Comparison of the Immunogenicity of Various Booster Doses of Inactivated Polio Vaccine Delivered Intradermally Versus Intramuscularly to HIV-Infected Adults, J Infect Dis, 211 (2015) 1969-1976.
23. A. Anand, K. Zaman, C.F. Estivariz, M. Yunus, H.E. Gary, W.C. Weldon, T.I. Bari, M. Steven Oberste, S.G. Wassilak, S.P. Luby, J.D. Heffelfinger, M.A. Pallansch, Early priming with inactivated poliovirus vaccine (IPV) and intradermal fractional dose IPV administered by a microneedle device: A randomized controlled trial, Vaccine, 33 (2015) 6816-6822.
24. P. Johansen, T. Storni, L. Rettig, Z. Qiu, A. Der-Sarkissian, K.A. Smith, V. Manolova, K.S. Lang, G. Senti, B. Mullhaupt, T. Gerlach, R.F. Speck, A. Bot, T.M. Kundig, Antigen kinetics determines immune reactivity, Proc Natl Acad Sci U S A, 105 (2008) 5189-5194.
25. P. Albrecht, G. van Steenis, A.L. van Wezel, J. Salk, Standardization of poliovirus neutralizing antibody tests, Rev Infect Dis, 6 Suppl 2 (1984) S540-544.
26. M. Vogelbruch, B. Nuss, M. Korner, A. Kapp, P. Kiehl, W. Bohm, Aluminium-induced granulomas after inaccurate intradermal hyposensitization injections of aluminium-adsorbed depot preparations, Allergy, 55 (2000) 883-887.
27. C. Yang, H. Shi, J. Zhou, Y. Liang, H. Xu, CpG oligodeoxynucleotides are a potent adjuvant for an inactivated polio vaccine produced from Sabin strains of poliovirus, Vaccine, 27 (2009) 6558-6563.
28. A.J. Mohammed, S. AlAwaidy, S. Bawikar, P.J. Kurup, E. Elamir, M.M. Shaban, S.M. Sharif, H.G. van der Avoort, M.A. Pallansch, P. Malankar, A. Burton, M. Sreevatsava, R.W. Sutter, Fractional doses of inactivated poliovirus vaccine in Oman, N Engl J Med, 362 (2010) 2351-2359.

29. S. Resik, A. Tejeda, P.M. Lago, M. Diaz, A. Carmenates, L. Sarmiento, N. Alemani, B. Galindo, A. Burton, M. Friede, M. Landaverde, R.W. Sutter, Randomized controlled clinical trial of fractional doses of inactivated poliovirus vaccine administered intradermally by needle-free device in Cuba, J Infect Dis, 201 (2010) 1344-1352.
30. S. Resik, A. Tejeda, R.W. Sutter, M. Diaz, L. Sarmiento, N. Alemani, G. Garcia, M. Fonseca, L.H. Hung, A.L. Kahn, A. Burton, J.M. Landaverde, R.B. Aylward, Priming after a fractional dose of inactivated poliovirus vaccine, N Engl J Med, 368 (2013) 416-424.
31. D. Soonawala, P. Verdijk, A.J. Wijmenga-Monsuur, C.J. Boog, P. Koedam, L.G. Visser, N.Y. Rots, Intradermal fractional booster dose of inactivated poliomyelitis vaccine with a jet injector in healthy adults, Vaccine, 31 (2013) 3688-3694.
32. C.F. Estivariz, H. Jafari, R.W. Sutter, T.J. John, V. Jain, A. Agarwal, H. Verma, M.A. Pallansch, A.P. Singh, S. Guirguis, J. Awale, A. Burton, S. Bahl, A. Chatterjee, R.B. Aylward, Immunogenicity of supplemental doses of poliovirus vaccine for children aged 6-9 months in Moradabad, India: a community-based, randomised controlled trial, Lancet Infect Dis, 12 (2012) 128-135.
33. S. Resik, A. Tejeda, O. Mach, M. Fonseca, M. Diaz, N. Alemany, G. Garcia, L.H. Hung, Y. Martinez, R. Sutter, Immune responses after fractional doses of inactivated poliovirus vaccine using newly developed intradermal jet injectors: a randomized controlled trial in Cuba, Vaccine, 33 (2015) 307-313.
34. U. Klein, R. Dalla-Favera, Germinal centres: role in B-cell physiology and malignancy, Nat Rev Immunol, 8 (2008) 22-33.
35. D. Gatto, S.W. Martin, J. Bessa, E. Pellicioli, P. Saudan, H.J. Hinton, M.F. Bachmann, Regulation of memory antibody levels: the role of persisting antigen versus plasma cell life span, J Immunol, 178 (2007) 67-76.
36. A. Shaulov, K. Murali-Krishna, CD8 T cell expansion and memory differentiation are facilitated by simultaneous and sustained exposure to antigenic and inflammatory milieu, J Immunol, 180 (2008) 1131-1138.
37. M.F. Bachmann, R.R. Beerli, P. Agnellini, P. Wolint, K. Schwarz, A. Oxenius, Long-lived memory CD8$^+$ T cells are programmed by prolonged antigen exposure and low levels of cellular activation, Eur J Immunol, 36 (2006) 842-854.
38. G. Iezzi, K. Karjalainen, A. Lanzavecchia, The duration of antigenic stimulation determines the fate of naive and effector T cells, Immunity, 8 (1998) 89-95.
39. T.M. Kundig, A. Shahinian, K. Kawai, H.W. Mittrucker, E. Sebzda, M.F. Bachmann, T.W. Mak, P.S. Ohashi, Duration of TCR stimulation determines costimulatory requirement of T cells, Immunity, 5 (1996) 41-52.
40. C. Liard, S. Munier, A. Joulin-Giet, O. Bonduelle, S. Hadam, D. Duffy, A. Vogt, B. Verrier, B. Combadiere, Intradermal immunization triggers epidermal Langerhans cell mobilization required for CD8 T-cell immune responses, J Invest Dermatol, 132 (2012) 615-625.
41. M. Merad, M.G. Manz, H. Karsunky, A. Wagers, W. Peters, I. Charo, I.L. Weissman, J.G. Cyster, E.G. Engleman, Langerhans cells renew in the skin throughout life under steady-state conditions, Nat Immunol, 3 (2002) 1135-1141.

SUPPLEMENTARY MATERIALS

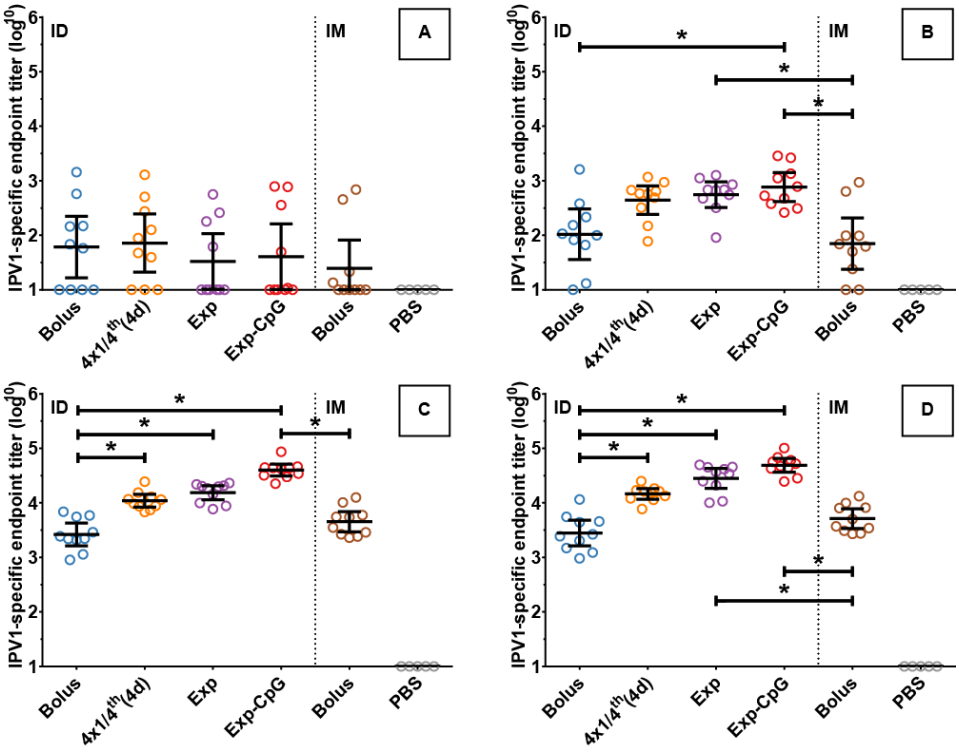

Supplementary Fig. 1 (S1) IPV1-specific serum IgG antibody responses of study 1, at 7 days (**A**, day 7) and 14 days (**B**, day 14) past the prime immunization course or 7 days (**C**, day 28) and 14 days (**D**, day 35) past the booster immunization course. Dosing schedules are presented in Table 1. Formulations were delivered intradermally by hollow microneedle-mediated microinjections (ID) or intramuscularly by conventional 26G hypodermic needles (IM). Bars represent the mean IPV1-specific IgG titer, the error bars the 95% confidence interval and an asterisk (*) designates a statistical significant difference ($p < 0.05$).

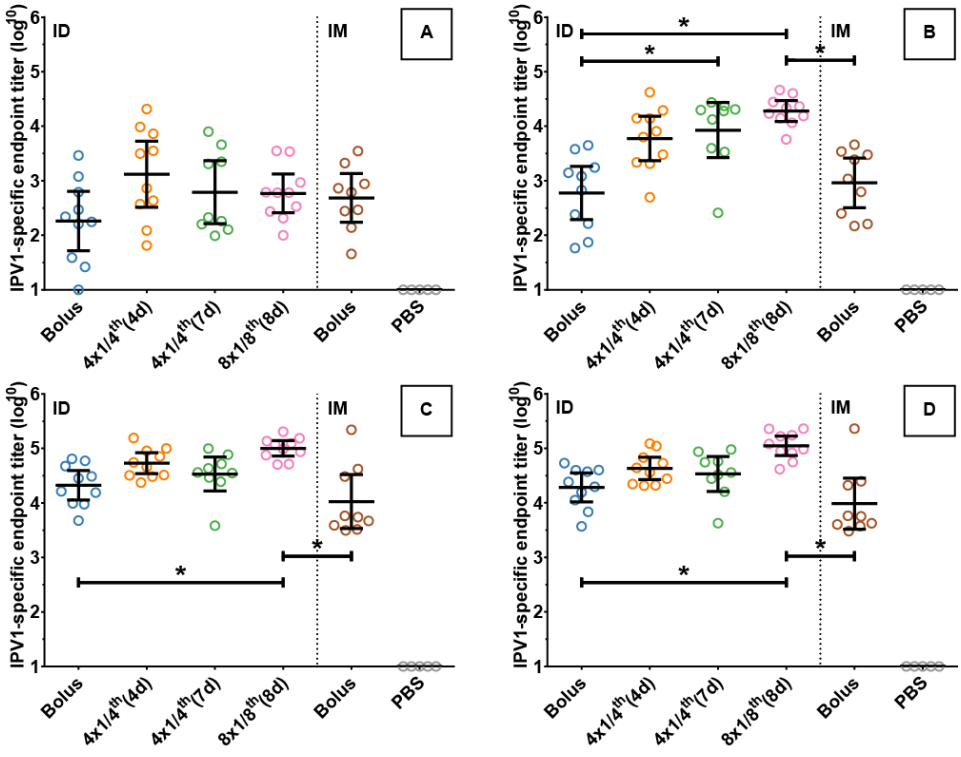

Supplementary Fig. 2 (S2) IPV1-specific serum IgG responses of study 2, at 7 days (**A**, day 7), 14 days (**B**, day 14), 28 days (**C**, day 28) and 35 days (**D**, day 35) past the prime immunization course. Dosing schedules are presented in Table 2. Formulations were delivered intradermally by hollow microneedle-mediated microinjections (ID) or intramuscularly by conventional 26G hypodermic needles (IM). Bars represent the mean IPV1-specific IgG titer, the error bars the 95% confidence interval and an asterisk (*) designates a statistical significant difference ($p < 0.05$).

5

Diphtheria toxoid and N-trimethyl chitosan layer-by-layer coated pH-sensitive microneedles induce potent immune responses upon dermal vaccination in mice

J. Control. Release, 262 (2017) 28-36

Pim Schipper[1], Koen van der Maaden[1], Vincent Groeneveld[1], Mitchel Ruigrok[1], Stefan Romeijn[1], Sven Uleman[3], Cees Oomens[2], Gideon Kersten[1,3], Wim Jiskoot[1], Joke Bouwstra[1]

[1] Division of Drug Delivery Technology, Cluster BioTherapeutics, Leiden Academic Centre for Drug Research, Leiden University, Leiden, The Netherlands

[2] Soft Tissue Biomechanics and Engineering, Department of Biomedical Engineering, Eindhoven University of Technology, Eindhoven, The Netherlands

[3] Intravacc (Institute for Translational Vaccinology), Bilthoven, The Netherlands

ABSTRACT

Dermal immunization using antigen-coated microneedle arrays is a promising vaccination strategy. However, reduction of microneedle sharpness and the available surface area for antigen coating is a limiting factor. To overcome these obstacles, a layer-by-layer coating approach can be applied onto pH-sensitive microneedles. Following this approach, pH-sensitive microneedle arrays (positively charged at coating pH 5.8 and nearly uncharged at pH 7.4) were alternatingly coated with negatively charged diphtheria toxoid (DT) and N-trimethyl chitosan (TMC), a cationic adjuvant. First, the optimal DT dose for intradermal immunization was determined in a dose-response study, which revealed that low-dose intradermal immunization was more efficient than subcutaneous immunization and that the EC_{50} dose of DT upon intradermal immunization is 3-fold lower, as compared to subcutaneous immunization. In a subsequent immunization study, microneedle arrays coated with an increasing number (2, 5, and 10) of DT/TMC bilayers resulted in step-wise increasing DT-specific immune responses. Dermal immunization with microneedle arrays coated with 10 bilayers of DT/TMC (corresponding with ±0.6 µg DT delivered intradermally) resulted in similar DT-specific immune responses as subcutaneous immunization with 5 µg of DT adjuvanted with aluminum phosphate (8-fold dose reduction). Summarizing, the layer-by-layer coating approach onto pH-sensitive microneedles is a versatile method to precisely control the amount of coated and dermally-delivered antigen that is highly suitable for dermal immunization.

5

GRAPHICAL ABSTRACT

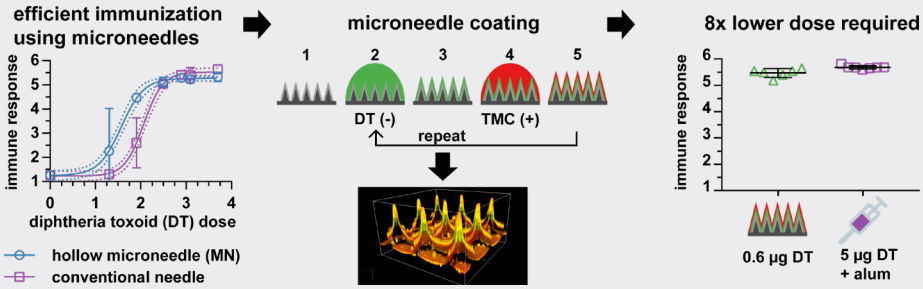

INTRODUCTION

Intradermal immunization has several benefits over conventional immunization by intramuscular bolus injection, as the skin is easily accessible and intradermal immunization is potentially pain-free. Moreover, superior immunization responses resulting from intradermal immunization as compared to conventional intramuscular immunization were reported for hepatitis B [1, 2], influenza [3-8] and polio [9-11]. This may be caused by the specialized dendritic cell subsets that are present in high numbers in the skin [12]. To deliver a sufficient amount of antigen to these cells, the physical barrier of the skin, the stratum corneum, must be overcome [13]. For this purpose microneedles can be used, which are needle-like structures used to pierce the stratum corneum in a minimally-invasive way. Several technologies for microneedle-mediated vaccine delivery are under development [14], such as coated microneedle arrays.

The amount of antigen delivery by coated microneedle arrays may be limited, because of the limited surface area available for coating. Therefore, different approaches have been developed to increase the amount of coated antigen. For example, dipping low-density microneedle arrays in an antigen-containing viscous solution leads to thick coatings containing a high amount of antigen (2 μg) [15, 16]. However, applying the dip-coating technique to high-density microneedle arrays results in blunting of the microneedles, which may impair the skin penetration ability of the microneedles [15, 17-19].

An alternative coating approach resulting in a thin coating is to modify the microneedle surface to control the antigen coating onto microneedle arrays and subsequent release into the skin by pH-dependent electrostatic interactions. In this approach, a negatively charged antigen adheres to a microneedle surface that is positively charged at a coating pH of 5.8. Upon piercing these antigen-coated pH-sensitive microneedles into skin, the electrostatic interactions between the antigen and the microneedles surface cease. This is caused by shifting the pH from a slightly acidic one (of the coating solution) towards a slightly alkaline one (physiological pH (7.4) of the skin). This pH-change induces a change in microneedle surface charge from positive to neutral, respectively [20]. Such pH-sensitive microneedle surface modifications allow to efficiently coat thin layers of antigens onto high-density microneedle arrays and for a controllable and effective antigen delivery.

However, the limitation of this manner of antigen-coating is that only low amounts of antigens can be coated onto microneedle arrays. This limitation can be overcome by using a layer-by-layer coating approach [21-23]. To effectively increase the amount of

antigen coated onto microneedle arrays, multiple layers of antigen and polymer are stacked onto one another, utilizing electrostatic interactions between antigen and polymer. Using this approach, high-density microneedle arrays were successfully coated with inactivated polio vaccine (IPV) particles and the adjuvant N-trimethyl chitosan (TMC) [24]. However, this approach was not yet examined for subunit vaccines such as diphtheria toxoid (DT), which is used in all pediatric vaccination programs worldwide.

In this study, a layer-by-layer coating approach of DT (a negatively charged antigen above a pH of 5) and the adjuvant TMC (a positively charged polymeric adjuvant) on high-density microneedle arrays modified with a pH-sensitive microneedle-surface was developed. It was demonstrated that the amount of DT coated onto the microneedle array was reproducible and the dermally-delivered amount of antigen was tuned by selecting the number of coated DT/TMC bilayers. Furthermore, the DT/TMC-coated microneedle arrays were capable of inducing potent and functional DT-specific immune responses upon dermal application in mice.

MATERIALS

The materials are provided in Supplementary data S1.

METHODS

Preparation of fluorescently labeled DT, aluminum phosphate-adsorbed DT and (fluorescently labeled) TMC

To visualize DT and/or TMC adhesion to microneedle arrays and release into skin, DT and TMC were fluorescently labeled. DT was fluorescently labeled with Alexa Fluor® 488 (DT-AF488) according to the manufacturer's protocol. TMC with a 15% quaternization degree was synthesized as described elsewhere [25], and was fluorescently labeled with rhodamine B isothiocyanate (TMC-RHO) as previously reported [26]. To quantify the delivery of DT into skin, DT was fluorescently labeled with a near-infrared fluorescent label IRDye® 800CW (DT-IRDYE800) according to the manufacturer's protocol. Aluminum phosphate-adsorbed DT (DT-ALUM) was prepared in a DT:alum ratio of 1:30 (w/w) and the adsorption was between 70 and 80% as determined by a DT-specific ELISA, as described elsewhere [27].

DT/TMC layer-by-layer coating approach for high-density microneedle arrays

To coat DT and TMC onto high-density microneedle arrays *via* a layer-by-layer coating approach, the following procedures were used. High-density silicon microneedle arrays with 576 microneedles on a 5x5 mm backplate (microneedle density of 2304 microneedles/cm^2) and a microneedle length of 220 µm were kindly provided by Robert Bosch GmbH (Stuttgart, Germany). In order to produce pH-sensitive microneedle surfaces with a surface pK_a of 6.9, the surfaces of microneedle arrays were chemically modified with a pyridine functional group, as explained in detail elsewhere [20, 24]. Consequently, at a coating pH of 5.8, the microneedle surfaces are positively charged, while (unlabeled and fluorescently labeled) DT is negatively charged and (unlabeled and fluorescently labeled) TMC is positively charged. Subsequently, a layer-by-layer coating approach was used to coat multiple layers of negatively charged DT and positively charged TMC by electrostatic interactions onto the microneedle arrays, as schematically represented in Fig. 1. Optimization of the coating procedure is described in Supplementary data S2. Some studies required the microneedle arrays to be coated with fluorescently labeled DT and fluorescently labeled TMC. For these studies, plain DT was replaced by either fluorescently labeled DT-AF488 or DT-IRDYE800 and plain

TMC was replaced by fluorescently labeled TMC-RHO. The fluorescence of (unlabeled and fluorescently labeled) DT and fluorescently labeled TMC was measured on a Tecan Infinite M1000 plate reader (Männedorf, Switzerland) at excitation and emission wavelengths shown in Table 1.

Table 1 Excitation and emission wavelengths of DT and TMC used for fluorimetric assays (for details, see methods section).

Compound	Fluorescence	Excitation wavelength (nm)	Emission wavelength (nm)
DT	Intrinsic	280	320
DT-AF488	Extrinsic	490	525
DT-IRDYE800	Extrinsic	774	789
TMC-RHO	Extrinsic	550	580

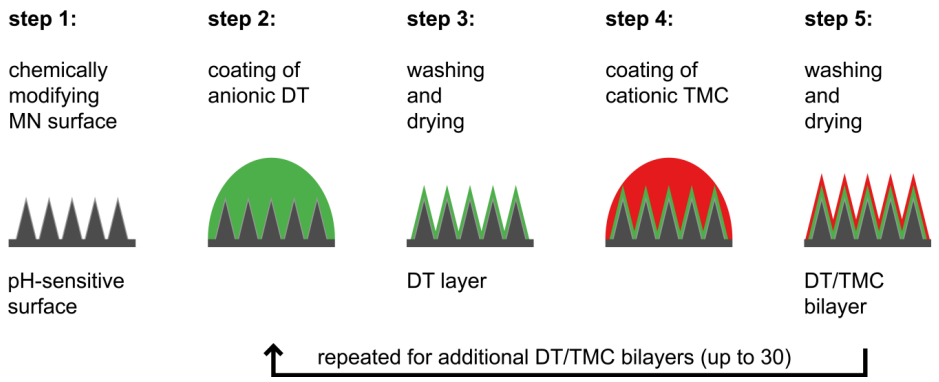

Fig. 1 Schematic illustration of the layer-by-layer coating approach of pH-sensitive microneedle surfaces.

To make use of the electrostatic interactions in the layer-by-layer coating approach, a 1 mM EDTA buffer at pH 5.8 was used as coating buffer, with DT or TMC in a concentration of 40 µg/mL. The first layer of DT was coated by applying a 50 µL droplet of the DT solution onto the pH-sensitive surface of the microneedle array for 30 min at room temperature. Then, the microneedle arrays were washed with 450 µL coating buffer. Subsequently, the microneedle arrays were dried under a flow of nitrogen gas. After drying, a layer of TMC was applied onto the DT-coated surface of the microneedle array, followed by washing and drying, as described above. Then a subsequent DT/TMC bilayer was coated onto the surface of the microneedle arrays, as described above, until the preselected number of DT/TMC bilayers was coated onto the microneedle arrays. The amount of coated DT or TMC, was determined by measuring the fluorescence of DT or fluorescently labeled DT-AF488, DT-IRDYE800 or TMC-RHO in the non-adhered fraction in each of the wash samples.

Scanning electron microscopy (SEM) and confocal laser scanning microscopy (CLSM) imaging of DT/TMC coated microneedle arrays

SEM imaging of DT/TMC coated microneedle arrays was performed to inspect the microneedle tip sharpness, geometry and surface morphology of the microneedles on a FEI NOVA nanoSEM 200 in high-voltage mode (10.0 kV). To this end, 4 microneedle arrays coated with 5 bilayers of DT/TMC and as control, 4 microneedle arrays with only a pH-sensitive surface (plain microneedle arrays) were imaged.

To visualize the distribution of DT and TMC on the surface of DT/TMC coated microneedles, CLSM imaging of microneedle arrays coated with 5 bilayers of fluorescently labeled DT-AF488/TMC-RHO was performed. CLSM was performed by utilizing a Nikon TE2000-E inverted microscope and a Nikon C1 confocal unit (Amsterdam, The Netherlands), in conjunction with a Nikon CFI Plan-Apochromat λ DM 20x (numerical aperture 0.75) objective. An argon laser (488 nm, laser intensity 75 and gain 106) and a 515/30 nm emission filter were used to visualize fluorescently labeled DT-AF488, while a diode-pumped solid-state laser (561 nm, laser intensity 75 and gain 95) and a 590/50 nm emission filter were used to visualize fluorescently labeled TMC-RHO. Nikon NIS Elements software version 4.20.00 was utilized for scan acquisition and analysis. The xy resolution was 1.10 µm/pixel and xyz scans were taken in steps of 2 µm.

Antigenicity and structural integrity of coated DT

To assess whether coated DT remained antigenic, DT or fluorescently labeled DT-AF488 released *in vitro* from 4 microneedle arrays coated with 5 bilayers of DT/TMC or DT-AF488/TMC-RHO, was examined by DT-specific ELISA or fluorescence measurements, respectively. To assess the structural integrity of coated DT, the integrity of *in vitro* released DT-AF488 was determined by measuring the molecular weight by non-reducing SDS-PAGE. *In vitro* release was triggered by submerging DT/TMC coated microneedles in release buffer (5 mM EDTA with 0.9% (w/v) sodium chloride) at pH 7.4, which induces a change to a (nearly) neutral surface charge on the pH-sensitive microneedle surfaces, loss of electrostatic interactions of the DT/TMC bilayers with the microneedle surface and subsequently release of DT and TMC, as explained in detail elsewhere [20]. More detailed procedures for this experiment are provided in Supplementary data S3.

Delivery of DT/TMC into the skin by DT/TMC coated microneedle arrays

Visualization of fluorescently labeled DT-AF488/TMC-RHO delivery into human skin

Human skin was obtained from a local hospital and prepared as described in Supplementary data S4. To examine whether fluorescently labeled DT-AF488 and TMC-RHO can be delivered into human skin by coated microneedle arrays, microneedle arrays

coated with 5 bilayers of fluorescently labeled DT-AF488/TMC-RHO were applied onto *ex vivo* human skin fixed on Styrofoam, by impact insertion using an in-house designed microneedle applicator. An average insertion speed of 0.5 m/s by the microneedle applicator was set on a uPRAX Microsolutions microneedle applicator controller (The Hague, The Netherlands). After insertion, the microneedle arrays were fixed onto the skin by applying a force of 5 N on top of the microneedle array. After 90 min, the microneedle arrays were withdrawn from the skin and immediately prepared for CLSM imaging by fixing the skin in a sample holder. The skin was imaged by CLSM using the same equipment as described above, except that a Nikon CFI Plan-Apochromat λ 4x (numerical aperture 0.2) objective was used. A laser intensity of 75 and gain 95 for the 488 nm laser were used to visualize fluorescently labeled DT-AF488, while a laser intensity of 75 and gain 86 for the 561 nm laser were used to visualize fluorescently labeled TMC-RHO. The xy resolution was 5.18 µm/pixel and xyz scans were taken in steps of 5 µm. The focal plane of the scans was parallel to the surface of the skin.

Quantification of dermally-delivered DT

To study the effect of the number of DT/TMC bilayers on the dermally-delivered DT dose, microneedle arrays coated with an increasing number of fluorescently labeled DT-IRDYE800/TMC bilayers were applied onto *ex vivo* human or mouse skin. The delivered DT dose was quantified by using an intradermally injected calibration curve.

For this purpose, an in-house developed system consisting of a single hollow microneedle and a hollow microneedle applicator was used in conjunction with a uPRAX microneedle applicator controller and a syringe pump (NE-300, Prosense, Oosterhout, The Netherlands). This system allowed for intradermal microinjections at a pre-determined skin depth and an accurate volume [10]. The near-infrared fluorescence of the delivered DT-IRDYE800 was measured in a Perkin-Elmer IVIS Lumina Series III *in vivo* imaging system (Waltham, MA, USA), by using a 745 nm excitation wavelength and an ICG emission filter, acquisition time 4 s, F-stop 2, binning 4 and field of view of 12.5 cm. Perkin-Elmer Living Image software version 4.3.1.0 was used for image acquisition and analysis. Background measurements were taken from control regions of the skin.

Quantification of DT delivered into *ex vivo* human skin by DT/TMC coated microneedle arrays was performed as follows. Microneedle arrays coated with 5 bilayers of fluorescently labeled DT-IRDYE800/TMC were applied onto *ex vivo* human skin for a period of either 30 or 90 min. A calibration curve in *ex vivo* human skin was obtained by intradermal microinjections with an injection volume varying between 0.5 and 20 µL at a DT-IRDYE800 concentration of 150 µg/mL and at an injection depth of 150 µm.

As all immunization studies were performed in mice, quantification of DT delivered by DT/TMC coated microneedle arrays into *ex vivo* mouse skin was also examined. Microneedle arrays coated with either 1, 2, 5, 10 or 20 bilayers of fluorescently labeled DT-IRDYE800/TMC were applied onto *ex vivo* mouse skin for a period of 90 min. A calibration curve in *ex vivo* mouse skin was obtained by intradermal microinjections with injection volumes varying between 0.1 and 10 µL at a DT-IRDYE800 concentration of 300 µg/mL and at an injection depth of 150 µm.

Immunization studies

Animal studies were performed in compliance with the guidelines and regulations enforced by Dutch laws and the Dutch animal ethic committee. These studies were approved by the "Dierexperimentencommissie Universiteit Leiden" under number 14166. Female BALB/c (BALB/cAnNCrl, strain code 028, 6 weeks of age on arrival) were obtained from Charles River, Saint-Germain-sur-l'Arbresle, France. The mice were housed in groups of 4 in a controlled environment subjected to the guidelines of the animal facilities of the Leiden Academic Centre for Drug Research, Leiden University. The mice were randomly assigned to the immunization groups (8 animals per group) and were first acclimatized for 2 weeks after arrival before a study started.

Dose-response study of intradermally- and subcutaneously-delivered DT

To determine the required amount of DT to be delivered by the DT/TMC coated microneedle arrays for sufficient DT-specific immune responses, a DT dose-response study was performed. DT-specific immune responses were determined after intradermal or subcutaneous immunization. DT doses ranging between 0.02 and 5 µg were examined. Detailed experimental descriptions are provided in Supplementary data S5.

Immunization study with DT/TMC coated microneedle arrays

The potential for a dermally applied DT/TMC coated microneedle array to induce DT-specific immune responses was investigated and compared to immunization by an intradermal injection with a single hollow microneedle or a subcutaneous injection. All immunization groups are provided in Table 2.

Immunization was performed at day 1 (prime immunization), day 22 (boost immunization) and day 43 (2nd boost immunization). One day prior to immunization by a DT/TMC coated microneedle array or a single hollow microneedle, the mice were shaved (an area of 4 cm^2 on the left posterior flank). Serum was collected from each mouse one day prior to immunization. Venous blood (200 µL) was drawn by tail vein incision and was collected in a 0.8 mL MiniCollect® tube, which was stored on ice before centrifugation

at 3000g at room temperature for 10 min to isolate serum. At day 63, all mice were sacrificed and bled by incision of the hind leg main artery. This blood was collected in 2.5 mL Vacuette® tubes and stored on ice before centrifugation at 2000g at room temperature for 10 min to isolate serum. Sera were stored at -80 °C until analysis. All mice were immobilized for 90 min by anesthesia with 1% isoflurane (with 100% oxygen as carrier gas) prior to and during immunization. During anesthesia, the eyes of the mice were protected by oculentum simplex.

The following immunization procedures were included in the study:

1. Dermal immunization was performed by applying a microneedle array coated with 2, 5 or 10 bilayers of DT/TMC to the skin. The selected number of coated DT/TMC bilayers was based on two factors: i) the DT-specific immune responses resulting from DT delivered into the skin by a single hollow microneedle as observed in the DT dose-response study and ii) the amount of fluorescently labeled DT-IRDYE800 delivered by microneedle arrays coated with 2, 5 and 10 bilayers into *ex vivo* mouse skin. The DT/TMC coated microneedle arrays were applied onto shaved mouse skin at a speed of 0.5 m/s by the in-house designed impact insertion microneedle applicator in conjunction with a uPRAX microneedle applicator controller and were held in the skin with dermal tape and a specially designed clothespin for 90 min.

2. As control to the dermal immunization with a DT/TMC coated microneedle array, intradermal immunization by microinjection with a single hollow microneedle was performed with i) 0.31 µg DT and ii) 0.31 µg DT mixed with 0.31 µg TMC, using an injection volume of 10 µL at injection depth of 150 µm. The injected DT dose was based on the amount of fluorescently labeled DT-IRDYE800 delivered by a microneedle array coated with 5 bilayers into *ex vivo* mouse skin. The TMC dose was based on the nearly 1:1 coating ratio of DT and TMC. The intradermal microinjections were performed as described above.

3. As controls to the (intra-)dermal immunization, a group of mice received subcutaneous injections of 100 µL *via* a conventional 26G hypodermic needle of i) 0.31 µg DT ii) 5 µg DT and 150 µg $AlPO_4$ (DT-ALUM) as positive control or iii) phosphate buffered saline (PBS) pH 7.4 as mock treatment.

Table 2 Immunization study with DT/TMC coated microneedle arrays.

The study parameters of the various immunization groups are summarized below. The following abbreviations are used. D: dermal, ID: intradermal, MN: microneedle, SC: subcutaneous.

Immunization route	Application method	Group name	DT dose (µg)
D	Coated MN array	2 bilayers DT/TMC	0.05*
		5 bilayers DT/TMC	0.3*
		10 bilayers DT/TMC	0.6*
ID	Single hollow MN	ID DT control	0.31
		ID DT/TMC control	0.31 (+0.31 µg TMC)
SC	Conventional 26G hypodermic needle	SC DT control	0.31
		DT-ALUM**	5 (+ 150 µg $AlPO_4$)
		PBS pH 7.4***	0

* As determined by the amount of DT delivered from microneedle arrays coated with fluorescently labeled DT-IRDYE800/TMC into *ex vivo* mouse skin.

** DT adjuvanted with aluminum phosphate (as positive control).

*** PBS pH 7.4 mock treated group (as negative control).

Determination of DT-specific serum IgG titers and diphtheria toxin-neutralizing antibody titers

To measure DT-specific total IgG, IgG1 and IgG2a titers in serum, an ELISA was performed, of which a detailed description of the procedures is provided in Supplementary data S6. Determination of the antibody titer capable of neutralizing active diphtheria toxin (DTx) was performed as described elsewhere [27].

Statistical analysis

Graphs were plotted as mean (±SEM or ±95% confidence interval for the immunization studies) and statistics were performed by using GraphPad Prism (v.7.00, GraphPad Software, LaJolla, CA, USA). To statistically compare groups amongst each other, Kruskall-Wallis tests with Dunn's post-hoc tests were performed because DT-specific IgG midpoint titers and DTx neutralizing antibody titers were non-normally distributed. Differences were considered significant at $p < 0.05$.

RESULTS

DT/TMC layer-by-layer coating approach for high-density microneedle arrays

Variations in the coating procedure were examined in order to maximize the amount of coated DT for each individual bilayer (see Supplementary data S2 for details). The optimal DT and TMC coating concentrations were 40 µg/mL, which were used for further experiments.

To determine whether an increased number of coated DT/TMC layers resulted in an increased amount of coated DT and TMC, microneedle arrays were coated with up to 30 bilayers of fluorescently labeled DT-AF488 and TMC-RHO. As shown in Fig. 2, 30 bilayers of DT-AF488/TMC-RHO were successfully coated onto the microneedle arrays and the amount of coated DT-AF488 and TMC-RHO increased linearly for up to 30 bilayers. The slopes in Fig. 2 represent the mean amount of coated DT-AF488 and TMC-RHO per bilayer, being 334.1 ng/bilayer (R^2 = 0.9963) for DT-AF488 and 251.5 ng/bilayer (R^2 = 0.9983) for TMC-RHO. The coating was not linear in the first layers, as demonstrated by the intersect with the y-axis, which is -543.8 ng and -89.0 ng for DT-AF488 and TMC-RHO, respectively. After 30 bilayers of DT-AF488/TMC-RHO were coated, 9.67 (±0.51) µg DT-AF488 and 7.58 (±0.38) µg TMC-RHO were cumulatively coated onto the microneedle arrays. Therefore, the ratio of coated DT to TMC was 1.3:1. Furthermore, a coating of 5 bilayers of fluorescently labeled DT-AF488/TMC-RHO resulted in a coated amount of 1.20 (±0.09) µg DT-AF488, while a coating of 5 bilayers of DT/TMC resulted in a coated amount of 2.08 (±0.14) µg DT. These results indicate that DT is coated more efficiently onto the microneedle arrays than fluorescently labeled DT-AF488.

SEM and CLSM imaging of DT/TMC coated microneedle arrays

SEM imaging was performed to determine whether the microneedle tip sharpness, geometry, and surface morphology of microneedles coated with 5 bilayers of DT/TMC were maintained. As demonstrated in Fig. 3A and B, a similar geometry with a tip diameter of < 1 µm and surface morphology were obtained for both plain and coated microneedles.

To visualize the distribution of DT and TMC over the surface of DT/TMC coated microneedles, CLSM imaging was performed on microneedles coated with 5 bilayers of fluorescently labeled DT-AF488/TMC-RHO. As demonstrated in Fig. 3C, DT-AF488 and TMC-RHO were indeed both coated onto the microneedles.

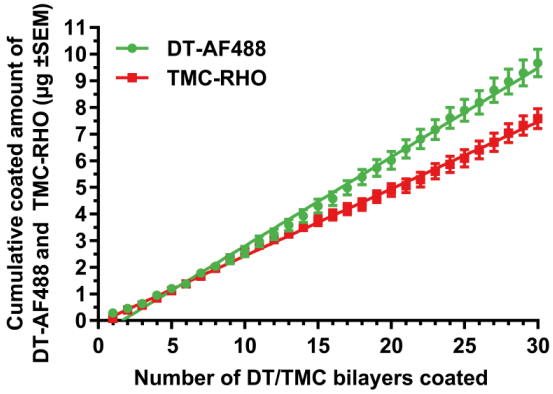

Fig. 2 Coating 30 bilayers of fluorescently labeled DT-AF488 and TMC-RHO.
Cumulative amounts of coated fluorescently labeled DT-AF488 and TMC-RHO by applying 30 DT-AF488/TMC-RHO bilayers onto microneedle arrays *via* a layer-by-layer coating approach. The mean cumulative amounts ± SEM of DT-AF488 (green dots) and TMC-RHO (red squares) coated onto the microneedle array are presented as a function of the number of coated DT-AF488/TMC-RHO bilayers (n = 14).

Antigenicity and structural integrity of coated DT

To assess whether coated DT remained antigenic, DT or fluorescently labeled DT-AF488 released *in vitro* from 4 microneedle arrays coated with 5 bilayers of DT/TMC or DT-AF488/TMC-RHO, was examined by DT-specific ELISA or fluorescence measurements, respectively. The release of DT and DT-AF488 (amount released/amount coated*100%) from the coated microneedle arrays was similar at 28.5% (±0.5) and 29.0% (±2.0) (mean ± SEM), respectively, suggesting that the antigenicity of coated and released DT was preserved.

Non-reducing SDS-PAGE was performed to determine the structural integrity of the coated DT. Fluorescently labeled DT-AF488 released *in vitro* from microneedle arrays coated with 30 bilayers of DT-AF488 and TMC-RHO was analyzed together with control samples of DT-AF488 diluted from stock solution and a mixture of DT-AF488 and TMC-RHO taken from stock solutions. The molecular weight of the coated and released DT-AF488 was comparable to that of the DT-AF488 control samples. Moreover, no bands indicative of fragments or covalent aggregates were observed (data not shown).

Altogether, these results indicate that DT retained its structural integrity and antigenicity after it was released from the microneedle surfaces.

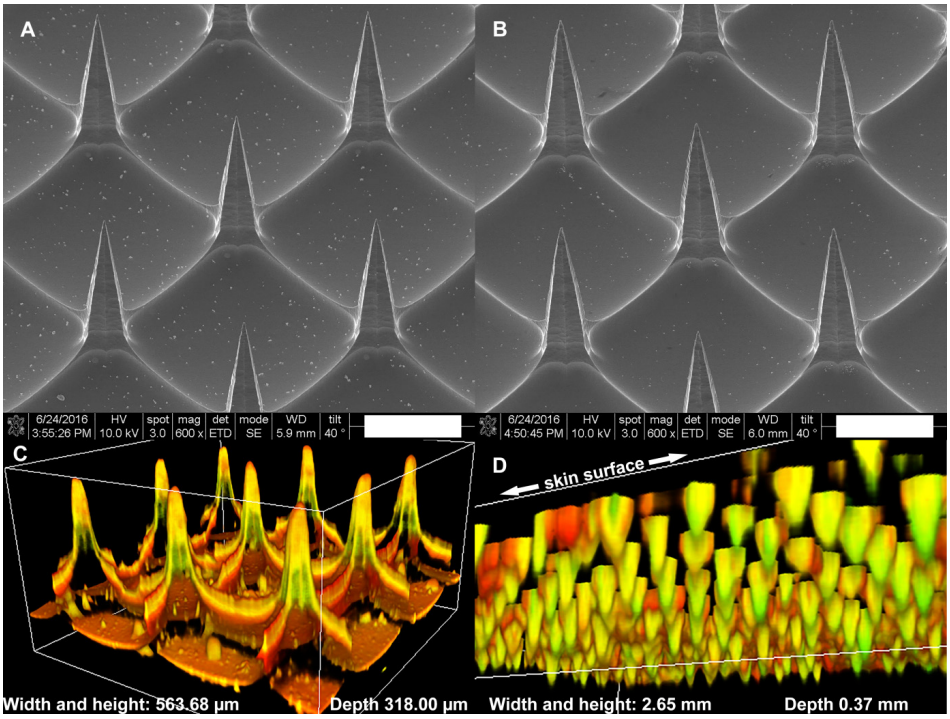

Fig. 3 SEM and CLSM imaging of DT/TMC coated microneedle arrays.

Representative SEM images of plain microneedles (**A**) and microneedles coated with 5 bilayers of DT/TMC (**B**) at 600x magnification, size bars represent 100 µm. Representative CLSM images of (**C**) microneedles coated with 5 bilayers of fluorescently labeled DT-AF488 and TMC-RHO (10x objective) and (**D**) DT-AF488 and TMC-RHO that are released into *ex vivo* human skin, after microneedles coated with 5 bilayers of fluorescently labeled DT-AF488 and TMC-RHO were applied and held in the skin for 90 min and subsequently removed before imaging (4x objective). The images are overlays of DT-AF488 fluorescence represented in green and TMC-RHO fluorescence represented in red.

Visualization of fluorescently labeled DT-AF488/TMC-RHO delivery into human skin

To examine whether fluorescently labeled DT-AF488 and TMC-RHO can be delivered into skin from coated microneedle arrays, microneedle arrays coated with 5 bilayers of DT-AF488/TMC-RHO were applied by impact-insertion and held in *ex vivo* human skin for 90 min. Immediately after withdrawal of the coated microneedles, CLSM imaging of the skin at the injection site was performed. From the image in Fig. 3D, showing fluorescence in the conduits in the skin from both DT-AF488 (green) and TMC-RHO (red), it is clear that DT-AF488 and TMC-RHO were successfully delivered into the skin after application and withdrawal of the DT-AF488/TMC-RHO coated microneedle array.

Quantification of dermally-delivered DT

To quantitatively determine the amount of DT delivered by DT/TMC coated microneedle arrays into the skin, microneedle arrays coated with 5 bilayers of fluorescently labeled DT-IRDYE800/TMC were used. Initially, *ex vivo* human skin studies were conducted to determine the effect of the application period of DT/TMC coated microneedle arrays on the amount of dermally-delivered DT. After application periods of 30 and 90 min, 184 (±16) ng and 293 (±46) ng DT were delivered, respectively. Because a 90 min application period was superior in comparison to a 30 min application period, a 90 min application period was used in subsequent studies.

As the immunization studies with DT/TMC coated microneedle arrays were carried out in mice, subsequent studies were performed on *ex vivo* mouse skin. To determine how the amount of dermally-delivered DT depends on the number of coated DT/TMC bilayers, the amount of dermally-delivered DT by microneedle arrays coated with either 1, 2, 5, 10 or 20 bilayers of fluorescently labeled DT-IRDYE800/TMC was quantified. The amount of dermally-delivered DT-IRDYE800 was linearly dependent on the number of bilayers coated onto the microneedle arrays, as shown in Fig. 4. The slope coefficient for DT-IRDYE800 delivery into *ex vivo* mouse skin was 67.5 ng/layer with a R^2 of 0.9967.

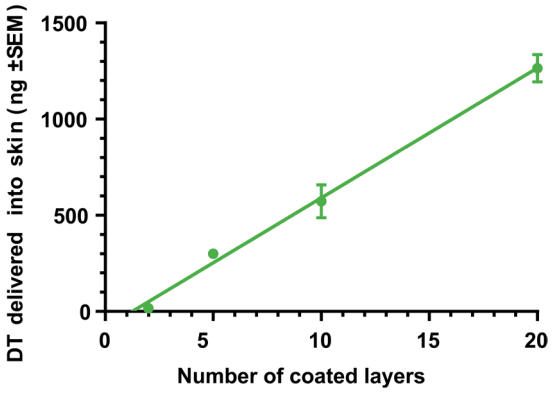

Fig. 4 Quantification of DT delivered into *ex vivo* mouse skin.

Quantification of the amount of fluorescently labeled DT-IRDYE800 (mean ± SEM, *n* = 3) dermally delivered into *ex vivo* mouse skin by microneedle arrays coated with an increasing number of bilayers of fluorescently labeled DT-IRDYE800/TMC.

Dose-response study of intradermally- and subcutaneously-delivered DT

To determine the required amount of dermally-delivered DT for the induction of DT-specific immune responses, a dose-response study was performed. DT was delivered intradermally by using a single hollow microneedle or subcutaneously by a conventional 26G hypodermic needle. The DT-specific IgG responses after the 2nd booster immunization are presented in Fig. 5A (for responses after prime and 1st booster immunization and IgG1:IgG2a ratios see Supplementary data S5). As shown in Fig. 5A, after the 2nd booster immunization, the midpoint (EC_{50}) of the intradermal curve (37 ng) was significantly lower (± 3-fold) than the subcutaneous curve (116 ng). This indicated that higher DT-specific IgG titers using lower DT doses are to be expected from intradermal immunization as compared to subcutaneous immunization. With regard to dose selection, although a DT dose of 0.02 µg already resulted in DT-specific IgG responses, a 0.3 µg dose resulted in similar responses as a 5 µg dose (16.6-fold lower). Moreover, as shown in Fig. 5B, a minimum DT dose of 0.3 µg was required for DTx neutralization titers, whilst a 0.78 µg dose resulted in similar DTx neutralization titers in comparison to a 5 µg dose (6.4-fold lower). Therefore, a minimum dose of 0.3 µg DT is required to be delivered by DT/TMC coated microneedle arrays to induce potent DT-specific IgG titers and DTx neutralization responses.

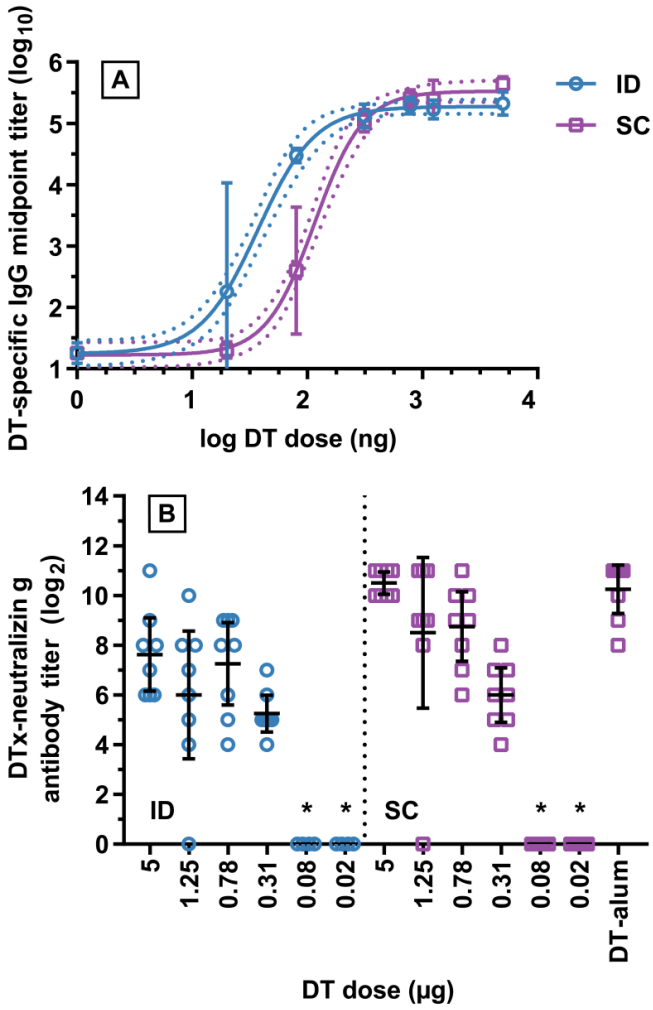

Fig. 5 A dose-response study of DT delivered into the skin.

DT-specific immune responses as a result of intradermal (ID) and subcutaneous (SC) delivery of doses ranging from 0.02 to 5 µg after the 2nd boost immunization. The DT-specific IgG midpoint titers (**A**) and DTx neutralization titers (**B**) are represented by blue circles (ID) and purple squares (SC), respectively. The DT-specific IgG responses were used to plot a 4-parameter fit (solid line) and a 95% confidence interval of that fit (dotted line) in (**A**) (n = 8). The blue and purple lines represent the fit for intradermal and subcutaneous delivery, respectively. Black lines represent the mean ± 95% confidence interval and stars represent a significant decrease ($p < 0.05$) in (**B**) (n = 8).

Immunization study with DT/TMC coated microneedle arrays

To study the potential to induce immunization of dermally-delivered DT by DT/TMC bilayer coated microneedle arrays, the DT-specific immune responses as a function of the number of DT/TMC bilayers (2, 5 and 10) coated onto the microneedle arrays was investigated in an immunization study. As 0.3 µg DT is required to induce DT-specific immune responses upon intradermal immunization (based on results of the dose-response study), microneedle arrays should be coated with at least 5 DT/TMC bilayers (see delivery studies in *ex vivo* skin).

The DT-specific IgG titers increased with an increasing number of coated DT/TMC bilayers after every subsequent immunization (prime, boost and 2nd boost), as shown in Fig. 6A-C. The higher response owing to immunization with an increased number of coated DT/TMC bilayers was also reflected in the DTx neutralization titers after the 2nd boost immunization, as shown in Fig. 6D. After every subsequent immunization, DT-specific IgG titers and DTx neutralization titers resulting from dermal immunization with microneedle arrays coated with 10 bilayers of DT/TMC (corresponding with approximately 0.6 µg delivered DT) and subcutaneous immunization with 5 µg DT-ALUM were not significantly different. The addition of TMC to the DT formulation for intradermal immunization with a single hollow microneedle did not result in increased DT-specific responses. As demonstrated in Fig. 6E, a stepwise decrease in IgG1:IgG2a ratio was observed for immunization by microneedle arrays coated with 2, 5 and 10 bilayers of DT/TMC.

DT-specific responses resulting from subcutaneous immunization with or without anesthesia were similar (data not shown), demonstrating that anesthesia had no effect on the DT-specific immune responses. PBS pH 7.4 mock treatment did not result in any DT-specific IgG titers.

Upon comparing immunization routes, dermal immunization with microneedle arrays coated with 5 or 10 DT/TMC bilayers or intradermal immunization with a single hollow microneedle resulted in higher DT-specific IgG titers in comparison to subcutaneous immunization after the prime and boost immunization. The DT-specific IgG titers of dermal or intradermal and subcutaneous immunization were only comparable after the 2nd boost immunization. These results indicate that dermal or intradermal immunization resulted in a faster development of IgG responses than subcutaneous immunization. A similar trend was observed for the DTx neutralization titers.

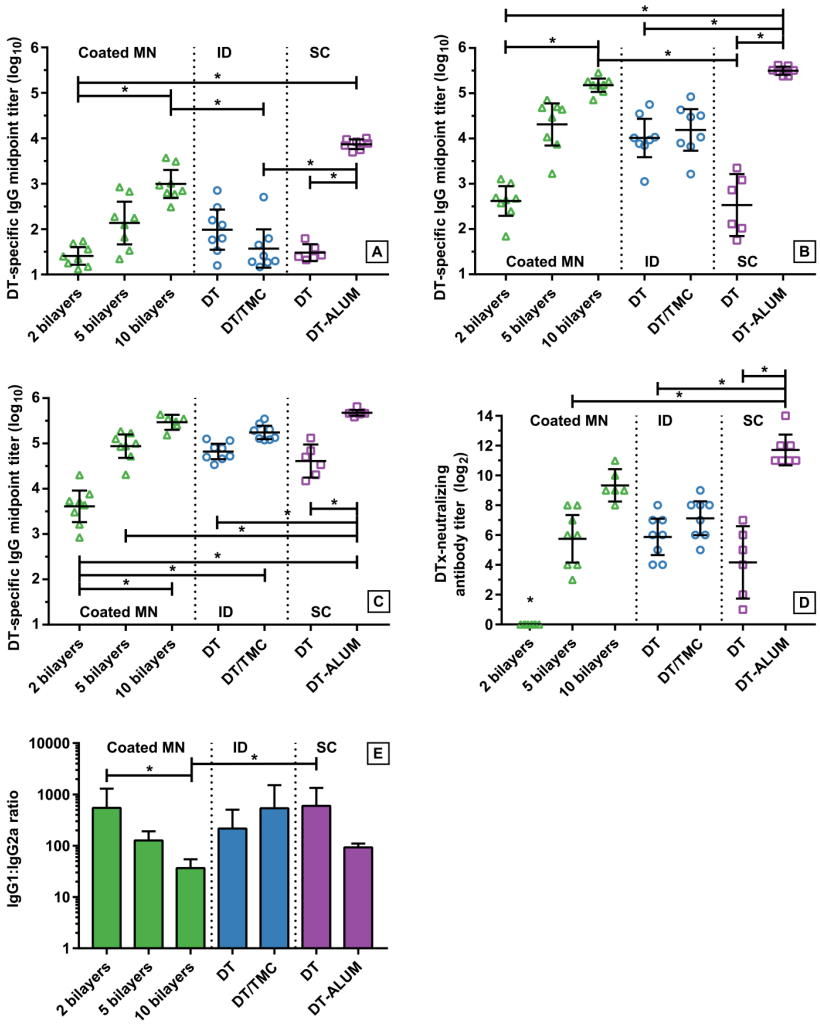

Fig. 6 Immunization study with DT/TMC coated microneedle arrays.

Assessment whether DT/TMC coated microneedle arrays induce DT-specific immune responses, in which a microneedle array coated with an increasing number of DT/TMC bilayers is applied onto the skin and compared to intradermal and subcutaneous control groups (see Table 2). Presented are the DT-specific IgG midpoint titers 21 days past prime immunization (**A**), boost immunization (**B**) and 2nd boost immunization (**C**) resulting from DT immunization *via* the dermal route by a DT/TMC coated microneedle array (coated MN, green triangles or bars), intradermal route by a single hollow microneedle (ID, blue circles or bars) or subcutaneous route by a conventional 26G hypodermic needle (SC, purple squares or bars). DTx neutralization titers (**D**) and IgG1:IgG2a ratios (**E**) were determined in serum at 21 days past the 2nd boost immunization as well. Black lines and bars represent mean ± 95% confidence interval (n = 8) and stars represent a significant increase ($p < 0.05$).

DISCUSSION

In this study, it was demonstrated that the DT/TMC layer-by-layer coating approach on pH-sensitive high-density microneedle arrays offers a tunable vaccine delivery system. The amount of DT that was coated and delivered into the skin was reproducible and could be tuned by selecting the number of coated DT/TMC bilayers. Moreover, dermal immunization of mice by using the DT/TMC coated microneedle arrays resulted in strong functional DT-specific immune responses.

DT/TMC layer-by-layer coating approach for high-density microneedle arrays

The amount of coated DT or TMC incremented linearly with each increasing bilayer of DT/TMC coated onto the microneedle arrays. This was also observed for coating IPV and TMC onto high-density microneedle arrays utilizing a similar layer-by-layer coating approach [24]. This demonstrates that a layer-by-layer coating procedure onto pH-sensitive microneedles is a versatile method to precisely control the amount of coated antigen by selecting the number of coated bilayers. Furthermore, this coating procedure may be applicable, not only to proteins, but also to nanoparticles.

Moreover, the microneedle tips of microneedles coated with 5 bilayers of DT/TMC had a tip diameter < 5 μm, which is required for effortless skin penetration [28]. Coating high-density microneedle arrays while preserving sharp microneedle tips is possible, by using this layer-by-layer coating approach or a nitrogen jet drying coating approach [17, 29], while dip-coating approaches resulted in blunt microneedle tips [15, 17–19]. Furthermore, viscosity enhancers, lyoprotectants or surfactants are not required for this layer-by-layer coating approach, which simplifies the formulation, while coating a high amount of antigen in a thin layer onto the microneedle arrays.

Delivery of DT/TMC into the skin by DT/TMC coated microneedle arrays

Using CLSM, we demonstrated that the DT and TMC delivered by DT/TMC coated microneedle arrays were co-localized in the conduits in the skin, but this method is not suitable to quantify the amount of DT within the skin. For this reason, we measured the near-infrared fluorescence intensity in the skin of DT-IRDYE800 delivered by the coated microneedle arrays.

Although precise dosing has been considered critical in dermal immunization [13, 14], it only has been convincingly addressed in a limited number of studies [30–32]. In the current study, we demonstrate that a linear increase in coated DT with an increasing numbers of DT/TMC bilayers also resulted in a linearly increased amount of DT delivered into

skin, allowing to select a precise dose that is reproducibly delivered into the skin. The delivery efficiency (amount released/amount coated onto the microneedle array*100%) of 16.7% in *ex vivo* mouse skin was comparable to that reported (between 7.6 and 37.5%) for other dry coating approaches for high-density microneedle arrays [29, 32-35].

Immunization studies

Coated microneedle arrays

Dermal immunization by microneedle arrays coated with 10 DT/TMC bilayers led to similar DT-specific immune responses compared with subcutaneous immunization by 5 µg DT-ALUM. The dose delivered in the skin by these coated microneedle arrays was determined at about 0.6 µg, i.e., about 8-fold lower than the subcutaneous dose. Moreover, coated microneedle arrays are easier to use for (intra-) dermal immunization compared to hollow microneedles, which require a sophisticated applicator [14]. Additionally, dry vaccine formulations generally are more stable than liquid ones [14, 15, 18, 33]. Altogether, this demonstrates the potential of antigen-coated microneedle arrays as an alternative for subcutaneous immunization.

The accuracy at which the DT dose was delivered in the skin by selecting an increasing number of DT/TMC bilayers coated onto the microneedle arrays was reflected in the corresponding increasing levels of DT-specific immune responses. For example, dermal immunization with microneedle arrays coated with 5 bilayers of DT/TMC, corresponding with a DT dose of 0.3 µg delivered into the skin, resulted in similar DT-specific immune responses as intradermal immunization with 0.3 µg DT delivered by a single hollow microneedle.

Application mode of the DT/TMC coated microneedle arrays

A supposed drawback of coated microneedle arrays is the lengthy application period of 90 min in the skin to deliver a sufficient amount of antigen. For this reason, in a pilot study a short-lasting repetitive application mode was investigated to strongly reduce the required application time. By using the impact insertion applicator system, microneedle arrays coated with 5 bilayers of DT/TMC were repeatedly applied onto the skin for 10 applications at a frequency of 1 Hz (1 application per second, 10 s total, with an application time of 0.5 s per application). Intriguingly, 10 repeated applications in 10 s resulted in similar DT-specific immune responses as a single 90 min application (Supplementary data S7). Therefore, this application mode permits very short application times, which may increase the attractiveness of the use of coated microneedle arrays even more, from a patient compliance perspective.

Influence of TMC

TMC was used as a poly-cation to enable layer-by-layer coating (as DT is negatively charged at coating pH) and because it has been reported to enhance DT-specific immune responses upon intradermal immunization [26]. However, in the current study only a mild increase in DT-specific immune responses (not significant) was observed, likely because much lower DT and TMC doses were used.

Intradermal versus subcutaneous immunization

It became evident in both immunization studies that (intra-)dermal immunization is more efficient at inducing DT-specific immune responses at low doses as compared to subcutaneous immunization. This high immunization efficiency at low antigen doses could lead to dose-sparing and thereby cost reduction of vaccination programs, which is especially of interest to low-income countries [36].

For both intradermal and subcutaneous immunization, humoral immune responses were dominant over cellular immune responses. This is represented by a high IgG1:IgG2a ratio, as humoral immune responses are characterized by the production of IgG1 antibodies, and cellular immune responses are characterized by the production of IgG2a antibodies [37, 38]. Surprisingly, in contrast to subcutaneous immunization (less dominant humoral immune responses at low antigen doses), upon intradermal immunization the humoral immune responses became predominant at low antigen doses in a dose-dependent manner.

CONCLUSION

In this study, we examined a layer-by-layer coating approach to coat high-density microneedle arrays with DT as anionic antigen and TMC as counter poly-cation and adjuvant. This coating approach allowed to control the amount of DT coated onto the microneedle arrays and delivered into the skin, whilst maintaining tip sharpness and integrity of the coated DT. After studying dose-response of DT immunization *via* the intradermal and subcutaneous route, it was demonstrated that intradermal immunization at low DT doses resulted in superior immune responses compared to subcutaneous immunization. Furthermore, we have demonstrated that immunization by DT/TMC coated microneedle arrays induced strong DT-specific immune responses. Summarizing, the layer-by-layer coating approach onto pH-sensitive microneedles is a versatile method to precisely control the amount of microneedle-coated and dermally-delivered antigen, which is highly-suitable for dermal immunization.

ACKNOWLEDGEMENTS

The authors kindly thank Dr. Michael Stumber (Robert Bosch GmbH) for supplying the microneedle arrays. The authors thank Dr. Reza Nejadnik and Anne France Beker their contributions to the SEM imaging, Dr. Juha Mönkare and Guangsheng Du for their contributions to the *in vivo* studies and Dr. Anne Römgens for stimulating discussions related to this study.

REFERENCES

1. H. Micozkadioglu, A. Zumrutdal, D. Torun, S. Sezer, F.N. Ozdemir, M. Haberal, Low dose intradermal vaccination is superior to high dose intramuscular vaccination for hepatitis B in unresponsive hemodialysis patients, Ren Fail, 29 (2007) 285-288.
2. T. Propst, A. Propst, K. Lhotta, W. Vogel, P. Konig, Reinforced intradermal hepatitis B vaccination in hemodialysis patients is superior in antibody response to intramuscular or subcutaneous vaccination, Am J Kidney Dis, 32 (1998) 1041-1045.
3. F.S. Quan, Y.C. Kim, A. Vunnava, D.G. Yoo, J.M. Song, M.R. Prausnitz, R.W. Compans, S.M. Kang, Intradermal vaccination with influenza virus-like particles by using microneedles induces protection superior to that with intramuscular immunization, J Virol, 84 (2010) 7760-7769.
4. R. Arakane, R. Annaka, A. Takahama, K. Ishida, M. Yoshiike, T. Nakayama, F. Takeshita, Superior immunogenicity profile of the new intradermal influenza vaccine compared to the standard subcutaneous vaccine in subjects 65 years and older: A randomized controlled phase III study, Vaccine, 33 (2015) 6650-6658.
5. D. Holland, R. Booy, F. De Looze, P. Eizenberg, J. McDonald, J. Karrasch, M. McKeirnan, H. Salem, G. Mills, J. Reid, F. Weber, M. Saville, Intradermal influenza vaccine administered using a new microinjection system produces superior immunogenicity in elderly adults: a randomized controlled trial, J Infect Dis, 198 (2008) 650-658.
6. E.V. Vassilieva, H. Kalluri, D. McAllister, M.T. Taherbhai, E.S. Esser, W.P. Pewin, J.A. Pulit-Penaloza, M.R. Prausnitz, R.W. Compans, I. Skountzou, Improved immunogenicity of individual influenza vaccine components delivered with a novel dissolving microneedle patch stable at room temperature, Drug Deliv Transl Res, 5 (2015) 360-371.
7. D.G. Koutsonanos, E.V. Vassilieva, A. Stavropoulou, V.G. Zarnitsyn, E.S. Esser, M.T. Taherbhai, M.R. Prausnitz, R.W. Compans, I. Skountzou, Delivery of subunit influenza vaccine to skin with microneedles improves immunogenicity and long-lived protection, Sci Rep, 2 (2012) 357.
8. Y.C. Kim, F.S. Quan, D.G. Yoo, R.W. Compans, S.M. Kang, M.R. Prausnitz, Improved influenza vaccination in the skin using vaccine coated microneedles, Vaccine, 27 (2009) 6932-6938.
9. P. Schipper, K. van der Maaden, S. Romeijn, C. Oomens, G. Kersten, W. Jiskoot, J. Bouwstra, Repeated fractional intradermal dosing of an inactivated polio vaccine by a single hollow microneedle leads to superior immune responses, J Control Release, (2016).
10. P. Schipper, K. van der Maaden, S. Romeijn, C. Oomens, G. Kersten, W. Jiskoot, J. Bouwstra, Determination of Depth-Dependent Intradermal Immunogenicity of Adjuvanted Inactivated Polio Vaccine Delivered by Microinjections via Hollow Microneedles, Pharm Res, 33 (2016) 2269-2279.
11. J. Cadorna-Carlos, E. Vidor, M.C. Bonnet, Randomized controlled study of fractional doses of inactivated poliovirus vaccine administered intradermally with a needle in the Philippines, Int J Infect Dis, 16 (2012) e110-116.
12. C. Levin, H. Perrin, B. Combadiere, Tailored immunity by skin antigen-presenting cells, Hum

Vaccin Immunother, 11 (2015) 27-36.

13. S.M. Bal, Z. Ding, E. van Riet, W. Jiskoot, J.A. Bouwstra, Advances in transcutaneous vaccine delivery: do all ways lead to Rome?, J Control Release, 148 (2010) 266-282.
14. K. van der Maaden, W. Jiskoot, J. Bouwstra, Microneedle technologies for (trans)dermal drug and vaccine delivery, J Control Release, 161 (2012) 645-655.
15. H.S. Gill, M.R. Prausnitz, Coated microneedles for transdermal delivery, J Control Release, 117 (2007) 227-237.
16. J.M. Song, Y.C. Kim, P.G. Barlow, M.J. Hossain, K.M. Park, R.O. Donis, M.R. Prausnitz, R.W. Compans, S.M. Kang, Improved protection against avian influenza H5N1 virus by a single vaccination with virus-like particles in skin using microneedles, Antiviral Res, 88 (2010) 244-247.
17. X. Chen, T.W. Prow, M.L. Crichton, D.W. Jenkins, M.S. Roberts, I.H. Frazer, G.J. Fernando, M.A. Kendall, Dry-coated microprojection array patches for targeted delivery of immunotherapeutics to the skin, J Control Release, 139 (2009) 212-220.
18. H.S. Gill, M.R. Prausnitz, Coating formulations for microneedles, Pharm Res, 24 (2007) 1369-1380.
19. J.A. Matriano, M. Cormier, J. Johnson, W.A. Young, M. Buttery, K. Nyam, P.E. Daddona, Macroflux microprojection array patch technology: a new and efficient approach for intracutaneous immunization, Pharm Res, 19 (2002) 63-70.
20. K. van der Maaden, H. Yu, K. Sliedregt, R. Zwier, R. Leboux, M. Oguri, A. Kros, W. Jiskoot, J. Bouwstra, Nanolayered chemical modification of silicon surfaces with ionizable surface groups for pH-triggered protein adsorption and release: application to microneedles, J. Mater. Chem. B, 1 (2013) 4466-4477.
21. P.C. DeMuth, X. Su, R.E. Samuel, P.T. Hammond, D.J. Irvine, Nano-layered microneedles for transcutaneous delivery of polymer nanoparticles and plasmid DNA, Adv Mater, 22 (2010) 4851-4856.
22. P.C. DeMuth, J.J. Moon, H. Suh, P.T. Hammond, D.J. Irvine, Releasable layer-by-layer assembly of stabilized lipid nanocapsules on microneedles for enhanced transcutaneous vaccine delivery, ACS Nano, 6 (2012) 8041-8051.
23. P.C. DeMuth, Y. Min, B. Huang, J.A. Kramer, A.D. Miller, D.H. Barouch, P.T. Hammond, D.J. Irvine, Polymer multilayer tattooing for enhanced DNA vaccination, Nat Mater, 12 (2013) 367-376.
24. K. van der Maaden, E. Sekerdag, P. Schipper, G. Kersten, W. Jiskoot, J. Bouwstra, Layer-by-Layer Assembly of Inactivated Poliovirus and N-Trimethyl Chitosan on pH-Sensitive Microneedles for Dermal Vaccination, Langmuir, 31 (2015) 8654-8660.
25. S.M. Bal, B. Slutter, E. van Riet, A.C. Kruithof, Z. Ding, G.F. Kersten, W. Jiskoot, J.A. Bouwstra, Efficient induction of immune responses through intradermal vaccination with N-trimethyl chitosan containing antigen formulations, J Control Release, 142 (2010) 374-383.
26. S.M. Bal, Z. Ding, G.F. Kersten, W. Jiskoot, J.A. Bouwstra, Microneedle-based transcutaneous immunisation in mice with N-trimethyl chitosan adjuvanted diphtheria toxoid formulations, Pharm Res, 27 (2010) 1837-1847.

27. B. Metz, W. Jiskoot, W.E. Hennink, D.J. Crommelin, G.F. Kersten, Physicochemical and immunochemical techniques predict the quality of diphtheria toxoid vaccines, Vaccine, 22 (2003) 156-167.
28. A.M. Romgens, D.L. Bader, J.A. Bouwstra, F.P. Baaijens, C.W. Oomens, Monitoring the penetration process of single microneedles with varying tip diameters, J Mech Behav Biomed Mater, 40 (2014) 397-405.
29. X. Chen, A.S. Kask, M.L. Crichton, C. McNeilly, S. Yukiko, L. Dong, J.O. Marshak, C. Jarrahian, G.J. Fernando, D. Chen, D.M. Koelle, M.A. Kendall, Improved DNA vaccination by skin-targeted delivery using dry-coated densely-packed microprojection arrays, J Control Release, 148 (2010) 327-333.
30. G. Widera, J. Johnson, L. Kim, L. Libiran, K. Nyam, P.E. Daddona, M. Cormier, Effect of delivery parameters on immunization to ovalbumin following intracutaneous administration by a coated microneedle array patch system, Vaccine, 24 (2006) 1653-1664.
31. G.J. Fernando, X. Chen, T.W. Prow, M.L. Crichton, E.J. Fairmaid, M.S. Roberts, I.H. Frazer, L.E. Brown, M.A. Kendall, Potent immunity to low doses of influenza vaccine by probabilistic guided micro-targeted skin delivery in a mouse model, PLoS One, 5 (2010) e10266.
32. G.J. Fernando, X. Chen, C.A. Primiero, S.R. Yukiko, E.J. Fairmaid, H.J. Corbett, I.H. Frazer, L.E. Brown, M.A. Kendall, Nanopatch targeted delivery of both antigen and adjuvant to skin synergistically drives enhanced antibody responses, J Control Release, 159 (2012) 215-221.
33. X. Chen, G.J. Fernando, M.L. Crichton, C. Flaim, S.R. Yukiko, E.J. Fairmaid, H.J. Corbett, C.A. Primiero, A.B. Ansaldo, I.H. Frazer, L.E. Brown, M.A. Kendall, Improving the reach of vaccines to low-resource regions, with a needle-free vaccine delivery device and long-term thermostabilization, J Control Release, 152 (2011) 349-355.
34. G.J. Fernando, J. Zhang, H.I. Ng, O.L. Haigh, S.R. Yukiko, M.A. Kendall, Influenza nucleoprotein DNA vaccination by a skin targeted, dry coated, densely packed microprojection array (Nanopatch) induces potent antibody and CD8(+) T cell responses, J Control Release, 237 (2016) 35-41.
35. M.L. Crichton, A. Ansaldo, X. Chen, T.W. Prow, G.J. Fernando, M.A. Kendall, The effect of strain rate on the precision of penetration of short densely-packed microprojection array patches coated with vaccine, Biomaterials, 31 (2010) 4562-4572.
36. A. Wagstaff, Poverty and health sector inequalities, Bull World Health Organ, 80 (2002) 97-105.
37. J.T. Collins, W.A. Dunnick, Germline transcripts of the murine immunoglobulin gamma 2a gene: structure and induction by IFN-gamma, Int Immunol, 5 (1993) 885-891.
38. E. Severinson, C. Fernandez, J. Stavnezer, Induction of germ-line immunoglobulin heavy chain transcripts by mitogens and interleukins prior to switch recombination, Eur J Immunol, 20 (1990) 1079-1084.

SUPPLEMENTARY MATERIALS

S1 MATERIALS

Ultrapure water (type 1, resistivity 18.2 MΩ·cm at 25 °C) was produced by an Elga Purelab Ultra and was used to prepare aqueous solutions. DT (12.25 mg/mL in Phosphate buffered saline (PBS) pH 7.4) was kindly provided by Intravacc (Bilthoven, The Netherlands). Alexa Fluor® 488 protein labeling kit and 1-Step™ Ultra TMB-ELISA substrate solution were purchased from Thermo Fisher Scientific (Waltham, MA, USA). IRDye® 800CW protein labeling kit was obtained from Li-cor (Lincoln, NE, USA). Adju-Phos® (aluminum phosphate) was purchased from Brenntag (Ballerup, Denmark). Rhodamine B isothiocyanate, ethylenediaminetetraacetic acid (EDTA), sodium chloride, glycine, sodium carbonate, sodium bicarbonate, bovine serum albumin (BSA), glycerol, acetic acid ≥99.7% (v/v), methanol ≥99.9% (v/v), ethanol 96% (v/v), polysorbate 20 and sulfuric acid (95-98%) were ordered at Sigma-Aldrich (Zwijndrecht, The Netherlands). Nitrogen and oxygen gas were purchased from Linde Gas (Schiedam, The Netherlands). Tris(hydroxymethyl)aminomethane-hydrochloride (TRIS-HCL), sodium dodecyl sulfate (SDS), 7.5% polyacrylamide (pre-cast) gels, reference molecular weight ladders and fixative enhancer were ordered at Bio-Rad (Hercules, CA, USA). Parafilm M® was obtained from Bemis (Monceau-sur-Sambre, Belgium). Styrofoam (5 cm thick) was purchased from a local hardware store. Polystyrene 48-well and 96-well microtiter plates, 0.8 and 2.5 mL Vacuette® Z serum separator clot activator premium tubes were ordered at Greiner Bio-One (Alphen aan den Rijn, The Netherlands). PBS pH 7.4 (163.9 mM Na^+, 140.3 mM Cl^-, 8.7 mM HPO_4^{2-} and 1.8 mM $H_2PO_4^-$, pH 7.4) was purchased from B. Braun Melsungen, Melsungen, Germany. PBS pH 7.2 (160.6 mM Na^+, 155.2 mM Cl^-, 2.7 mM HPO_4^{2-}, 1.5 mM $H_2PO_4^-$ and 1.5 mM K^+, pH 7.2) was ordered at Gibco (Thermo Fisher Scientific (Waltham, MA, USA)). Rompun® (20 mg/mL xylazine, Bayer B.V., Mijdrecht, The Netherlands), Nimatek® (100 mg/mL ketamine, Eurovet Animal Health B.V., Bladel, The Netherlands) and oculentum simplex were obtained from a local pharmacy. IsoFlo® (isoflurane 100% w/w) was ordered at Abbott Laboratories, Maidenhead, UK. Horseradish peroxidase-conjugated goat-anti-rat IgG, IgG1 and IgG2a were obtained from Southern Biotech, Birmingham, AL, USA.

S2 OPTIMIZATION OF THE DT/TMC LAYER-BY-LAYER COATING APPROACH FOR HIGH-DENSITY MICRONEEDLE ARRAYS

METHODS

Variations in the coating procedure were examined in order to maximize the amount of coated DT for each individual bilayer. Firstly, the influence of the DT concentration in the coating formulation on the cumulative amount of coated DT over 5 bilayers of DT/TMC was determined. The DT concentration was varied from 10 to 40 µg/mL in the coating

buffer (1 mM EDTA buffer at pH 5.8), while the TMC concentration was kept constant at 10 µg/mL in the coating buffer. Secondly, the influence of TMC on the cumulative amount of coated DT over 5 bilayers of DT/TMC was examined. The TMC concentration was varied from 10 to 40 µg/mL in the coating buffer, while the DT concentration was kept constant at 40 µg/mL in the coating buffer.

RESULTS

As shown in Supplementary Fig. S2A, the cumulative amount of DT coated over 5 bilayers of DT/TMC was highest, when a DT concentration of 40 µg/mL was used. As shown in Supplementary Fig. S2B, the cumulative amount of DT coated over 5 bilayers of DT/TMC was highest when a TMC concentration of 40 µg/mL was used.

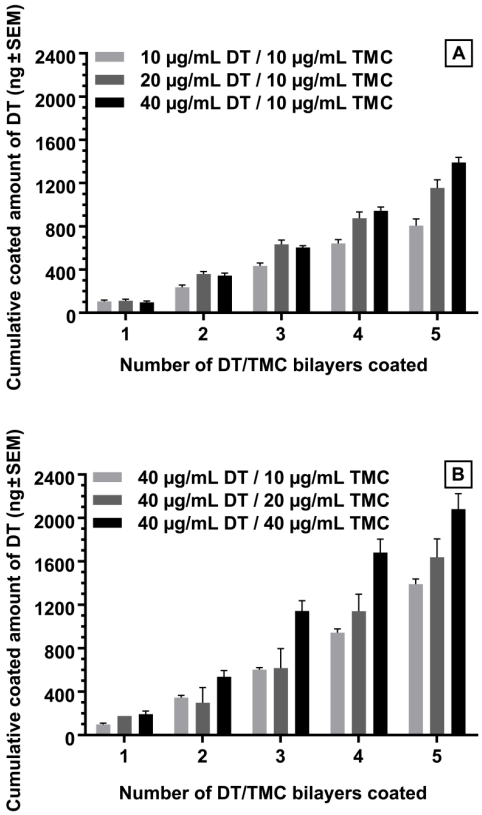

Supplementary Fig. S2 Optimization of the DT/TMC layer-by-layer coating approach.

Effects of variations in the DT/TMC layer-by-layer coating approach on the cumulative amount of coated antigen. The mean cumulative amount ± SEM of coated DT after each incrementally coated DT/TMC bilayer is presented in (**A**) for different DT coating concentrations and a constant TMC coating concentration and in (**B**) for different TMC coating concentrations and a constant DT coating concentration (n = 8).

S3 ANTIGENICITY AND STRUCTURAL INTEGRITY OF COATED DT

METHODS

To assess whether coated DT remained antigenic, DT or fluorescently labeled DT-AF488 released *in vitro* from 4 microneedle arrays coated with 5 bilayers of DT/TMC or DT-AF488/TMC-RHO, was examined by DT-specific ELISA or fluorescence measurements, respectively. To initiate the DT release *in vitro*, each DT/TMC or DT-AF488/TMC-RHO coated microneedle array was placed in a well of a 48-well plate and 500 µL of release buffer (5 mM EDTA at pH 7.4 with 0.9% (w/v) sodium chloride) was added, followed by a 30 min incubation period at room temperature. The release of DT/TMC *in vitro* was triggered by changing the pH-sensitive microneedle surfaces from cationic to neutral by a pH-shift from slightly acidic towards physiological pH (7.4), as explained in detail elsewhere [S3-1]. Subsequently, DT or fluorescently labeled DT-AF488 was quantified in the supernatant: DT by a DT-specific sandwich ELISA (performed as described elsewhere [S3-2]) and fluorescently labeled DT-AF488 by fluorescence.

To assess the structural integrity of coated DT, 4 microneedle arrays were coated with 30 bilayers of fluorescently labeled DT-AF488/TMC-RHO. After *in vitro* release of the coated DT-AF488 as described above, the integrity of DT-AF488 was determined by measuring the molecular weight of released DT-AF488 by non-reducing SDS-PAGE as follows. The *in vitro* released fluorescently labeled DT-AF488, reference DT-AF488, fluorescently labeled TMC-RHO and a mixture of DT-AF488 and TMC-RHO (weight ratio 1:1), were mixed 1:1 with sample buffer (60 mM TRIS-HCL pH 6.8, 25% (v/v) glycerol and 2% (w/v) SDS), of which 50 µL was loaded onto a 7.5% polyacrylamide gel. Reference molecular weight ladders were added as well, after which samples were electrophoretically separated at 80 Volts for 10 min followed by 120 Volts for 45 min in running buffer (25 mM TRIS-HCL pH 8.3, 192 mM glycine, 0.1% (w/v) SDS). Subsequently, gels were fixated in fixation buffer (50% (v/v) methanol, 10% (v/v) acetic acid and 10% (v/v) fixative enhancer) in the dark on an orbital shaker for 20 min before analysis by fluorescence detection by a Bio-Rad ChemiDoc MP gel imaging system (Hercules, CA, USA). Fluorescently labeled DT-AF488 and TMC-RHO and the molecular weight ladder were detected by fluorescence by using settings to detect AF488, rhodamine and Cy5, respectively. Bio-Rad Image Lab™ software version 4.1 was used for image acquisition and analysis.

REFERENCES

[S3-1] K. van der Maaden, H. Yu, K. Sliedregt, R. Zwier, R. Leboux, M. Oguri, A. Kros, W. Jiskoot, J. Bouwstra, Nanolayered chemical modification of silicon surfaces with ionizable surface groups for pH-triggered protein adsorption and release: application to microneedles, J Mater Chem B, 35 (2013) 4466-4477.

[S3-2] G.F. Kersten, W. Jiskoot, T. Hazendonk, E.C. Beuvery, In vitro determination of antigen quality: biosensor analysis and fluorescence spectroscopy, Dev Biol Stand, 92 (1998) 295-300.

S4 PREPARATION OF *EX VIVO* SKIN

To examine the DT/TMC delivery into skin, *ex vivo* human and *ex vivo* mouse skin were used. Abdominal *ex vivo* human skin was obtained from local hospitals after cosmetic surgery. The subcutaneous fat was removed and the skin was cleaned as described below. Cleaning was performed by using PBS pH 7.4, 70% (v/v) ethanol and PBS pH 7.4 again. The skin was then dermatomed to 600 µm thickness by using a Padgett Electro Dermatome Model B dermatome (Kansas City, MO, USA) and it was frozen at -80 °C in a Petri dish containing a wetted tissue, to prevent excess drying during thawing. *Ex vivo* mouse skin was isolated from BALB/c mice, immediately after being sacrificed, and was frozen at -80 °C in a Petri dish containing a wetted tissue. Prior to use, *ex vivo* human or mouse skin was thawed at 37 °C, the mouse skin was shaved and the skin was cleaned. Subsequently, the skin was slightly pre-stretched by pinning the skin on a flat piece of Parafilm-covered Styrofoam.

S5 DOSE-RESPONSE STUDY OF INTRADERMALLY- AND SUBCUTANEOUSLY-DELIVERED DT

METHODS

DT-specific immune responses resulting from intradermal DT immunization were compared to those resulting from subcutaneous DT immunization. For the intradermal immunization, a single hollow microneedle was used in combination with the single hollow microneedle applicator system, to perform intradermal microinjections at a pre-defined skin injection volume and -depth of 10 µL and 150 µm, respectively [S5]. Subcutaneous immunization groups received an injection of 100 µL with a conventional 26G hypodermic needle in the skin-fold of the neck. For both immunization routes, mice were immunized with a DT dose of 5, 1.25, 0.78, 0.31, 0.08 or 0.02 µg. As positive control,

one group received subcutaneous injections of 5 µg DT and 150 µg $AlPO_4$ (DT-ALUM). A mock treated group received subcutaneous injections of PBS pH 7.4. Immunization was performed at day 1 (prime immunization), day 22 (boost immunization) and day 43 (2nd boost immunization). Mice that were assigned to intradermal immunization, were shaved (an area of 4 cm^2 on the left posterior flank) one day prior to immunization, at day 0, 21 and 42, and were immobilized during immunization by anesthesia with a mixture of ketamine (150 mg/kg) and xylazine (10 mg/kg). During anesthesia, the eyes of the mice were covered by oculentum simplex for protection of the eyes. Serum was collected from all mice one day prior to immunization. Venous blood (200 µL) was drawn by tail vein incision and was collected in a 0.8 mL MiniCollect® tube, which was stored on ice before centrifugation at 3000g at room temperature for 10 min to isolate serum, which was stored at -80 °C until analysis. At day 63, all mice were sacrificed and bled by incision of the hind leg main artery. This blood was collected in 2.5 mL Vacuette® tubes and stored on ice before centrifugation at 2000g at room temperature for 10 min to isolate serum, which was stored at -80 °C until analysis. Dose-response titration curves were calculated by a 4-parameter fit on the log10 values of the DT dose (in ng) versus the DT-specific total IgG midpoint titers.

RESULTS

After the prime immunization at day 21, DT-specific IgG titers resulting from intradermal and subcutaneous delivery were equal at low doses, as shown in Supplementary Fig. S5A. Although DT-specific IgG titers resulting from subcutaneous delivery at the highest dose of 5 µg appeared higher compared to intradermal delivery, this was not significant ($p = 0.16$). The bottom, top, hillslope and the midpoint (EC_{50}) of the dose-response curves resulting from intradermal or subcutaneous delivery were similar.

Three weeks after the first boost immunization, DT-specific IgG titers resulting from intradermal delivery were increased in comparison to subcutaneous delivery when lower DT doses were injected, as shown in Supplementary Fig. S5B. The bottom and hillslope of the dose-response curves resulting from intradermal or subcutaneous delivery were similar. However, the midpoint (EC_{50}) of the intradermal curve (89 ng) was significantly lower than the subcutaneous curve (194 ng). This indicated that higher DT-specific IgG titers using lower doses are to be expected from intradermal delivery compared to subcutaneous delivery. Contrarily, the top of the subcutaneous curve (4.655) was significantly increased compared to the intradermal curve (4.177). This indicated that higher DT-specific IgG titers are to be expected from subcutaneous delivery compared to intradermal delivery, when a high DT dose is injected. However, direct comparisons of equal doses injected intradermally or subcutaneously did not result in statistically

significant differences.

Three weeks after the second booster immunization, DT-specific IgG titers resulting from intradermal delivery were again increased compared to subcutaneous delivery when lower DT doses were injected, as shown in Supplementary Fig. S5C (which is a copy of Fig. 5A). However, at this time point, intradermal and subcutaneous delivery resulted in similar DT-specific IgG titers when higher DT doses were injected. In detail, the bottom, top and hillslope of the dose-response curves resulting from intradermal or subcutaneous delivery were similar. However, the midpoint (EC_{50}) of the intradermal curve (37 ng) was again significantly lower (± 3-fold) than the subcutaneous curve (116 ng). This indicated that higher DT-specific IgG titers using lower doses are to be expected from intradermal delivery as compared to subcutaneous delivery.

As shown in Supplementary Fig. S5D, the IgG1:IgG2a ratio was determined at day 63 and similar ratios for all tested doses were observed, with the exception of the 0.02 µg DT dose injected subcutaneously. A trend towards a higher IgG1:IgG2a ratio was observed for intradermal immunization with lower DT doses. PBS pH 7.4 mock treatment did not result in any DT-specific IgG titers.

REFERENCES

[S5] P. Schipper, K. van der Maaden, S. Romeijn, C. Oomens, G. Kersten, W. Jiskoot, J. Bouwstra, Determination of Depth-Dependent Intradermal Immunogenicity of Adjuvanted Inactivated Polio Vaccine Delivered by Microinjections via Hollow Microneedles, Pharm Res, 33 (2016) 2269-2279.

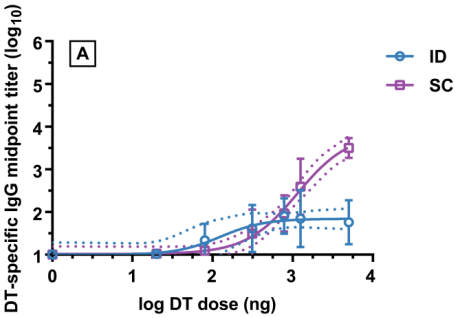

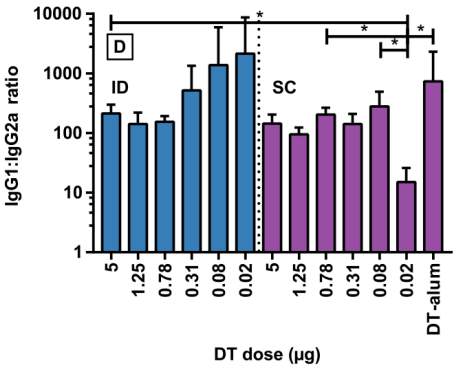

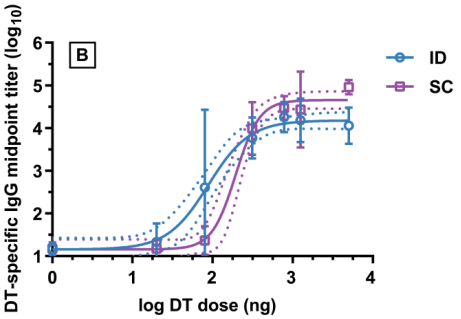

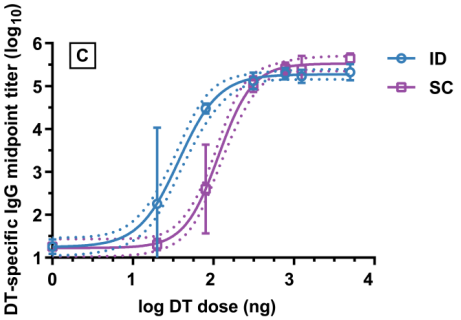

Supplementary Fig. S5 Dose-response study of intradermally- and subcutaneously-delivered DT.

Dose-response study, in which DT-specific immunization responses were investigated as a result of intradermal (ID) and subcutaneous (SC) delivery at doses ranging from 0.02 to 5 µg. The DT-specific IgG midpoint titers 21 days past prime immunization (**A**), boost immunization (**B**) and 2nd boost immunization (**C**) as a result of intradermal or subcutaneous delivery of different DT doses

are represented by blue circles and purple squares, respectively, which represent the mean ± 95% confidence interval (n = 8). These DT-specific IgG responses were used to plot a 4-parameter fit (solid line) and a 95% confidence interval of that fit (dotted line). The blue and purple lines represent the fit for intradermal and subcutaneous delivery, respectively.

IgG1:IgG2a ratios (**D**) were determined in serum at 21 days past the 2nd boost immunization as function of delivery route and DT dose as well. Blue and purple bars represent mean ± 95% confidence interval (n = 8) for intradermal and subcutaneous delivery, respectively, and stars represent a significant increase ($p < 0.05$).

S6 DETERMINATION OF DT-SPECIFIC SERUM IgG TITERS BY ELISA

METHODS

To measure DT-specific total IgG, IgG1 and IgG2a titers in serum, an indirect ELISA was performed. To coat the wells of a polystyrene 96-well microtiter plate, 100 µL of 1.4 µg/mL DT in 0.05 M bicarbonate buffer pH 9.6 was added per well and incubated overnight at 4 °C. Next, a washing step was performed utilizing a Tecan 96PW plate washer and wash buffer (PBS pH 7.2 and 0.05% (v/v) polysorbate 20). A blocking step was then performed by adding 150 µL/well of 1% (w/v) BSA dissolved in PBS pH 7.2 and incubation for 1 hour at 37 °C. Afterwards, a washing step was performed and threefold serial dilutions of serum samples were made in assay buffer (PBS pH 7.2, 0.5% (w/v) BSA and 0.05% (v/v) polysorbate 20) in the 96-well plate at 100 µL/well. Afterwards, plates were incubated at 37 °C for 2 h, followed by a washing step. Subsequently, 100 µL/well of horseradish peroxidase-conjugated goat-anti-mouse IgG, IgG1 or IgG2a was added to the wells in a 5000-fold dilution in assay buffer. Afterwards, plates were incubated at 37 °C for 1.5 hour, followed by a double washing step. Next, 100 µL/well of TMB substrate solution was added and incubated for 10 min at room temperature. The reaction was stopped by adding 100 µL/well of 2 M sulfuric acid. Finally, sample absorbance was measured at 450 nm on a Tecan Infinite M1000 plate reader. Midpoint titers were determined as the logIC50 of the 4-parameter fit on the log10 values of the dilution factor versus the 450 nm absorbance.

S7 COMPARISON BETWEEN A SINGLE INSERTION AND REPEATED INSERTIONS OF DT/TMC COATED MICRONEEDLE ARRAYS ON DT-SPECIFIC IMMUNE RESPONSES

Microneedle arrays coated with 5 bilayers of DT/TMC were applied onto shaved mouse skin by impact insertion at a speed of 0.5 m/s by the in-house designed impact insertion microneedle applicator, which was controlled by a uPRAX microneedle applicator

controller. To investigate the possibility to reduce the application time, microneedle arrays coated with 5 bilayers of DT/TMC were applied by (see Fig. S7):

i. A single application of 90 min
ii. 10 applications at a frequency of 1 Hz (1 application per second, 10 s total, with an application time of 0.5 s per application)

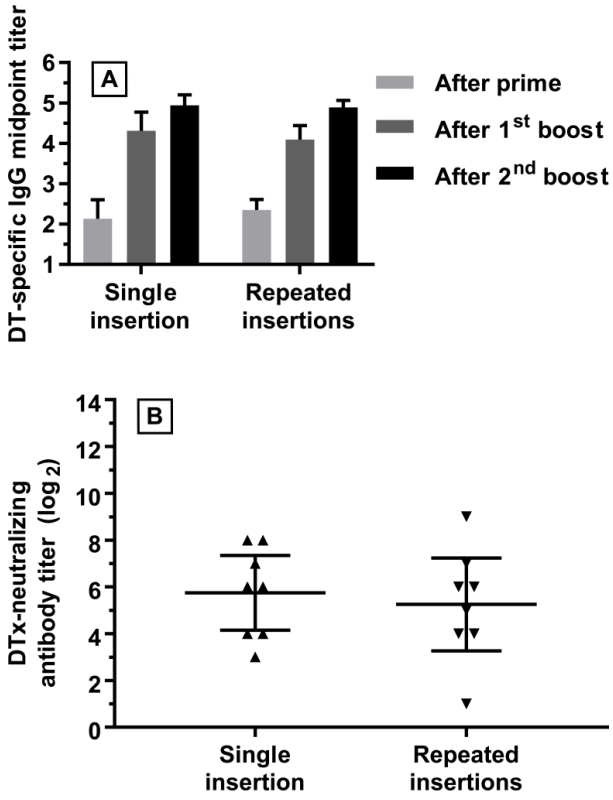

Supplementary Fig. S7 Comparison between a single insertion and repeated insertions of DT/TMC coated microneedle arrays on DT-specific immune responses.

Comparison of DT/TMC coated microneedle arrays to induce DT-specific responses, in which microneedle arrays coated with 5 bilayers of DT/TMC were pierced into the skin and kept for 90 min onto the skin (single insertion) or were repeatedly inserted in the skin for 10 applications at a frequency of 1 Hz (1 application per second, 10 s total, with an application time of 0.5 s per application). Presented are the DT-specific IgG midpoint titers (**A**) 21 days past prime immunization (light gray bars), past 1st boost immunization (gray bars) and past 2nd boost (black bars). DTx neutralization titers were determined in serum at 21 days past the 2nd boost immunization as well (**B**). Bars represent mean ± 95% confidence interval (n = 8).

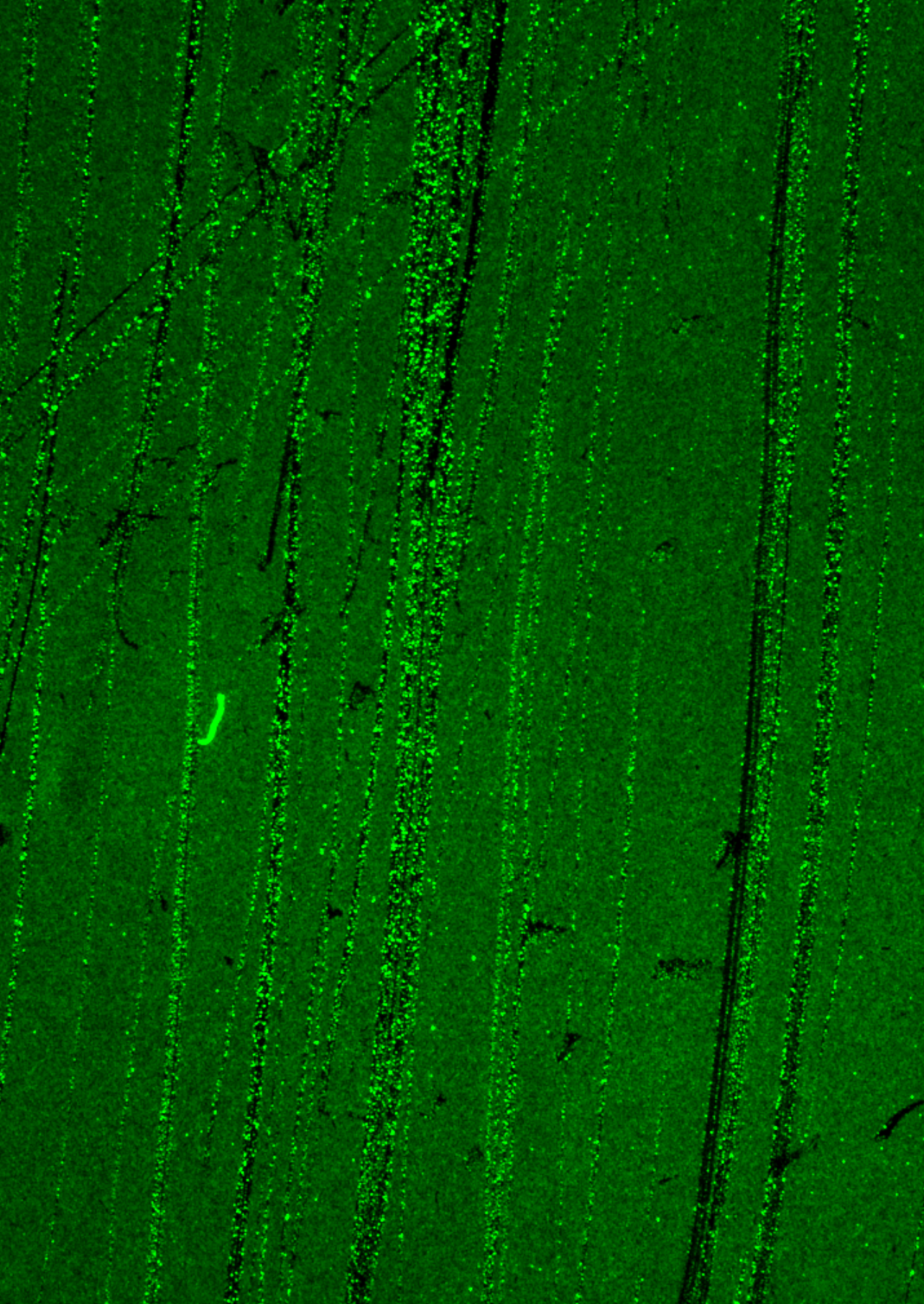

6

Chemical modifications of gold surfaces with basic groups and a fluorescent nanoparticle adhesion assay to determine their surface pK_a

Submitted to Langmuir

P. Schipper[1,*], K. van der Maaden[1,*], W. Jiskoot[1], J.A. Bouwstra[1]

* authors contributed equally

[1] Division of Drug Delivery Technology, Cluster BioTherapeutics, Leiden Academic Centre for Drug Research, Leiden University, Leiden, the Netherlands

ABSTRACT

PURPOSE

For pharmaceutical, biological and biomedical applications the functionalization of gold surfaces with pH-sensitive groups has great potential. The aim of this work was to modify gold surfaces with pH-sensitive groups and to determine the pK_a of the modified gold surfaces using a fluorescent nanoparticle adhesion assay.

METHODS

To introduce pH-sensitive groups onto gold surfaces, we modified gold-coated silicon slides with four different bases: 4-mercaptopyridine (4-MP), 4-pyridylethylmercaptan (4-PEM), 4-aminothiophenol (4-ATP), and 2-mercaptoethylamine (2-MEA). To screen whether the modifications were successful, the binding of negatively charged fluorescently labeled nanoparticles to the positively charged surfaces was visualized by fluorescence microscopy. Next, the pK_a of the modified surfaces was determined by quantifying the pH-dependent adhesion of the fluorescently labeled nanoparticles with fluorescence spectroscopy.

RESULTS

Fluorescence microscopy showed that the gold surfaces were successfully modified with the four different basic molecules. Moreover, fluorescence spectroscopy revealed that fluorescently labeled negatively charged nanoparticles bound onto gold surfaces that were modified with one of the four bases in a pH-dependent manner. By quantifying the adsorption of negatively charged fluorescently labeled nanoparticles onto the functionalized gold surfaces and using the Henderson-Hasselbalch equation, the pK_a of these surfaces was determined to be 3.7±0.1 (4-MP), 5.0±0.1 (4-PEM), 5.4±0.1 (4-ATP), and 7.4±0.3 (2-MEA).

CONCLUSION

We successfully functionalized gold surfaces with four different basic molecules, yielding modified surfaces with different pK_a values as determined with a fluorescent nanoparticle adhesion assay.

GRAPHICAL ABSTRACT

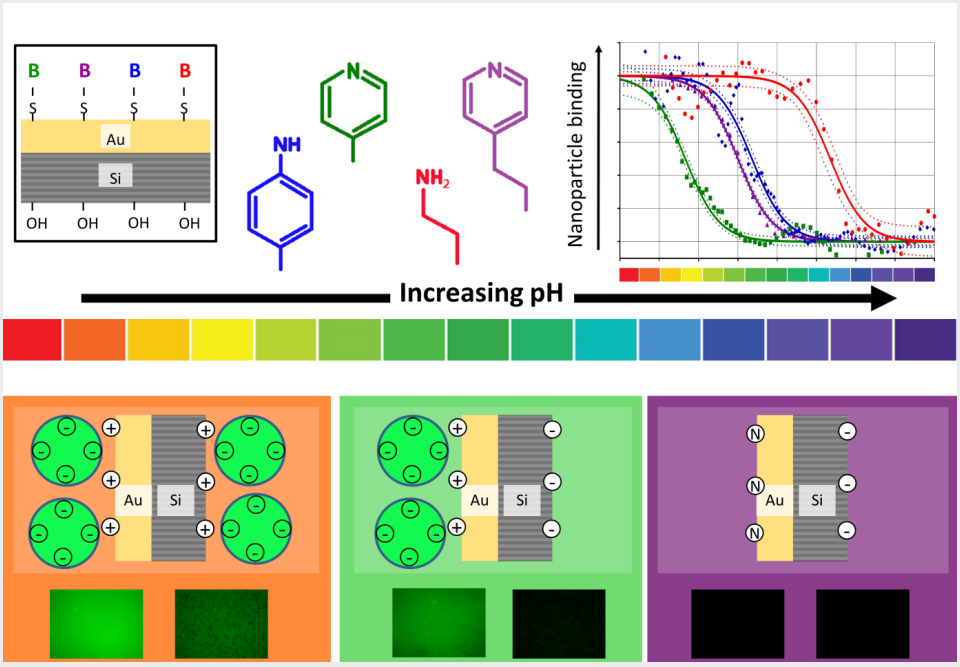

INTRODUCTION

Gold microstructures and nanoparticles are often researched for pharmaceutical, biological and biomedical applications, because of their biocompatible nature [1]. Microneedles, for example, which are needle-like structures with micrometer dimensions that are used for minimally-invasive and pain free dermal drug delivery or sampling of biological fluids [2] that are made of silicon have been coated with a layer of gold [3-5]. Such gold-coated silicon microneedles have been functionalized in order to detect vancomycin [3]. Furthermore, gold nanoparticles are used for the delivery of genes [6] and anticancer drugs [7, 8]. To further extend the applicability of gold microstructures and nanoparticles for pharmaceutical purposes, their surfaces can be functionalized with pH-sensitive groups. This will enable the immobilization/desorption of DNA, proteins, antigens and nanoparticles *via* electrostatic interactions onto/from gold microstructures and nanoparticles as a function of the pH. Importantly, the success of pH-dependent drug delivery will depend on the pK_a of functionalized gold surfaces, which in turn depends on the choice of the functional group and has to be experimentally confirmed.

Fluorescent nanoparticles can be used to investigate the surface properties of chemically-modified surfaces. Recently, we developed a fluorescent nanoparticle adhesion assay (FNAA) to determine the pK_a of silicon surfaces that are modified with acidic and basic molecules [9]. This method is based upon pH-dependent adsorption of cationic or anionic fluorescent nanoparticles onto surfaces with an opposite charge *via* electrostatic interactions. So far, the FNAA has been used to determine the pK_a of silicon surfaces modified with amine groups (APTES) [9], carboxylic groups [9], and pyridine groups [10, 11]. Besides, this method was used to analyze more complex surfaces (i.e., determination and design of the isoelectric point of chemically-modified silicon surfaces) [11]. Furthermore, since most methods are not suitable to detect more than one pK_a value [12], the FNAA could be an attractive method to analyze surfaces that have more than one pK_a value [9]. So far, the FNAA has not been used to determine the pK_a of surfaces other than silicon.

In this work we modify gold-coated silicon surfaces with a panel of basic molecules. Such modified surfaces are potentially suitable for pharmaceutical applications. Besides, we used negatively charged fluorescently labeled nanoparticles and fluorescence microscopy to study the success of the modifications. Moreover, we show that by determining the pH-dependent fluorescent nanoparticle adhesion onto gold-coated silicon slides, the pK_a of gold surfaces modified with a variety of basic molecules can be determined.

MATERIALS

Acetone (puriss.), methanol (HPLC grade), hydrogen peroxide (30% w/w, puriss. p.a.), hydrochloric acid (HCl, 37%, ACS reagent grade), 4-mercaptopyridine (4-MP), 4-pyridylethylmercaptan (4-PEM), 4-aminothiophenol (4-ATP), 2-mercaptoethylamine (2-MEA), ethylenediaminetetraacetic acid (EDTA, ACS reagent grade), and 100-nm fluorescent orange sulfate-modified polystyrene latex beads were purchased from Sigma-Aldrich, Zwijndrecht, the Netherlands. Absolute ethanol (dehydrated, HPLC grade) was purchased from Biosolve, Valkenswaard, the Netherlands. Concentrated sulfuric acid (95-98%, ACS reagent grade) and sodium hydroxide (NaOH, ACS reagent grade) were ordered from Boom, Meppel, the Netherlands. Ultrapure deionized Milli-Q (MQ) water with a resistivity of 18 MΩ·cm at 25 °C was produced by an ELGA Purelab Ultra water purification system. BrandTech Scientific 1.5 mL cuvettes were purchased at VWR, Ede, the Netherlands. Parafilm M® was obtained from Bemis (Monceau-sur-Sambre, Belgium). Black flat-bottom polystyrene 96-wells plates were obtained from Greiner Bio-One, Alphen a/d Rijn, the Netherlands.

METHODS

Preparation of silicon slides and gold-coated silicon slides

Silicon wafers with <100> orientation and a thickness of 500 µm, one side of which was coated with a 1000 Å gold layer (Sigma-Aldrich), were diced into slides of 1x1 cm by using a General Signal Micro Automation Model 602M dicing saw in conjunction with Disco ZH05 series dicing saws, (further referred to as gold-coated silicon slides, having a gold-coated surface area of 1 cm^2 on one side and a non-coated (plain) silicon surface area of 1 cm^2 on the other side). To study non-specific nanoparticle binding onto the (non-coated) silicon side of the gold-coated silicon slides, plain 2-side polished silicon wafers with <100> orientation and a thickness of 300 µm, which were cut into slides of 1x1 cm (further referred to as silicon control slides, having a total silicon surface area of 2 cm^2, obtained from Tyndall National Institute, Cork, Ireland), were used as a control.

Surface modification

To obtain chemically-modified gold surfaces with pH-sensitive groups, gold-coated silicon slides were modified with four different gold-reactive molecules from which it was expected that they result in different surface pK_a values, as schematically represented in Fig. 1. To simultaneously modify up to 45 silicon slides, polychlorotrifluoroethylene

coating containers were developed by the fine mechanical department of Leiden University. Prior to the introduction of pH-sensitive surface groups, the slides were cleaned with acetone and methanol, and were subsequently dried in a vacuum oven at 50 °C for 30 min. To remove residual organic contaminants, the slides were incubated in a piranha solution (7:3 (v/v) mixture of sulfuric acid and hydrogen peroxide) for 60 min at 120 °C. *Caution: piranha solution is an extremely corrosive mixture that should be treated with utmost carefulness.* After removal of the piranha solution, the slides were washed with MQ water until the pH was above 5. Next, the slides were sequentially washed with methanol and dried.

To obtain pH-sensitive groups onto the gold-coated silicon slides, the slides were incubated overnight in a 10 mM solution of a gold-specific reactant (4-MP, 4-PEM, 4-ATP, or 2-MEA) in absolute ethanol at room temperature whilst gently rocking. Finally, non-reacted chemicals were removed by extensively washing the slides sequentially with absolute ethanol and methanol, after which the slides were dried. Slides were stored under vacuum until use. Silicon control slides, which were used to correct for non-specific binding onto the silicon side of the gold-coated slides, were treated with the same procedure as gold-coated silicon slides.

Colloidal stability of nanoparticles as function of pH

The pH-dependent colloidal stability of the 100-nm fluorescently labeled sulfate-modified negatively charged nanoparticles was assessed to investigate whether these nanoparticles are suitable to be used to determine the surface pK_a of the gold-coated silicon slides in the selected pH-range (2 to 10). To this end, the pH-dependent hydrodynamic diameter and polydispersity index (PDI) of these nanoparticles were determined by using dynamic light scattering and the ζ-potential by using Laser Doppler electrophoresis on a Zetasizer Nano (Malvern Instruments).

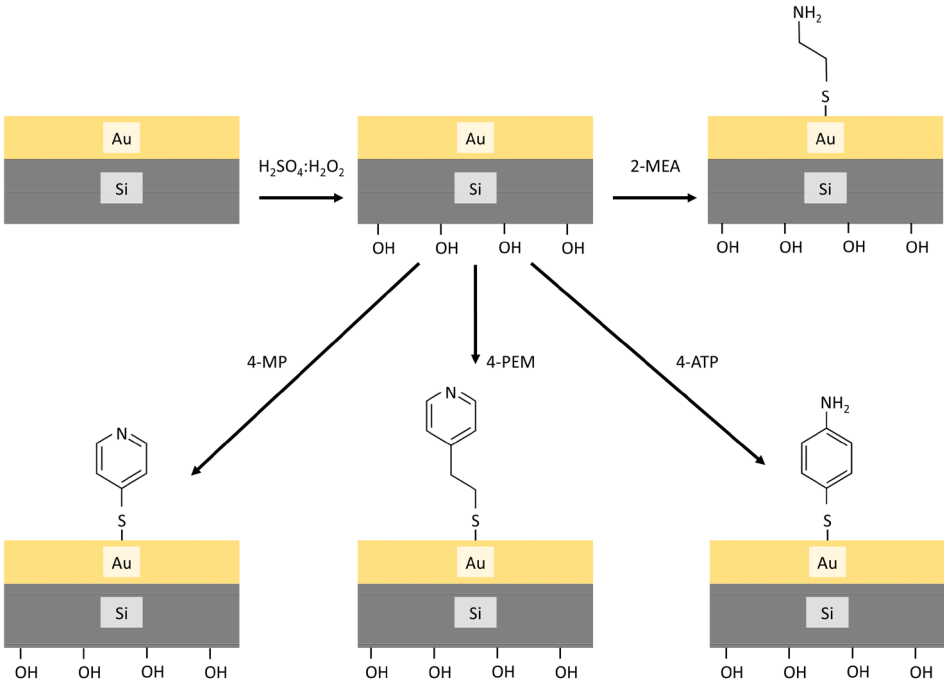

Fig. 1 Introduction of pH-sensitive groups onto gold-coated silicon surfaces. Abbreviations: 2-MEA (2-mercaptoethylamine); 4-MP (4-mercaptopyridine); 4-PEM (4-pyridylethylmercaptan); 4-ATP (4-aminothiophenol).

Fluorescence microscopy for qualitative assessment of surface modification

To qualitatively assess the success of the modification of the gold-coated silicon slides, the adhesion of negatively charged fluorescently labeled nanoparticles at three pH values was imaged by using fluorescence microscopy. To this end, chemically-modified gold-coated silicon slides were incubated with 1 µL/mL nanoparticle dispersions in 1 mM EDTA buffers with pH values of 2.0, 2.5 and 7.5. After 2 h the slides were washed with a 1 mM EDTA buffer having the same pH as the nanoparticle dispersion, and dried by using a gentle air stream. The slides were imaged by using a Nikon Eclipse E600 with a GFP filter set in conjunction with a Photometrics Coolsnap-pro CF monochrome camera and Media Cybernetics imaging software.

Fluorescent nanoparticle adhesion assay

To investigate the applicability of the FNAA to determine the pK_a of functionalized gold surfaces, the surface pK_a of the chemically-modified gold-coated silicon slides

was determined by using the general principles of the FNAA [9]. This assay is based on electrostatic interactions between electrochemically-charged surfaces and oppositely charged nanoparticles as a function of the pH. Because only one side of the gold-coated silicon slides was modified with pH-sensitive groups, the FNAA was adapted to determine the surface pK_a of the chemically-modified gold-coated side (i.e., for each pH determination nanoparticle adhesion was determined for gold-coated silicon slides and silicon control slides).

For each titration, 1 µL/mL nanoparticle dispersions in 1 mM EDTA with pH values from 10.5 to 2 (in steps of approximately 0.5 pH values per dispersion) were prepared by using 0.1 or 0.01 M HCl to adjust the pH. At each pH value 750 µL of the nanoparticle dispersion was transferred to a 1.5 mL cuvette in triplicate. Next, to each of these cuvettes 1) a gold-coated silicon slide, 2) a silicon control slide, or 3) no silicon slide (control) was added, which were subsequently sealed with Parafilm® and covered in aluminum foil to protect the fluorescent nanoparticles from light. For each chemically-modified gold-coated silicon slide a titration was performed at least twice. After 4 h of shaking at 500 rpm (IKA VXR Basic Vibrax orbital shaker), from each sample two aliquots of 200 µL were transferred to a flat-bottom black 96-wells plate. The fluorescence was measured on a Tecan Infinite® M1000 plate reader at an excitation wavelength of 520 nm and an emission wavelength of 540 nm.

Surface-specific nanoparticle binding

To determine the surface-specific binding of nanoparticles onto chemically-modified gold surfaces, first the pH-dependent binding percentage of nanoparticles per cm^2 onto the silicon control slides (B_{Si}) was calculated according to equation 1:

$$B_{Si} = (1 - [Fluo_{Si} / Fluo_{contr}]) / 2 * 100\% \quad \text{(Eqn. 1)}$$

Where $Fluo_{Si}$ is the fluorescence of the nanoparticle dispersion that was incubated with a silicon control slide; and $Fluo_{contr}$ is the fluorescence of the nanoparticle dispersion that was not incubated with a silicon slide, which served as a control for non-specific adhesion of nanoparticles to the cuvette.

Next, the total binding of nanoparticles onto the gold-coated silicon slides (B_{Au}) as a function of the pH was calculated according to equation 2:

$$B_{Au} = (1 - [Fluo_{Au} / Fluo_{contr}]) * 100\% \quad \text{(Eqn. 2)}$$

Where $Fluo_{Au}$ is the fluorescence of the nanoparticle dispersion that was incubated with a gold-coated silicon slide. Binding data was smoothed by averaging the binding percentage at five successive pH values.

Because the gold-coated silicon slides expose 1 cm^2 silicon surface (non-coated side), the percentage of specific binding of nanoparticles onto the chemically-modified gold side ($B_{Au\text{-}specific}$) was calculated by subtracting the percentage of the nanoparticles that bound onto 1 cm^2 silicon surface (B_{Si}) from B_{Au}, see equation 3:

$$B_{Au\text{-}specific} = B_{Au} - B_{Si} \qquad \text{(Eqn. 3)}$$

Calculation of surface pK_a

To compare the binding of nanoparticles onto the different functionalized gold surfaces, first the minimum (B_{min}) and maximum (B_{max}) percentage of nanoparticle binding onto each chemically-modified gold-coated surface was calculated (horizontal bottom and top asymptote, respectively), according to equation 4:

$$B_{Au\text{-}specific} = B_{min} + ([B_{max} - B_{min}] / [1 + 10^{(pKa - pH)}]) \qquad \text{(Eqn. 4)}$$

Next, for each functionalized gold surface, at each pH value nanoparticle binding was normalized between the minimum and maximum binding according to equation 5:

$$\text{Norm. surface charge} = ([B_{Au\text{-}specific} - B_{min}] / [B_{max} - B_{min}]) * 100\% \qquad \text{(Eqn. 5)}$$

Finally, the normalized surface charge was plotted as a function of the pH and an S-shaped curve with its 95% confidence interval was calculated according to the Henderson-Hasselbalch equation. The pK_a was defined and calculated as the mid-point of the S-shaped curve. All calculations were performed by using GraphPad Prism (v.7.00, GraphPad Software, LaJolla, CA, USA).

RESULTS

pH-dependent stability of nanoparticles

To determine the pK_a of gold surfaces that have been modified with basic molecules by using oppositely charged (sulfate-modified) nanoparticles, the nanoparticles should be physicochemically stable in the investigated pH-range. As shown in Fig. 2, the hydrodynamic diameter (94±1 nm), PDI (0.16±0.01), and ζ-potential (-58±6 mV) of the negatively charged nanoparticles did not noticeably change in the investigated pH range (pH 2 – 10). Besides, no significant difference in fluorescence was observed in a pH range between 3-12. So, these nanoparticles are suitable to be used to analyze gold surfaces that have been modified with basic groups having surface pK_as ranging from 3-9.

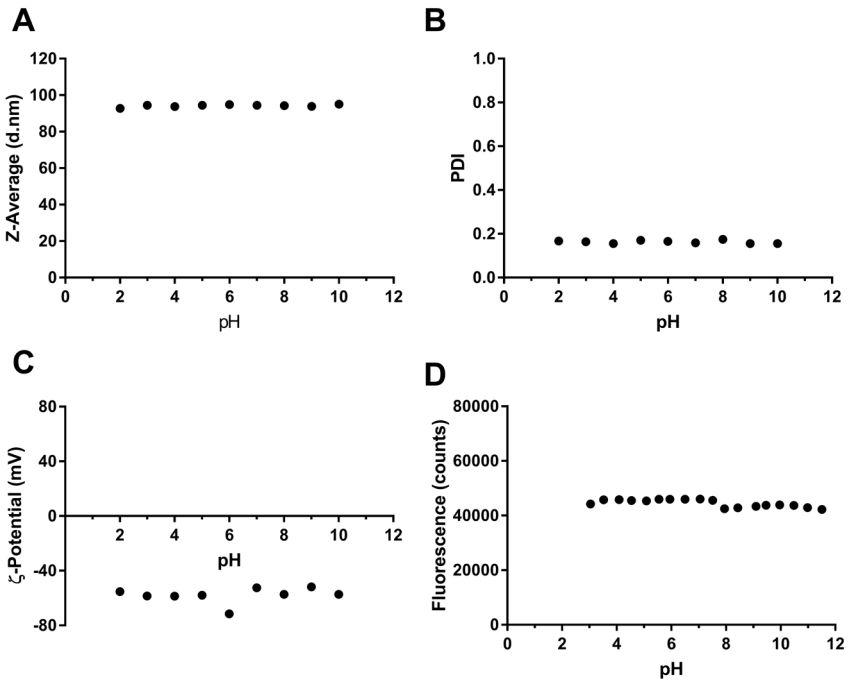

Fig. 2 pH-dependent hydrodynamic diameter (**A**), polydispersity index (PDI, **B**), ζ-potential (**C**), and fluorescence (**D**) of fluorescently labeled sulfate modified negatively charged polystyrene nanoparticles.

Assessment of surface modification

The success of the chemical modification of the gold surfaces was assessed by imaging the adhesion of the negatively charged fluorescently labeled nanoparticles at three different pH values onto the gold-coated silicon slides using fluorescence microscopy. As shown in Fig. 3, the nanoparticles bound onto plain (uncoated) silicon surfaces at a pH value of 2, but hardly bound at pH values of 2.5 and 7.5. Furthermore, they did not bind onto non-modified gold surfaces. In contrast, the fluorescently labeled negatively charged fluorescent nanoparticles bound onto the chemically-modified gold surfaces in a pH dependent manner. Therefore, this data qualitatively shows that the modification of the gold surfaces with the four basic molecules was successful.

pK_a determination of chemically-modified gold surfaces

After it was shown that the gold surfaces were successfully modified with a panel of basic groups, the FNAA (see materials and methods) was performed. As shown in Fig. 4 (left side), the binding of negatively charged nanoparticles onto the chemically-modified gold-coated silicon slides and the silicon control slides was determined as a function of the pH. Because the fluorescently labeled negatively charged nanoparticles also bound onto uncoated silicon surfaces at low pH values, the binding of these nanoparticles onto the gold-coated silicon slides was corrected for nanoparticle adhesion onto the silicon side according to equation 3. As shown in Fig. 4 (right side), the maximum binding of negatively charged nanoparticles onto gold surfaces (pH ~2.5) modified with 2-MEA, 4-MP, or with 4-PEM was comparable (21±4%, 26±14% and 25±3%, respectively), but higher for 4-ATP-coated gold surfaces (41±15%).

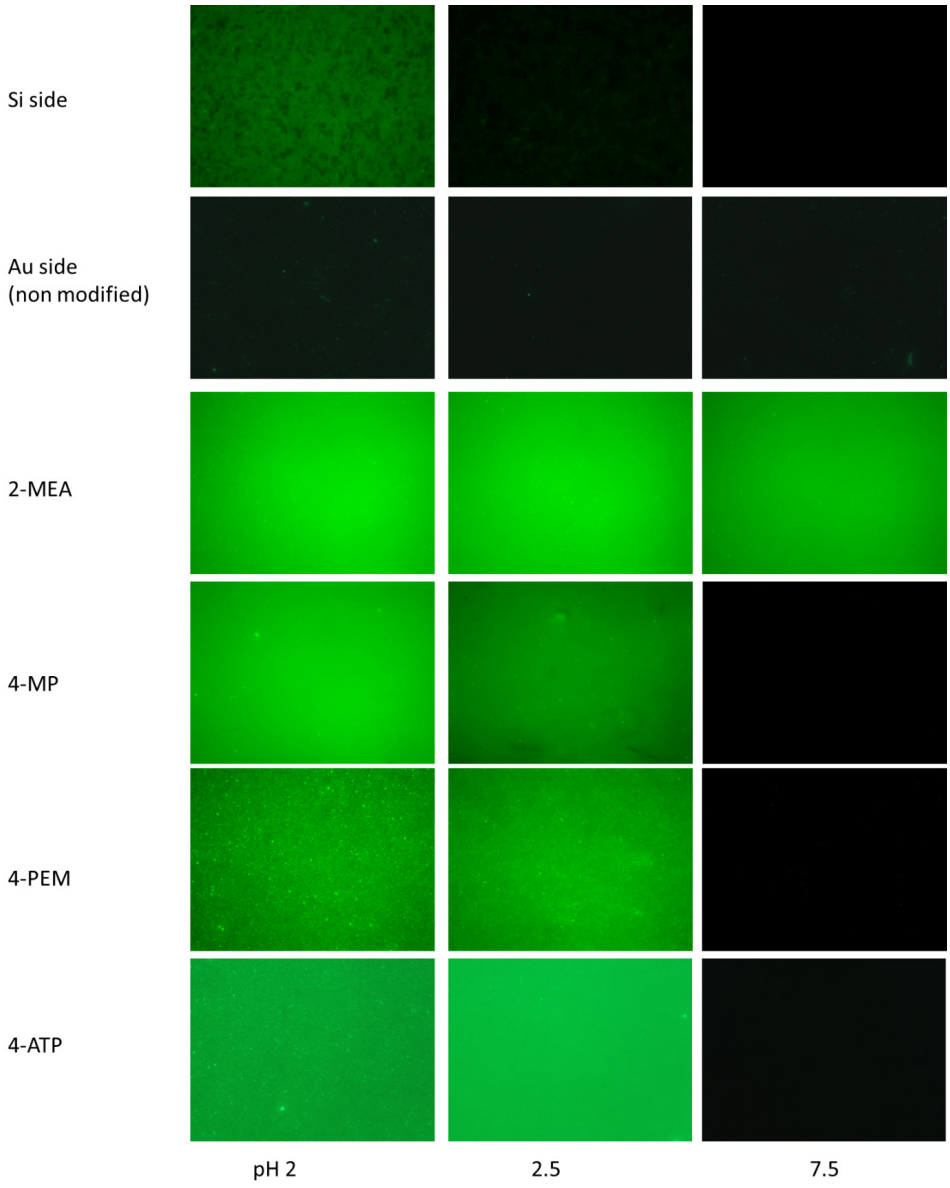

Fig. 3 Representative fluorescence microscopy images (200x magnification) of silicon and chemically-modified gold-coated silicon surfaces that had been incubated with negatively charged fluorescently labeled nanoparticles at different pH values. Abbreviations: 2-MEA (2-mercaptoethylamine); 4-MP (4-mercaptopyridine); 4-PEM (4-pyridylethylmercaptan); 4-ATP (4-aminothiophenol).

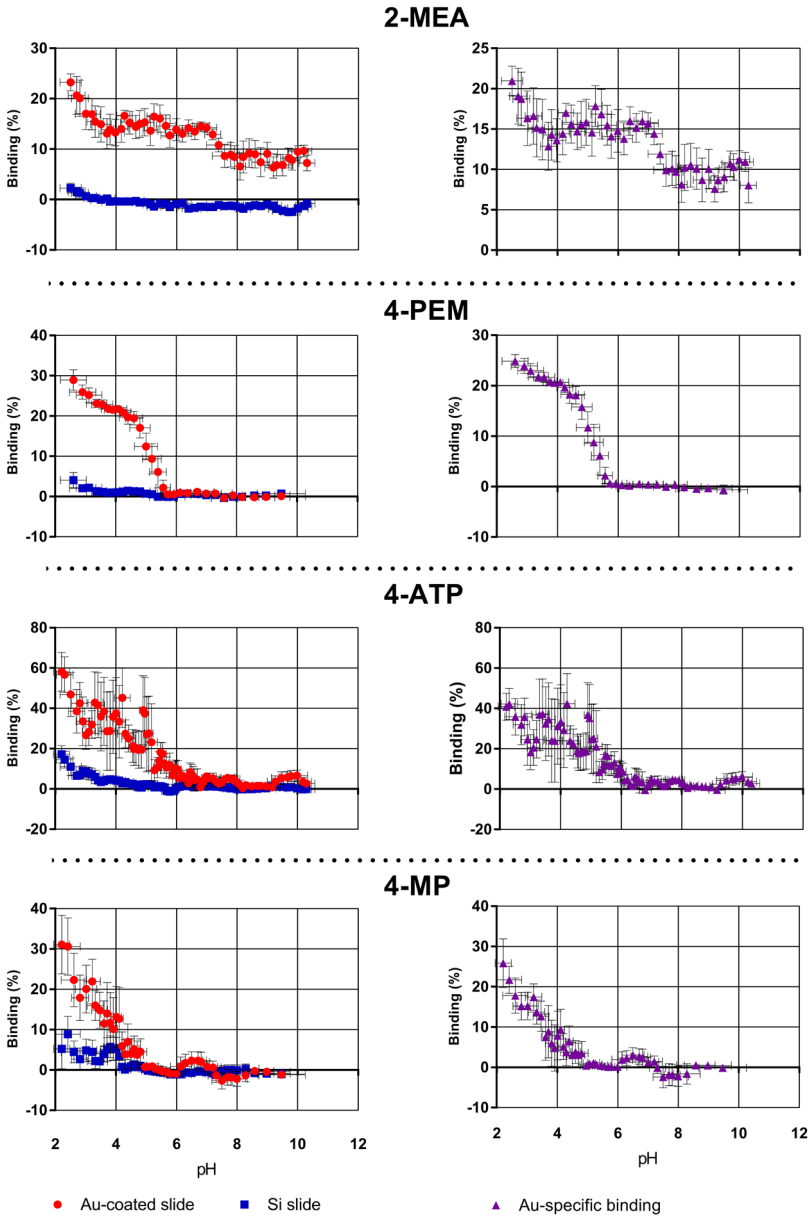

Fig. 4 Results of FNAA of negatively charged fluorescently labeled nanoparticles onto silicon slides (B_{Si}) and gold coated silicon slides modified with pH-sensitive groups (B_{Au} ,left), and gold coated silicon slides corrected for nanoparticle adhesion onto the silicon side ($B_{Au\text{-}specific}$,right). Abbreviations: 2-MEA (2-mercaptoethylamine); 4-MP (4-mercaptopyridine); 4-PEM (4-pyridylethylmercaptan); 4-ATP (4-aminothiophenol). Values are represented as mean ± SEM.

To calculate the pK_a value of gold surfaces that were modified with basic groups, the pH-dependent binding of the negatively charged fluorescently labeled nanoparticles onto the gold-coated silicon slides was normalized to the minimum and maximum binding (normalized surface charge) according to equation 5. As shown in Fig. 5, the normalized surface charge of the gold-coated silicon surfaces modified with the four different gold-specific modifiers were significantly distinguishable from each other (as the 95% confidence intervals did not overlap between normalized surface charges of 10% to 90%). The calculated pK_a values were 7.4±0.3 (2-MEA), 3.7±0.1 (4-MP), 5.0±0.1 (4-PEM), and 5.4±0.1 (4-ATP). These data show that the FNAA is a powerful tool to distinguish between pH-sensitive surface groups having different pK_a values on gold surfaces that are modified with basic molecules.

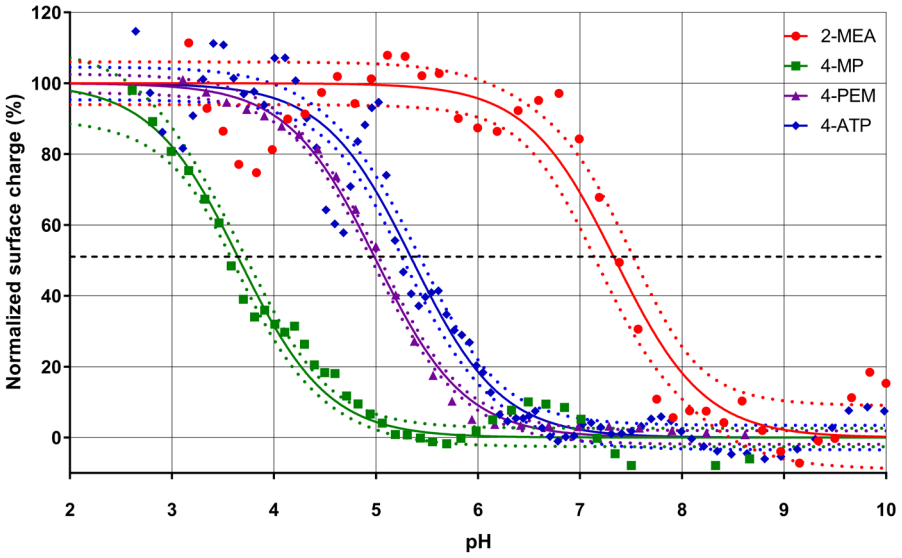

Fig. 5 Normalized surface charge of chemically-modified gold-coated silicon surfaces as a function of the pH, as determined by FNAA. The black dashed line indicates the surface pK_a where the normalized surface charge is 50% of its maximal value. Abbreviations: 2-MEA (2-mercaptoethylamine); 4-MP (4-mercaptopyridine); 4-PEM (4-pyridylethylmercaptan); 4-ATP (4-aminothiophenol). Values are represented as mean ± 95% confidence intervals (dotted lines).

DISCUSSION

Well-characterized functionalized gold surfaces have great potential for pharmaceutical, biological and biomedical applications, such as DNA delivery [6], pH-dependent drug delivery to cancer cells [13], and biosensors [3]. In this work, gold surfaces were successfully modified with a panel of different basic molecules, which was confirmed by using negatively charged fluorescently labeled nanoparticles and fluorescence microscopy. Such a method using nanoparticles and fluorescence microscopy is a fast, easy and cheap approach to check whether the surface modification is successful.

The modification of gold-coated silicon slides with 4-MP, 4-PEM, and 4-ATP resulted in pH-sensitive surfaces that are highly positively charged in a (slightly) acidic environment and that are (almost) uncharged at physiological pH (7.4). Therefore, these surface modifiers have potential for, e.g., pH-dependent drug delivery whereby anionic drugs may be adhered to the gold surface at (slightly) acidic pH (positively charged surface) and can be released at physiological pH (non-charged surface) [10, 14]. However, the binding of negatively charged nanoparticles onto 2-MEA-modified gold surfaces decreased from 20% to 10%, but did not reach 0%, indicating that 2-MEA surfaces have two surface pK_a values, one of which is above 10 (2-MEA in solution has a pK_a of 10). Similarly to 2-MEA on gold (ethylamine surface groups), APTES-modified silicon (propylamine surface groups) resulted in surfaces having two pK_as, one of 7 and the second of 10 [9]. However, the potential second surface pK_a was not further investigated, because the binding of negatively charged nanoparticles at higher pH values is not relevant under physiological conditions and therefore was outside the scope of this research.

To determine the pK_a of functionalized surfaces, a variety of methods have been developed, such as an indirect laser-induced temperature jump method [15], interfacial impedance [16, 17], differential capacitance measurements [18], reductive desorption [19], electrochemical titration [20, 21], piezoelectric quartz crystal microbalance [22], surface potential measurements [23, 24], optical absorption spectroscopy [25], surface enhanced Raman scattering [26-29], chemical force microscopy [30], faradaic impedance titration [31], and contact angle titration [29]. However, most of these methods require expensive equipment, are complicated, or lack accuracy because of their invasive character [9, 32]. As fluorescence spectroscopy is widely available in pharmaceutical and biological laboratories, a FNAA may be a good alternative to the methods described above. However, a FNAA as previously reported [9] is not directly applicable to determine the surface pK_a of gold-coated silicon surfaces that have been modified with basic molecules, which was therefore adapted in this study.

In this research it was shown that negatively charged fluorescently labeled nanoparticles bound onto plain silicon surfaces at low pH values. This was expected because the isoelectic point of silicon surfaces containing silanol groups is between 0.5-3.5 [33]. Below the isoelectric point the surface is positively charged and capable of binding negatively charged nanoparticles. Therefore, the adhesion of nanoparticles onto gold-coated silicon slides was corrected for the adhesion of nanoparticles onto the silicon side.

The surface pK_as obtained by using a FNAA was compared to surface pK_a values reported in the literature (shown in Table 1). This shows that different surface pK_a values have been found for the same chemically-modified gold surfaces when using different methods (e.g., (Fourier transform)- surface enhanced Raman scattering, chemical force microscopy, faradaic impedance titration [12, 18, 19, 26, 28-31]). The surface pK_a values obtained by using the FNAA (at least for 2-MEA and 4-MP) are in the same range as the values reported in the literature. To our knowledge, in the literature there is only one report where two of the same gold reactive molecules have been used as in this study. In that study by Bryant and Crooks the surface pK_a of gold surfaces modified with 4-MP and 4-ATP were determined by using differential interfacial capacitance [18]. Although the surface pK_a values obtained in our study using the FNAA were about 1 pK_a unit lower, the relative difference between the two chemically-modified gold surfaces was similar to the difference found by them (~2 pK_a units difference). Therefore, these results show that the FNAA is a powerful tool to study nanoparticle-surface interaction and is a fairly easy and cheap alternative to conventional methods to determine the surface pK_a of chemically-modified gold surfaces.

Table 1 Surface pK_a (with 95% confidence interval (CI)) of chemically-modified gold surfaces obtained by our fluorescent nanoparticle adhesion assay (FNAA) or *via* various methods reported in the literature. Abbreviations: 2-MEA (2-mercaptoethylamine); 4-MP (4-mercaptopyridine); 4-PEM (4-pyridylethylmercaptan); 4-ATP (4-aminothiophenol).

Gold-reactive molecule	pK_a FNAA (mean, 95% CI)	pK_a from literature	Method used in the literature	Reference #
2-MEA	7.4 (7.1-7.6)	3.4-5	Fourier transform (FT) surface enhanced Raman scattering (FT-SERS)	[26]
		5	FT-SERS	[27]
		6.4-6.8	Reductive desorption	[19]
		7	Chemical force microscopy	[30]
		8.6	Faradaic impendence titration	[31]
4-MP	3.7 (3.5-3.8)	3.9	SERS	[29]
		~4	Contact angle titration	[29]
		4.6	Differential interfacial capacitance	[18]
		5.3	SERS with Gouy-Chapmann model	[29]
		7.5	Cyclic voltammetry	[12]
4-PEM	5.0 (4.9-5.1)	3.3	FT-SERS (*Note: authors refer to unpublished work... and published the same work in 2 journals...*)	[28]
4-ATP	5.4 (5.2-5.5)	6.9	Differential interfacial capacitance	[18]

CONCLUSION

In this work we have successfully modified gold surfaces with a panel of basic groups with different pK_a values that are potentially useful for pharmaceutical applications. We have shown that the success of the modification of gold surfaces with basic molecules can be assessed easily and fast by using negatively charged fluorescently labeled nanoparticles and fluoresce microscopy. Finally, by determining the pH-dependent nanoparticle adhesion onto gold-coated silicon slides corrected for nanoparticle adhesion onto the silicon side, the pK_a of gold surfaces modified with a variety of basic molecules can be determined.

REFERENCES

1. R. Shukla, V. Bansal, M. Chaudhary, A. Basu, R.R. Bhonde, M. Sastry, Biocompatibility of gold nanoparticles and their endocytotic fate inside the cellular compartment: a microscopic overview, Langmuir, 21 (2005) 10644-10654.
2. K. van der Maaden, W. Jiskoot, J. Bouwstra, Microneedle technologies for (trans)dermal drug and vaccine delivery, J Control Release, 161 (2012) 645-655.
3. S.A. Ranamukhaarachchi, C. Padeste, M. Dubner, U.O. Hafeli, B. Stoeber, V.J. Cadarso, Integrated hollow microneedle-optofluidic biosensor for therapeutic drug monitoring in sub-nanoliter volumes, Sci Rep-Uk, 6 (2016).
4. T.W. Prow, X. Chen, N.A. Prow, G.J. Fernando, C.S. Tan, A.P. Raphael, D. Chang, M.P. Ruutu, D.W. Jenkins, A. Pyke, M.L. Crichton, K. Raphaelli, L.Y. Goh, I.H. Frazer, M.S. Roberts, J. Gardner, A.A. Khromykh, A. Suhrbier, R.A. Hall, M.A. Kendall, Nanopatch-targeted skin vaccination against West Nile Virus and Chikungunya virus in mice, Small, 6 (2010) 1776-1784.
5. G.J. Fernando, X. Chen, T.W. Prow, M.L. Crichton, E.J. Fairmaid, M.S. Roberts, I.H. Frazer, L.E. Brown, M.A. Kendall, Potent immunity to low doses of influenza vaccine by probabilistic guided micro-targeted skin delivery in a mouse model, PLoS One, 5 (2010) e10266.
6. Y. Ding, Z. Jiang, K. Saha, C.S. Kim, S.T. Kim, R.F. Landis, V.M. Rotello, Gold nanoparticles for nucleic acid delivery, Mol Ther, 22 (2014) 1075-1083.
7. E.C. Dreaden, L.A. Austin, M.A. Mackey, M.A. El-Sayed, Size matters: gold nanoparticles in targeted cancer drug delivery, Ther Deliv, 3 (2012) 457-478.
8. E. Spyratou, M. Makropoulou, E.P. Efstathopoulos, A.G. Georgakilas, L. Sihver, Recent Advances in Cancer Therapy Based on Dual Mode Gold Nanoparticles, Cancers (Basel), 9 (2017).
9. K. van der Maaden, K. Sliedregt, A. Kros, W. Jiskoot, J. Bouwstra, Fluorescent nanoparticle adhesion assay: a novel method for surface pK_a determination of self-assembled monolayers on silicon surfaces, Langmuir, 28 (2012) 3403-3411.
10. K. van der Maaden, H.X. Yu, K. Sliedregt, R. Zwier, R. Leboux, M. Oguri, A. Kros, W. Jiskoot, J.A. Bouwstra, Nanolayered chemical modification of silicon surfaces with ionizable surface groups for pH-triggered protein adsorption and release: application to microneedles, J Mater Chem B, 1 (2013) 4466-4477.
11. K. van der Maaden, J. Tomar, W. Jiskoot, J. Bouwstra, Chemical modifications of silicon surfaces for the generation of a tunable surface isoelectric point, Langmuir, 30 (2014) 1812-1819.
12. T.d.F. Paulo, H.D. Abruna, I.C. Diogenes, Thermodynamic, kinetic, surface pK_a, and structural aspects of self-assembled monolayers of thio compounds on gold, Langmuir, 28 (2012) 17825-17831.
13. A. Madhusudhan, G.B. Reddy, M. Venkatesham, G. Veerabhadram, D.A. Kumar, S. Natarajan, M.Y. Yang, A. Hu, S.S. Singh, Efficient pH dependent drug delivery to target cancer cells by gold nanoparticles capped with carboxymethyl chitosan, Int J Mol Sci, 15 (2014) 8216-8234.
14. K. van der Maaden, E.M. Varypataki, S. Romeijn, F. Ossendorp, W. Jiskoot, J. Bouwstra, Ovalbumin-coated pH-sensitive microneedle

arrays effectively induce ovalbumin-specific antibody and T-cell responses in mice, Eur J Pharm Biopharm, 88 (2014) 310-315.

15. J.F. Smalley, L. Geng, A. Chen, S.W. Feldberg, N.S. Lewis, G. Cali, An indirect laser-induced temperature jump study of the influence of redox couple adsorption on heterogeneous electron transfer kinetics, J Electroanal Chem, 549 (2003) 13-24.
16. M. Opallo, J. Dojlido, Dissociation Equilibrium of Ortho-Phthalic Acid on the Mercury-Electrode, J Electroanal Chem, 127 (1981) 211-217.
17. J. Dojlido, M. Dmowskastanczak, Z. Galus, Adsorption and Dissociation Equilibrium of Benzoic-Acid on Mercury-Electrode, J Electroanal Chem, 94 (1978) 107-122.
18. M.A. Bryant, R.M. Crooks, Determination of Surface pK_a Values of Surface-Confined Molecules Derivatized with pH-Sensitive Pendant Groups, Langmuir, 9 (1993) 385-387.
19. H. Munakata, D. Oyamatsu, S. Kuwabata, Effects of omega-functional groups on pH-dependent reductive desorption of alkanethiol self-assembled monolayers, Langmuir, 20 (2004) 10123-10128.
20. J.W. Zhao, L.Q. Luo, X.R. Yang, E.K. Wang, S.J. Dong, Determination of surface pK(a) of SAM using an electrochemical titration method, Electroanal, 11 (1999) 1108-1111.
21. Z. Dai, H.X. Ju, Effect of chain length on the surface properties of omega-carboxy alkanethiol self-assembled monolayers, Physical Chemistry Chemical Physics, 3 (2001) 3769-3773.
22. K. Sugihara, K. Shimazu, K. Uosaki, Electrode potential effect on the surface pK(a) of a self-assembled 15-mercaptohexadecanoic acid monolayer on a gold/quartz crystal microbalance electrode, Langmuir, 16 (2000) 7101-7105.
23. J.J. Betts, B.A. Pethica, The Ionization Characteristics of Monolayers of Weak Acids and Bases, T Faraday Soc, 52 (1956) 1581-1589.
24. J. Caspers, E. Goormaghtigh, J. Ferreira, R. Brasseur, M. Vandenbranden, J.M. Ruysschaert, Acido-Basic Properties of Lipophilic Substances - a Surface-Potential Approach, J Colloid Interf Sci, 91 (1983) 546-551.
25. K.S. Mayya, V. Patil, M. Sastry, On the stability of carboxylic acid derivatized gold colloidal particles: The role of colloidal solution pH studied by optical absorption spectroscopy, Langmuir, 13 (1997) 3944-3947.
26. X.W. Cao, Study of electrode potential effect on acid-base behavior of omega-functionalized self-assembled monolayers using Fourier transform surface-enhanced Raman scattering spectroscopy, J Raman Spectrosc, 36 (2005) 250-256.
27. K. Nishiyama, A. Kubo, A. Ueda, I. Taniguchi, Surface pK(a) of amine-terminated self-assembled monolayers evaluated by direct observation of counter anion by FT-surface enhanced Raman spectroscopy, Chem Lett, (2002) 80-81.
28. K. Nishiyama, M. Tsuchiyama, A. Kubo, H. Seriu, S. Miyazaki, S. Yoshimoto, I. Taniguchi, Conformational change in 4-pyridineethanethiolate self-assembled monolayers on Au(111) driven by protonation/deprotonation in electrolyte solutions, Physical Chemistry Chemical Physics, 10 (2008) 6935-6939.

29. H.Z. Yu, N. Xia, Z.F. Liu, SERS titration of 4-mercaptopyridine self-assembled monolayers at aqueous buffer/gold interfaces, Analytical Chemistry, 71 (1999) 1354-1358.
30. E.W. van der Vegte, G. Hadziioannou, Acid-base properties and the chemical imaging of surface-bound functional groups studied with scanning force microscopy, J Phys Chem B, 101 (1997) 9563-9569.
31. V. Molinero, E.J. Calvo, Electrostatic interactions at self assembled molecular films of charged thiols on gold, J Electroanal Chem, 445 (1998) 17-25.
32. H.X. He, C.Z. Li, J.Q. Song, T. Mu, L. Wang, H.L. Zhang, Z.F. Liu, Force titration of a carboxylic acid terminated self-assembled monolayer using chemical force microscopy, Mol. Cryst. Liq. Cryst. Sci. Technol. Sect. A-Mol. Cryst. Liq. Cryst., 294 (1997) 99-102.
33. X.D. Liu, J. Cheng, X.C. Lu, R.C. Wang, Surface acidity of quartz: understanding the crystallographic control, Physical Chemistry Chemical Physics, 16 (2014) 26909-26916.

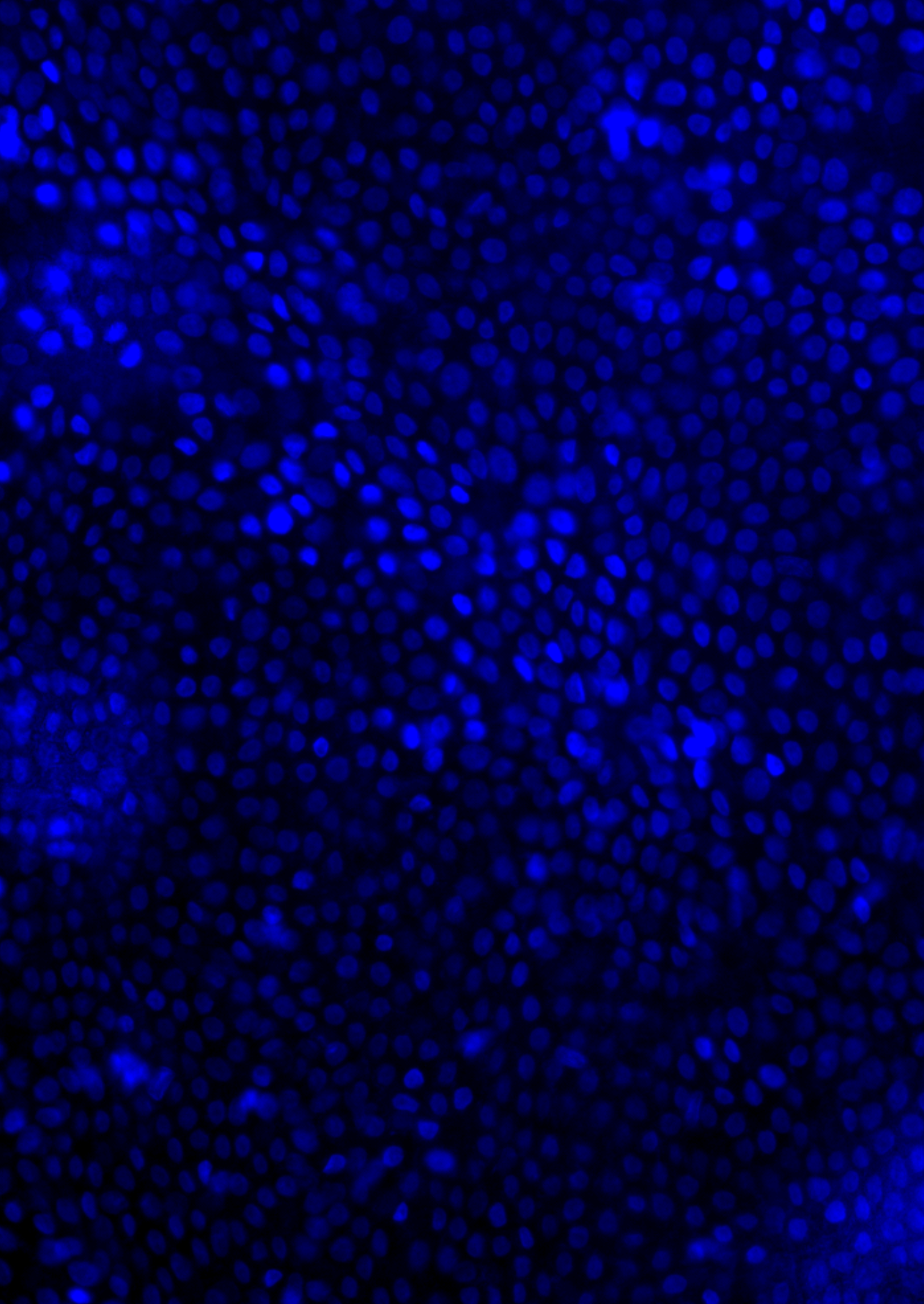

7

Summary, prospects and conclusion

SUMMARY

Classically, the intramuscular and subcutaneous routes are used to administer vaccines using hypodermic needles. In recent decades, the interest in methods to administer vaccines intradermally has increased, as it has become evident that the skin contains a much higher number of immune cells in comparison to muscle or subcutis tissue [1-6]. The skin may therefore provide a more efficient route for immunization, perhaps even with a lower vaccine dose, while retaining safety and efficacy [1-6]. For example, a 60-80% dose reduction for intradermal rabies vaccination compared to intramuscular vaccination has been reported [7-9]. Dose sparing has also been reported for vaccination against hepatitis B [10, 11], influenza [12-17] and polio [18, 19] *via* the intradermal administration route as compared to intramuscular administration.

To administer vaccines into the skin, the physical obstruction provided by the stratum corneum must be bypassed in order to deliver the vaccine to the immune cells in the skin. The stratum corneum is the outermost layer of the skin and has a thickness of ca. 15-20 μm [20]. The stratum corneum can be bypassed by using microneedles that are long enough to cross the stratum corneum. In addition, the microneedles should be short enough to avoid reaching nerve endings and thereby avoiding any pain sensation. As such, the advent of microneedles has paved the way for potentially pain-free and minimally invasive intradermal immunization [21]. Microneedle-mediated intradermal vaccination offers additional advantages over classical intramuscular and subcutaneous vaccination, which use hypodermic needles. The use of hypodermic needles results in painful injections, carries a risk for needle re-use and needle-stick injuries and has the downside of requiring trained personnel to perform the injections. As microneedles are short, can be designed for single use and are easy to administer, they may alleviate the problems associated with hypodermic needles.

Of the several types of microneedles available [21], the focus in this thesis is on the use of hollow microneedles and coated microneedles. Hollow microneedles are hollow-bore needles of micrometer scale. The hollow microneedle is inserted into the skin, after which a liquid formulation flows through the bore of the needle, effectively injecting the formulation into the skin. In the research described in this thesis, a single hollow microneedle was used in conjunction with an injection system. Coated microneedles are prepared from solid microneedles, which are usually produced in arrays of needles protruding from a backplate. The surfaces of these arrays of solid microneedles are coated with a vaccine and after insertion into the skin, the coating is released. The design and usage of microneedles and microneedle arrays may affect the immune

responses, especially as the density and type of immune cells depend on the depth in skin at which the antigen is administered.

Dendritic cells (DCs) are immune cells, specialized in the initiation of antigen-specific immune responses. Various subsets of DCs are located at different depths in the skin. The Langerhans cell (LC) is a type of DC which resides exclusively in the epidermis (upper layer of the skin), while the dermal DCs (DDCs) reside exclusively in the dermis (skin layer located underneath the epidermis) [1]. As explained in more detail in the introduction of this thesis in *chapter 1*, three subsets of DCs are known to reside in human skin, which have seemingly distinct immunological roles. LCs seem to specialize in cytotoxic T cell responses, whereas $CD14^+$ DDCs seem more likely to induce humoral responses and $CD1a^+$ DDCs are somewhat in between. How these subsets of DCs are most efficiently triggered to enhance or shift the immune response to the benefit of intradermal vaccination is not fully understood. Therefore, the aim of the research described in *chapters 2 and 3* was to unravel the dependency of immune responses on the depth at which the antigen is administered into skin.

In *chapter 2* it is described how the performance of a single hollow microneedle injection system was improved to achieve accurate injections at various depths in skin using hollow microneedles. These improvements allowed for accurate microinjections into rat skin at predetermined injection depths (varying between 50-900 µm), injection volumes (1-100 µL) and injection rates (up to 60 µL/min). After establishing the accuracy of depth-controlled microinjections, the dependency of monovalent inactivated polio vaccine serotype 1 (IPV1)-specific immune responses on the intradermal injection depth of IPV1 was investigated. The use of a classic adjuvant, i.e. aluminum salts, is prohibited in intradermal immunization due to toxicity. Therefore, IPV1-specific immune response-enhancing effects of adjuvants CpG oligodeoxynucleotide 1826 (CpG) or cholera toxin (CT) in intradermal immunization were also investigated. IPV1-specific immune responses resulting from microinjections of IPV1 at skin depths ranging between 50-550 µm resulted in similar IgG and virus-neutralizing antibody titers against IPV1 and did not differ from conventional intramuscular immunization. Furthermore, IPV1 adjuvanted with either CpG or CT was administered by intradermal microinjections at a depth in skin of 400 µm and by intramuscular administration. Regardless of administration method, CpG or CT adjuvanted IPV1 immunization resulted in significantly (7-fold) increased IPV1-specific IgG titers. Although IPV1-specific immune responses were unaffected by intradermal injection depth, they were enhanced by CpG and CT, which indicates that both adjuvants are promising candidates to enhance intradermal IPV1 immunization, as an alternative to aluminum salts.

In *chapter 3*, the aim was to determine whether migration of, maturation of and antigen uptake by LCs, $CD1a^+$ and $CD14^+$ DDCs differ as a result of administration of antigen at various doses (1-50 µg) or injection depths (50-1000 µm) in *ex vivo* human skin. Ovalbumin (OVA) was selected as model antigen. By using a skin explant model, after injection of antigen into skin, migrated skin cells were collected. Next, the migration, maturation and OVA uptake were determined per skin DC subset by using flow cytometric analysis. Increasing OVA doses resulted in a trend of enhanced migration of LCs, whilst it resulted in statistically significant decreased migration of $CD1a^+$ and $CD14^+$ DDCs. Moreover, increasing OVA doses only resulted in increased maturation of $CD1a^+$ DDCs, determined as increased expression of costimulatory molecule CD86. Furthermore, the amount of OVA uptake and percentage of OVA-containing cells was enhanced for Langerhans cells (12-99%) and $CD1a^+$ DDCs (91-99%) with increasing OVA dose. Antigen uptake by $CD14^+$ DDCs was most efficient, as demonstrated by a seemingly saturated amount of OVA uptake and very high percentage of OVA-containing cells (±99%), even at the lowest dose tested. The amount of OVA uptake by $CD14^+$ DDCs was followed by that of $CD1a^+$ DDCs and LCs, which demonstrated a 3.5-fold lower and 15.7-fold lower amount of OVA uptake, respectively, at the highest tested dose. The migration of, maturation of and OVA uptake by LCs, $CD1a^+$ and $CD14^+$ DDCs were independent of the injection depth. After determination of the diffusion coefficient of OVA in human skin, it was found that the diffusion coefficient of OVA was high enough to obscure any effect of the injection depth. Nonetheless, intradermal microinjection by using a single hollow microneedle with a 50-fold reduced injection volume resulted in similar antigen uptake as compared to an intradermal injection using a conventional hypodermic needle-and-syringe. Thus, by using hollow microneedles, the injection volume for intradermal injections may be strongly reduced, avoiding discomfort associated with intradermal injections with larger injection volumes (100-200 µL) [19].

Upon invading the skin, a pathogen will increase in numbers exponentially during infection, simultaneously growing the immune response. Therefore, it was hypothesized that mimicking a natural infection during intradermal immunization will enhance vaccine-specific immune responses. In *chapter 4*, the aim was to determine whether IPV1-specific responses could be enhanced by repeated intradermal injections of fractional IPV1 doses, compared to a single intradermal or intramuscular bolus injection. Intradermal microinjections through a single hollow microneedle were compared to intramuscular injections through a hypodermic needle. Rats were immunized intradermally with 5 D-antigen units (DU) of IPV1 at 150 µm skin depth. This dose was administered as a bolus, or in a repeated fractional dosing schedule: 4 doses of 1.25 DU (1/4th of total dose) were administered on four consecutive days or every other day; 8 doses of 0.625 DU (1/8th of

total dose) were administered on eight consecutive days; or 4 exponentially increasing doses (0.04, 0.16, 0.8 and 4 DU), either with or without an exponentially increasing CpG oligodeoxynucleotide 1826 (CpG) dose, were administered on four consecutive days. All of these repeated fractional dosing schedules resulted in up to ca. 10-fold higher IPV1-specific IgG responses in comparison to intradermal and intramuscular bolus dosing. IPV1 combined with adjuvant CpG in exponential dosing did not significantly increase the IPV1-specific IgG responses further. In conclusion, repeated fractional intradermal IPV1 dosing leads to superior IPV1-specific IgG responses without the use of adjuvants. Based on results in this study, it is expected that a controlled release delivery system simulating repeated fractional dosing will result in enhanced antigen-specific immune responses, while only using a single administration.

A benefit of using coated microneedle arrays is that the vaccine is in a solid state. Therefore, vaccine coated to microneedle arrays is expected to be more stable at room temperature as compared to liquid vaccine formulations. In addition, coated microneedles are easier to apply than hollow microneedles, which rely on a pumping mechanism to flow liquids through the bore of the needle. In order to prepare coated microneedle arrays, pH-sensitive microneedle surfaces provide a method to adhere antigen to the microneedle surface during coating and to release antigen upon piercing the skin, depending amongst others on the environmental pH and surface pK_a. However, the surface area of the microneedles piercing the skin is a limiting factor for the amount of vaccine that can be coated onto the microneedle array. To increase the surface area available for coating on the microneedle array, two approaches were investigated in *chapters 5 and 6*.

A layer-by-layer coating approach effectively stacks alternating positively and negatively charged layers of coating onto the microneedle surfaces, thereby increasing the amount of vaccine coated onto the microneedle array. The aim of the work described in *chapter 5* was to examine whether a layer-by-layer antigen-coating approach on pH-sensitive modified silicon surfaces of microneedles can be used for intradermal immunization. Following this approach, pH-sensitive silicon surfaces of high-density microneedle arrays (positively charged at coating pH 5.8 and nearly uncharged at pH 7.4) were alternatingly coated with negatively charged diphtheria toxoid (DT, an anionic antigen) and positively charged N-trimethyl chitosan (TMC, a cationic polymer with adjuvant function). In a dose-response study, the required DT dose for sufficient DT-specific immune responses was first determined. In this dose-response study, intradermal immunization using a single hollow microneedle was compared to subcutaneous immunization using a hypodermic needle. This study revealed that low-dose intradermal immunization is more efficient

than subcutaneous immunization and that the EC_{50} dose of DT (dose resulting in half of maximum effect) upon intradermal immunization is 3-fold lower, as compared to subcutaneous immunization. After selecting the DT doses that were required to be administered intradermally for sufficient DT-specific immune responses, the DT/TMC layer-by-layer coating approach was optimized. It was demonstrated that the amount of DT coated onto the microneedle array is reproducible and the intradermally-administered amount of antigen can be tuned by selecting the number of coated DT/TMC bilayers. In a subsequent immunization study, microneedle arrays were coated with an incrementally increasing number (2, 5, and 10) of DT/TMC bilayers and intradermal immunization using these microneedle arrays resulted in incrementally increasing DT-specific immune responses. Intradermal immunization using microneedle arrays coated with 10 bilayers of DT/TMC (corresponding with about 0.6 µg DT delivered intradermally) resulted in similar DT-specific immune responses as subcutaneous immunization with 5 µg of DT adjuvanted with aluminum phosphate, which is an 8-fold dose reduction of DT. In *chapter 5*, it was demonstrated that the layer-by-layer coating approach onto pH-sensitive microneedles is a versatile method to precisely control the amount of coated and intradermally-administered vaccine and that this approach is highly suitable for intradermal immunization for DT.

Another approach to increase the surface area available for coating on microneedle arrays, is to create a sponge-like gold surface on top of a silicon surface [22]. To this end, gold ions were sputtered onto silicon surfaces, creating a sponge-like surface, greatly increasing the surface available for coating. In *chapter 6*, the aim was to evaluate the possibilities to create pH-sensitive surface-functionalization on gold surfaces, to eventually enable antigen coating for use on coated microneedles. To this aim, gold surfaces were functionalized with pH-sensitive basic groups and the pK_a of the functionalized gold surfaces were determined by using a fluorescent nanoparticle adhesion assay. As demonstrated by the binding of negatively charged fluorescently labeled nanoparticles to the positively charged functionalized gold surfaces, as visualized by fluorescence microscopy, gold-coated silicon slides were successfully modified with four different bases: 4-mercaptopyridine (4-MP), 4-pyridylethylmercaptan (4-PEM), 4-aminothiophenol (4-ATP), and 2-mercaptoethylamine (2-MEA). By quantifying the pH-dependent adsorption of negatively charged fluorescently labeled nanoparticles onto the functionalized gold surfaces with fluorescence spectroscopy and by using the Henderson-Hasselbalch equation, the pK_a of these surfaces was determined to be 3.7±0.1 (4-MP), 5.0±0.1 (4-PEM), 5.4±0.1 (4-ATP), and 7.4±0.3 (2-MEA). In conclusion, gold surfaces were successfully functionalized with four different basic molecules, yielding modified surfaces with different pK_a values.

PROSPECTS

The single hollow microneedle injection system: the next step in development

After improvements were made to the single hollow microneedle injection system as described in *chapter 2*, this system was used extensively in several studies described in this thesis. Major advantages of the system are its accuracy in injection volume, -depth and -rate. This accuracy in injection parameters allowed to study several hypotheses regarding depth-controlled intradermal vaccine administration. In addition, this system was used to perform intradermal microinjections in mice, rat and (*ex vivo*) human skin.

Although this injection system is impressive in its accuracy and flexibility in injection parameters, it is rather large and too complicated to be used by untrained personnel. So, the single hollow microneedle injection system should be miniaturized and made user-friendly. Miniaturization could be achieved using a small pump and reservoir for the solution for injection, as it was proven in *chapter 3* that a very small injection volume still resulted in adequate antigen uptake by skin immune cells. User-friendly operation could be achieved by opting for fixed injection parameters, removing the need for flexibility and extensive configuration before injection, whilst simplifying and miniaturizing the design. Results from *chapters 2 and 3* indicate that the requirement for depth-controlled administration in skin is not strict, which allows for a fixed injection depth.

Ideally a single device is designed, consisting of a single hollow microneedle or an array of hollow microneedles, in combination with a reservoir for the solution for injection and a method to flow the solution through the bore of the needle (e.g., by using a pump or pressure) into the skin. In addition, the device should be safe to use, by preventing premature actuation (i.e., before the injection site is targeted) and by preventing needle-stick injuries by retracting the needle(s) after use. In a most optimistic view, the device is ready to be deployed for administration by non-medically trained personnel, to enlarge access to vaccines in more difficult to reach areas in the world, where vaccination coverage is low due to lack of medically trained personnel.

Depth-controlled intradermal immunization

One of the aims of this thesis was to investigate the effect of administering a vaccine at various depths in skin on vaccine-specific immune responses. The rationale stems from the distinct immune functions of the various skin DC subsets residing at different depths in skin: by administering a vaccine at a specific depth in skin, different skin DC subsets may be targeted, exploiting these distinct immune functions. However, the results described in *chapters 2 and 3* indicate no great influence of depth-controlled

intradermal vaccine administration on vaccine-specific immune responses. These results suggest that there is no strict requirement with respect to the injection depth when using hollow microneedles or the length of the microneedle when using solid (dissolvable or coated) microneedles (or microneedle arrays). However, as outlined in *chapter 3*, the diffusion coefficient in skin of the model antigen, OVA (±42 kDa [23]), might be high enough to possibly obscure a depth-dependent effect on antigen uptake by DCs in skin. Nevertheless, also for IPV1, which is a particulate antigen of about 30 nm in diameter [24, 25], no dependency on the injection depth was observed in *chapter 2*. Since most vaccines consist of particulate antigens larger than IPV1, such as (partially) inactivated viruses, bacteria, and alum-adsorbed antigens, it will be interesting to investigate whether the conclusions for depth-controlled administration of OVA and IPV1 can be extrapolated to such larger particulate antigens, which are expected to diffuse slower through the different layers of the skin.

As studies described in this thesis investigating depth-controlled intradermal immunization were performed solely using a liquid formulation, it will be interesting to evaluate vaccine-specific immune responses resulting from intradermal immunization with solid (dissolvable or coated) microneedles of different length, as it is expected that the intradermal diffusion profile of an antigen being released from solid microneedles differs from that of an antigen that is formulated in a liquid and delivered *via* a hollow microneedle.

Dosing schedule

In *chapter 4*, alternative IPV1 dosing schedules to conventional bolus dosing were examined. The dosing schedule was demonstrated to influence the IPV1-specific immune responses. Specifically, injection of 1/4 of the total dose on four consecutive days or every other day; 1/8 of the total dose on eight consecutive days; or 4 exponentially increasing doses, either with or without an exponentially increasing CpG dose, all resulted in increased IPV1-specific immune responses. A prolonged dosing schedule most probably leads to an antigen depot being formed in germinal centers and it has been shown that such a depot is needed for B-cells to proliferate into plasma B-cells and memory B-cells [26, 27]. These results indicate that a prolonged-release formulation (releasing antigen over several days) may enhance the immune response. Therefore, it will be of interest to design a (micro- or nanoparticulate) formulation that is capable of delivering the vaccine in multiple doses (perhaps using multiple layers of degradation and antigen release), exploiting the prolonged dosing schedule effect as demonstrated in *chapter 4*. In a study investigating different particulate formulations, it was elegantly shown that OVA was released in burst at first, but then was released linearly with time for lipid bilayer coated OVA encapsulated mesoporous silica nanoparticles [28]. This type of

antigen release is continuous, instead of the immediate fractional dosing per day studied in *chapter 4*. Investigating these types of antigen release profiles head-to-head will be interesting, in order to determine which release profile is needed for optimal vaccine-specific immune responses. This information may then be used to develop particulate or microneedle designs further, possibly by using solid microneedle (arrays) combining antigen burst-release with prolonged antigen release [29-32], ideally with particulate systems with different release rates, simulating fractionated dosing.

The future of intradermal immunization

The intradermal immunization route has been quoted as being more efficient than other immunization routes. Intradermal rabies immunization resulted in a 60-80% dose reduction compared to intramuscular immunization [7-9]. Moreover, dose sparing has been reported for intradermal immunization (compared to conventional intramuscular immunization) for hepatitis B [10, 11] and influenza [12-17]. The results described in *chapter 5* clearly indicate that a lower DT dose is required when immunizing *via* the intradermal route compared to the conventional subcutaneous route in mice. To consolidate whether the intradermal route is truly more efficient in comparison to the conventional intramuscular route, more of such preclinical dose-response studies comparing both routes are required. Such studies will lay a foundation for multi-armed clinical trials in humans studying intradermal versus conventional routes at different doses, to provide evidence whether dose-sparing is a possibility by using intradermal immunization. Comparative studies in humans are limited, but are needed to validate whether the intradermal route is also more efficient in humans.

The best evidence in humans of increased immune responses after intradermal immunization in comparison to conventional intramuscular immunization has been demonstrated by using IPV. Intradermal immunization of IPV in naïve newborn infants resulted in either similar [18, 33] or inferior [34-36] seroconversion rates, compared to intramuscular immunization. In addition, intradermal booster immunization of previously IPV vaccinated adults resulted in either similar [19, 37] or inferior [38, 39] seroconversion rates, compared to intramuscular immunization. However, intradermal immunization in these studies was performed with 1/5th of a full IPV dose and was compared to intramuscular immunization with a full IPV dose. It is not known why this 1/5 dose was chosen and whether it was based on an explorative dose-response study, which is required to properly design such studies.

Besides efficacy, the safety of a vaccine is an important aspect as well. Regulatory authorities will balance an application for marketing authorization of the vaccine based

on safety and efficacy data. Moreover, at the time of writing, the vaccination coverage is decreasing [40-42]. This is due to numerous reasons, including religious and philosophical reasons [43], but also false claims of adverse effects of vaccines [44-46]. For these reasons, the regulatory and public attention to vaccine safety is high. It is therefore imperative to maintain a high level of (public) confidence for new intradermal vaccine administration devices. As such, in the design of human clinical trials, a risk-based assessment on expected adverse events is to be included.

However, to move into clinical trials, the concepts described in this thesis for hollow and coated microneedles need to be developed into a (drug) product. Major hurdles to take are, for example, the production of the antigen(s), the (removal of) impurities from the bulk product, the excipients and perhaps adjuvant(s) to be used in the formulation of the vaccine, the stability, shelf-life and storage conditions. Another concern is the sterility of the product. Perhaps it is easier to achieve sterility for liquid formulations *via* conventional procedures, than for layer-by-layer coated microneedles, for which new procedures will have to be developed.

Intradermal immunization by using the hollow microneedle approach in comparison to the coated microneedle approach

In this thesis, vaccines administered by using either a single hollow microneedle injection system or a coated microneedle array have been studied. As summarized in Table 1, both of the two approaches to deliver vaccines intradermally have distinct advantages and disadvantages.

Development of a production process for liquid formulations combined with hollow microneedle(s) and applicators will be easier in comparison to development of a production process for coated microneedle arrays. Although technical difficulties producing the microneedles themselves will be similar, especially the solution for injection is easier to develop than a dry formulation of a vaccine coated onto a microneedle array. A solution for injection to be administered by hollow microneedle(s) is either already available or knowledge and experience in producing one is more readily available. Marketing authorization of a hollow microneedle-based vaccine may be easier as well, as regulatory experience is available for the solution for injection formulation and the medical device will be subjected to regulations for an injection device, for which regulatory experience exists as well. Thus, the hollow microneedle approach has a large potential to generate a marketable product within a reasonable amount of time.

Table 1 Comparison of intradermal immunization by using coated microneedle arrays vs. hollow microneedles.

	Hollow microneedles		Coated microneedle arrays	
	Advantages	**Disadvantages**	**Advantages**	**Disadvantages**
Formulation	• Formulations readily available • Shorter development times for the formulation • Development of a multivalent formulation is relatively easy • No vaccine is wasted during production of the product • No limits on dose	• A concentrated antigen formulation may need to be developed • Requires cold-chain supply	• Potentially does not require cold-chain supply	• Extensive reformulation needed • More extensive development times for the formulation • Multivalent formulations more difficult • Coating procedure may lead to substantial wastage of vaccine • Limited dose requires potent antigen or formulation
Injection	• Very accurate dosing	• Risk of leakage during administration, especially for arrays • Risk of microneedle clogging	• No increased risk of leakage for arrays • No risk of microneedle clogging	• Dosing accuracy difficult to control, depending on external factors
Device	• Controllable injection parameters	• Complex device • Pump required	• Simple device • No pump required	• Injection parameters not controllable

Although the coated microneedle approach may have a longer route and higher hurdles to overcome before being developed into a product ready for marketing authorization, it has unique advantages over the hollow microneedle approach. As the coated microneedle approach is based on a dry-coated vaccine, it is expected that the vaccine is more stable than a liquid vaccine formulation [47, 48], potentially avoiding the need for a cold-chain supply. This makes the coated microneedle approach an ideal candidate for a vaccine that can be used in extreme environments with high or low temperatures, or where a cold-chain supply is not supported. In addition, coated microneedles do not require a complicated device to apply them into the skin. This would help spread vaccine coverage in remote locations in the world, as untrained personnel should be able to administer the vaccine to the population. Or, in case of a pandemic, self-administration could help spread vaccine coverage quickly.

In summary, although both approaches have unique advantages over one another, hollow microneedle-based vaccines are a more realistic approach and may be expected sooner on the market than coated microneedles-based vaccines.

CONCLUSION

In this thesis, several aspects of microneedle-mediated intradermal vaccination were explored. It was demonstrated that vaccine-specific immune responses are not dependent on the intradermal administration depth of the vaccine. In contrast, by providing a prolonged exposure to the vaccine through repeated fractional doses that were intradermally delivered *via* a hollow microneedle, vaccine-specific immune responses were significantly increased. Furthermore, it was demonstrated that a layer-by-layer coating approach on solid microneedles allows for a dose-tunable and simple administration of vaccine. These layer-by-layer coated microneedles were utilized for effective immunization and might provide an escape from cold-chain supply.

REFERENCES

1. C. Levin, H. Perrin, B. Combadiere, Tailored immunity by skin antigen-presenting cells, Hum Vaccin Immunother, 11 (2015) 27-36.
2. J.F. Nicolas, B. Guy, Intradermal, epidermal and transcutaneous vaccination: from immunology to clinical practice, Expert Rev Vaccines, 7 (2008) 1201-1214.
3. R.B. Belshe, F.K. Newman, J. Cannon, C. Duane, J. Treanor, C. Van Hoecke, B.J. Howe, G. Dubin, Serum antibody responses after intradermal vaccination against influenza, N Engl J Med, 351 (2004) 2286-2294.
4. B. Bonnotte, M. Gough, V. Phan, A. Ahmed, H. Chong, F. Martin, R.G. Vile, Intradermal injection, as opposed to subcutaneous injection, enhances immunogenicity and suppresses tumorigenicity of tumor cells, Cancer Res, 63 (2003) 2145-2149.
5. S. Kaushik, A.H. Hord, D.D. Denson, D.V. McAllister, S. Smitra, M.G. Allen, M.R. Prausnitz, Lack of pain associated with microfabricated microneedles, Anesth Analg, 92 (2001) 502-504.
6. S.M. Bal, Z. Ding, E. van Riet, W. Jiskoot, J.A. Bouwstra, Advances in transcutaneous vaccine delivery: do all ways lead to Rome?, J Control Release, 148 (2010) 266-282.
7. M.J. Warrell, K.G. Nicholson, D.A. Warrell, P. Suntharasamai, P. Chanthavanich, C. Viravan, A. Sinhaseni, M.K. Chiewbambroongkiat, X. Pouradier-Duteil, C. Xueref, et al., Economical multiple-site intradermal immunisation with human diploid-cell-strain vaccine is effective for post-exposure rabies prophylaxis, Lancet, 1 (1985) 1059-1062.
8. B.P. Quiambao, E.M. Dimaano, C. Ambas, R. Davis, A. Banzhoff, C. Malerczyk, Reducing the cost of post-exposure rabies prophylaxis: efficacy of 0.1 ml PCEC rabies vaccine administered intradermally using the Thai Red Cross post-exposure regimen in patients severely exposed to laboratory-confirmed rabid animals, Vaccine, 23 (2005) 1709-1714.
9. A. Ambrozaitis, A. Laiskonis, L. Balciuniene, A. Banzhoff, C. Malerczyk, Rabies post-exposure prophylaxis vaccination with purified chick embryo cell vaccine (PCECV) and purified Vero cell rabies vaccine (PVRV) in a four-site intradermal schedule (4-0-2-0-1-1): an immunogenic, cost-effective and practical regimen, Vaccine, 24 (2006) 4116-4121.
10. T. Propst, A. Propst, K. Lhotta, W. Vogel, P. Konig, Reinforced intradermal hepatitis B vaccination in hemodialysis patients is superior in antibody response to intramuscular or subcutaneous vaccination, Am J Kidney Dis, 32 (1998) 1041-1045.
11. H. Micozkadioglu, A. Zumrutdal, D. Torun, S. Sezer, F.N. Ozdemir, M. Haberal, Low dose intradermal vaccination is superior to high dose intramuscular vaccination for hepatitis B in unresponsive hemodialysis patients, Ren Fail, 29 (2007) 285-288.
12. Y.C. Kim, F.S. Quan, D.G. Yoo, R.W. Compans, S.M. Kang, M.R. Prausnitz, Improved influenza vaccination in the skin using vaccine coated microneedles, Vaccine, 27 (2009) 6932-6938.
13. D. Holland, R. Booy, F. De Looze, P. Eizenberg, J. McDonald, J. Karrasch, M. McKeirnan, H. Salem, G. Mills, J. Reid, F. Weber, M. Saville, Intradermal influenza vaccine administered using a new microinjection system produces superior

immunogenicity in elderly adults: a randomized controlled trial, J Infect Dis, 198 (2008) 650-658.

14. F.S. Quan, Y.C. Kim, A. Vunnava, D.G. Yoo, J.M. Song, M.R. Prausnitz, R.W. Compans, S.M. Kang, Intradermal vaccination with influenza virus-like particles by using microneedles induces protection superior to that with intramuscular immunization, J Virol, 84 (2010) 7760-7769.
15. D.G. Koutsonanos, E.V. Vassilieva, A. Stavropoulou, V.G. Zarnitsyn, E.S. Esser, M.T. Taherbhai, M.R. Prausnitz, R.W. Compans, I. Skountzou, Delivery of subunit influenza vaccine to skin with microneedles improves immunogenicity and long-lived protection, Sci Rep, 2 (2012) 357.
16. E.V. Vassilieva, H. Kalluri, D. McAllister, M.T. Taherbhai, E.S. Esser, W.P. Pewin, J.A. Pulit-Penaloza, M.R. Prausnitz, R.W. Compans, I. Skountzou, Improved immunogenicity of individual influenza vaccine components delivered with a novel dissolving microneedle patch stable at room temperature, Drug Deliv Transl Res, 5 (2015) 360-371.
17. R. Arakane, R. Annaka, A. Takahama, K. Ishida, M. Yoshiike, T. Nakayama, F. Takeshita, Superior immunogenicity profile of the new intradermal influenza vaccine compared to the standard subcutaneous vaccine in subjects 65 years and older: A randomized controlled phase III study, Vaccine, 33 (2015) 6650-6658.
18. J. Cadorna-Carlos, E. Vidor, M.C. Bonnet, Randomized controlled study of fractional doses of inactivated poliovirus vaccine administered intradermally with a needle in the Philippines, Int J Infect Dis, 16 (2012) e110-116.
19. S.B. Troy, D. Kouiavskaia, J. Siik, E. Kochba, H. Beydoun, O. Mirochnitchenko, Y. Levin, N. Khardori, K. Chumakov, Y. Maldonado, Comparison of the Immunogenicity of Various Booster Doses of Inactivated Polio Vaccine Delivered Intradermally Versus Intramuscularly to HIV-Infected Adults, J Infect Dis, 211 (2015) 1969-1976.
20. J. van Smeden, M. Janssens, G.S. Gooris, J.A. Bouwstra, The important role of stratum corneum lipids for the cutaneous barrier function, Biochim Biophys Acta, 1841 (2014) 295-313.
21. K. van der Maaden, W. Jiskoot, J. Bouwstra, Microneedle technologies for (trans)dermal drug and vaccine delivery, J Control Release, 161 (2012) 645-655.
22. R. Zhang, H. Olin, Porous Gold Films-A Short Review on Recent Progress, Materials (Basel), 7 (2014) 3834-3854.
23. A.D. Nisbet, R.H. Saundry, A.J. Moir, L.A. Fothergill, J.E. Fothergill, The complete amino-acid sequence of hen ovalbumin, Eur J Biochem, 115 (1981) 335-345.
24. S.Y. Tzeng, K.J. McHugh, A.M. Behrens, S. Rose, J.L. Sugarman, S. Ferber, R. Langer, A. Jaklenec, Stabilized single-injection inactivated polio vaccine elicits a strong neutralizing immune response, Proc Natl Acad Sci U S A, 115 (2018) E5269-E5278.
25. J.M. Hogle, M. Chow, D.J. Filman, Three-dimensional structure of poliovirus at 2.9 A resolution, Science, 229 (1985) 1358-1365.
26. D. Gatto, S.W. Martin, J. Bessa, E. Pellicioli, P. Saudan, H.J. Hinton, M.F. Bachmann, Regulation of memory antibody levels: the role of persisting

antigen versus plasma cell life span, J Immunol, 178 (2007) 67-76.

27. U. Klein, R. Dalla-Favera, Germinal centres: role in B-cell physiology and malignancy, Nat Rev Immunol, 8 (2008) 22-33.
28. G. Du, R.M. Hathout, M. Nasr, M.R. Nejadnik, J. Tu, R.I. Koning, A.J. Koster, B. Slutter, A. Kros, W. Jiskoot, J.A. Bouwstra, J. Monkare, Intradermal vaccination with hollow microneedles: A comparative study of various protein antigen and adjuvant encapsulated nanoparticles, J Control Release, 266 (2017) 109-118.
29. M. Zaric, O. Lyubomska, O. Touzelet, C. Poux, S. Al-Zahrani, F. Fay, L. Wallace, D. Terhorst, B. Malissen, S. Henri, U.F. Power, C.J. Scott, R.F. Donnelly, A. Kissenpfennig, Skin dendritic cell targeting via microneedle arrays laden with antigen-encapsulated poly-D,L-lactide-co-glycolide nanoparticles induces efficient antitumor and antiviral immune responses, ACS Nano, 7 (2013) 2042-2055.
30. P.C. Demuth, W.F. Garcia-Beltran, M.L. Ai-Ling, P.T. Hammond, D.J. Irvine, Composite dissolving microneedles for coordinated control of antigen and adjuvant delivery kinetics in transcutaneous vaccination, Adv Funct Mater, 23 (2013) 161-172.
31. M. Leone, J. Monkare, J.A. Bouwstra, G. Kersten, Dissolving Microneedle Patches for Dermal Vaccination, Pharm Res, 34 (2017) 2223-2240.
32. J. Monkare, M. Pontier, E.E.M. van Kampen, G. Du, M. Leone, S. Romeijn, M.R. Nejadnik, C. O'Mahony, B. Slutter, W. Jiskoot, J.A. Bouwstra, Development of PLGA nanoparticle loaded dissolving microneedles and comparison with hollow microneedles in intradermal vaccine delivery, Eur J Pharm Biopharm, 129 (2018) 111-121.
33. A.J. Mohammed, S. AlAwaidy, S. Bawikar, P.J. Kurup, E. Elamir, M.M. Shaban, S.M. Sharif, H.G. van der Avoort, M.A. Pallansch, P. Malankar, A. Burton, M. Sreevatsava, R.W. Sutter, Fractional doses of inactivated poliovirus vaccine in Oman, N Engl J Med, 362 (2010) 2351-2359.
34. A. Anand, K. Zaman, C.F. Estivariz, M. Yunus, H.E. Gary, W.C. Weldon, T.I. Bari, M. Steven Oberste, S.G. Wassilak, S.P. Luby, J.D. Heffelfinger, M.A. Pallansch, Early priming with inactivated poliovirus vaccine (IPV) and intradermal fractional dose IPV administered by a microneedle device: A randomized controlled trial, Vaccine, 33 (2015) 6816-6822.
35. S. Resik, A. Tejeda, P.M. Lago, M. Diaz, A. Carmenates, L. Sarmiento, N. Alemani, B. Galindo, A. Burton, M. Friede, M. Landaverde, R.W. Sutter, Randomized controlled clinical trial of fractional doses of inactivated poliovirus vaccine administered intradermally by needle-free device in Cuba, J Infect Dis, 201 (2010) 1344-1352.
36. S. Resik, A. Tejeda, R.W. Sutter, M. Diaz, L. Sarmiento, N. Alemani, G. Garcia, M. Fonseca, L.H. Hung, A.L. Kahn, A. Burton, J.M. Landaverde, R.B. Aylward, Priming after a fractional dose of inactivated poliovirus vaccine, N Engl J Med, 368 (2013) 416-424.
37. D. Soonawala, P. Verdijk, A.J. Wijmenga-Monsuur, C.J. Boog, P. Koedam, L.G. Visser, N.Y. Rots, Intradermal fractional booster dose of inactivated poliomyelitis vaccine with a jet injector in healthy adults, Vaccine, 31 (2013) 3688-3694.

38. C.F. Estivariz, H. Jafari, R.W. Sutter, T.J. John, V. Jain, A. Agarwal, H. Verma, M.A. Pallansch, A.P. Singh, S. Guirguis, J. Awale, A. Burton, S. Bahl, A. Chatterjee, R.B. Aylward, Immunogenicity of supplemental doses of poliovirus vaccine for children aged 6-9 months in Moradabad, India: a community-based, randomised controlled trial, Lancet Infect Dis, 12 (2012) 128-135.
39. S. Resik, A. Tejeda, O. Mach, M. Fonseca, M. Diaz, N. Alemany, G. Garcia, L.H. Hung, Y. Martinez, R. Sutter, Immune responses after fractional doses of inactivated poliovirus vaccine using newly developed intradermal jet injectors: a randomized controlled trial in Cuba, Vaccine, 33 (2015) 307-313.
40. P.M. Frew, A.K. Fisher, M.M. Basket, Y. Chung, J. Schamel, J.L. Weiner, J. Mullen, S.B. Omer, W.A. Orenstein, Changes in childhood immunization decisions in the United States: Results from 2012 & 2014 National Parental Surveys, Vaccine, 34 (2016) 5689-5696.
41. C. Hough-Telford, D.W. Kimberlin, I. Aban, W.P. Hitchcock, J. Almquist, R. Kratz, K.G. O'Connor, Vaccine Delays, Refusals, and Patient Dismissals: A Survey of Pediatricians, Pediatrics, 138 (2016).
42. H.J. Larson, A. de Figueiredo, Z. Xiahong, W.S. Schulz, P. Verger, I.G. Johnston, A.R. Cook, N.S. Jones, The State of Vaccine Confidence 2016: Global Insights Through a 67-Country Survey, EBioMedicine, 12 (2016) 295-301.
43. N.S. Clemmons, P.A. Gastanaduy, A.P. Fiebelkorn, S.B. Redd, G.S. Wallace, C. Centers for Disease, Prevention, Measles - United States, January 4-April 2, 2015, MMWR Morb Mortal Wkly Rep, 64 (2015) 373-376.
44. J.S. Gerber, P.A. Offit, Vaccines and autism: a tale of shifting hypotheses, Clin Infect Dis, 48 (2009) 456-461.
45. I.o. Medicine, Adverse Effects of Vaccines: Evidence and Causality, The National Academy Press, Washington, DC, USA, 2012.
46. M.A. Maglione, L. Das, L. Raaen, A. Smith, R. Chari, S. Newberry, R. Shanman, T. Perry, M.B. Goetz, C. Gidengil, Safety of vaccines used for routine immunization of U.S. children: a systematic review, Pediatrics, 134 (2014) 325-337.
47. X. Chen, G.J. Fernando, M.L. Crichton, C. Flaim, S.R. Yukiko, E.J. Fairmaid, H.J. Corbett, C.A. Primiero, A.B. Ansaldo, I.H. Frazer, L.E. Brown, M.A. Kendall, Improving the reach of vaccines to low-resource regions, with a needle-free vaccine delivery device and long-term thermostabilization, J Control Release, 152 (2011) 349-355.
48. H.S. Gill, M.R. Prausnitz, Coating formulations for microneedles, Pharm Res, 24 (2007) 1369-1380.

7

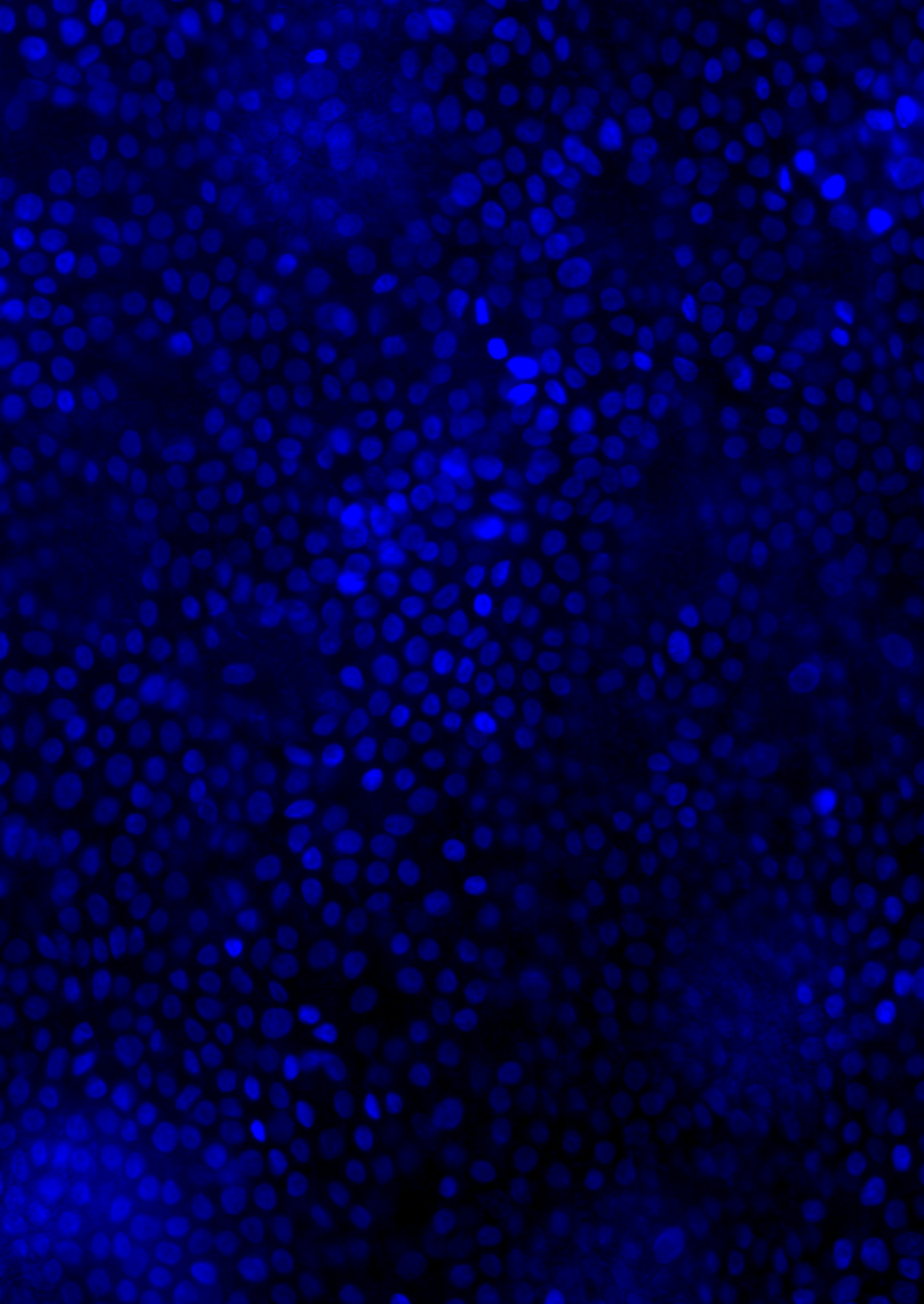

A

Nederlandse samenvatting
Curriculum Vitae
List of publications
List of abbreviations

NEDERLANDSE SAMENVATTING

Een uitleg van de onderstreepte woorden is te vinden in de verklarende woordenlijst.

INLEIDING

Het belang van vaccineren

Het belang van vaccineren staat soms ter twijfel. Ten onrechte, want vaccineren voorkomt ernstige ziektes. Ziektes die in de vorige eeuw nog verantwoordelijk waren voor ziekenhuisopname, permanente schade en sterfte, voornamelijk onder kinderen, komen tegenwoordig weinig voor dankzij grootschalige vaccinatieprogramma's. Behalve leed, worden ook medische kosten bespaard door te investeren in vaccinatieprogramma's.

Hoe werkt een vaccin

Het afweersysteem weert ziekteverwekkers uit ons lichaam. Afweercellen zijn de soldaten van het afweersysteem. Zij staan op wacht en starten een afweerreactie als zij een ziekteverwekker ontdekken. Deze afweerreactie is zeer belangrijk om de ziekteverwekker uit het lichaam te weren.

Een vaccin is een spuitje met daarin een samenstelling van (i) een verzwakte of gedode ziekteverwekker, of een onderdeel daarvan, (ii) een adjuvans en (iii) verschillende hulpstoffen om het vaccin stabiel en werkzaam te houden. Een dergelijke samenstelling wordt ook wel een vaccinformulering genoemd. Na vaccinatie reageren de afweercellen op het vaccin en proberen het vaccin af te weren. Met succes, want het vaccin is immers onschadelijk. Omdat een vaccin in zekere mate lijkt op de echte ziekteverwekker, leren de afweercellen de ziekteverwekker te herkennen en af te weren. Hierdoor zijn de immuuncellen in staat bij een infectie de echte ziekteverwekker te herkennen en te neutraliseren.

Soms is een vaccin niet succesvol om het afweersysteem een ziekteverwekker te leren herkennen of afweren. In dat geval wordt de ziekteverwekker niet herkend door de afweercellen na vaccinatie of treden de afweercellen niet afdoende op tegen de ziekteverwekker na vaccinatie. In een dergelijk geval wordt een adjuvans aan het vaccin toegevoegd. Een adjuvans maakt de afweercellen actief en spoort deze aan tot actie. Een adjuvans is dus een hulpstof die het vaccin werkzamer maakt. Daarnaast is het mogelijk dat er meerdere vaccins worden samengevoegd tot één combinatievaccin. Het voordeel van een combinatievaccin is dat er minder prikken nodig zijn.

De traditionele manieren van vaccineren

De meeste vaccins worden via een injectienaald in een spier of onderhuids ingespoten.

Deze manier van vaccineren kan als traditioneel beschouwd worden. In de afgelopen jaren is de belangstelling om vaccins op andere manieren toe te dienen echter toegenomen, omdat deze mogelijk effectiever zijn.

Eén van deze andere manieren van vaccineren is het injecteren van een vaccin in de huid. De huid bevat namelijk veel meer afweercellen dan spieren. Daarom zal vaccineren via de huid effectiever kunnen zijn dan vaccinatie via de spier. Zoveel effectiever, dat er wellicht een lagere dosis vaccin nodig zal zijn. Dit wordt ook wel dosisbesparing genoemd.

In de wetenschappelijke literatuur is bijvoorbeeld beschreven dat er bij vaccinatie via de huid van hondsdolheidsvaccin (rabiësvaccin) een 60-80% lagere dosis nodig is ten opzichte van toediening in de spier. Dosisbesparing is ook beschreven voor vaccinatie tegen hepatitis B, griep (influenza) en polio, wanneer vaccinatie via de huid werd vergeleken met vaccinatie via de spier.

Beschermende functies van de huid

De huid heeft een beschermende functie voor het lichaam. Eén van deze beschermende functies is het buiten het lichaam houden van ziekteverwekkers. Zo is er bijvoorbeeld een fysieke blokkade, welke wordt verzorgd door de buitenste laag van de huid, de hoornlaag. De hoornlaag is zeer dun, ongeveer 15-20 micrometer (ofwel ongeveer één vijftigste millimeter) dik. Echter, de fysieke blokkade van de hoornlaag houdt ook vaccins buiten de huid. Om vaccins in de huid toe te dienen, moet de hoornlaag omzeild worden. Wanneer er naalden gebruikt worden die lang genoeg zijn om de hoornlaag te passeren, kan het vaccin afgeleverd worden bij de afweercellen in de huid. Wanneer de naalden bovendien kort genoeg zijn, kan een pijnsensatie vermeden worden. Pijnreceptoren liggen namelijk diep in de huid. Micronaalden zijn dunne naaldjes met een lengte van slechts 50-1000 micrometer (ofwel één twintigste tot 1 millimeter) en voldoen aan deze eigenschappen. De ontwikkeling van micronaalden kan daarom leiden tot een manier voor pijnloze vaccinatie.

Nadelen van traditionele vaccinatie met een injectienaald

Hoewel traditionele vaccinatie door middel van een injectienaald effectief is, zijn er een aantal nadelen bij het gebruik van injectienaalden. Behalve dat injecties met injectienaalden pijnlijk zijn, is er ook een risico dat de injectienaalden hergebruikt worden, waardoor een risico op infectie ontstaat. Daarnaast is er een risico voor prikaccidenten met infectie als gevolg. Tot slot kunnen de injecties alleen uitgevoerd worden door personen die daarvoor geschoold zijn. Omdat micronaalden zo kort zijn, voor eenmalig gebruik ontworpen kunnen worden en gemakkelijk te gebruiken zijn, kunnen micronaalden de nadelen van injectienaalden mogelijk vermijden.

Micronaalden

Om vaccinatie via de huid mogelijk te maken, zijn er diverse typen micronaalden ontwikkeld. In dit proefschrift wordt onderzoek beschreven waarin twee typen micronaalden gebruikt worden voor vaccinatie: holle en gecoate micronaalden.

Holle micronaalden lijken enigszins op traditionele injectienaalden, maar hebben veel kleinere afmetingen. Holle micronaalden worden in de huid geprikt, waarna een vloeibare vaccinformulering door het holle gedeelte van de naald de huid in vloeit, met behulp van een injectiepomp.

In het in dit proefschrift beschreven onderzoek werd een enkele holle micronaald gebruikt in combinatie met een applicator- en injectiesysteem (zie figuur 1). Een applicatorsysteem is nodig om de holle micronaald nauwkeurig op een gewenste diepte in de huid aan te brengen. Een injectiesysteem is nodig om een gewenste dosis van het vaccin nauwkeurig toe te dienen. De diepte waarop de micronaalden in de huid gebracht worden is van belang, omdat het aantal en het type afweercellen in de huid afhankelijk is van de diepte in de huid. Zowel het aantal als het type afweercellen dat bereikt wordt zou de effectiviteit van de vaccinatie kunnen beïnvloeden.

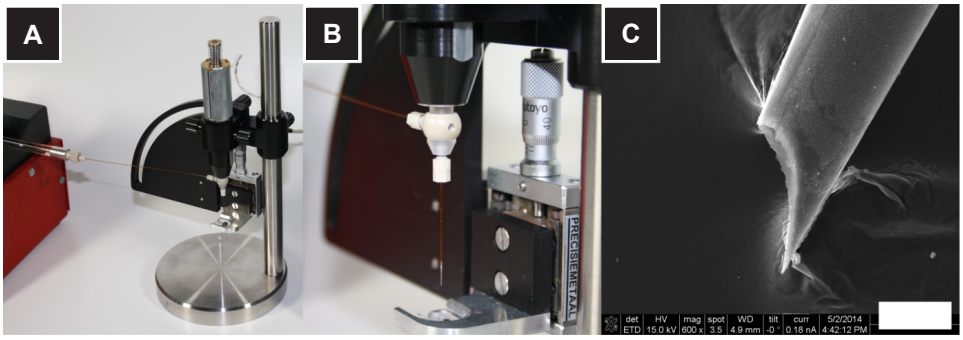

Figuur 1 Beelden van het applicator- en injectiesysteem voor enkele holle micronaalden (**A** en **B**) met een enkele holle micronaald daaraan bevestigd (**B**) en een zeer sterk vergroot beeld van een enkele holle micronaald (**C**, de witte balk representeert 0,05 mm, ofwel één twintigste millimeter).

Het tweede type in dit proefschrift beschreven micronaalden voor vaccinatie zijn gecoate micronaalden, waarvoor massieve micronaalden gebruikt worden. Deze worden veelal geproduceerd in rijen welke uit een plaatje steken; dit geheel wordt gewoonlijk aangeduid met de term micronaalden-array (zie figuur 2A en 2B). Vervolgens wordt

het oppervlak van de micronaalden op zo'n array gecoat met vaccin (zie figuur 2C). Na het inbrengen in de huid van met vaccin gecoate micronaalden-arrays, laat de coating van de micronaaldoppervlakken los. De vaccincoating blijft achter in de huid nadat de micronaalden-arrays verwijderd zijn (zie figuur 2D). De afweercellen in de huid reageren vervolgens op het vaccin.

Het voordeel van met vaccin gecoate micronaalden-arrays is dat zij, in vergelijking met een holle micronaald, zeer eenvoudig in de huid ingebracht kunnen worden. Zo eenvoudig dat men het in principe zelf zou kunnen doen, mits daarvoor een zeer simpel micronaald-toedieningsapparaatje ontworpen wordt. Het nadeel is echter dat de hoeveelheid vaccin dat gecoat kan worden op de micronaalden-arrays beperkt is door het relatief kleine beschikbare oppervlak voor vaccincoating. De hoeveelheid vaccin dat gecoat kan worden kan verhoogd worden door het vergroten van het beschikbare oppervlak voor vaccincoating.

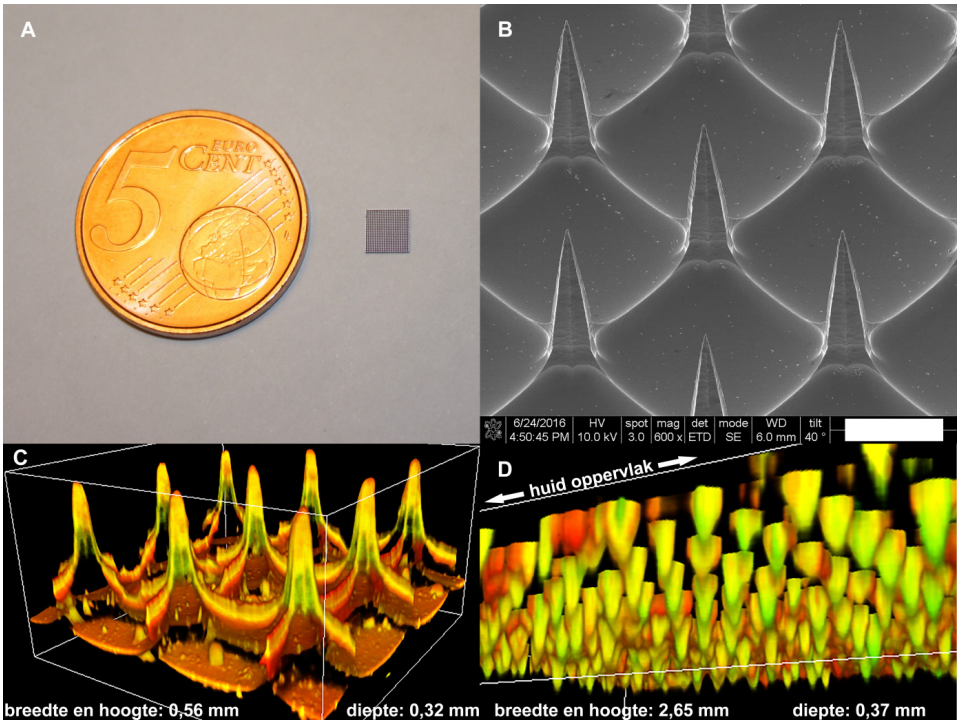

Figuur 2 Beelden van micronaalden-arrays. Een overzichtsbeeld van een micronaalden-array met 576 massieve micronaalden op een 5x5 mm plaatje is weergegeven in **A** en een 600x vergroot beeld daarvan is weergegeven in **B** (witte balk representeert 0,1 mm, ofwel één tiende millimeter). Beelden van de coating (groene en rode kleur) op een met vaccin gecoate micronaald-array is weergegeven

in **C**. Beelden van coating afgegeven in de huid, nadat een met vaccin gecoate micronaald-array in de huid is gebracht en verwijderd, is weergegeven in **D**.

DOELSTELLINGEN VAN HET IN DIT PROEFSCHRIFT BESCHREVEN ONDERZOEK

De doelstellingen van het in dit proefschrift beschreven onderzoek zijn:

- Inzicht verkrijgen in het effect van de injectiediepte in de huid op de afweerreactie tegen een vaccin.
- Inzicht verkrijgen in de afweerreactie na vaccinatie via de huid gedurende meerdere dagen, ten opzichte van een éénmalige injectie, waarbij de totale hoeveelheid vaccin gelijk is.
- Opzetten van een methode waarin vaccin en adjuvans afwisselend laag-voor-laag op micronaalden-arrays worden aangebracht, om de hoeveelheid aangebracht vaccin op de micronaalden-arrays te vergroten voor vaccinatiedoeleinden.
- Opzetten van methoden om goudoppervlakken te veranderen, met als doel de hoeveelheid te coaten vaccin op goud-gecoate micronaalden-arrays te vergroten.

SAMENVATTING

Dendritische cellen (DCs) zijn afweercellen welke gespecialiseerd zijn in het neutraliseren van ziekteverwekkers en het op gang brengen van verdere afweerreacties. DCs zijn daarom erg belangrijk bij vaccinatie. Zoals in detail is uitgelegd in de inleiding van dit proefschrift (*hoofdstuk 1)*, bevinden zich drie verschillende typen DCs in de humane huid. Elk type DC in de huid heeft een andere functie in de afweer tegen ziekteverwekkers. Bovendien verblijven deze drie typen DCs in verschillende hoeveelheden op verschillende dieptes in de huid. Daarom is de sterkte van de verschillende afweerreacties wellicht afhankelijk van de diepte waarop het vaccin in de huid wordt toegediend. Het onderzoek dat is beschreven in *hoofdstukken 2 en 3* heeft daarom tot doel om te bepalen of de afweerreacties op vaccinatie beïnvloed worden door de diepte waarop het vaccin in de huid wordt toegediend.

In *hoofdstuk 2* is beschreven hoe het applicator- en injectiesysteem voor een holle micronaald is verbeterd ten opzichte van het initiële ontwerp. Het injectiesysteem werd lekkage-vrij gemaakt door kritieke onderdelen te vervangen door onderdelen bestendig tegen hoge druk. Door deze verbeteringen is het mogelijk met een enkele holle micronaald in mensen- en rattenhuid te injecteren met een precieze injectiediepte, injectievolume en injectiesnelheid. Vervolgens is onderzocht of specifiek tegen geïnactiveerd poliovaccin serotype 1 (IPV1) gerichte afweerreacties in ratten beïnvloed worden door de injectiediepte.

Tevens is onderzocht of de IPV1-specifieke afweerreacties versterkt kunnen worden door adjuvantia aan de IPV1-vaccinformulering toe te voegen. Uit dit onderzoek is gebleken dat IPV1-specifieke afweerreacties onafhankelijk zijn van de diepte waarop IPV1 met behulp van een holle micronaald in de huid wordt geïnjecteerd. Tevens is gebleken dat vaccinatie via de huid net zo effectief is als vaccinatie via de spier. Bovendien leidt toevoeging van een adjuvans (CpG oligodeoxynucleotide 1826 (CpG) of choleratoxine (CT)) aan de IPV1-vaccinformulering tot een verhoging van IPV1-specifieke afweerreacties ten opzichte van een IPV1-vaccinformulering zonder adjuvans, ongeacht het type adjuvans (CpG of CT) of de toedieningsroute (via de huid of de spier). Beide adjuvantia zijn dus veelbelovende kandidaten om het effect van IPV1-vaccinatie via de huid te verbeteren.

In *hoofdstuk 3* is onderzocht of de afweerreacties van de drie typen DCs in humane huid veranderen, wanneer verschillende doses vaccin worden geïnjecteerd of wanneer een vaccin op verschillende dieptes in de huid wordt geïnjecteerd. Nadat de DCs in de huid vaccin opnemen, worden zij geactiveerd en migreren vervolgens naar dieper gelegen weefsels in het lichaam om daar afweerreacties op gang te brengen. Daarom zijn er drie reacties van de DCs op vaccinatie onderzocht: de hoeveelheid opgenomen vaccin, de mate van DC-activatie en de mate van migratie van de drie typen DCs in humane huid. Uit deze studies is gebleken dat de drie verschillende typen DCs in humane huid van elkaar verschillen in de mate waarin zij het vaccin opnemen, de mate waarin zij geactiveerd worden en de mate van migratie. Het is gebleken dat deze uitkomsten ook afhankelijk zijn van de geïnjecteerde dosis. Echter, de mate van vaccinopname, DC-activatie en -migratie wordt niet beïnvloed door de injectiediepte in de huid. Nader onderzoek heeft uitgewezen dat het vaccin zich zo snel door de huid beweegt dat het alle lagen van de huid kan bereiken gedurende de duur van het experiment. Het injectievolume is echter ook van belang, voornamelijk voor de mate van irritatie en pijnsensatie in de huid nadat een vaccin in de huid is geïnjecteerd. Het is gebleken dat injecties in de huid met holle micronaalden en een zeer klein injectievolume tot vergelijkbare afweerreacties leiden als injecties met een normale injectienaald en een groot injectievolume.

Tijdens een natuurlijke infectie kan een ziekteverwekker de huid binnen dringen en exponentieel in aantal toenemen tijdens deze infectie. Door deze sterke groei in aantallen ziekteverwekkers kan de omvang van de afweerreactie toenemen. Daarom is, zoals beschreven in *hoofdstuk 4*, onderzocht of de afweerreactie toeneemt door de vaccindosis over meerdere dagen te verspreiden, al dan niet in een exponentieel toenemende dosis. Immers, als het toedienen van vaccin een natuurlijk verloop volgt, blijft de afweerreactie gestimuleerd voor langere tijd, waardoor meer afweercellen aangetrokken zouden kunnen worden.

Het doel van de studies beschreven in *hoofdstuk 4* is dan ook om te bepalen of IPV1-specifieke afweerreacties worden versterkt, wanneer een dosis IPV1 in meerdere delen wordt opgesplitst en toegediend gedurende meerdere dagen, ten opzichte van een gelijke éénmalige dosis IPV1. Voor verspreide toediening zijn verschillende doseringsschema's gebruikt, namelijk vaccinatie gedurende 4 of 8 dagen, om de dag of exponentieel toenemend (gedurende 4 dagen en al dan niet met CpG toegevoegd), welke zijn vergeleken met een éénmalige toediening. De doseringsschema's waarbij vaccin is geïnjecteerd in de huid gedurende meerdere dagen, al dan niet met een exponentieel toenemende dosis, resulteert in een 10-voudige verhoging van IPV1-specifieke afweerreacties in vergelijking met een éénmalige dosering geïnjecteerd in huid of spier. IPV1 gecombineerd met adjuvans CpG in een exponentieel toenemend doseringsschema verhoogt de IPV1-specifieke afweerreacties niet verder. Samengevat is gebleken dat het toedienen van IPV1 in de huid gedurende meerdere dagen tot superieure IPV1-specifieke afweerreacties leidt, waarbij het gebruik van een adjuvans geen toegevoegde waarde heeft.

Naast studies gebruikmakend van holle micronaalden zijn er ook studies uitgevoerd gebruikmakend van gecoate massieve micronaalden-arrays. Gecoate massieve micronaalden-arrays kunnen worden gemaakt door gebruik te maken van pH-gevoelige oppervlakken. De lading van pH-gevoelige micronaaldoppervlakken is afhankelijk van de pH van de omgeving waarin de oppervlakken zich bevinden. Tijdens het coaten wordt een relatief lage pH gebruikt. Bij een lage pH zijn de micronaaldoppervlakken positief geladen. Daardoor kan een negatief geladen vaccin zich aan de micronaaldoppervlakken hechten. Omdat de pH in de huid neutraal is en de lading van de micronaaldoppervlakken afhankelijk is van de pH, wordt de lading op het oppervlak minder. Daardoor verzwakt ook de binding tussen vaccin en micronaaldoppervlak. Hierdoor laat het vaccin los van de micronaaldoppervlakken nadat de micronaalden-arrays in de huid zijn ingebracht.

Zoals eerder beschreven, is de hoeveelheid vaccin die gecoat kan worden op massieve micronaalden-arrays beperkt door het geringe beschikbare oppervlak voor vaccincoating. Het in de *hoofdstukken 5 en 6* beschreven onderzoek had daarom tot doel methoden te ontwikkelen om meer vaccin op de micronaalden-arrays te coaten, door gebruikmaking van pH-gevoelige oppervlakken en methoden om het beschikbare oppervlak voor vaccincoating te vergroten.

In het onderzoek beschreven in *hoofdstuk 5* is een laag-voor-laag coatingsmethode ontwikkeld, gebruikmakend van micronaalden-arrays met pH-gevoelige oppervlakken. Tevens zijn in *hoofdstuk 5* micronaalden-arrays die op deze manier gecoat zijn getest op

geschiktheid voor vaccinatiedoeleinden.

In de eerste stap zijn pH-gevoelige oppervlakken gecreëerd door chemische modificatie van micronaaldoppervlakken die bestaan uit silicium. In de tweede stap zijn deze pH-gevoelige oppervlakken van de micronaalden-arrays afwisselend gecoat met negatief geladen difterietoxoïde (DT, een vaccin) en positief geladen N-trimethylchitosan (TMC, een polymeer met adjuvansfunctie).

Uit een dosis-responsstudie is gebleken dat de minimaal benodigde DT-dosis voor het opwekken van meetbare DT-specifieke afweerreacties ongeveer 300 nanogram is. Daarna is de methode om diverse DT/TMC-lagen op de micronaalden-arrays te coaten geoptimaliseerd. Hierbij is gebleken dat reproduceerbare hoeveelheden DT op de micronaalden-arrays gecoat kunnen worden. Bovendien is gebleken dat de hoeveelheid gecoat DT op de micronaalden-arrays verhoogd kan worden door een groter aantal DT/TMC-lagen aan te brengen. Daarnaast is gebleken dat de hoeveelheid in de huid afgeleverd vaccin mede bepaald wordt door het aantal gecoate DT/TMC-lagen.

In een daaropvolgende vaccinatiestudie in muizen is aangetoond dat vaccinatie met micronaalden-arrays gecoat met een stapsgewijs toenemend aantal DT/TMC-lagen resulteert in stapsgewijs toenemende DT-specifieke afweerreacties. Vaccinatie met behulp van micronaalden-arrays gecoat met 10 DT/TMC-lagen (overeenkomend met ongeveer 0,6 microgram in de huid toegediend DT) resulteert in vergelijkbare DT-specifieke afweerreacties als onderhuidse vaccinatie met 5 microgram DT gecombineerd met adjuvans. Dit is een 8-voudige dosisbesparing. Uit de resultaten beschreven in *hoofdstuk 5* blijkt dat de laag-voor-laag DT/TMC-coatingsmethode op pH-gevoelige micronaaldoppervlakken een veelbelovende manier is om DT-vaccinatie via de huid mogelijk te maken.

Een andere methode om het beschikbare oppervlak voor vaccincoating op micronaalden-arrays te vergroten, is het creëren van een sponsachtig goudoppervlak bovenop het siliciumoppervlak van de micronaalden-arrays. Om dit vergrote oppervlak te benutten, is in *hoofdstuk 6* tot doel gesteld om methoden op te zetten voor chemische modificatie van goudoppervlakken, zodat pH-gevoelige oppervlakken gecreëerd kunnen worden.

Zoals eerder beschreven, bepaalt de pH van de omgeving of en wanneer een pH-gevoelig oppervlak in staat is om vaccin te binden en in de huid af te geven, als gevolg van een samenspel tussen pH en pK_a-waarde. De pH waarbij 50% van de oppervlakmoleculen een lading heeft en de andere helft neutraal is, wordt de pK_a-

waarde genoemd. Om te bepalen bij welke pH een oppervlak geladen is, is het van belang deze pK_a-waarde te meten. Daarom is in het in *hoofdstuk 6* beschreven onderzoek de pK_a-waarde van de gemodificeerde goudoppervlakken bepaald. Uit deze studies is gebleken dat goudoppervlakken met succes gemodificeerd kunnen worden met vier verschillende moleculen, die na chemische reactie met het goudoppervlak resulteren in goudoppervlakken met vier verschillende p*K*a-waarden.

CONCLUSIE

Met het in dit proefschrift beschreven onderzoek is meer inzicht verkregen in verschillende aspecten van vaccinatie via de huid met behulp van micronaalden. Vaccin-specifieke afweerreacties blijken niet afhankelijk te zijn van de diepte waarop het vaccin in de huid wordt toegediend. Vaccin-specifieke afweerreacties blijken daarentegen aanzienlijk te worden verhoogd, wanneer het vaccin gedurende meerdere dagen in de huid wordt toegediend. Verder bieden zowel holle micronaalden als laag-voor-laag gecoate massieve micronaalden met pH-gevoelige micronaaldoppervlakken mogelijkheden om eenvoudig, doeltreffend en mogelijk pijnloos te vaccineren via de huid.

VERKLARENDE WOORDENLIJST

- **Adjuvans (meervoud: adjuvantia)**: een stof die de afweerreactie tegen een vaccin kan versterken.
- **Afweercellen**: lichaamscellen betrokken bij het neutraliseren van ziekteverwekkers.
- **Afweerreactie**: reactie van het lichaam gericht op het neutraliseren van ziekteverwekkers.
- **Afweersysteem**: systeem van reacties van het lichaam betrokken bij de neutralisatie van ziekteverwekkers.
- **Applicator- en injectiesysteem**: een combinatie van een applicatorsysteem, welke nodig is om een holle micronaald op een nauwkeurige manier in de huid te brengen, en een injectiesysteem, welke nodig is om de gewenste dosis van het vaccin nauwkeurig toe te dienen (zie figuur 1).
- **Chemische modificatie (van een oppervlak)**: het aanpassen van de eigenschappen van een oppervlak door chemische reacties uit te voeren op het oppervlak, met als doel het oppervlak een functie uit te kunnen laten voeren (bijvoorbeeld een pH-gevoelig oppervlak).
- **Dendritische cellen (DCs)**: afweercellen betrokken bij eerste reacties van het lichaam op ziekteverwekkers door de binnendringende ziekteverwekkers onschadelijk te maken en verdere afweerreacties op gang te brengen.
- **Difterie**: een ziekte veroorzaakt door *Corynebacterium diphtheriae*, een bacterie die gifstoffen maakt welke kunnen leiden tot beschadiging van de hartspier en zenuwstelsel. Onbehandeld is de ziekte vaak dodelijk: difterie was één van de meest voorkomende doodsoorzaken bij kinderen, totdat vaccinatie tegen difterie routinematig werd toegepast.
- **Difterietoxoïde**: het werkzame bestandsdeel in een vaccin tegen difterie.
- **Dosis-responsstudie**: studie waarbij de relatie wordt onderzocht tussen een gegeven dosis en het effect daarvan.
- **DT-specifieke afweerreacties**: afweerreacties van het lichaam, welke specifiek gericht zijn tegen DT (difterietoxoïde). De hoogte van deze afweerreacties zegt iets over de mate van bescherming tegen difterie.
- **Geïnactiveerd polio vaccin serotype 1 (IPV1)**: vaccin tegen polio, gebaseerd op gedood (geïnactiveerd) poliovirus (sero-)type 1.
- **Griep (influenza)**: een ziekte veroorzaakt door het influenzavirus. Infectie van de luchtwegen met influenzavirus leidt bij de meeste mensen tot aanzienlijke ziekteverschijnselen en soms zelfs tot sterfte.
- **Hepatitis B**: een leverontsteking die wordt veroorzaakt door het hepatitis B-virus, welke kan leiden tot levercirrose en leverkanker.
- **Hondsdolheid (rabiës)**: een ernstige ziekte als gevolg van een infectie met het

rabiësvirus, meestal door een beet van een door rabiës besmet dier (onder andere honden, vossen, vleermuizen en katten). Hondsdolheid is uiterst gevaarlijk voor mensen en het leidt onbehandeld tot de dood.

- **Infectie**: het binnendringen en zich vestigen van een ziekteverwekker in een levend wezen.
- **IPV1-specifieke afweerreacties**: afweerreacties van het lichaam, welke specifiek gericht zijn op de afweer van IPV1 (geïnactiveerd polio vaccin serotype 1). De hoogte van deze afweerreacties zegt iets over de mate van bescherming tegen polio.
- **Microgram**: één microgram is gelijk aan één miljoenste gram.
- **Micrometer**: één micrometer is een duizendste van een millimeter.
- **Micronaalden-array**: één of meerdere rijen van micronaalden, welke uit een plaatje steken (zie figuur 2).
- **Nanogram**: één nanogram is gelijk aan één miljardste gram.
- **N-trimethylchitosan (TMC)**: een polymeer met adjuvansfunctie.
- **Polio (poliomyelitis)**: een virusziekte welke een ontsteking van de grijze stof in het ruggenmerg veroorzaakt. Dit leidt tot ongeneeslijke verlammingen en blijvende spierzwakte, bij groeiende kinderen ook tot misvormingen of soms tot de dood als de ademhalingsspieren verlamd raken.
- **Polymeer**: aaneenschakeling van identieke of soortgelijke moleculen die chemisch aan elkaar zijn gekoppeld.
- **Vaccin**: (farmaceutisch) preparaat waarmee tegen een ziekte wordt gevaccineerd.
- **Vaccinatieprogramma**: een schema waarmee een overheid een aantal als essentieel beoordeelde vaccinaties aanbeveelt of verplicht stelt.
- **Vaccineren**: het toedienen van een vaccin.
- **Vaccinformulering**: een samenstelling van (i) een verzwakte of gedode ziekteverwekker, of een onderdeel daarvan, (ii) een adjuvans en (iii) verschillende hulpstoffen om het vaccin stabiel en werkzaam te houden.
- **Ziekteverwekker**: micro-organisme (zeer klein levend wezen) of virus dat een infectieziekte veroorzaakt.

CURRICULUM VITAE

Pim Schipper was born on the 22nd of December 1985 in Alkmaar. After graduating from the Murmellius Gymnasium in Alkmaar in 2004, he started his study Pharmacy at Utrecht University. He performed his research project at the 1st Department of Medicine, University Medical Center Hamburg-Eppendorf, Hamburg, Germany, resulting in his master thesis entitled "CD55 and CD59 expression on erythrocytes and leukocytes of patients with EAHEC O104:H4 infection". In August 2012, he obtained his pharmacist (PharmD) degree.

In May 2012, he started his PhD project at Leiden University under the supervision of Prof. Dr. Joke A. Bouwstra, Prof. Dr. Wim Jiskoot (Division of BioTherapeutics, Leiden Academic Centre for Drug Research (LACDR), Leiden University) and Prof. Dr. Ir. Cees W.J. Oomens (Soft Tissue Engineering and Mechanobiology, Department of Biomedical Engineering, Eindhoven University of Technology). The research performed during his PhD project is described in this thesis.

In August 2017 he started as Regulatory Project Leader at the College ter Beoordeling van Geneesmiddelen - Medicines Evaluation Board (CBG-MEB), which is the Dutch national independent authority in drug regulatory affairs.

LIST OF PUBLICATIONS

P. Schipper, K. van der Maaden, T.M.M. van Capel, A.M. Römgens, C.W. Oomens, E.C. de Jong, J. Bouwstra, Antigen uptake by skin dendritic cells as function of antigen dose and intradermal injection depth, Manuscript in preparation.

P. Schipper*, K. van der Maaden*, W. Jiskoot, J. Bouwstra, Chemical modifications of gold surfaces with basic groups and a fluorescent nanoparticle adhesion assay to determine their surface pK_a, Manuscript submitted.

P. Schipper, K. van der Maaden, V. Groeneveld, M. Ruigrok, S. Romeijn, S. Uleman, C. Oomens, G. Kersten, W. Jiskoot, J. Bouwstra, Diphtheria toxoid and N-trimethyl chitosan layer-by-layer coated pH-sensitive microneedles induce potent immune responses upon dermal vaccination in mice, J Control Release, 262 (**2017**) 28-36.

P. Schipper, K. van der Maaden, S. Romeijn, C. Oomens, G. Kersten, W. Jiskoot, J. Bouwstra, Repeated fractional intradermal dosing of an inactivated polio vaccine by a single hollow microneedle leads to superior immune responses, J Control Release, 242 (**2016**) 141-147.

P. Schipper, K. van der Maaden, S. Romeijn, C. Oomens, G. Kersten, W. Jiskoot, J. Bouwstra, Determination of depth-dependent intradermal immunogenicity of adjuvanted inactivated polio vaccine delivered by microinjections via hollow microneedles, Pharm Res, 33 (**2016**) 2269-2279.

K. van der Maaden, E. Sekerdag, **P. Schipper**, G. Kersten, W. Jiskoot, J. Bouwstra, Layer-by-layer assembly of inactivated poliovirus and N-trimethyl chitosan on pH-sensitive microneedles for dermal vaccination, Langmuir, 31 (**2015**) 8654-8660.

W. Dammermann*, **P. Schipper***, S. Ullrich, K. Fraedrich, J. Schulze zur Wiesch, T. Fründt, G. Tiegs, A. Lohse, S. Lüth, Increased expression of complement regulators CD55 and CD59 on peripheral blood cells in patients with EAHEC O104:H4 infection, PLoS One, 8 (**2013**) e74880.

* Authors contributed equally

LIST OF ABBREVIATIONS

Abbreviation	Meaning
2-MEA	2-mercaptoethylamine
4 x 1/4th (4 d)	four 1/4th doses administered over four consecutive days
4 x 1/4th (7 d)	four 1/4th doses administered on every other day over seven days
4-ATP	4-aminothiophenol
4-MP	4-mercaptopyridine
4-PEM	4-pyridylethylmercaptan
8 x 1/8th (8 d)	eight 1/8th doses administered over eight consecutive days
APC	antigen-presenting cell
BSA	bovine serum albumin
CI	95% confidence interval
CLSM	confocal laser scanning microscopy
CpG	CpG oligodeoxynucleotide 1826
CT	cholera toxin
CTL	cytotoxic T-lymphocyte
D	dermal
DC	dendritic cell
DC-shMN-iSystem	digitally-controlled single hollow microneedle injection system
DDC	dermal dendritic cell
DT	diphtheria toxoid
DT-AF488	diphtheria toxoid conjugated with Alexa Fluor® 488
DT-ALUM	aluminum phosphate-adsorbed diphtheria toxoid
DT-IRDYE800	diphtheria toxoid conjugated with near-infrared fluorescent label IRDye® 800CW
DTx	diphtheria toxin
DU	D-antigen units
EDTA	ethylenediaminetetraacetic acid
Exp	four exponentially increasing doses administered over four consecutive days
Exp-CpG	four exponentially increasing doses combined with adjuvant CpG administered over four consecutive days
FCS	fetal calf serum
FNAA	fluorescent nanoparticle adhesion assay

Abbreviation	Meaning
FRAP	fluorescence recovery after photobleaching
FT	Fourier transform
FT-SERS	Fourier transform surface enhanced Raman scattering
H&E	hematoxylin and eosin
HCl	hydrochloric acid
HMN	hollow microneedle
ID	intradermal
ID-bolus	intradermal bolus immunization
IM	intramuscular
IM-bolus	intramuscular bolus immunization
IMDM	Iscove's modified Dulbecco's medium
IPV	inactivated polio vaccine
IPV1	monovalent inactivated polio vaccine serotype 1
LC	Langerhans cell
LSD	least significant difference
MFI	median fluorescence intensity
MN	microneedle
MQ	ultrapure deionized Milli-Q water
NaOH	sodium hydroxide
OPV	oral polio vaccine
OVA	ovalbumin
OVA-AF488	ovalbumin conjugated with Alexa Fluor® 488
OVA-FITC	ovalbumin conjugated with FITC
PBS	phosphate buffered saline
PDI	polydispersity index
SC	subcutaneous
SDS	sodium dodecyl sulfate
SEM	scanning electron microscopy
SERS	surface enhanced Raman scattering
TMB	3,3'5,5'-tetramethylbenzidine
TMC	N,N,N-trimethyl chitosan
TMC-RHO	N,N,N-trimethyl chitosan (TMC) conjugated with rhodamine B isothiocyanate
TRIS-HCL	tris(hydroxymethyl)aminomethane hydrochloride
VN	virus neutralization